



Kipingu, Andrea Martin (2025) *Modelling population dynamics to inform the evaluation of vector control tools in semi-field and field settings*. PhD thesis.

<https://theses.gla.ac.uk/85104/>

Copyright and moral rights for this work are retained by the author

A copy can be downloaded for personal non-commercial research or study, without prior permission or charge

This work cannot be reproduced or quoted extensively from without first obtaining permission from the author

The content must not be changed in any way or sold commercially in any format or medium without the formal permission of the author

When referring to this work, full bibliographic details including the author, title, awarding institution and date of the thesis must be given

Enlighten: Theses

<https://theses.gla.ac.uk/>
research-enlighten@glasgow.ac.uk



College of Medical, Veterinary and Life Sciences

School of Biodiversity, One Health and Veterinary Medicine

**Modelling population dynamics to inform the evaluation of vector
control tools in semi-field and field settings**

Submitted in fulfilment of the requirements for the degree of
Doctor of Philosophy

By

Andrea Martin Kipingu

Submitted on 3rd January 2025 to the University of Glasgow

Abstract

Malaria remains one of the most common life-threatening vector-borne diseases worldwide, with an estimated 263 million global cases and 597,000 deaths per year, 94% and 95% of which occur in sub-Saharan African countries, respectively. In sub-Saharan Africa, Tanzania accounts for approximately 3.3% and 4.3% of all malaria cases and deaths, placing it among the leading four countries responsible for just over half of global malaria deaths. Malaria is transmitted to humans through a bite by an infected female *Anopheline* mosquito. In Dar es Salaam, Tanzania, *An. gambiae s.l.* (i.e., *An. gambiae s.s.*, *An. arabiensis* and *An. merus*) is the most important species in terms of malaria transmission, followed by *An. funestus*. Vector control remains the most effective strategy against malaria. The main malaria vector control interventions are insecticide-treated bed nets and indoor residual spraying; both were very successful but were not enough to eliminate transmission, so there is a continuous search for new tools and strategies for deployment.

Development of interventions typically starts in the laboratory and then moves to the semi-field system before going to the field; thus, we need robust ways to assess them at all these levels. Experiments for testing vector control interventions in semi-field systems serve as a cost-effective link between laboratory and field trials, enabling researchers to evaluate interventions or their combinations in controlled conditions. One way to achieve reliable outcomes is to design semi-field experiments with adequate statistical power. Evaluating power is crucial for determining necessary resources, including finances, time, and participants. However, power analysis is rarely done, possibly due to limitations in technical skills and the availability of tools such as software.

Furthermore, assessment of interventions in the field settings needs to not only determine the impact on population size but also regulatory processes (such as negative density dependence and positive density dependence known as Allee effect) that regulate populations. Negative density dependence is a regulatory process which typically operates in immature mosquitoes where growth rates decline at high densities, mainly caused by resource competition. Allee effect is another process operating in adult mosquitoes where population crash if density is low, mainly caused by mate limitation. Understanding the impacts on population

dynamics and how low populations are regulated in the field settings could provide critical insights into how to improve vector control strategies. This is because at low densities, regulatory processes, particularly negative density dependence and Allee effects, have implications for vector suppression and elimination plans. However, the existence of Allee effects in the field settings with low mosquito population densities and their implications for vector control interventions is still unknown.

The main aim of this PhD thesis was to improve the evaluation of malaria vector control interventions. This was done through a combination of theoretical and statistical modelling approaches applied to both semi-field and field settings. There were three specific research aims: 1) how can vector control experimental designs be improved in semi-field systems? 2) what are the trade-offs between mosquito population regulatory mechanisms at low densities? and 3) do key mosquito population regulatory processes emerge from large-scale vector control?

To achieve aim 1, a simulation-based power analysis framework from a generalised linear mixed model was developed to assess how many chambers, sampling frequency and sampling size in semi-field systems would provide enough power to determine the impact of interaction between two tools, here pyriproxyfen autodissemination and the widespread insecticide-treated bed nets against malaria vector *An. arabiensis* across a range of commonly used semi-field experimental designs, such as single vs. combined interventions and short- vs. long-term experiments.

Results showed that the higher the effect sizes, the higher the power, but power also increased with the number of chambers, sampling frequency, and number of mosquitoes, while high variation between chambers reduced power. A generalisable power analysis framework was provided and can be used widely for other vector control tools, experimental scenarios and also other vectors.

For aim 2, a simulation model based on an age-structured population model was developed to quantify trade-offs between negative density dependence and the Allee effect and how these impact the outcomes of interventions.

Results showed that while in isolation, these mechanisms are not able to drive the population into extinction, their co-existence can accelerate population extinction as populations become smaller. A combination of negative density dependence, the Allee effect, and sustained larvicidal intervention led to a

decline in mosquito populations to levels from which they could not recover. Conversely, the combination of negative density dependence, the Allee effect, and short-term larvicidal applications did not decrease mosquito populations to lower levels enough to prevent a rebound. Understanding regulatory processes like Allee effects can support vector control by highlighting resilient and vulnerable aspects of the mosquito's life cycle stages to interventions, and potentially accelerating malaria elimination.

To address aim 3, a population dynamics model was developed using the Bayesian state-space modelling approach. Initially, the model was fitted to simulated data to determine whether my framework would be able to quantify Allee effects if they exist in the wild. Results showed that the framework was indeed able to capture the life history traits, including negative density dependence and Allee effects. Subsequently, the model was fitted to female adult *An. gambiae* data from Dar es Salaam, Tanzania, to identify the presence of Allee effects in natural settings and quantify the impacts of a larvicide intervention.

Results showed that there was no evidence of the Allee effect in the *An. gambiae* mosquito data from Dar es Salaam despite the larviciding having reduced the population by 60.92%. When planning for future malaria vector control strategies, it is essential to consider Allee effects, if they exist, fewer resources could result in better outcomes, similar to deploying more resources.

In conclusion, the methods and findings presented in this thesis will help future research to evaluate vector control interventions or their combinations in SFS and field settings. This thesis contributed to a general understanding of the trade-offs between negative density dependence and Allee effects and how they can contribute to vector control and accelerate malaria elimination. The Bayesian state-space modelling framework developed in this thesis will aid further research in identifying Allee effects in different settings with low mosquito population densities.

Table of Contents

Abstract	ii
List of Tables	x
List of Figures	xi
Acknowledgement	xv
Author's Declaration.....	xvii
List of Abbreviations.....	xviii
Chapter 1 General Introduction	19
1.1 The problem of malaria	19
1.1.1 Malaria burden	19
1.1.2 Malaria transmission and mosquito life cycle	19
1.2 Malaria vector control	20
1.2.1 Importance of malaria vector control	20
1.2.2 Current, novel and future vector control tools	22
1.2.3 Assessment of vector control tools	23
1.3 Importance of population dynamics for vector control	24
1.3.1 Negative density dependence	25
1.3.2 Allee effects.....	25
1.4 Modelling of vector population dynamics	26
1.4.1 Theoretical models of population dynamics.....	26
1.4.2 Applied models of vector population dynamics.....	29
1.4.3 Models to assess the impact of vector control tools	31
1.5 Description of the research gap and objectives.....	32
1.5.1 Aim 1) How can vector control experimental designs be improved in semi-field systems?.....	34
1.5.2 Aim 2): What are the trade-offs between mosquito population regulatory mechanisms at low densities?	34
1.5.3 Aims 3) Do key mosquito regulatory mechanisms emerge from large-scale vector control?.....	34
1.6 Case studies.....	35

1.6.1	The design of vector control semi-field experiments	35
1.6.2	Large-scale larvicidal control in Dar es Salaam, Tanzania	36
Chapter 2	A power analysis framework to aid the design of robust semi-field vector control experiments.....	38
	Abstract.....	38
2.1	Introduction.....	40
2.2	Methods.....	44
2.2.1	Overview of experimental design choices	44
2.2.2	Approach for short-term experiments testing single and combined interventions	47
2.2.3	Approach for long-term experiments testing single and combined interventions	48
2.2.4	Power estimation	49
2.2.5	Tutorial - practical application.....	50
2.2.6	Type I error rate	55
2.3	Results	56
2.3.1	Short-term experiments testing single and combined interventions	56
2.3.2	Long-term experiments testing single and combined interventions	58
2.3.3	Inter-chamber variance affects power	59
2.4	Discussion.....	61
2.5	Conclusion.....	65
Chapter 3	Implications of the trade-offs between negative density dependence and the Allee effect for the malaria vector control endgame	66
	Abstract.....	66
3.1	Introduction.....	68
3.2	Methods.....	71
3.2.1	Study design	72
3.2.2	Stage-structured population model formulation.....	72

3.2.3	Leslie Matrix for estimation of adult mosquitoes' population growth rate	76
3.2.4	Role of negative density dependence and Allee effect in regulating mosquito populations	78
3.2.5	Impacts of negative density dependence and Allee effects on sustained and short-termed interventions.....	79
3.2.6	Trade-offs between negative density dependence and the Allee effect	80
3.3	Results	82
3.3.1	Adult mosquitoes' population growth rate	82
3.3.2	Role of negative density dependence and Allee effect in regulating mosquito populations	83
3.3.3	Impacts of negative density dependence and Allee effects on sustained and short-term interventions.....	85
3.3.4	Trade-offs between negative density dependence and Allee effect in the mosquito population regulation	87
3.4	Discussion.....	89
3.5	Conclusion.....	92
Chapter 4	Identifying the Allee effects impacting <i>Anopheles gambiae</i> populations in the field	94
	Abstract.....	94
4.1	Introduction.....	95
4.2	Methods.....	98
4.2.1	Large-scale larvicidal control programme in Dar es Salaam	98
4.2.2	Longitudinal surveillance of <i>An. gambiae</i> in Dar es Salaam.....	98
4.2.3	Simulated data: adult female <i>An. gambiae</i> population abundance	99
4.2.4	Environmental data.....	99
4.2.5	Bayesian state-space models (SSMs)	100
4.2.5.1	Biological process: Mosquito life cycle	100
4.2.5.2	Observational processes	105

4.2.6	Model fitting and outputs.....	109
4.3	Results	110
4.3.1	Allee effects are identifiable with simulated data.....	110
4.3.2	Population dynamics of <i>An. gambiae</i> mosquitoes in Dar es Salaam	111
4.3.3	Allee effects could not be identified from the Dar es Salaam field data	115
4.3.4	Larvicidal in Dar es Salam decreased mosquito abundance through reductions in larval survival.....	116
4.4	Discussion.....	118
4.5	Conclusion.....	123
Chapter 5	General Discussion and Conclusions.....	124
5.1	The role of simulations for evaluating vector control interventions. ..	124
5.2	Implications of vector population regulation for malaria vector control efforts.....	126
5.3	Leveraging population dynamics modelling for effective malaria vector control	128
5.4	Future work	129
5.5	Conclusions.....	130
Chapter 6	List of Appendices	132
Appendix A	Supplementary materials for Chapter 2	132
Appendix A.1	List of articles selected for a simple review of the use of power to justify the sample size.	132
Appendix B	Supplementary materials for Chapter 3	135
Appendix B.1	Dynamics of female adult <i>An. gambiae</i> mosquito data from the field	135
Appendix B.2	Weekly rainfall across wards during the large scale larvicidal control programme in Dar es Salaam.....	136
Appendix B.3	Figure showing centered average weekly rainfall across wards (black) and population dynamics without intervention (blue) during the large- scale larvicidal control in Dar es Salaam, Tanzania.....	136

Appendix B.4	Tables of selected combinations of negative density dependence (DD), the Allee effect variations (AE) and Larvicides application (LA)	137
Appendix B.5	Population without negative density dependence	147
Appendix B.6	Trade-offs between the negative density dependence and the Allee effects by probability of extinction	147
Appendix B.7	R script for a simulation model in Chapter 3	149
Appendix B.8	Conversion of original parameters values to values per week	151
Appendix C	Supplementary materials for Chapter 4	152
Appendix C.1	Female adult mosquito data from data from Dar es Salaam, Tanzania, aggregated weekly	152
Appendix C.2	Total number of traps per each ward	152
Appendix C.3	Weekly current rainfall per ward	153
Appendix C.4	Weekly cumulative rainfall for each ward	153
Appendix C.5	Average weekly temperature across wards	154
Appendix C.6	Representation of statistical distributions shape or rate parameters of priors using means and variances	154
Appendix C.7	Trace plots of model fitting using the simulated data	155
Appendix C.8	Prior and posterior distributions of model fitting using the simulated data	155
Appendix C.9	Observed vs. predicted adult mosquito averaged across wards . ..	156
Appendix C.10	ACFs for the simulated data	156
Appendix C.11	Trace plots of model fitted to field data	157
Appendix C.12	Prior vs. posterior distribution of model fitting using field data	158
Appendix C.13	Observed vs. estimated mosquitoes for each ward	158
Appendix C.14	Observed vs. estimated mosquitoes across wards	159
Appendix C.15	Bayesian state-space model JAGS code	159
List of References	163

List of Tables

Table 2.1: Experimental design scenarios, study variables and simulated values for short- and long-term experiments. An estimated variance (EV) between chambers of 0.1807 was used in this study, estimated by fitting a negative binomial GLMM to the mesocosm experimental data (165).....	45
Table 3.1: Description and parameter values used in the simulation model, with respective literature sources. Only estimates per week were used during the simulation. How original biological values converted to per week values are shown in Appendix B.8.....	81
Table 4.1: Description of prior and posterior distributions. For each parameter in the model, a brief description of its biological meaning, the mean values obtained from the literature, and how these were transformed first into weekly values (the time unit of the SSM model) and then as parameters of their corresponding prior distribution are provided. Finally, for the posterior distributions, the mean and 95% credible intervals (CIs) are provided, and to maintain biological meaning, parameter values representing mean survival were transformed into logit (i.e., log odds of survival) using logit function.	107

List of Figures

- Figure 2.1: Picture of a semi-field system at the Ifakara Health Institute (Tanzania) with (A) the replicated outdoor environment separated by nets keeping mosquitoes inside. Inside the semi-field system, there are the number of (B) chambers within which there are (C, D) artificial larval habitats and vegetation and (E) emergence traps for monitoring emerging mosquitoes..... 43
- Figure 2.2: Change in expected mosquito counts over 3 months (12 weeks), comparing the use of ITN and PPFa interventions in a semi-field experiment, showing how much faster the number of mosquitoes is reduced in the chambers combining both ITN and PPFa with (red) and without (blue) interaction than would be expected based on the single effects of PPFa (dark red) and ITN (purple) or no intervention (black)..... 55
- Figure 2.3: Statistical power obtained from different short-term SFE designs. Top panels (a and b) show the power expected when testing single interventions (ITN) and bottom panels when testing combined interventions (ITN and PPFa; c and d) with increasing (a and c) number of chambers per treatment or (b and d) number of mosquitoes recaptured. Different coloured lines correspond to varying effects or interaction sizes, i.e., % reduction in mosquito population. The dashed line is 80% power, and the dot-dashed shows a 5% power which is a type I error rate, which is the expected power when the effect size is zero. Error bars show 95% confidence intervals. Estimated variance (EV) was used in both (a-d) while 50 mosquitoes were used in (a) and (c), and 4 chambers per treatment in (b) and (d). 57
- Figure 2.4: Statistical power obtained from different long-term SFE designs. Top panels (a, b and c) show the power expected when testing single interventions (ITN) and bottom panels when testing combined interventions (ITN and PPFa; d, e and f) with increasing (a and d) number of chambers per treatment or (b and e) frequency of sampling or (c and f) number of mosquitoes to sample. Different coloured lines correspond to varying effects or intervention sizes, i.e., % reduction in mosquito population. The dashed line is 80% power and the dot-dashed shows 5% power which is a type I error rate, which is the expected power when the effect size is zero. Error bars show 95% confidence intervals. Estimated variance (EV) was used in both (a-f). A total of 10 mosquitoes and weekly sampling were used in (a) and (d), four chambers per treatment and 10 mosquitoes in (b) and (e), and four chambers per treatment and weekly sampling in (c) and (f). The main effects used for ITN and PPFa in (d-f) are 80% and 70%, respectively..... 59

- Figure 2.5: The effect of varying inter-chamber variance on the relationship between power and the number of chambers per treatment. Inter-chamber variance was varied from the estimated variance of 0.1807 (EV, solid line which corresponds to a red line in Figure 2.3c) to half (dashed line), double (dotted), and quintuple (dash-dotted line) its original value. Error bars show 95% confidence intervals. The red colour represents the target non-zero interaction effect (80% was used here) and the blue colour type I error rate (0% interaction effect). The two-dashed line is the 80% power, and the long-dashed line (black colour) is the nominal type I error rate of 5%. In this case, a total of 50 recaptured mosquitoes were used and the main effects explored for ITN and PPFa were 80% and 70%, respectively. 61
- Figure 3.1: Low-density population dynamics. The population growth rate is less than 1 above the carrying capacity K and below the critical population threshold K^- . A black line indicates negative density dependence, whereas a blue and red line indicates positive density dependence (i.e., weak, and strong Allee effects, respectively). 71
- Figure 3.2: Schematic representation of the model showing stages of the mosquito life cycle together with the predictors of the life-history traits. Arrows correspond to the transition from one stage to another. Larvae I correspond to early instar larvae, while Larvae II correspond to late instar larvae. 76
- Figure 3.3: Population growth as estimated through (a) a Leslie matrix method and (b) direct calculations from the simulation model (i.e., an average across 100 simulations all initialised at 800 female mosquitoes). The dashed line indicates the threshold of the population growth rate where the population declines when the rate is below this point. 83
- Figure 3.4: Role of DD and AE in regulating mosquito populations without a larvicidal intervention. (a) Three DD levels, $2.75e-05$, $5.5e-05$ and $2.2e-04$, were used, keeping Allee effects constant at 360. The red colour corresponds to DD3 when $AE=0$, (b) Three AE levels, 180, 360 and 720, were used, keeping DD constant at $5.5e-05$, and (c) Percentage of population change (relative to the initial size of 800 mosquitoes) after 193 weeks when DD and AE mean values $5.5e-05$ and 360 were varied across a range of values from 90% reduction to 100% or 300% increase. The percentage of population change was averaged over 100 simulations. 84
- Figure 3.5: Mosquito populations regulated by (a, c, e) negative density dependence at levels $2.75e-05$, $5.5e-05$ and $2.2e-04$ setting the Allee effect (C) constant to 360 and (b, d, f) Allee effects at levels 180, 360 and 720 keeping

- negative density dependence constant at $5.5e-05$. Larvicidal treatment was applied in three regimes, (a, b) sustained larvicidal application, (c, d) a single short application and (e, f) two short applications. 86
- Figure 3.6: Heat maps showing the probability of extinction (averaged over 100 iterations) by week 193 after varying across a range of values from 90% reduction to 100% increase in sustained larvicidal effect size, 0.25, and (a) negative density dependence effect size, $5.5e-05$, setting Allee effect constant or (b) Allee effect size, 360, setting negative density dependence constant. 87
- Figure 3.7: Heat maps showing the population growth rates averaged over 100 simulations for each percentage increase or decrease in negative density dependence and the Allee effect mean values, $5.5e-05$ and 360, respectively; (a) without intervention, (b) with two short applications of intervention, (c) single short application of intervention and (d) with sustained intervention. 89
- Figure 4.1: Monthly mosquito population abundance data showing (a) the sum of all traps per ward and (b) the sum of all traps across wards before and during a large-scale larvicidal control programme conducted from 2004 to 2008 in three administrative municipalities of Dar es Salaam, Tanzania.100
- Figure 4.2: Schematic of the life cycle model. At each life stage (i.e., adults, Larvae I, Larvae II and Pupae) mosquitoes transition from one stage to another (arrows) by surviving and some of these transitions (i.e., Larvae I to Larvae II and Larvae II to Pupae) are influenced by ecological factors. The Greek letters reflect the parameters in the model.....105
- Figure 4.3: An illustration of prior (black) and posterior (red) estimates of (a) negative density dependence, (b) Allee effect, (c) per capita fecundity and (d) adult survival in the y-axis for each of the probability of observations (pobs) in the x-axis. The error bars represent means and 95% CIs of the prior and posterior distributions.....110
- Figure 4.4: Accuracy of model estimates using pobs of 0.1. Histograms of prior (grey) and posterior (light blue) distributions for (a) negative density dependence and (b) the Allee effect with lines indicating the true values (red), median of the posterior distribution (blue) and 95% CIs of the posterior distributions (dashed grey).111
- Figure 4.5: (a) Illustration of the reconstruction of the total population abundances of *An. gambiae* adult mosquitoes across all wards: The y-axis is observed (black), predicted mean mosquito population abundance (predNa) (red), 2.5% and 97.5% quantiles (sky blue) of predicted population abundance, while the

x-axis is the time in weeks. (b) Goodness of fit: observed vs. predicted total population abundances of *An. gambiae* adult mosquitoes across wards, where the diagonal solid line corresponds to the 1:1 line.112

Figure 4.6: Illustration of the reconstruction of the population abundances of *An. gambiae* adult mosquitoes for selected wards. The y-axis is the number of adult mosquitoes, and the x-axis is the time in weeks. The black colour shows the observed data collected in the field for 193 weeks from April 2005 to December 2008. The red shows the mean mosquito population abundance (predNa) estimated by SSM for a similar time interval with corresponding 2.5% and 97.5% quantiles of estimated population abundance (predNa) (sky blue).112

Figure 4.7: Histograms of prior and posterior distributions of selected parameters showing mean (a) larval survival, (b) pupal survival, (c) adult survival, (d) per capita fecundity, the effect of (e) negative density dependence, (f) current rainfall (g) temperature on larval survival and (h) the Allee effect. The grey colour is the prior distribution, and the light blue colour is the posterior distribution.114

Figure 4.8: Effects of negative density dependence on mean larval survival as regulated by cumulative rainfall of (a) 0 mm (no rainfall), (b) 31 mm (medium across the year or lower during the rainy season), and (c) 331 mm (maximum/peak during the rainy season), all at different larval abundances. The grey colour is the mean larval survival, the brown colour is survival at 100 larvae, and the dark golden colour is survival at 500 larvae.....115

Figure 4.9: The evidence of whether Allee effects exist in the *An. gambiae* mosquito population in Dar es Salaam. Panel (a) shows priors in grey colour and posterior predictions in light blue colour for the Allee effect, C. Panel (b) shows the predicted overall mean fecundity in grey colour and overall predicted fecundity after the Allee effect in red colour, all based on an estimated average number of female adult mosquitoes across wards and weeks (i.e., N=52).116

Figure 4.10: The effects of larvicides alone on larvae: (a) Histogram of estimated mean survival with (red) and without (grey) larvicides and (b) the estimated female adult mosquito abundance averaged across wards before (black) and during (red) the larvicidal programme, where each line represents the abundance per each phase of larvicide application which included a total of 3, 6, and 6 wards in the first, second and third phase, respectively.117

Acknowledgement

I take this wonderful opportunity to express my gratitude to the Almighty God for his everlasting love, mercy, and grace towards me and my entire family and for guiding me to complete my PhD journey. My PhD journey has brought me to an amazing experience with both ups and downs, but in the end, it turned out to be a feeling of great pleasure and happiness.

I want to thank my supervisors at the University of Glasgow, Dr Mafalda Viana, Dr Paul Johnson, and Prof Dan Haydon, for their unwavering support and guidance throughout my PhD studies. As a former mathematics teacher, early days of my PhD posed significant challenges in grasping fundamental concepts including vector biology. However, they guided me towards a complex modelling project and consistently supported me whenever I encountered difficulties. I want to express my gratitude to Dr Samson Kiware, my local supervisor and mentor at Ifakara Health Institute (IHI), Tanzania. Dr Kiware played a crucial role since the time I was an intern at IHI, and he ensured a smooth beginning of my PhD studies and great support throughout this PhD especially during my visits to IHI. I am grateful for the support from Dr Dickson Lwatoejera during my time at IHI and for sharing with me data to be used as part of this PhD. I am also thankful to Dr Proper Chaki from IHI and Dr Kija Ng'habi from Mbeya College of Health and Allied Sciences, University of Dar es Salaam, for sharing their data with me and permitting me to use the data as part of my PhD project. I am grateful for being awarded a 4-year full scholarship under the LKAS leadership grant, which covered full course fees and provided a stipend throughout my PhD studies.

I am grateful to the Data Science and Mathematical Modelling team members at IHI for their support and advice throughout my PhD journey. As colleagues, they tried to motivate me and ensured I did not give up on this journey. I am also thankful to the Entomological and Laboratory Technicians and Research Scientists at IHI who supported me, especially during my visits to the institute's semi-field systems facilities (known as Mosquito City) at Kingani, Ifakara, Tanzania. Specifically, I thank Hamis Kunambi, Yohana Mwalugelo, Dr Najat Kahamba, and Dr Halfan Ngowo for their assistance during the visit.

I am grateful to my colleagues and postgraduate research students at the University of Glasgow for their invaluable support and guidance throughout my PhD studies. I particularly would like to extend special thanks to the following colleagues with whom I had the privilege of meeting or working together at the university and who generously spent their valuable time with me: Dr Cyrus Kavwele, Dr Dennis Minja, Dr Zabibu Kabalika, Dr Prince Ubiaru, Dr Najat Kahamba, Christina Makungu, Majaliwa Masolele, Mecklina Mbundi, Victoria Githu, and Houssein Kimario along with his family. I am deeply grateful for their unwavering support to me and my family.

I would like to express my gratitude to my PhD viva examiners, Prof Thomas Smith from the Swiss Tropical and Public Health Institute and Dr Luca Nelli from the University of Glasgow, for their insightful comments and suggestions, which significantly enhanced this thesis. I also wish to acknowledge the support of the viva convenor, Dr Taya Forde, for creating a conducive environment and smooth coordination during my viva.

I would also like to be grateful to Dr Nkuba Nyerere Mbeho for advice and mentorship from the very beginning. Although Dr Mbeho was not directly involved in my PhD studies, he will still be remembered as the first person to introduce me to the field of Mathematical modelling during my undergraduate studies at Sokoine University of Agriculture and since then I have held it tight and never looked back.

Finally, I want to express my deepest gratitude to my family here in Glasgow and my parents and relatives back home in Tanzania for their unwavering support and prayers throughout my PhD journey. I am grateful to my beloved parents, Pastor Martin Kipingu and Stellan Kipingu, whose unwavering prayers, trust, and belief in me from the very beginning have played a fundamental role throughout my studies. More importantly, I am thankful to my lovely wife, Hilda Kipingu, and my wonderful daughter, Abigail Kipingu, for their incredible and irreplaceable support throughout my PhD studies. Hilda's relentless support, heartfelt encouragement and prayers and enduring faith never wavered, even during the toughest times.

“Our help is in the name of the LORD, who made heaven and earth”

Psalms 124:8

Author's Declaration

I, Andrea Martin Kipingu, hereby confirm that the work presented in this thesis is entirely my original work. Whenever information has been obtained from other sources, I have made a diligent effort to acknowledge its source by citing and referencing the relevant literature. I acknowledge the contributions of all co-authors, as well as my supervisors, Dr Mafalda Viana, Dr Paul Johnson, Prof Daniel Haydon and Dr Samson Kiware. The copyright of this thesis is retained by the author. Researchers are permitted to reproduce, distribute, or transmit this thesis, provided that they appropriately acknowledge the author per accepted academic practice. Furthermore, I confirm that no part of this work has been submitted as part of any other degree at the University of Glasgow, or any other institution and that this thesis did not exceed the prescribed word limit.

List of Abbreviations

AE	Allee effects
ANOVA	Analysis of variance
ATSB	Attractive toxic sugar baits
CDC	Centre for Disease Control
COVID-19	Corona Virus Disease 2019
DD	Negative density dependence
DDT	Dichlorodiphenyltrichloroethane
EL	Eave Louvers
EV	Estimated variance
GLMMs	Generalized linear mixed-effects models
GLMs	Generalized linear models
H1	Alternative hypothesis
HLC	Human Landing Catch
IM	Ivermectin
ITNs	Insecticide-treated bed nets
IRS	Indoor residual spraying
IVM	Integrated vector management
LLINs	Long-lasting insecticidal nets
LRT	Likelihood ratio tests
LSM	Larval Source Management
PPFa	Pyriproxyfen autodissemination
SFEs	Semi-field experiments
SFS	semi-field systems
SSM	State-space modelling
SWAT	Soil and Water Assessment Tool
UMCP	Urban Malaria Control Programme
VCTs	Vector control tools

Chapter 1 General Introduction

1.1 The problem of malaria

1.1.1 Malaria burden

Malaria remains the most common life-threatening vector-borne disease worldwide. It causes high morbidity and mortality, with an estimated 263 million global cases and 597,000 deaths per annum, of which sub-Saharan African countries contributed 93.5% and 95.3% of cases and deaths, respectively (1). In sub-Saharan Africa, Tanzania accounts for around 3.3% of all malaria cases and 4.3% of malaria-related deaths, placing it among the four countries experiencing just over half of all malaria deaths worldwide (1). There has been a decline in global annual malaria case incidence per 1000 population at risk from 79 in 2000 to 60.4 in 2023 and annual mortality rate per 100,000 population at risk from 28.5 in 2000 to 13.7 in 2023, with the proportion of deaths among children aged under five years, the most vulnerable group, declining from 86.7% in 2000 to 73.7% in 2023 (1). This success in sub-Saharan African countries, including Tanzania, was primarily due to vector control, i.e., long-lasting insecticide-treated bed nets and indoor residual spraying (2-6). However, in recent years, global malaria cases have unexpectedly increased from 212 million in 2015 to 249 million in 2022 before rising again to 263 in 2023 (1,7,8). This increase was likely caused by a combination of factors, including widespread insecticide and behavioural resistance of malaria vectors that allow them to evade the control, COVID-19 and disruption of services from early 2020 due to COVID-19 or impacts from climate change (7-11). Given this current malaria landscape, there is a need for a deeper understanding of how current and new malaria vector control measures impact vector populations and also how those tools could be better used to control and eliminate malaria vectors.

1.1.2 Malaria transmission and mosquito life cycle

The protozoan parasite of the genus *Plasmodium* is the main cause of human malaria infections. There are five species of *Plasmodium*, i.e., *P. falciparum*, *P. malariae*, *P. ovale*, *P. vivax* and *P. knowlesi*, but among these, *P. falciparum* is the most predominant and important in terms of deaths in Africa (12,13). Malaria is a vector-borne disease transmitted by female anopheline mosquitoes of three

main species: *Anopheles gambiae* s.s., *An. arabiensis* and *An. funestus*. The mosquito carries malaria parasites and transmits the infections when feeding on humans; however, not all anopheline mosquitoes are regarded as malaria vectors (14,15). Epidemiologically, the intensity of malaria transmission is determined by various factors such as mosquito density (16), lifespan (17,18), biting behaviour (19,20), fitness and the overall capacity to transmit malaria parasites (21,22). Since the current malaria vaccine is not widely available and not effective for all age groups (23,24), reduction and/or elimination of vector populations remains the most efficient strategy for preventing malaria transmission (14).

Mosquitoes undergo distinct life stages, starting from the aquatic phases of egg, larva and pupa to the terrestrial adult stage (25,26). Female adult mosquitoes lay 50-200 eggs in breeding habitats such as water bodies, which then hatch into larvae (26). The larval stage is further divided into two main instar stages known as early and late instar larval stages. Over about two weeks, the larvae require resources such as temperature, which typically ranges between 23°C and 31°C (27), and feed on microorganisms such as bacteria, yeasts and protozoa (26). The late instar larvae transform into pupae, which takes approximately 2 to 4 days. During their brief life, pupae do not feed and finally emerge as adult mosquitoes (26). Initially, after emergence from pupae, both female and male adults feed on plant nectar. Subsequently, the female mosquitoes proceed to feed on blood (25). Adult female and male mate, and after mating, the female adult begins seeking a blood meal to develop and lay eggs (oviposition). The process from when the mosquito seeks and feeds on blood to the oviposition of eggs is referred to as the gonotrophic cycle, which normally takes 2-4 days (25,28,29). The entire life cycle of a mosquito takes roughly about a month (30); therefore, throughout the project, all the model developments will be assumed to take the same life cycle period.

1.2 Malaria vector control

1.2.1 Importance of malaria vector control

Vector control is a highly effective method for preventing malaria transmission that works by directly targeting disease-transmitting vectors (14,31,32). Such control measures increase vector mortality, hence reducing vector abundance, and as a consequence, they bring a reduction in malaria incidence, prevalence,

morbidity, and mortality (33). There are multiple tools for malaria vector control, but currently, chemical control using insecticides against adult mosquitoes is by far the most widespread (34). The main two vector control tools are 1) insecticide-treated bed nets (ITNs), which, in addition to the physical protection against mosquito bites, the chemical in them (typically pyrethroids) kills the mosquitoes upon contact with the net, and 2) indoor residual spraying (IRS) with insecticides, which kills mosquitoes that rest on interior house surfaces such as walls and roofs (14,35). In sub-Saharan Africa, where malaria is endemic, ITNs alone resulted in a 68% decline in malaria transmission, while IRS alone contributed to a 13% decline between 2000 and 2015 (2). ITN is the most common and efficient vector control method in Tanzania, followed by IRS, but they are facing challenges because of insecticide resistance and changes in mosquito and human behaviours (36-39). The current Tanzania Demographic and Health Survey and Malaria Indicator Survey have shown that the use of ITNs in Dar es Salaam, Tanzania, is more widespread (whereby 71.8% of households have at least one ITN in their houses) (40) compared to other malaria vector control interventions including larviciding (41), mosquito repellents (36,42) and mosquito-proofed housing (43). However, the majority of the households in Dar es Salaam and other regions of Tanzania prefer mosquito nets during the rainy season because of more mosquitoes, and do not like to sleep under the net, or some even sleep outside during the dry season (especially when the weather is too warm) because of fewer or no mosquitoes (44-46). Additional supplementary control measures such as larviciding also exist, but mostly in urban areas (41,47,48). Instead of targeting adult mosquitoes, larvicide works by reducing larval survival and impairing larval development (49). Although larviciding can be effective in reducing the adult mosquito population, the population can rebound once the larviciding stops. For instance, a semi-field experiment for malaria mosquito control conducted in southern Tanzania in rice paddy farms used bio-larvicide mixed with fertiliser and revealed a significant reduction of mosquito larval density in areas with the intervention, although adult mosquitoes continued to exist in these settings at low densities (48). Despite the efforts to reduce malaria vector populations through ITN, IRS and larvicides, malaria persists due to difficulties in maintaining the populations under control and even eliminating them. These challenges may indicate that, as currently implemented, these interventions may not be as efficient in decreasing mosquito populations to extinction and achieving malaria elimination as one would hope

for. There are several reasons for this, including the lack of understanding of how widespread implementation of the intervention should be or how difficult it is to sustain it over a long time. Therefore, identifying problems such as population rebound and what is causing them is critical to enhancing vector control strategies, not only to take advantage of them but also to understand how to deploy the strategy and to prevent the evolution of resistance.

1.2.2 Current, novel and future vector control tools

To minimise the threats to the effectiveness of core malaria vector control interventions and target mosquitoes from multiple directions, supplementary, combined and innovative vector control interventions are highly recommended (35,50,51). Different deployment strategies, which are combined approaches for vector control include topical repellents to prevent mosquito bites, insecticide-treated clothing to reduce exposure to mosquitoes, spatial or airborne repellents to create barriers against mosquitoes, space spraying to control adult mosquitoes, and housing modifications to prevent their entry (50). Other strategies for malaria vector control include Larval Source Management (LSM), a supplementary intervention which targets the immature, aquatic stages of mosquitoes (i.e., the larvae and pupae) to reduce the abundance of adult mosquitoes. LSM comprises four types: habitat modification, habitat manipulation, larviciding and biological control (52). Still, there is a growing interest among researchers in using LSM as part of combined strategies for malaria vector control due to its effectiveness in various settings where it has been implemented (41,47,53-57). Several other innovations aiming to close gaps in anti-malaria efforts include improved nets with expanded chemistries to defeat insecticide resistance, such as new Interceptor® G2 nets treated with both pyrethroid and chlorfenapyr (58-60). Additional novel methods for malaria vector control include the use of mosquito nets treated with pyriproxyfen alone or in combination with pyrethroid (60-62). Moreover, a new method of vector control involves ivermectin, i.e., the use of animals or humans who can actively contribute by taking endectocides or drugs that, once ingested, affect mosquitoes that come into contact with them (63,64). Other novel vector control tools include the use of genetically engineered fungal pathogens of anophelines to kill wild mosquito populations (65) and natural *Wolbachia* infections to manipulate mosquito reproduction and immunity thereby limiting the spread of disease pathogens (66). Furthermore, gene drive, one of the most

promising technologies, is gaining interest for its implementation in semi-field and field conditions following successful results in laboratory settings (67). Despite the availability of various vector control tools, malaria persists, highlighting the need for more development of future vector control methods to target factors such as insecticide resistance, behavioural change by mosquitoes and impacts of climate change.

1.2.3 Assessment of vector control tools

Vector control tools (VCTs) have a significant role in preventing vector-borne disease, and their efficacy is typically assessed in different settings, including laboratory, semi-field, or field conditions (68,69). The assessment process typically commences in the laboratory, where experiments are carried out under controlled insectary conditions using colonised mosquitoes (70). These laboratory experiments are resource-intensive, i.e., they require substantial investments in terms of finances, time and specialised technical expertise. Typically, after successful initial testing in the laboratory, VCTs undergo further evaluation in semi-field systems. Semi-field experiments (SFEs) are conducted in simulated field conditions within semi-field systems, which can be self-contained habitats placed within the natural ecosystem of a disease vector. These can range in size and conditions and can contain all the requisites for the completion of the vector life cycle (71–75) or be clean rooms with bare grounds (76–82), where either field-collected mosquitoes or those reared in the laboratory are used (68,70,83). SFEs provide researchers with an opportunity to closely and directly observe mosquito behaviours and their interactions with the environment. Various types of data that result from the SFEs include counts of mosquito abundances and the proportions or number of mosquitoes in different categories such as alive unfed, alive fed, dead unfed or dead fed. Ensuring reliable outcomes from SFEs requires careful design that includes adequate statistical power; however, power analysis is often neglected either due to lack of its importance among researchers, insufficient technical knowledge or lack of software tools to perform the analysis. Power refers to the probability of identifying a particular effect in a research study, assuming it exists (84). While standard analytical power analysis methods are available, they typically address only simpler analyses such as t-tests, ANOVA or chi-squared tests (85,86). Unfortunately, these standard methods are inadequate for analysing semi-field experiments as they typically do not accommodate

multiple levels of random variation (e.g., variation among observation within chambers or variation between chambers), of which are common in SFE. Consequently, there remains a need to develop power analysis methods that can effectively address these levels of random variations as well as accommodate various types of response data. The semi-field assessment provides valuable insights into the behaviour and effectiveness of VCTs in conditions that closely emulate natural settings. Once VCTs have been successfully tested in SFEs, they are normally subjected to small- or large-scale evaluation in the field. Field studies encompass trials conducted directly in natural breeding habitats using natural vector populations (68), providing valuable insights into the effectiveness of control interventions in the natural settings where disease transmissions occur. By assessing VCTs in laboratory, semi-field, and field conditions, researchers gain a comprehensive understanding and data on the efficacy and practical applicability of these important tools in controlling vector-borne diseases. To ensure reliable results, experiments that are conducted to evaluate and assess VCTs should be rigorously designed.

1.3 Importance of population dynamics for vector control

Population dynamics, as a branch of ecology, examines the changes in population size or density over time and space for one or multiple species. In the context of vector control, population dynamics is important as it provides empirical data for quantifying population trends and addressing key research questions related to control efforts (87). For instance, population dynamics have been used to inform the types of interventions needed, the timing and the strategy for their implementation, the projected size of mosquito populations over time and how their stability and response to interventions or their combinations differ across species (63,88). More importantly, population dynamics can be used to explore causal processes influencing population variations, such as how environmental factors, vector controls, and ecological processes impact mosquito population sizes (63,87,88). Negative density dependence and positive density dependence (known as Allee effects) are two examples of ecological processes that regulate population dynamics (89). However, the relative importance of the Allee effects in regulating mosquito populations is largely unknown. Therefore, there is a need to have a deep understanding of the malaria vectors and their ecological processes to inform the design and evaluation of malaria vector controls as well as describe

the failure and success of the deployed control measures. More detailed explanations of the two examples of ecological processes are provided in subsections 1.3.1 and 1.3.2 below.

1.3.1 Negative density dependence

Negative density dependence is a population regulation process that has been shown to exist in *An. gambiae* populations at the larvae stage (90-94), meaning their per capita growth rate increases as populations decline, for instance, through strong competition in larval habitats that is alleviated as population size declines. The evidence for this comes mostly from laboratory experiments with *An. gambiae*, showing that competition between larvae for food and other resources such as space affects their population densities (93,94). There have also been studies conducted in semi-natural conditions using artificial larval habitats to demonstrate the existence of negative density dependence in *An. gambiae* larvae (90,91). With less space (e.g., small water pools), the competition between larvae will increase. This competition will then result in a decrease in the larval population, which in turn will release some space again to accommodate more larvae. Modelling studies found that negative density dependence in larval development time is more significant than in survival, and models that ignore negative density dependence do not adequately capture the dynamics of mosquito abundance data (95). Ignoring endogenous regulatory processes (such as negative density dependence) may result in the exaggeration of predictions of the effectiveness of vector controls, for example believing that an intervention will have the same influence on destabilising malaria vectors in both low- and high-density populations (96). A consequence of negative density dependence is that control measures may become proportionately less effective as mosquito populations decline because the surviving individuals have a much higher per capita growth rate than those in high density.

1.3.2 Allee effects

Even though malaria vectors are generally considered negative density-dependent, there exists an opposing scenario where small vector populations may experience Allee effects, i.e. positive density dependence, in which the per capita population reproduction rate reduces with population size (89). In other words, if

individual fitness is reduced as population size decreases, then the population is exhibiting an Allee effect, which decides the extinction or conservation of that population (97). Allee effects are common in animal populations and can increase the risk of stochastic extinction in small populations (89,97). Evidence of the Allee effects exists across multiple taxa such as birds (98-100), fish (101-103), mammals (104-106), reptiles or amphibians (107) and other aquatic (97,108,109) and terrestrial invertebrates (110-113). The primary mechanisms for Allee effects include mate-limitation (in mammals, reptiles or amphibians, invertebrates), cooperative defence, feeding and breeding (in birds, fish, terrestrial invertebrates, mammals), predation (in fish, mammals, terrestrial invertebrates), pollination failure and inbreeding (in plants) (97,108). For instance, Angulo *et al.* demonstrated that Allee effects played an important role in the conservation of endangered northern island fox populations on the California Channel Islands. Their research revealed that a predation-driven Allee effect significantly impacted adult fox survival, attributed to Golden Eagles (106). Consequently, the control of Golden Eagles was implemented to reduce predation and recover fox densities (114-117). In mosquitoes, Allee effects are expected to mainly operate at the adult level, where mating becomes limited at low population size. Consequently, female's probability of mating declines due to fewer males available, leading to potential population crashes (118). There is still limited information on how other mechanisms such as cooperation, cannibalism or predation could lead to the Allee effects in mosquito populations. Understanding the mechanisms that lead to Allee effects in mosquitoes and account for their consequences are vital components in understanding the ecology of vector populations and improve vector control (119,120). However, it is not yet known whether Allee effects exist in vector populations or what are the implications for vector control.

1.4 Modelling of vector population dynamics

1.4.1 Theoretical models of population dynamics

Mathematical models can be used to understand or predict population dynamics, e.g., vector populations, species communities, and ecosystems, as they enable defining the complexity of the system without directly disrupting it (121,122). Theoretical models provide a deeper mechanistic understanding, allowing

predictions into future population dynamics and parameter space where empirical data is limited or unavailable. For example, for vector populations, while experiments in laboratory settings using laboratory-colonised vectors are useful to explore single population parameters in detail (e.g., survival or fecundity) (68,88), modelling is a simplification of natural world phenomena. Field experiments are more realistic and capture the interacting population parameters not only within individuals and populations but within the ecosystem; however, they are challenging to track, cost more resources, and can risk changing or destroying the system's ecology (121). Models describing vector population dynamics can be used to support malaria control programs (e.g., national malaria control programs and other stakeholders). For instance, Kiware *et al.* developed a mosquito population dynamics model (known as Vector Control Optimization Model) using systems of ordinary differential equations. They aimed to describe mosquito life and feeding cycles to assess and optimise the effectiveness of combined vector control interventions at varying coverages for suppressing dominant malaria vectors in sub-Saharan Africa. The model simulations indicated that utilising insecticide-treated nets at a coverage of 50% or 80%, in combination with larvicides, endectocide-treated cattle, and attractive toxic sugar baits at coverages of 80%, 50% and 50%, respectively, led to significant reduction in mosquito populations and effectively drove them to extinction (123). Wu *et al.* developed an advanced patch-based differential equation modelling framework that expands the Ross-Macdonald model to facilitate planning, monitoring, and evaluation of *Plasmodium falciparum* malaria control efforts. Within their model framework, they have devised innovative algorithms specifically for simulating adult mosquito demography, dispersal, and egg laying in response to resource availability. Through this framework, they have introduced new formulas to characterise mosquito parasite dispersal and spatial dynamics under steady-state conditions, encompassing human biting rates, vectorial capacity matrix, and threshold conditions (124). Xing *et al.* developed and analysed a discrete-time model of a stage-structured mosquito population to investigate the impact of a constant birth rate (i.e., adult fecundity) on the mosquito population's inherent net reproductive number (i.e., the expected number of female mosquitoes that a single female adult produces in her entire lifetime (125)), and how these factors contribute to population persistence or extinction. The results indicated that a per capita fecundity of 12 eggs led to an inherent net reproductive number greater

than 1, suggesting mosquito persistence. Their findings emphasised that continuous or seasonal persistence or extinction of the mosquito populations depends on the magnitude of the inherent net reproductive number. Consequently, controlling adult fecundity could potentially lead to the elimination of mosquito population (30). Ngwa formulated a deterministic differential equation model to analyse population dynamics of malaria vectors to understand conditions necessary for the existence and stability of a non-zero steady-state vector population density. The findings indicate that mosquito reproduction number is a determining factor for establishment and persistence of vector population, as it must exceed unity for this persistence to occur (126), consistent with the findings reported by Xing *et al.* (30), Lu and Li (125). In their study, Lutambi *et al.* developed an ordinary differential equation model of the mosquito life cycle to explore the impact of dispersal and uneven distribution of resources on the distribution and dynamics of mosquito populations to inform vector control measures (127). Their findings indicated the association between resource heterogeneity, dispersal, spatial distribution, and mosquito population dynamics. Furthermore, they highlighted the potential of randomly distributing repellents to reduce the distance travelled by mosquitoes, offering a promising strategy for vector control (127). Depinay *et al.* presented a simulation model of African malaria vectors to gain insights into the dynamics of vector populations and the underlying key mechanisms. The study revealed that abiotic factors (i.e., temperature and rainfall) were pivotal in both aquatic and adult stages of mosquitoes, leading to an initial population peak following a dry period. Similarly, biotic factors (i.e., larval competition, predation and dispersal) significantly influenced fluctuations in mosquito population sizes, where temperature was identified as a key determinant in species dispersal (128). Okuneye *et al.* developed a deterministic, weather-driven model to examine the population dynamics of immature and mature mosquitoes for better vector control efforts. They sought to assess how temperature and rainfall impacted mosquito population abundance in three sub-Saharan African countries, i.e., South Africa, Nigeria and Kenya. Their findings revealed that mosquito abundance peaks at mean temperature and rainfall ranging between 22-25 °C and 98-121 mm in South Africa, 24-27°C and 113-255 mm in Nigeria, and 20.5-21.5 °C and 70-120 mm in Kenya. Their study highlighted the importance of intensifying vector control efforts during periods when weather conditions are conducive to mosquitoes (129). Despite their

importance, theoretical models may be limited in offering practical and more actionable information because they do not necessarily utilise real world data although sometimes their parameter values can be informed by empirical data. Therefore, it is of great importance that while these models examine the dynamics of vector populations, they must also take into account various biological mechanisms that operate in varying vector densities. Incorporating both negative density dependence and Allee effects in the modelling of mosquito population dynamics has been limitedly explored in most of the models. Yet, it is unclear why both processes have been overlooked, but this could be due to a lack of knowledge of their importance, difficulties in setting density dependence models or a deficiency of empirical data that could help study them more explicitly. Failure to include regulatory processes such as negative density dependence and Allee effects is to potentially underestimate their impacts on the vector population dynamics, which in turn has an impact on vector control and elimination processes.

1.4.2 Applied models of vector population dynamics

Applied population dynamics models differ from theoretical models in that they are designed to use real-world data to provide insights into the dynamics of actual populations. However, the process is often simplified due to constraints such as computational power and data availability. By using data fitting techniques, these applied models can offer more practical and actionable information about how populations change over time. This approach allows researchers and policymakers to understand better and address real-world population dynamics and their implications. Applied models that explain vector population dynamics use data either from laboratory, semi-field or field trials. When fitted to data, models can be used to study and identify ecological behaviours related to population or disease dynamics. For example, Ngowo *et al.* developed Bayesian state-space models (SSMs) based on wild *An. funestus* life history traits to quantify the impact of negative density dependence and seasonal fluctuations. The results showed that the pattern of the adult survival and fecundity varied highly across the year, but negative density dependence had less importance on the survival of wild *An. funestus* mosquitoes compared to rainfall and temperature (88). In their study, Christiansen-Jucht *et al.* developed a model based on a system of differential equations to evaluate the temperature- and age-dependent survival and mortality

of *Anopheles gambiae* s.s. mosquitoes across their life cycle stages. The model was fitted to a longitudinal dataset of vector abundance spanning 36 months in sub-Saharan Africa, considering both data that incorporated age dependence and those that did not. The model fitting showed that both temperature and age significantly influenced the survival and mortality of mosquitoes at all stages. Notably, the model accounting for age dependence consistently provided a better fit to the data compared to the model that ignored age dependence (130).

Abdelrazec and Gumel developed a stage-structured model based on a system of ordinary differential equations to analyse the population dynamics of mosquitoes. Their study aimed to investigate the impact of temperature and rainfall variability on mosquito abundance. The model incorporated two different functional forms of egg oviposition rate: the Verhulst-Pearl logistic and Maynard-Smith-Slatkin functions were used. The model was fitted to the mosquito surveillance and weather data from the Peel region of Ontario, Canada. The findings suggested that the Maynard-Smith-Slatkin function was more ecologically appropriate for modelling the egg oviposition process compared to the Verhulst-Pearl logistic function. Moreover, the results indicated a peak in mosquito abundance at temperature and rainfall values ranging from 20°C to 25°C and 15mm to 35mm, respectively (131).

Ezanno et al. developed a weather-driven model based on a system of ordinary differential equations to predict and compare population dynamics of three mosquito species of *Anopheles*, *Culex* and *Aedes* in south France. The model was fitted to the longitudinal data on host-seeking adult female mosquitoes collected using CDC-light traps at two settings in southern France. The results have indicated that the predicted population abundance of *Anopheles hyrcanus*, *Culex pipiens*, and *Aedes caspius* differed, where *Aedes caspius* showed higher annual variations across settings. Moreover, adult mosquito emergence appeared to be an important factor in the population dynamics across species, suggesting that vector control measures must precisely target all aspects associated with mosquito emergence (132).

Walker *et al.* developed a discrete-time model of mosquito larval population dynamics to assess how larval density affects larval survival and development time. The model's validity was verified using publicly available semi-field data on larval density and pupation time collected during a six-month experiment. The study revealed that negative density dependence in larval development time may be more significant than in survival. Furthermore, the results showed that models without negative density

dependence do not adequately capture the trends in mosquito data (95). El Moustaid and Johnson developed a dynamical model of mosquito density using a system of ordinary differential equations to assess different methods for quantifying mosquito populations and suggest various dynamical system models that take into account mosquito life cycle traits at different temperature regimes. In their findings, models demonstrated different patterns at varying temperatures, and these patterns matched the observed population data (133). Biswas *et al.* developed and analysed a deterministic model for Zika to evaluate the impact of human awareness in combination with vector control measures. The model was calibrated, and parameters were estimated using reported Zika-infected human data from Colombia. Their study results showed that as the rate of sexual transmission increased, the density of exposed and infected human populations also increased, suggesting that Zika virus transmission between humans could be controlled by controlling sexual transmissions (134). Abiodun *et al.* developed an ordinary differential equation model to analyse how temperature and water availability impact the population dynamics of *Anopheles* mosquito. The model was designed to evaluate the impact of climate on the gonotrophic cycle and abundance of populations by analysing the mosquito life cycle. The ambient temperature data used for the model was obtained from KwaZulu-Natal Province, South Africa, while mosquito abundance data was obtained from New Halfa town, eastern Sudan. The results indicated that larvae abundance reached its lowest level between October and June, increased between June and October, and peaked in August, reflecting dry and rainy seasons. High temperatures during the dry season had a significant impact on larvae and other immature mosquitoes, as breeding habitats dried up quickly during the summer (135). The studies above demonstrated the crucial role of using data in calibrating models to understand the dynamics of disease vectors. Population dynamics models are widespread, but none has investigated the role of Allee effects in malaria mosquitoes and the relative impacts on the overall population dynamics.

1.4.3 Models to assess the impact of vector control tools

Population models provide descriptions, explanations, and predictions of phenomena such as growth, reproduction or disease transmission from one stage to another. However, one of their powerful uses is the assessment of the impact of vector controls on population dynamics. There are not many such models for

Anopheles mosquito control. A couple of notable exceptions include White *et al.*, who developed a simple model which accounted for both aquatic and adult stages of *An. gambiae* to explore the individual and combined impacts of long-lasting insecticidal nets (LLINs), IRS, larvicides, and pupacides. Their modelling work revealed that a combination of interventions that target both stages of the mosquito life cycle led to a substantial reduction in mosquito density (92). Ng'habi *et al.* developed SSMs fitted to data from replicated mesocosms to assess the impact on *An. arabiensis* of LLINs alone and in combination with insecticidal eave louvres or treatment of cattle with endectocide Ivermectin. According to their results, LLINs alone reduced mosquito survival by 91% and almost eliminated the mosquito populations when combined with Ivermectin (63). Marshall *et al.* developed a model to study the sugar-feeding behaviour of mosquitoes using field data from Mali. Their goal was to estimate sugar-feeding rates of adult mosquitoes at different ages and evaluate the potential of attractive toxic sugar baits (ATSB) in controlling mosquito populations. The model and fitted parameters were then incorporated into another larger integrated vector management (IVM) model that includes LLINs and IRS to assess the potential contribution of ATSB to future IVM programmes. Their findings indicated that younger mosquitoes had a higher estimated sugar-feeding rate compared to older mosquitoes. Additionally, they found that ATSB feeding rate of 50% or more had a greater impact than combining LLINs and IRS (136). Chitnis *et al.* developed a mathematical model to assess the comparative effectiveness of ITNs and IRS with dichlorodiphenyltrichloroethane (DDT) or bendiocarb, whether applied alone or in combination, in Namawala, Tanzania, where *An. gambiae* was the primary malaria vector. Their research indicated that the optimal use of ITNs was more effective in preventing mosquitoes and providing greater personal protection compared to IRS with DDT or bendiocarb. According to their findings, the combination of ITNs and IRS was more effective than ITNs alone only when IRS was implemented at high coverage levels (137). As examples, these studies have effectively highlighted the significance of using models to study the impacts of malaria vector controls in different settings.

1.5 Description of the research gap and objectives

Briefly, this PhD project focused on exploring two distinct approaches to making a vector control intervention readily available for public use. Firstly, the project

involved the evaluation of vector control interventions in semi-field systems. Secondly, the project entailed the assessment of the efficacy of vector control interventions in the field. Vector control experiments in semi-field systems serve as a cost-effective link between laboratory experiments and field trials, enabling researchers to evaluate the effectiveness of potential vector control interventions or their combinations in controlled conditions. However, for SFEs to be useful, they must be designed to provide reliable results; one way to ensure this reliability is by achieving adequate statistical power. Evaluating the statistical power of an experimental design is critically important to help determine the required resources, including finances, time and participants. Despite its importance, power analysis is rarely conducted for SFEs. Limitations to performing power analysis may include a lack of awareness of its importance, technical expertise, and availability of tools such as software for performing power analysis. The assessment of the efficacy of vector control intervention in the field involves assessing their impact on natural vector populations by taking into account the ecology of vector populations to see how interventions might be impacting particular regulatory processes of the mosquitoes and how we can use these processes to improve vector control in the field. Although it is accepted that understanding the impact of interventions on population dynamics is important for improving vector control strategies, there is still a lack of knowledge about how population regulatory mechanisms, such as Allee effects and density dependence act, interact with each and interventions and their implications for sustainability of vector control. Understanding the population regulatory mechanisms triggered by vector control when populations become smaller can provide useful insights into how they might impede or facilitate elimination of vector-transmitted diseases such as malaria.

This PhD project aimed to fill this knowledge gap by improving and determining the effectiveness of malaria vector control interventions on mosquito populations through a combination of theoretical and statistical modelling approaches. Specifically, there were the following three aims as described in subsections 1.5.1, 1.5.2, and 1.5.3 below:

1.5.1 Aim 1) How can vector control experimental designs be improved in semi-field systems?

This objective was addressed in Chapter 2 where a power analysis framework and tutorial were developed to inform the design of vector control experiments in semi-field systems. Generalised linear mixed-effect models were used to simulate and fit the data and quantify power of a single intervention or two in combination across a range of scenarios including short and long-term semi-field experimental experiments. Expected results here include the amount of power versus number of chambers, sampling frequency and sampling size. The study described in this chapter has been submitted as an article to the Malaria Journal.

1.5.2 Aim 2): What are the trade-offs between mosquito population regulatory mechanisms at low densities?

This aim was addressed in Chapter 3 where the trade-offs between negative density dependence and the Allee effect and its implications for the malaria vector control and elimination processes were explored. This was done using a simulation technique based on a stage-structured population model adapted to a large-scale larviciding intervention in Dar es Salam as a case study. The expected outcomes from this objective include weekly larval, pupal and adult mosquito abundances, growth rates and probabilities of population extinction.

1.5.3 Aims 3) Do key mosquito regulatory mechanisms emerge from large-scale vector control?

This objective was addressed in Chapter 4. Here, the model developed in Chapter 3 was adapted to a Bayesian SSM framework. First, this framework was tested with data from the simulation adapted in Chapter 3 and then fit it to the vector surveillance data from the Dar es Salam larviciding case study. The expected outcomes from this aim include posterior prediction means of the model parameters, predicted weekly average mosquito abundances across chains and iterations per individual wards and across wards as well as per intervention phase and across phases.

In Chapter 5, a discussion was provided for the main topics covered in Chapter 2, Chapter 3 and Chapter 4, and their contribution to the wider research area, along

with the overall project implications, limitations, challenges, suggestions for future research, and conclusion.

1.6 Case studies

1.6.1 The design of vector control semi-field experiments

One of the important aspects of an experimental design is determining the sample size, which can be the number of chambers per treatment, the number of mosquitoes, the number of participants or the number of mosquito traps. There are multiple methods of sample size calculations, which may include random sampling or power analysis. Power refers to the probability of uncovering an effect if it exists (84). Underpowered experiments normally utilise small sample sizes, which may result in study failure to detect the target effect and ineffective statistical analyses. Overpowered experiments normally use large sample sizes, leading to statistically significant results but with an unnecessary number of samples, higher costs and ethical concerns (138). Power analysis is one of the robust methods to inform the designs of vector control experiments; however, it is rarely used, partly due to a lack of knowledge among researchers, for example, knowledge of what power analysis is, what information it can provide and how it works (139). The limited use of the power analysis methods highlights the need to develop a generalisable framework and provide a step-by-step guide on its use to improve the designs of vector control semi-field experiments.

This first case study involves the use of power analysis methods to inform the designs of vector control experiments in semi-field systems. Specific Aim 1 in subsection 1.5.1 was addressed using this case study where a simulation-based power analysis framework using the generalised linear mixed-effect models (GLMMs) was developed and its use was step-by-step demonstrated and provided as a tutorial in an open-source software environment R. Here, power analysis methods were provided to inform the designs of a single vector control intervention (in this case, ITN alone) and in combination (in this case, ITN and autodissemination of pyriproxyfen (PPFa)). This framework is generalisable, meaning it can incorporate any other intervention apart from ITN and/or PPFa. Conducting a thorough power analysis to inform the designs of semi-field experiments (SFEs) is an important step of ensuring reliable results.

1.6.2 Large-scale larvicidal control in Dar es Salaam, Tanzania

Dar es Salaam is the biggest city in Tanzania, located on the eastern coast of the country along the shores of the Indian Ocean. Malaria is considered one of the main serious health problems in Dar es Salaam, with a prevalence rate of 1% among children aged 6 to 59 months (40). *Anopheles gambiae s.l.* is the most important mosquito species in terms of malaria transmission in urban Dar es Salaam, whereas other key species such as *An. funestus* exists at a very low abundance (140). In Dar es Salaam, malaria transmission typically peaks in one or two weeks following the rainy season and eventually declines to very low levels during the dry period (47). Apart from the rainy season, where larval density increases, socio-economic activities and urban land use, such as small-scale farming in backyard gardens and irrigation by tap water, increase the chance of creating breeding habitats, especially during the dry season (141). In Dar es Salaam, a range of mosquito control measures, including installation of ceiling boards, window screening, coils, repellents, indoor residual spraying (IRS) and insecticide-treated bed nets (ITNs), are usually being utilised by the community in their everyday lives. Larviciding was also one of the city's control measures carried out under the supervision of the Urban Malaria Control Programme (UMCP). The choices over each of these measures are primarily influenced by factors such as affordability and community's knowledge and perception on the effectiveness and potential health risks associated with each intervention (47).

A large-scale community-based larvicidal intervention was carried out in Dar es Salaam, Tanzania, from 2004 to 2008 as part of the UMCP with the primary aim of developing a sustainable larval control measure as one of the key components of malaria control strategy (41). The programme achieved substantial success, leading to a decrease in malaria prevalence from 28% to less than 2% between the years 2004 and 2008 (142). These low population densities are the main reason we are using this data and set up as a case study to investigate the presence of Allee effects.

During this programme, trained community members were tasked with surveilling larval habitats, applying larvicides to these habitats, and collecting adult mosquitoes (143). At the time of implementation, Dar es Salaam was divided into three administrative municipalities, which were further unequally divided into 73

wards. Out of the total 73 wards, larviciding activities were undertaken only in 15 specific wards across three distinct phases. The preparatory activities for the programme commenced in 2004, but weekly female adult mosquito collection only took place for 47 weeks (out of the total 193) between 2005 and 2006, before starting larvicides application to the larval habitats. The larvicides application began in 2006 by treating 3 wards in the first phase, followed by an additional 6 wards making a total of 9 wards in the second phase, and the remaining 6 wards were included in the last phase, making a total of 15 wards all covered with larvicides (41,47).

Chapter 2 A power analysis framework to aid the design of robust semi-field vector control experiments

This Chapter has been submitted as a research article and is currently under peer review in the Malaria Journal as: Andrea M. Kipingu, Dickson W. Lwatoejera, Kija R. Ng'habi, Samson S. Kiware, Mafalda Viana, Paul C.D. Johnson. (2024). A power analysis framework to aid the design of robust semi-field vector control experiments.

A preprint of this manuscript was published in the Research Square 2024: <https://doi.org/10.21203/rs.3.rs-4970151/v1>

Abstract

Semi-field experiments are an efficient way of assessing the impacts of potential new vector control tools (VCTs) before field trials. However, their design is critically important to ensure their results are unbiased and informative. An essential element of the design of semi-field experiments is power analysis, which empowers researchers to ensure that only designs with adequate statistical power are adopted. In this study, a methodology was developed, and its use was demonstrated in a tutorial, to determine the required number of semi-field chambers, sampling frequency and the number of mosquitoes required to achieve sufficient power for evaluating the impact of a single VCT or two in combination. By analysing data simulated from a generalized linear mixed-effects model, power was estimated for various experimental designs, including short- (24 hours) vs. long-term (3 months) experiments and single vs. combined application of interventions (e.g., insecticide-treated nets combined with pyriproxyfen autodissemination). Although power increased with increasing number of chambers, sampling frequency and the number of mosquitoes, the number of chambers and variance between chambers were the dominant factors determining power relative to all other design choices. High variance between chambers decreased power, highlighting the importance of making conditions similar among chambers, by reducing variation if possible and by rotating variables if not. As compared to a single intervention, an additional intervention required an increase in the number of chambers, while short and long experiments were similar in

terms of key aspects such as the number of chambers per treatment. Determining the most efficient experimental design for a semi-field experiment will depend on a balance of design choices and resource constraints. The power analysis framework and tutorial provided here can aid in the robust design of these widely used experiments and ultimately facilitate the development of VCTs.

2.1 Introduction

Vector control remains one of the most efficient strategies against malaria. Widespread vector control tools such as insecticide-treated nets (ITNs) and indoor residual spraying (IRS), were major factors in the decline in malaria cases, responsible for 68% and 13% reductions in cases, respectively, across sub-Saharan Africa from 2000 to 2015 (2). However, due to changes in human behaviour (144), the development of mosquito behavioural and insecticide resistance (19,145,146), and changing mosquito species composition (147-150), these interventions have not been sufficient to continue or improve the trend of declining malaria cases, so they need to be complemented with other tools (52,151-153).

New interventions are initially tested in the laboratory for safety and efficacy before moving to the field. Laboratory studies are relatively inexpensive but do not provide evidence of how well an intervention works in the field. In contrast, field studies can provide such evidence but generally require a substantial investment of resources such as time, effort and money. Semi-field experiments (SFE) provide a relatively inexpensive bridge between laboratory and field experiments. SFEs for malaria vector control are conducted within semi-field systems (SFS) (Figure 2.1), which can be self-contained habitats placed within the natural ecosystem of a disease vector. These can range in size and conditions and can contain all the requisites for the completion of the vector life cycle (71–75) or be clean rooms with bare grounds (76–82). Additionally, SFS can be partitioned into compartments (hereafter ‘chambers’) into which mosquitoes are released or emerge and from which they are recaptured or sampled following exposure to the intervention being trialled. Because of their size, the number of chambers available in a SFS typically ranges between 2 to 16 (Figure 2.1).

SFE generally adopt one of two extremes of experimental designs: short-term, lasting 24 to 48 hours to investigate immediate effects on mosquito mortality; or long-term, >3 months to investigate dynamic effects that develop over several generations of the mosquito population. For example, interventions that are expected to have a large and fast impact on mortality such as pyrethroid or chlorfenapyr-based ITNs (154,155) could be tested as a short-term intervention in SFS, while those with slow or delayed impacts such as pyriproxyfen (an insect growth regulator typically used to control immature mosquitoes from growing into

adults) (156) or entomopathogenic fungi (65,157,158) might be better suited for long-term experiments. An additional important aspect of any experimental design is selecting designs that give adequate power (159,160). Power refers to the probability of identifying a particular effect in a research study, assuming it exists. In the case of SFE, design choices can mean the number of chambers, duration of the experiment, and number of mosquitoes to be recaptured or sampled (161). It can also mean the proportions or number of mosquitoes in different categories (for example, alive unfed, alive fed, dead unfed or dead fed) to be recovered. The ability to compare power between different designs allows researchers to make informed decisions about which of these designs is more likely to allow them to detect an effect of interest. More effective experimental design is crucial for optimising resources use, including finance and time. Enhanced experimental designs allow for the evaluation of vector control intervention in a shorter timeframe and in a more cost-effective way. By testing malaria vector interventions effectively, we can facilitate quicker field deployment and establish a pathway for novel interventions to transition swiftly from testing to field implementation. Ultimately, doing this will help increase availability of interventions for public use and in turn contribute to the global reduction in malaria cases.

Standard analytical power analysis methods available from software packages often only deal with simple analyses such as t-tests, ANOVA or chi-squared tests (85,86). Unfortunately, these are not suitable for analysing semi-field experiments as they generally do not allow count data outcomes (e.g., number of mosquitoes) and multiple levels of random variation (e.g., variation among observation within chambers or variation between chambers), both of which are common in SFE. Although there are few standard methods for count data, count distributions such as Poisson and negative binomial distributions are often underutilised. Poisson and negative binomial models more effective in accounting for overdispersion or under dispersion. There is a need for a power analysis framework that reflects how the resultant data from SFE will be analysed. There has been no systematic review to date of the use of power analysis in SFE. For illustration, articles were surveyed in *Malaria Journal* and *Parasites & Vectors* using the search terms “semi-field” and “mesocosm”. A total of 38 articles (19 from *Malaria Journal* and 19 from *Parasites & Vectors*) published between 2020 to 2023 that comprise SFE studies (n=25) or

hut trials (n=13) which would have been eligible for power analysis were selected (see a list of selected articles in Appendix A.1).

Furthermore, the review has also shown that data from SFEs are usually analysed using generalised linear models (GLMs; 26% of articles reviewed) or generalized linear mixed-effects models (GLMMs; 45% of articles reviewed). Therefore, a power analysis method that also incorporates a similar degree of complexity and flexibility as GLMs or GLMMs will give the most realistic power estimates. When conducting power analysis for GLMMs, it is usual to use an approach called Monte Carlo simulation because of the flexibility and accuracy it gives relative to analytical power analysis methods. Simulations are used to generate multiple datasets that are as similar as possible to the expected datasets resulting from the planned experiments. All simulated datasets are analysed, and the proportion of these datasets giving a significant result is our estimate of the probability of detecting an effect, i.e., the estimate of power. The use of simulation from GLMMs overcomes the limitations of traditional power analysis methods as GLMMs can account for multiple sources of random variation (84). The advantages of using simulation-based power analysis for overcoming the limitations of analytical methods are well-known and have been illustrated in several studies (84,162-164). However, these methods are little used in the design of vector control trials, specifically for SFE.

From the review, eleven (29%) of the selected articles used power analysis to justify the sample size (five from Malaria Journal and six from Parasites & Vectors), of which six shared the same author. Of the eleven articles that used power analysis, 5 articles used the simulation-based power analysis method, 1 article utilized a method for comparing proportions and 6 articles did not specify the power analysis methods used. Although this is a small sample, it suggests that power analysis is underutilized in vector control SFEs. This neglect may in part be attributed to the limitations associated with traditional power analysis approaches or lack of expertise. This study aims to address both of these obstacles by developing a power analysis framework for the design of SFE and providing step-by-step instructions on how to apply it.

To illustrate the value of power analysis to SFE design, guidance and tools are presented through reproducible examples that illustrate the trialling of two

malaria vector control interventions, applied independently or in combination (i.e., single and combined) under two experimental scenarios (short-term with static effects and long-term with dynamic effects). This study aimed to empower researchers conducting SFEs to estimate power across a range of experimental design scenarios. This knowledge of statistical power, in combination with knowledge of the costs and resource constraints specific to each design, will allow researchers to make informed choices between competing designs. Specifically, the objective was to develop a power analysis framework that can be used to explore the impact on power of varying (i) the number of chambers (i.e., SFS compartments) per treatment, (ii) the number of mosquitoes to be recaptured in the control chamber (for short-term SFEs, recaptured mosquitoes can be used as a proxy of how many mosquitoes should be released), or to be sampled after they emerge from a self-propagating population (for long-term SFEs), (iii) the frequency of sampling mosquitoes, (iv) the amount of variation between chambers, and (v) the chosen size of the intervention effect that can be detected (targeted effect size).



Figure 2.1: Picture of a semi-field system at the Ifakara Health Institute (Tanzania) with (A) the replicated outdoor environment separated by nets keeping mosquitoes inside. Inside the semi-field system, there are the number of (B) chambers within which there are (C, D) artificial larval habitats and vegetation and (E) emergence traps for monitoring emerging mosquitoes.

2.2 Methods

2.2.1 Overview of experimental design choices

Here, the assumption is that the aim of a vector control experiment is to identify whether the single intervention is better than the control, or if the combined intervention (i.e., there is an interaction effect) is better than expected based on combining (multiplying) the separate effects (i.e., there is no interaction effect). Here, two typical SFE design scenarios, trialling single (i.e., ITN alone) and combined (i.e., ITN and pyriproxyfen autodissemination) interventions were explored. Pyriproxyfen autodissemination (PPFa) is mosquito-assisted larviciding where adult female mosquitoes transfer pyriproxyfen to their aquatic habitats (156). Although the power analysis framework developed here incorporates two malaria vector control tools (VCTs), namely ITN and PPFa, in practice, these could be any VCTs with similar characteristics. In the SFE trialling single intervention, only power analysis methods and estimates were presented solely for ITN alone. To minimise redundancy in methodology, power analysis methods for SFE trialling PPFa alone were not included because the same approach used for ITN would apply to PPFa or any other single vector control intervention. Additionally, two experiment durations were studied: short-term i.e., lasting 24 to 48 hours, which intended to investigate immediate effects on mosquito mortality; and long-term, i.e. ≥ 3 months, which intended to investigate dynamic effects that develop over several generations of the mosquito population. For all the scenarios, different SFE designs were tried as follows. First, a varying number of chambers, i.e. 2, 4, 6, and 8 per treatment were used. Second, for frequency of sampling, the short-term experiment had a single sampling point at 24 hours but for the long-term experiment (i.e., an experiment taking 3 months) we explored different frequencies namely, monthly sampling consisting of 3 sampling points, fortnightly sampling consisting of 6 sampling points, weekly sampling consisting of 12 sampling points and daily sampling consisting of 90 sampling points. Third, different mosquito abundances recaptured in control chambers were set as 5, 10, 20, 30, 40, 50, 60, 70, 80, 90 and 100 mosquitoes for the short-term experiments while 1, 5, 10, 20 and 40 mosquitoes were used for the long-term experiments. Throughout this paper, recaptured mosquitoes (or mosquitoes to be recaptured)

will be specifically used as a proxy of how many mosquitoes need to be released in the control chamber for a short-term SFE.

In this power analysis framework, the target effect size for each intervention was defined as the proportion of mosquitoes remaining at the end of the experiment. E.g., for single interventions, assuming that ITNs result in an 80% reduction in mosquito populations and PPFa results in a 70% reduction, then 20% and 30% of mosquitoes will remain at the end of the experiment (Figure 2.2, purple and brown lines), respectively. For combined interventions, where ITNs and PPFa are implemented simultaneously but without interactions, the product of the final proportions, which results in $20\% \times 30\% = 6\%$ of mosquitoes remaining at the end of the experiment (Figure 2.2, blue line) was assumed. Finally, for combined interventions with interaction, an interaction effect of 50%, i.e., the 6% of mosquitoes remaining when no interaction occurred will be reduced to 3% when there is an interaction (Figure 2.2, red line). The example effect sizes given above for ITNs and PPFa are quite large; therefore, the power of our experimental designs to detect four smaller effect sizes and their combinations was explored. All scenarios and designs are summarized in Table 2.1. Here, zero intervention effect size (0% reduction in mosquito population) represents the null hypothesis. The purpose of including the 0% scenarios in the study was to compare the estimated and nominal (i.e., 5% power) type I rates.

Unexplained variation in abundance between chambers (here referred to as inter-chamber variance) is one of the determinants of the statistical power of any SFE study. To quantify the impact of lower and higher inter-chamber variance on statistical power, we used an estimated variance (EV) of 0.1807 based on published SFE data (165) and varied it by factors of 0.5 \times , 1 \times , 2 \times and 5 \times (Table 2.1).

Table 2.1: Experimental design scenarios, study variables and simulated values for short- and long-term experiments. An estimated variance (EV) between chambers of 0.1807 was used in this study, estimated by fitting a negative binomial GLMM to the mesocosm experimental data (165).

Experimental scenarios	Study variables	R object names	Simulated values

Short-term experiment for single and combined interventions	Number of chambers per treatment	n.ch.per.trt	2, 4, 6, 8
	Expected number of mosquitoes recaptured in the control group	lambda	5, 10, 20, 30, 40, 50, 60, 70, 80, 90, 100
	Target effect sizes for single intervention (as % reduction)	itn.effect, ppf.effect	0%, 40%, 50%, 60%, 80%
	Target interaction effect sizes for combined interventions (as % reduction in mosquito population)	ixn.effect	0%, 40%, 50%, 60%, 80%
	Inter-chamber variance, σ_c^2	chamber.var	0.0904, 0.1807, 0.3614, 0.9035
	Experimental time period	-	24 or 48 hours
Long-term experiment for single and combined interventions	Chambers per treatment	n.ch.per.trt	2, 4, 6, 8
	Sampling frequency (sampling points)	sampl.freq	Daily (90), weekly (12), bi-weekly (6), monthly (3)
	Expected number of mosquitoes to be sampled	lambda	1, 5, 10, 20, 40
	Target effect size for a single intervention	itn.time, ppf.time	0%, 40%, 50%, 60%, 80%
	Target interaction effect size for combined intervention	ixn.ppf.itn.time	0%, 40%, 50%, 60%, 80%
	Time variance, σ_T^2	time.var	0.2266
	Inter-chamber variance, σ_c^2	chamber.var	0.0904, 0.1807, 0.3614, 0.9035
	Experimental time period	-	12 weeks (i.e., 3 months)
Dispersion parameter of the negative binomial distribution, θ	theta	10	

2.2.2 Approach for short-term experiments testing single and combined interventions

This section covers the detailed statistical models for short-term SFE testing single and combined interventions where mosquitoes are trapped at a single time point. The number of mosquitoes trapped in the chamber j , y_j , were modelled as being drawn from a Poisson distribution, i.e., $y_j \sim Pois(\lambda_j)$. The natural log of expected mosquito counts in the chamber j , is given as

$$\log(\lambda_j) = \beta_0 + \beta_I ITN_j + c_j. \quad 2.1$$

where β_0 is the expected log abundance in an average control chamber where neither intervention is present. ITN_j represents a single ITN intervention that is static over time and is an indicator variable, i.e. 1 in chambers where the intervention is deployed and 0 otherwise. β_I is the coefficient of the covariate ITN_j and represents the multiplicative intervention effect size on the natural log scale. For example, if an intervention such as an ITN reduces mean vector abundance by 80%, the multiplicative effect is $e^{\beta_I} = 0.2$, and $\beta_I = \log(0.2)$. c_j is a normally distributed random effect representing variation between chambers that is not explained by the fixed effect of the intervention, such that $c_j \sim N(0, \sigma_c^2)$ where σ_c^2 is an inter-chamber variance. The decision to use Poisson distribution in the short-term SFEs was based on the fact that, with only a single time point available, the variability observed within a single chamber is limited to the between-chambers variance. With experimental hut systems that allow entry of wild mosquitoes, there will be more variability in mosquitoes trapped between huts and therefore overdispersed Poisson distribution will be appropriate to account for this overdispersion additional to between hut variation.

To test the interaction between two interventions, Equation 2.1 was extended to add two predictor terms such that,

$$\log(\lambda_j) = \beta_0 + \beta_I ITN_j + \beta_P PPF_j + \beta_{I,P} ITN_j PPF_j + c_j. \quad 2.2$$

where β_I (as in Equation 2.1) and β_P are the coefficients representing the effects of the covariates ITN_j and PPF_j , respectively, which are indicator variables (i.e., 0 or 1) representing the presence in chamber j of that specific intervention. $\beta_{I,P}$ is a coefficient of the covariate $ITN_j PPF_j$ which represents an interaction between

ITN and PPFa. Because $ITN_j PPF_j$ is the product of the ITN and PPFa indicator variables, it is also an indicator variable, which is 1 only when both interventions are present and 0 otherwise. The interaction coefficient $\beta_{I,P}$ indicates how much more rapidly mosquito abundances are reduced by the combined effect of ITN and PPFa compared to what would be expected by combining (multiplying) their individual effects.

2.2.3 Approach for long-term experiments testing single and combined interventions

This section provides a detailed model description of a more complex experimental design, a long-term semi-field experiment testing single and combined interventions where mosquitoes are trapped at multiple time points. The number of mosquitoes trapped at a time i in the chamber j , $y_{i,j}$, was modelled as being drawn from a negative binomial distribution, i.e., $y_{i,j} \sim NB(\lambda_{i,j}, \theta)$. The natural log of the expected number of mosquitoes trapped at a time i , in the chamber j , are given as

$$\log(\lambda_{i,j}) = \beta_0 + \beta_T t_{i,j} + \beta_I ITN_{i,j} + \beta_{T,I} t_{i,j} ITN_{i,j} + \tau_i + c_j.$$

2.3

where β_0 is the expected log count in a control chamber at the first time point. $\beta_{T,I}$ is the effect of an interaction between time and ITN on mosquito abundance. β_T is the effect of time only on mosquito abundance in control chambers and β_I is the effect of ITN only on mosquito abundance when time is zero. The effects of time and ITN (i.e., β_T and β_I) are assumed to be zero in the simulated data (Figure 2.2, black and purple colour), this is to help simplify the setting of experimental design choices when simulating the data. However, those effects assumed zero must still be included in the model because in real data it should not be assumed that their effects are zero.

τ_i and c_j are normally distributed random effects of time and chamber, respectively, such that $\tau_i \sim N(0, \sigma_\tau^2)$ and $c_j \sim N(0, \sigma_c^2)$ where σ_τ^2 and σ_c^2 are time and inter-chamber variances, respectively. τ is incorporated in Equation 2.3 because, for a long-term SFE, mosquito abundance is expected to vary randomly between time points.

The θ is the dispersion parameter of the negative binomial distribution and represents unexplained variation among observations within a single chamber at a single time point. The use of a negative binomial distribution in the long-term SFEs was due to the reason that, when data from multiple time points are available, it is possible to separate consistent variation between chambers from variation between observations within chambers.

To test the interaction between multiple interventions that have dynamic effects over time (see Figure 2.2), Equation 2.3 was extended to add four predictor terms such that,

$$\begin{aligned} \log(\lambda_{i,j}) = & \beta_0 + \beta_T t_{i,j} + \beta_I ITN_{i,j} + \beta_P PPF_{i,j} + \beta_{T,I} t_{i,j} ITN_{i,j} + \beta_{T,P} t_{i,j} PPF_{i,j} \\ & + \beta_{I,P} ITN_{i,j} PPF_{i,j} + \beta_{T,I,P} t_{i,j} ITN_{i,j} PPF_{i,j} + \tau_i + c_j. \end{aligned}$$

2.4

where $\beta_{T,I} t_{i,j} ITN_{i,j}$ corresponds to the change in abundance over time due to ITN relative to changes occurring in the control chambers and $\beta_{T,P} t_{i,j} PPF_{i,j}$ corresponds to the change in abundance over time due to PPFa relative to changes in the control chambers. $\beta_{T,I,P} t_{i,j} ITN_{i,j} PPF_{i,j}$ corresponds to the change in the combined treatment chambers relative to what would be expected by combining (multiplying) the effects of change over time from the single treatment chambers. β_T is the effect of time only in the control chamber, β_I is the effect of ITN only and β_P is the effect of PPFa only on mosquito abundance. $\beta_{T,I}$ and $\beta_{T,P}$ are the effects of the interaction between time and ITN or time and PPFa on mosquito abundance, respectively, while $\beta_{I,P}$ is the effect of the interaction between ITN and PPFa only on mosquito abundance. The effects of time, ITN, PPFa and ITNxPPF (i.e., β_T , β_I , β_P , and $\beta_{I,P}$) are assumed to be zero in the simulated data (Figure 2.2), however, they must still be included in the model because in real data they should not be assumed that their effects are zero. $\beta_{T,I,P}$ is the effect of the interaction between time, ITN and PPFa on mosquito abundance.

2.2.4 Power estimation

Based on Equations 2.1-2.4 and the parameter values in Table 1, 1000 data sets for each experimental scenario were simulated. The simulated datasets were analysed by fitting the generalised linear mixed-effect models (GLMMs) from which they were simulated and testing for the intervention effect using the glmer function of the lme4 R package (166), which fits GLMMs using maximum likelihood.

Power was estimated as the proportion of simulated datasets in which the null hypothesis of no intervention effect was rejected using a significance threshold of $p < 0.05$, where the p-value was calculated using Wald z-tests from the GLMMs. Sufficient power was defined as an estimated power of at least 80%. The number of simulated datasets of 1000 was chosen as a trade-off between adequate precision and feasible computation time (1000 data sets give a margin of error of $\pm 2.5\%$ when true power is 80%).

2.2.5 Tutorial – practical application

In this section, an R tutorial to illustrate a step-by-step estimation of the statistical power of a short-term SFE with a single intervention is provided. This tutorial is provided to empower researchers with little or no expertise in using a simulation-based power analysis for SFE. This tutorial covers a simple scenario only; however, one can expand this to accommodate more complex SFE scenarios such as additional interventions or long experiments with single or combined interventions. (see doi: [10.5281/zenodo.11186503](https://doi.org/10.5281/zenodo.11186503)) (167)

In sub-sections (i)-(iv) below, simulation and power analysis methods for a single data set are illustrated. Sub-sections (v)-(vii) show how to simulate multiple datasets and estimate power based on experimental scenarios and parameter choices in Table 2.1. The data sets were simulated under the assumption that the alternative hypothesis (H1) is true, i.e., the intervention effect is not zero (excluding scenarios when 0% effect was simulated). Some of the parameters e.g., *n.ch.per.trt* and *lambda* (Table 2.1) were chosen based on my knowledge/experience and per communication with other scientists. Other parameters e.g., *chamber.var* were estimated using the data from the previous SFE in Ng’habi et al (2018) (165).

The total number of chambers per treatment, *n.ch.per.trt*, indicates how many chambers known as “replicates” are present per treatment. In the R code below, varying SFE design choices were set and simulated either single or multiple data sets based on the assigned design choices followed by fitting the GLMM model to the simulated data. After GLMM model fitting, power estimation is performed by calculating a proportion of the simulated data set whose p-values are less than 0.05. The tutorial was implemented in R version 4.2.3 (168) using multiple libraries

including *ggplot2* (169) for producing plots, *lme4* for fitting GLMMs (166), and *dplyr* for data manipulations (170).

- i) The setting of experimental design scenarios and parameter choices in R

```
# design choices
n.ch.per.trt <- 4 # number of chambers per treatment
itn.lev <- 0:1 # ITN levels: 0 means no ITN and 1 means there is ITN
# make template data set representing design
dat <- expand.grid(replicates = 1:n.ch.per.trt, itn = itn.lev)
# create chambers/replicates id
dat$chamber <- factor(paste(dat$itn, dat$replicates, sep="-"))
# rearranging data set in a useful order
dat <- dat[, c("replicates", "itn", "chamber")]
dat

##   replicates itn chamber
## 1         1  0    0-1
## 2         2  0    0-2
## 3         3  0    0-3
## 4         4  0    0-4
## 5         1  1    1-1
## 6         2  1    1-2
## 7         3  1    1-3
## 8         4  1    1-4
```

Assign values for all parameters for fixed and random effects:

```
# parameter choices - fixed effects
# mean recaptured mosquito count in the control group
lambda <- 50
# proportion remaining in ITN chambers relative to control chambers
itn.effect <- 0.2 # this corresponds to 80% mortality from ITN
# assign chamber variance
chamber.var <- 0.1807
```

Calculate additive coefficients for fixed effect parameters by applying the log link function to the multiplicative effect of an intervention (i.e., $\log(0.2)$ for ITN).

```
# coefficients (parameter values) for all terms
b.0 <- log(lambda)
b.i <- log(itn.effect)
```

- ii) Simulation of a single data set.

After setting experimental design scenarios and parameter choices, the inter-chamber variance, a single data set can now be simulated. Using the simulated linear predictor (sum of terms which include coefficients e.g., β_0 as an intercept

and β_I as a slope with its associated explanatory variable), expected mosquito counts will then be generated using a Poisson distribution.

```
# simulate random effect variance per chamber
chamber.re <- rnorm(nlevels(dat$chamber), sd = sqrt(chamber.var))
names(chamber.re) <- levels(dat$chamber)
# simulate linear predictor (with fixed effects only)
# and add it to the dataset "dat" as a column named lin.pred
dat$lin.pred.fixed <- b.0 + b.i * dat$itn
# add random effects (chamber.re) to the linear predictor
dat$lin.pred <-
  dat$lin.pred.fixed + chamber.re[as.character(dat$chamber)]
# generate mosquito counts from a Poisson distribution
dat$mosquito.count <- rpois(nrow(dat), exp(dat$lin.pred))
# output the new data table "dat"
dat
## replicates itn chamber lin.pred.fixed lin.pred mosquito.count
## 1      1 0 0-1      3.91  3.97      66
## 2      2 0 0-2      3.91  3.87      50
## 3      3 0 0-3      3.91  3.37      38
## 4      4 0 0-4      3.91  3.72      34
## 5      1 1 1-1      2.30  3.03      19
## 6      2 1 1-2      2.30  2.22      12
## 7      3 1 1-3      2.30  1.67      10
## 8      4 1 1-4      2.30  2.11      12
```

- iii) Perform a statistical test for a simulated data set to calculate the p-value.

Fitting to the simulated data in “dat” the GLMM model using the *glmer* function. The model named “model.itn“ will incorporate a response variable which is the expected mosquito counts denoted by “mosquito.count”, a fixed effect for a single intervention (i.e., ITN alone) and a random effect between chambers. From the model summary, the p-value is extracted using the *coef()* function.

```
# load the lme4 package to fit the model
library(lme4)
# outputting the parameter estimates and the p-values
model.itn <- glmer(mosquito.count ~ itn+(1 | chamber), family="poisson", data=dat)
p <- coef(summary(model.itn))[2, "Pr(>|z|)"]
p
## 3.327833e-07
```

In this example, the p-value was 3.3×10^{-7} , which is less than 0.05, therefore a significant intervention effect was detected.

- iv) Power estimation for a single data set

In sub-sections (i-iii), an illustration of how to simulate and calculate a p-value for a single data was provided. Since power cannot be estimated from a single simulation, there is a need to simulate multiple data sets as shown in subsequent sections (v-vii).

v) Simulation of the multiple data sets.

A function called “sim.dat.fun” was created to automate the simulation process described in subsection (ii) above. The “sim.dat.fun” function takes a design table “dat”, coefficients “b.0” and “b.i” and inter-chamber variance “chamber.var” as input parameters. The function then produces a table “dat” containing mosquito counts as an output.

```
# function for simulating the data
# assign a function to simulate data as sim.dat.fun
# beginning of the function "sim.dat.fun"
sim.dat.fun <- function(dat,b.0,b.i,chamber.var){
  # simulate random effects for chambers
  chamber.re <- rnorm(nlevels(dat$chamber), sd = sqrt(chamber.var))
  names(chamber.re) <- levels(dat$chamber)
  # simulate linear predictor (with fixed effects only)
  # add the simulated data to dataset "dat" as a column named lin.pred
  dat$lin.pred.fixed <- b.0 + b.i * dat$itn
  # add random effect (chamber.re) to fixed linear predictors above
  dat$lin.pred <-
    dat$lin.pred.fixed + chamber.re[as.character(dat$chamber)]
  # generate mosquitoes counts as random data using Poisson
  dat$mosquito.count <-
    rpois(nrow(dat),exp(dat$lin.pred))
  # output the new data table "dat"
  dat
} # end of data simulation function "sim.dat.fun"

# assign the function output as simdat for easy referencing
simdat <- sim.dat.fun(dat,b.0,b.i,chamber.var)
# output the "simdat"
simdat
## replicates itn chamber lin.pred.fixed lin.pred mosquito.count
## 1      1 0 0-1      3.91 3.91      43
## 2      2 0 0-2      3.91 3.62      45
## 3      3 0 0-3      3.91 3.46      26
## 4      4 0 0-4      3.91 3.66      47
## 5      1 1 1-1      2.30 2.55      16
## 6      2 1 1-2      2.30 1.87      5
## 7      3 1 1-3      2.30 2.71      19
## 8      4 1 1-4      2.30 2.94      17
```

vi) Perform a statistical test for the simulated data sets to extract p-values.

In this case, a function called “sim.mos.pval” was created to automate the function “sim.dat.fun” and outputs p-values. The function “sim.mos.pval” will output the p-values from the GLMM model with a Poisson distribution. The fitted model denoted by “model.itn” will incorporate a response variable which is the expected mosquito counts denoted by “mosquito.count”, fixed effects which are ITN, and random effect between chambers.

```
# output the p-values
sim.mos.pval <- function(...){
  simdat2 <- sim.dat.fun(dat,b.0,b.i,chamber.var, theta)
  model.itn <- glmer(mosquito.count ~ itn+(1 | chamber),family="poisson",data=simdat
2)
  p <- coef(summary(model.itn))[2, "Pr(>|z|)"]
  c(p = p)
}
```

vii) Power estimation for multiple data sets

Here, a function “sim.pvals.list” was created to output power estimate by updating function “sim.mos.pval” multiple times based on the number of simulations “nsim” provided. Again, another function called “sim.pvals.list” was created to output a list of p-values by automating the function “sim.mos.pval” to simulate multiple data sets based on the number of simulations “nsim” assigned. Therefore, the percentage of the data sets whose p-values are less than 0.05 is the power estimate.

```
nsim <- 100
sim.pvals.list <-
  lapply(1:nsim, sim.mos.pval)
sim.pvals <- do.call("rbind", sim.pvals.list)
# estimate power as a proportion of datasets whose p-values p< 0.05.
n.sig <- sum(sim.pvals[, "p"] < 0.05)
power.estimate <- n.sig/nsim
# output power estimate
power.estimate
## [1] 0.96
```

For the simulations reported in the results sections, the power analysis methods illustrated in the tutorial above were used and expanded to estimate power for all combinations of scenarios, short- vs. long-term SFE and single vs. combined interventions. To promote reproducibility, the R codes used to produce the results and R tutorials for other SFE scenarios are freely available as R Markdown files for access on an online repository (see doi: [10.5281/zenodo.11186503](https://doi.org/10.5281/zenodo.11186503)) (167). Some of the parameter values were extracted using mesocosm experimental data from the previous study (see doi: <https://doi.org/10.1038/s41598-018-31805-8>) (165).

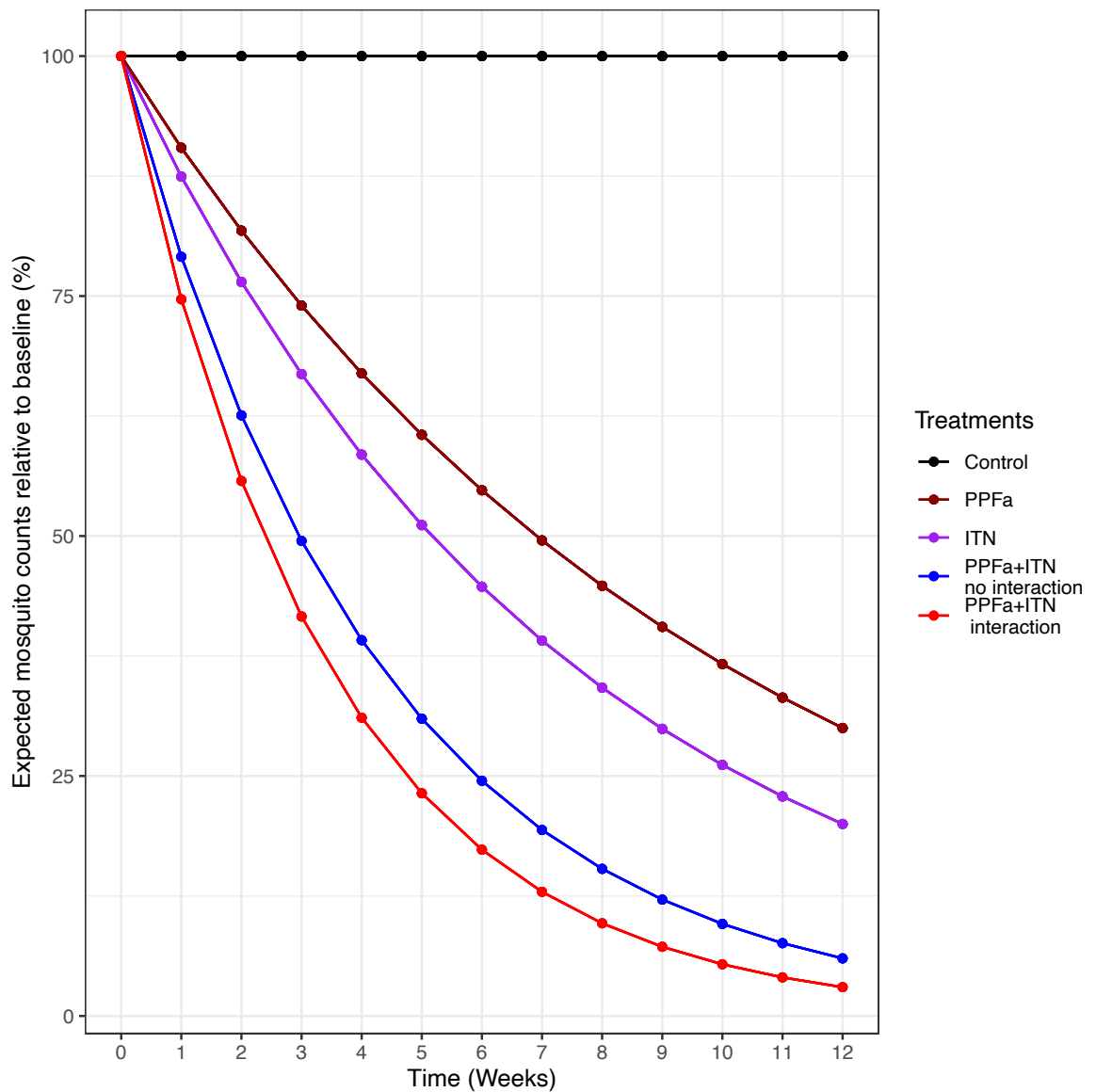


Figure 2.2: Change in expected mosquito counts over 3 months (12 weeks), comparing the use of ITN and PPFa interventions in a semi-field experiment, showing how much faster the number of mosquitoes is reduced in the chambers combining both ITN and PPFa with (red) and without (blue) interaction than would be expected based on the single effects of PPFa (dark red) and ITN (purple) or no intervention (black).

2.2.6 Type I error rate

Before reporting power estimates using GLMMs, it is recommended to check whether the estimated type I error rate (i.e. estimated power at zero effect size; Figure 2.3, dot-dashed lines) is equal to the nominal type I error rate, which here is 5%. Checking type I error rate estimates is useful for identifying inflated power estimates and more generally for identifying scenarios where GLMMs are unreliable. In our case study, some of the power estimates were inflated, particularly when the number of chambers per treatment was 2. For example, the type I error rate was 15% when there were 2 chambers per treatment for short-term SFEs (Figure 2.3a, c). However, the estimated type I error rates were less

severe (slightly inflated) in long-term SFEs at less than 8% (Figure 2.4). Type I error rate estimates across all scenarios were averaged at 8%, 3% higher than the nominal type I error rate (Figure 2.3 & Figure 2.4). Generally, the type I error rate was more inflated in short-term SFEs with scenarios that involve fewer than 6 chambers per treatment than in long-term SFEs testing single and combined interventions.

2.3 Results

2.3.1 Short-term experiments testing single and combined interventions

Power increased with increasing number of experimental chambers per treatment and the number of mosquitoes to be recaptured from each experimental chamber (Figure 2.3). Additionally, the target effect size of the interventions also had a large impact on power in each scenario. Power increased initially with recaptured mosquitoes, then plateaued for single interventions with around 50 mosquitoes, and combined interventions with around 80 mosquitoes (Figure 2.3a and b). Power was 87% at four chambers per treatment, 50 mosquitoes recaptured and 60% reduction in mosquito population (Figure 2.3a, blue solid line). A minimum of 10 mosquitoes would need to be recaptured in each treatment chamber to ensure at least 80% power assuming that the only interest is to detect effects at least as large as an 80% reduction in mosquito density (Figure 2.3b).

The higher the targeted interaction effect size, the higher the power of the experimental design. However, within target interaction effect sizes (Figure 2.3c and d), although there was an increase in power with an increasing number of chambers per treatment, adequate (> 80%) power could only be achieved at the highest interaction effect size (i.e., > 80% reduction) with a minimum of 6 chambers per treatment (Figure 2.3c). If a target interaction effect size results in a 60% or less reduction, none of the scenarios was sufficient to give enough power to detect the smallest effect of the intervention (Figure 2.3c). With four chambers per treatment, only designs recapturing at least 90 mosquitoes with a target interaction effect size of an 80% reduction in the mosquito population provided adequate power (Figure 2.3c). The increase in power above 80% at a minimum of 6 chambers per treatment and high target interaction effect size indicates the necessity for the SFE studies to consider the use of a large number of treatment

chambers (at least 4 and preferably 6 chambers) to ensure that the target treatment effects are detected. By comparing the results in Figure 2.3, testing a single intervention would require fewer chambers than would be required when testing combined interventions i.e., the increase in the number of interventions increases the number of chambers to be used per treatment. It should also be noted that designs with four or fewer chambers gave the most inflated type I error rates, suggesting that even the low levels of power achieved in these scenarios are likely to be inflated.

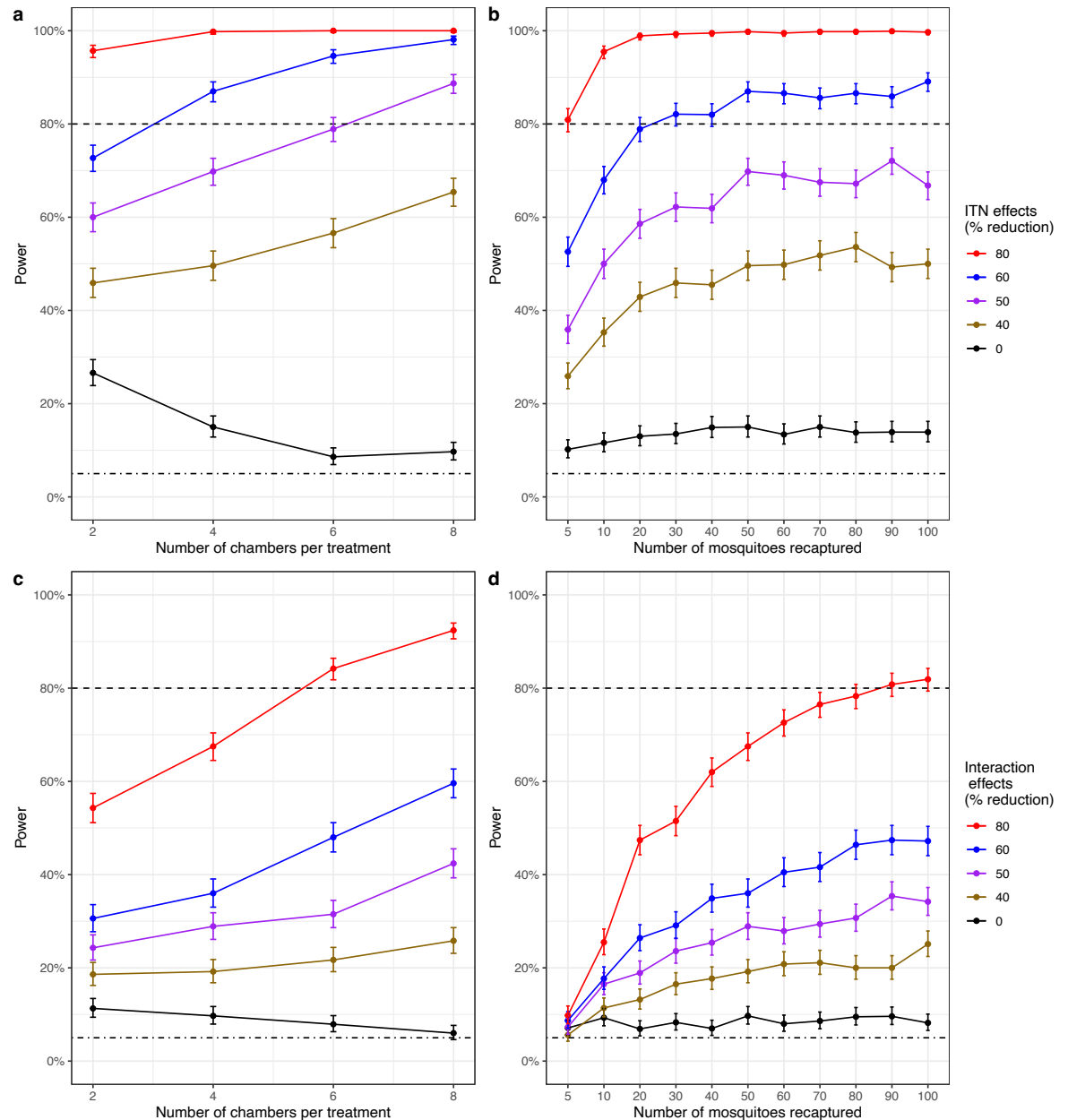


Figure 2.3: Statistical power obtained from different short-term SFE designs. Top panels (a and b) show the power expected when testing single interventions (ITN) and bottom panels (c and d) when testing combined interventions (ITN and PPFa) with increasing (a and c) number of chambers per treatment or (b and d) number of mosquitoes recaptured. Different coloured lines correspond to varying effects or interaction sizes, i.e., % reduction in mosquito population. The dashed line is 80% power, and the dot-dashed line shows a 5% power which is a type I error rate, which is the expected power when the effect size is zero. Error bars show

95% confidence intervals. Estimated variance (EV) was used in both (a-d) while 50 mosquitoes were used in (a) and (c), and 4 chambers per treatment in (b) and (d).

2.3.2 Long-term experiments testing single and combined interventions

Power was higher with more chambers, increased sampling frequency, and a higher number of mosquitoes to be sampled per chamber (Figure 2.4). Enough power was achieved at a minimum of 4 chambers per treatment (Figure 2.4a), weekly sampling (Figure 2.4b), and 10 mosquitoes to be sampled per week (Figure 2.4c) with only a 60% reduction in mosquito population by ITN. More than 90% power was achieved at 4 chambers per treatment (Figure 2.4d), weekly sampling (Figure 2.4e), and 10 mosquitoes to be sampled per week (Figure 2.4f) with an 80% reduction in population by ITN and PPFa interaction. The higher the ITN and PPFa interaction effect, the power of the experimental study was higher with the increased number of chambers per treatment, sampling frequency and mosquitoes to be sampled. 100% power was attained at the highest interaction effect (i.e., 80% reduction in mosquito population) by maximising either the number of chambers, sampling frequency, or the number of mosquitoes sampled (Figure 2.4d-f).

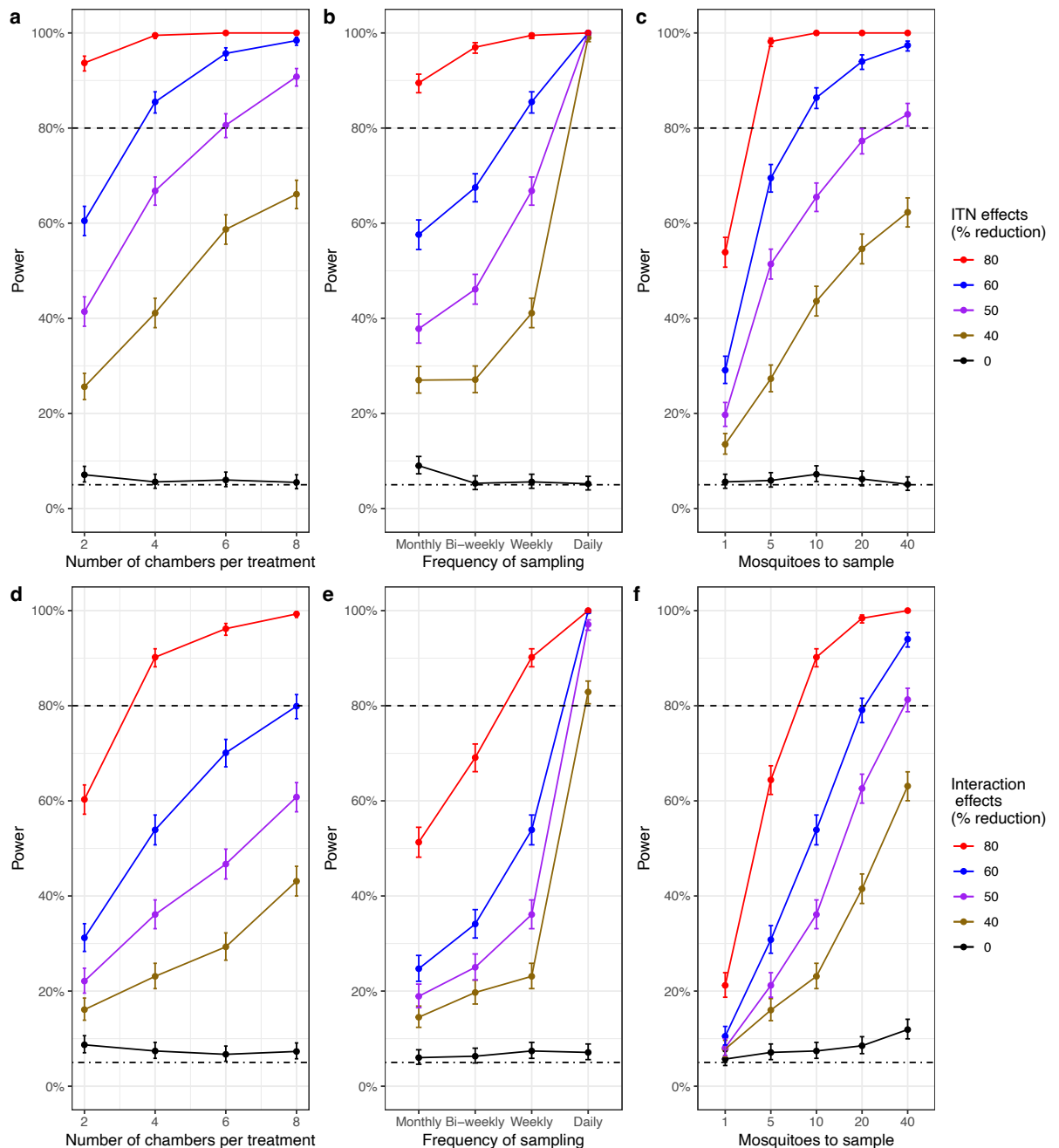


Figure 2.4: Statistical power obtained from different long-term SFE designs. Top panels (a, b and c) show the power expected when testing single interventions (ITN) and bottom panels (d, e and f) when testing combined interventions (ITN and PPFa; d, e and f) with increasing (a and d) number of chambers per treatment or (b and e) frequency of sampling or (c and f) number of mosquitoes to sample. Different coloured lines correspond to varying effects or intervention sizes, i.e., % reduction in mosquito population. The dashed line is 80% power and the dot-dashed shows 5% power which is a type I error rate, which is the expected power when the effect size is zero. Error bars show 95% confidence intervals. Estimated variance (EV) was used in both (a-f). A total of 10 mosquitoes and weekly sampling were used in (a) and (d), four chambers per treatment and 10 mosquitoes in (b) and (e), and four chambers per treatment and weekly sampling in (c) and (f). The main effects used for ITN and PPFa in (d-f) are 80% and 70%, respectively.

2.3.3 Inter-chamber variance affects power

The estimated type I error rate was 8% (i.e., 3% higher), except for when there were only 2 chambers per treatment for a short-term semi-field experiment (SFE)

testing combined interventions, which had a type I error rate $>9\%$. For the short-term SFE testing both single and combined interventions, the more variation between the treatment chambers the less power there was (Figure 2.5, dotted and dash-dotted red lines). In contrast, for the long-term SFE testing both single and combined interventions, different inter-chamber variances resulted in closely related power estimates. For estimated variance (EV, which corresponds to the red line in Figure 2.3c), power was 68.5% when 4 chambers per treatment were used and 50 mosquitoes recaptured, which increased to 84% and 91% at 6 and 8 chambers per treatment, respectively (Figure 2.5, solid red line). When the inter-chamber variance was halved to $EV/2$, 79% power was attained at only 4 chambers per treatment, but then increased to 90% and 97% at 6 and 8 chambers per treatment, respectively (Figure 2.5, dashed red line). In contrast, when inter-chamber variance was doubled to $EV \times 2$, power was 59.5%, 70.5% and 82% at 4, 6 and 8 chambers per treatment, respectively (Figure 2.5, dotted red line). Additionally, a fivefold increase in inter-chamber variance lowered power to below 60% irrespective of the used number of chambers per treatment (Figure 2.5, dash-dotted red line).

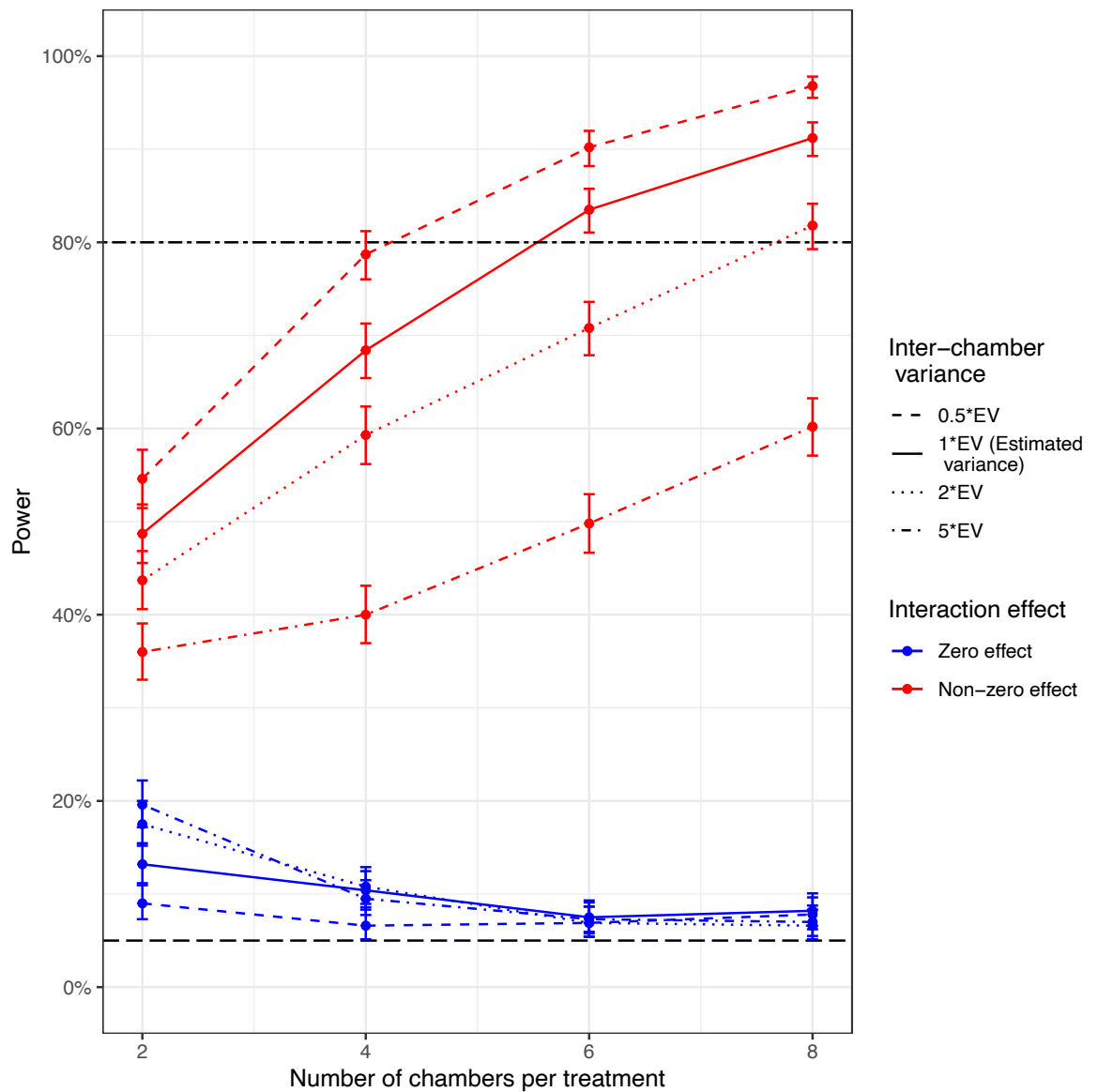


Figure 2.5: The effect of varying inter-chamber variance on the relationship between power and the number of chambers per treatment. Inter-chamber variance was varied from the estimated variance of 0.1807 (EV, solid line which corresponds to a red line in Figure 2.3c) to half (dashed line), double (dotted), and quintuple (dash-dotted line) its original value. Error bars show 95% confidence intervals. The red colour represents the target non-zero interaction effect (80% was used here) and the blue colour type I error rate (0% interaction effect). The two-dashed line is the 80% power, and the long-dashed line (black colour) is the nominal type I error rate of 5%. In this case, a total of 50 recaptured mosquitoes were used and the main effects explored for ITN and PPFa were 80% and 70%, respectively.

2.4 Discussion

This study provided guidance and a tool to empower semi-field experiment (SFE) researchers to explore the relationship between design choices and predicted power. It investigated the impact on power of varying the number of experimental chambers, the number of mosquitoes recaptured in the control (as a proxy for the

number released), the frequency of sampling adult mosquitoes, the amount of variation between chambers, and the size of the target intervention effect.

Before reporting simulation-based power estimates using GLMMs, it is beneficial to check whether the estimated type I error (i.e., false positive) rate is correct. Type I error rates, which are equivalent to estimated power at zero effect size, were inflated ($> 5\%$) for all experimental designs, suggesting that Wald z-tests from GLMMs fitted using maximum likelihood give inflated type I error rates. In our study, type I error rate inflation was particularly severe ($> 8\%$) for designs with fewer chambers per treatment (≤ 4), due to severely biased p-values generated from Wald z-tests. For a single analysis, this inflation problem can be resolved by adjusting p-values, for example using the function *simulateLRT* in the *DHARMA* R package which performs simulated likelihood ratio tests for GLMMs based on the parametric bootstrap (171,172). However, such simulation-based methods are too slow to be feasible as part of simulation-based power analysis. Therefore, in addition to identifying scenarios where power is likely to be over-estimated, estimating the type I error rate can also alert researchers to scenarios that generate potentially unreliable results from GLMMs, without this knowledge they might publish false positive results. On the other hand, simulation-based power analysis methods can be quite computationally intensive, especially when using standard computers such as laptops. However, there are potential effective strategies to alleviate these demands; two of the most commonly used methods include the use of computing clusters to distribute the workload across multiple processors and the use of cloud computing services where instead of running simulations directly on your personal computer, you run them on virtual computers as they can be accessed remotely (173).

One of the main findings of this study was that for most realistic SFE designs, the power estimate was below the conventional threshold for acceptability of 80%, except for experimental scenarios with an extremely large target effect size. That is to say, for the experimental scenarios covered in this study, current SFEs seem to be underpowered for more realistic effect sizes. It is perhaps one of the general limitations of SFE that unless we build a large-scale semi-field system with five or ten times as many chambers or, more realistically, repeat the experiment multiple times with rotated (e.g., using a Latin square design) or randomised chambers per treatment (which would effectively double or multiply the number of chambers),

it will be difficult to be able to detect anything less than very large effects. The power analysis framework presented here is intended to give SFE researchers the tools to decide how large a semi-field system would need to be, or how many repetitions of the experiment would be required, for a particular effect size of a given intervention.

Power was expected to increase with more chambers, more mosquitoes, higher sampling frequency and lower inter-chamber variation, but the relative importance of these factors in a range of realistic SFE scenarios was unknown. In this study, a realistic SFE required a minimum of 4 chambers to detect single (non-interaction) effects but may be underpowered for effects below a 40% reduction. To obtain adequate power and maintain an acceptable type I error rate, a minimum of 4 and preferably 6 chambers per treatment was required to detect higher interaction effects (i.e., $\geq 80\%$ reduction), suggesting that using designs with fewer chambers would have resulted in an underpowered study for lower effects. In general, we found that two chambers per treatment are too few and insufficient to ensure the detection of the interaction effect between PPFa and ITN. However, several ways may help increase the number of chambers per treatment, that do not involve building a large-scale semi-field system or repeating the experiment multiple times (71). For example, one may consider whether both single interventions are needed in the same experiment and potentially exclude the negative control.

Human Landing Catch (HLC) is one of the standard methods for sampling adult mosquitoes, however, it demands a lot of effort in terms of time, money, and logistics such as a trained supervisory team and supplies at the collection sites (174). Therefore, the selection of sampling frequency involves a balance between statistical power and the amount of resources to be invested in an experimental study, and our study illustrated how this balance point could be found. Although without providing scientific reasons, most studies with SFE consider weekly or bi-weekly sampling of mosquitoes (175). Results from this study indicated power increases as sampling frequency increases from monthly to daily. Under our study scenarios, bi-weekly sampling did not improve power substantially compared to monthly sampling, although even this small increase could bring borderline designs above 80% power.

It is difficult to obtain enough mosquitoes for use in the SFEs because of the high operational cost of rearing them in insectaries. Additionally, other species such *An. funestus* is even more challenging to maintain in insectary settings, making it hard to establish laboratory colonies (88). Due to its importance, researchers need to determine the number of mosquitoes they are supposed to use for SFEs, which will provide them with successful and informative experiments. Since there is no standard way to identify the total number of mosquitoes to be released, especially in long-term experiments, understanding the expected number of mosquitoes to be recaptured can be a good proxy to help determine how many mosquitoes should be released to maximize the power of the study. In a recent semi-field study by Mbuba *et al.* (176) in Tanzania aimed to evaluate two topical repellents against *Anopheles* mosquitoes, a total of 25 mosquitoes were released in each of the three treatment chambers, and the experiment was repeated if fewer than 50% of the released mosquitoes were recaptured in the negative control (176). Our findings indicated that recapturing 50 mosquitoes in six chambers per treatment achieved adequate power (> 80%) to detect an effect size of 50% reduction in mosquito abundance. Increasing variation between chambers in the mean number of mosquitoes recaptured resulted in lower power in the short-term SFEs and reducing inter-chamber variation increased power. In contrast, for the long-term SFEs, different inter-chamber variances resulted in similar power estimates. It is suggested that conditions should be kept as similar as possible across all treatment chambers, which can be done, for example, by rotating volunteers who capture mosquitoes or hosts for mosquitoes' blood meals.

While the power analysis methods presented here provide valuable insights into optimising SFE design, they also have limitations. The framework relies on simulation-based power analysis with GLMM-fitting methods, which have higher computational demands than traditional power analysis methods. The focus of this study was to develop a statistical power analysis framework and produce an R tutorial to assist in the design of robust vector control experiments in semi-field systems. Results for two specific scenarios are shown, but these can be easily adapted and extended to other intervention scenarios including long-term SFE with non-dynamic effects, or effects changing over time. As we adapted the framework from a Poisson to a Negative binomial model for the long-term experiment, other adaptations might be required. For example, a binomial model might be preferred in the presence of high variability in the recaptured mosquitoes

(e.g., associated with chamber variance) or high recapture rates as we would expect larger numbers of mosquitoes. Alternatively, a multinomial model could be a good option for complex dependencies between modes of action (177,178) such as having number of mosquitoes in various categories such as alive unfed, alive fed, dead unfed and dead fed. In addition, this framework could be used for other widely used experimental systems such as hut trials, where instead of chambers, outdoor experimental huts are used. The uptake of power analysis methods will improve the quality of SFE and as a consequence provide a more robust evaluation of the impacts of new vector control interventions on mosquito populations. Future research directions may include adapting the framework to different vector control experimental scenarios or exploring alternative SFS experimental designs. Additionally, future work may focus on expanding this work to a web-based application such as an R shiny application and R packages for an interactive power analysis framework.

2.5 Conclusion

Determining the most efficient experimental design for a semi-field experiment (SFE) will depend on a balance of design choices and resource constraints. The power analysis framework and tutorial provided here can aid researchers in the robust design of these widely used experiments and ultimately facilitate the development of new vector control tools. Due to its flexibility, this generic power analysis framework can be customised and adapted to inform designs of other vector control SFEs and experimental hut trials. The statistical power analysis framework presented here has already been successfully applied to inform the design of a vector control SFE in one of the semi-field systems at Ifakara, Tanzania.

Chapter 3 Implications of the trade-offs between negative density dependence and the Allee effect for the malaria vector control endgame

Abstract

Understanding the interplay between vector control and malaria mosquito population dynamics is critical to assessing and improving vector controls. Mosquito populations are regulated through a range of biotic and abiotic mechanisms, and among them, negative density dependence, where small populations grow more rapidly than large ones, is thought to be widespread. However, a positive density dependence at low population density, also known as the Allee effect where small populations die more rapidly, is also possible. Understanding the extent to which the Allee effect impacts mosquito populations is critical to predicting whether populations pushed close to extinction by interventions such as larvicide application will rebound or die out. Here, a stochastic simulation model based on a stage-structured population model was developed to investigate the roles of negative density dependence and the Allee effect, their impacts on the efficacy of sustained and short-termed larvicidal intervention, and their trade-offs in regulating mosquito populations. The model followed the stages of the mosquito life cycle, with life-history traits namely fecundity and larval, pupal, and adult survival defined as a function of density, larviciding, environmental variables and importantly the Allee effect. Negative density dependence was modelled as a modifier of larval survival and the Allee effect as a modifier of total fecundity. The model was iterated 100 times and calculated the quantiles of the key output measure, weekly adult mosquito abundance. While in isolation, varying density dependence and the Allee effect did not impact the population size in the long term, their combination seemed to accelerate population extinction. A combination of negative density dependence, the Allee effect, and sustained larvicidal intervention led to a decline in mosquito populations to levels from which they could not recover. In contrast, the combination of negative density dependence and the Allee effect, along with short-term larvicidal applications, did not result in a decline in mosquito populations to lower levels that would prevent rebound. Higher levels of the Allee effect, along with mid-level negative density dependence, led to a decline in the populations, and the risk of extinction increased as the duration of the

intervention increased. Understanding less studied regulatory processes like Allee effects can support vector control by highlighting both resilient and vulnerable aspects of the vector's life cycle stages to interventions. If present, we can potentially harness Allee effects to accelerate malaria elimination.

3.1 Introduction

Vector control remains one of the most efficient strategies against malaria (35,179). Implicitly, vector control reduces mosquito population sizes but maintaining the populations under control and even eliminating them remains challenging. A major reason is that as mosquito populations become smaller, a range of ecological changes, such as alterations in their per capita growth rate are likely to occur (180). These fluctuations in population size can occur naturally e.g., large seasonal fluctuations with the wet season or less pronounced and shorter-term fluctuations with changes in temperature or rainfall patterns (181), but understanding the population regulatory mechanisms triggered by vector control when populations become smaller can provide useful insight into how these mechanisms might impede or facilitate malaria elimination. Malaria vector control interventions might become proportionately less effective at low mosquito population density because the surviving individuals have a much higher per capita reproduction or growth rate than those in high densities. Settings with small mosquito population densities (e.g., Dar es Salaam and Zanzibar, Tanzania) reported a low level of persistent malaria transmission despite the effects of core and supplementary interventions. For instance, a large-scale larvicidal control in Dar es Salaam, Tanzania, led to a decline in the *Anopheles gambiae* mosquito population which typically prefer small and temporary breeding habitats, but there was still residual malaria (41,47). In Zanzibar, Tanzania, despite 77.8% of households having at least one insecticide-treated net (ITN), which is a core vector control intervention in the area (40), malaria transmission persisted but at low levels (184). With the use of key interventions, namely ITNs and Indoor residual spraying (IRS), mosquito populations are declining (2), but are difficult to knock down further or eliminate, allowing malaria to persist at low levels.

Mosquito populations seem to be density-dependent at the larval stages (90), meaning that the per capita growth rate is fastest when density is low (Figure 3.1, black line). Laboratory experiments with *Anopheles gambiae* showed that competition for resources at the larval stage is the major source of negative density dependence (90). With less space (e.g., small water pools) competition between larvae increases, which leads to larval population decline, and in turn, releases some space again to accommodate more larvae allowing the population to recover again. Consequently, an intervention might become proportionately

less effective as a population declines because surviving individuals have a higher per capita growth rate compared to those in high density. However, an opposing scenario is also possible, where small mosquito populations experience Allee effects, i.e., population growth rate reduces as the population declines (Figure 3.1, blue and red lines) (120). Allee effects arise from factors such as difficulty in finding a mate, limited cooperative behaviours, inbreeding and risk of predation, resulting in a higher risk of stochastic extinction as populations become smaller (89,97), and may operate at low or high levels. At low levels (corresponding to weak Allee effects), the per capita population growth reduces but remains positive (blue colour in Figure 3.1). In contrast, with higher levels of Allee effects, where the population growth rate falls below the threshold (critical population size) leading to extinction (185), the per capita population growth rate is negative and therefore the population is decreasing (Figure 3.1, red colour).

The occurrence and relative importance of density dependence and Allee effects have been demonstrated in various animals, grouped by taxonomic categories such as fish, reptiles, birds, mammals and insects, as well as in plant systems (186,187). For instance, for a new plant population, the presence of few plants impedes the transfer of conspecific pollen to extend the generation. The failure to transfer pollen when the total number of founder individual plants is not large enough to attract pollinators to regularly service plants growing close to them may result in the extinction of the new population (188,189). Allee effects have also been identified in vertebrates, where goldfish population size was observed to increase faster due to cooperation when several goldfish were placed in a water tank containing other goldfish (190). Similarly, experiments in mammals including deer mice and red-backed voles have demonstrated that high population size may stimulate reproduction, guarantee their survival, and increase protection against toxic reagents or predators, as opposed to low population size where reproduction was suppressed (191,192). Studies of Allee effects in insects are sparser, but sexually reproducing insects such as *Callosobruchus chinensis* and *Tribolium confusum* showed that difficulty in finding mates is the primary mechanism affecting their population dynamics at low population density, which led to population extinction (193). Potential mechanisms for Allee effects identified in invertebrate insects such as gypsy moth populations are difficulty in locating mates and risk of predation (113,194-197). Importantly, Allee effects have played a role in the control of biological invasions through the establishment and spread

of non-native species. The control of biological invasions has often been possible by limiting the mating of biological invaders such as invasive flies, *Philornis downsi*, or red turpentine beetle, *Dendroctonus valens*, (97,198). It is important to understand biotic traits like density dependence and Allee effects that act on small populations and have the capacity to allow population persistence or extinction.

There is currently no evidence from the field or laboratory experiments on the impacts of the Allee effects on malaria mosquitoes or any other vectors. However, previous modelling work predicted that gene drive would be more effective if a strong Allee effect exists in a low-density mosquito population where transgenic mosquitoes are released (199-203). Although the role of Allee effects in malaria vector population dynamics remains unknown, understanding how they might contribute to population regulation is critical for assessing vector control strategies, given their opposing implications for vector suppression and elimination plans. This study aimed to develop a stochastic simulation model based on a stage-structured population model to address the four research questions: (i) how is the mosquito population growth rate regulated over time? (ii) what are the roles of negative density dependence and the Allee effect in regulating mosquito populations at low densities? (iii) how do negative density dependence and the Allee effect impact the efficacy of the vector control interventions? and (iv) what are the trade-offs between density negative dependence and the Allee effect in regulating mosquito populations? Understanding the extent to which Allee effects might impact mosquito populations is critical to predicting whether populations can be pushed to extinction by interventions or if they will rebound. Simulations are useful because they allow us to explore a range of scenarios and identify which might be important to enhance our understanding of mosquito ecology to better design, assess and optimize vector controls.

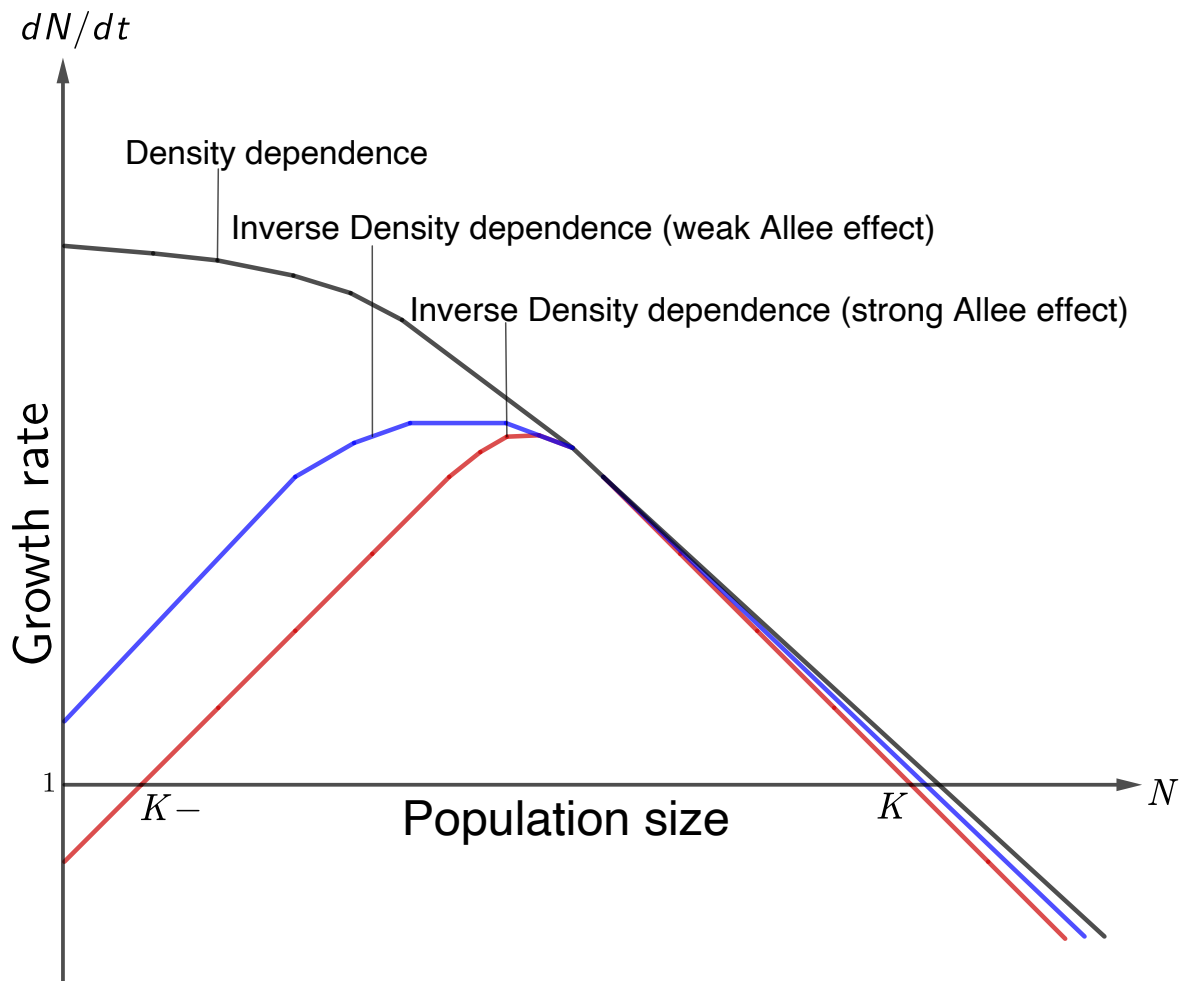


Figure 3.1: Low-density population dynamics. The population growth rate is less than 1 above the carrying capacity K and below the critical population threshold K_- . A black line indicates negative density dependence, whereas a blue and red line indicates positive density dependence (i.e., weak, and strong Allee effects, respectively).

3.2 Methods

To address the specific research questions, a stochastic simulation model was developed based on a stage-structured population model. Since the Allee and negative density dependence effects are expected to be most relevant when mosquito populations are low, the model emulated the study design of a large-scale larvicidal intervention in urban Dar es Salaam, Tanzania, which was shown to have reduced mosquito population size by 94.4%. From the population model, the Leslie matrix was also developed to explore the growth rate of a stable population as regulated by negative density dependence and the Allee effect.

3.2.1 Study design

Larvicide in urban Dar es Salaam (41) targeted 15 (out of 73) wards from 3 municipalities (5 wards each) and was deployed in three different phases (time periods) for 193 weeks from early 2005 to late 2008. In phase one, only three wards received a larvicidal treatment; in the second phase another 6 wards were added and in the last phase, the intervention was scaled up to cover all 15 wards. The type and amount of larvicides applied and intervention durations are described elsewhere (41,47,204). The dynamics generated in the simulation model are similar to the data from the larvicidal intervention in Dar es Salaam (as shown in Appendix B.1). Daily rainfall and temperature data from 2005-2008 were obtained from an open-source repository called Soil and Water Assessment Tool (SWAT) (205) and aggregated to mean weekly data (as shown in Appendix B.2, Appendix B.3 and Appendix C.5) to match the time unit in the model (for further details see section 3.2.2, Appendix B.2, Appendix B.3 and Appendix C.5). Since the rainfall and temperature data are not specific for each ward, it was assumed that the mean weekly rainfall and temperature in all fifteen wards from the three municipalities of urban Dar es Salaam were the same.

3.2.2 Stage-structured population model formulation

A simulation model was developed based on a stage-structured population model. The model follows a simplified mosquito life cycle with adult female mosquitoes laying eggs that hatch into early instars that develop into late instars. Late instars develop into pupae which later emerge as adult mosquitoes. Each of these stages is then linked through or impacted by rates or probabilities such as fecundity, larvae, pupae or adult survival and development (Figure 3.2).

Figure 3.2 illustrates the model, which is mathematically defined as follows: it is assumed that the larval (i.e., early instars, $N_{l,1}$, and late instars, $N_{l,2}$) survival probabilities, ρ_x (where x are either early instar larvae, $l, 1$, or late instar larvae, $l, 2$), are defined by binomial distributions, with linearised functions S_x , at ward i , and week t , through an inverse logit transformations such that,

$$\rho_x(i, t) = \frac{\exp(S_x(i, t))}{1 + \exp(S_x(i, t))}$$

Survival probability of early instars, $\rho_{l,1}$, was defined through an inverse logit transformation of linear function $S_{l,1}$, described as a function of the number of total larval abundance ($N_{l,1}+N_{l,2}$), rainfall (R), larvicides (LA) and temperature (T) such that:

$$S_{l,1}(i, t) = \beta_0 - \beta_1(1 - \beta_2 R(t))(N_{l,1}(i, t) + N_{l,2}(i, t)) + \beta_3 R(t) - \beta_4 LA(i, t) + \beta_5 T(t). \quad 3.2$$

where β_0 is the mean logit (i.e., log odds) of larval survival when all covariates are 0 (e.g., centred rainfall = 0 mm, larvicide = 0 and centred temperature = 0 °C). The parameters β_{1-2} describe the impact of negative density dependence on early instar larval survival, which is mainly regulated by rainfall and larval density. Specifically, β_1 is the effect size governing the impact of total larval abundance (i.e., $N_{l,1}$ and $N_{l,2}$) on early instar larval survival and here assumed to regulate the magnitude of negative density dependence. β_2 is a fraction of β_6 and β_1 (i.e., β_6 / β_1) where β_6 is the effect of the interaction between larval density and centred rainfall on early instar larval survival. β_3 is the effect of centred rainfall (R) on early instar larval survival. Parameters β_4 and β_5 are the effects of larvicides (LA) and centred temperature (T) on early instar larval survival, respectively. Temperature and rainfall were centred at their mean values of 27 °C and 56 mm respectively. That is, their means were subtracted so that each centred variable has a mean of zero, such that the intercepts of the survival and fecundity functions can be interpreted as logit survival probability conditional on mean temperature and rainfall.

The survival probability of late instars, $\rho_{l,2}$, was defined through an inverse logit transformation of the linear function $S_{l,2}$, and was structured similarly to Equation 3.1. Explicitly, the late instar linear function was written similar to the linear function of early larval instars (Equation 3.2) (i.e., $S_{l,1} = S_{l,2}$), hence, the parameter descriptions and values in functions $S_{l,1}$ and $S_{l,2}$ were similarly used in this study. Since the larval stage lasts for two weeks, it was divided into two stages, each lasting for one week. Dividing the larval stage into two stages aligns with the model development, which assumes one week for each stage of the mosquito life cycle. Throughout the text, negative density dependence (i.e., β_1) is regarded as a common parameter among the two larval stages.

Survival probability of pupae ρ_p (structured similarly to Equation 3.1) in ward i at week t was defined through an inverse logit transformation of the mean logit pupal survival (λ_0). On the other hand, weekly adult survival probability ρ_a in a ward i at week t was defined through an inverse logit transformation of the mean logit adult survival (α_0); this implicitly assumes that there is exponential survival of adult mosquitoes.

Mosquito fecundity was modelled as a Poisson process with mean b in the ward i and week t and linearised through an exponential transformation with temperature (T) which then regulated by the Allee effect parameter C , such that:

$$b(i, t) = 0.5 * \exp(\omega_0 + \omega_1 T(i, t)) * N_a(i, t) * \frac{Na(i, t)}{C + N_a(i, t)}$$

3.3

where ω_0 is the mean log per capita fecundity when the centred temperature is 0 °C and ω_1 is the weekly effect of temperature on fecundity. The Allee effect is emulated as the probability of mating, where the number of female adults, N_a , is scaled with a constant C . Specifically, the greater the value of C relative to N_a , the lesser the mating probability, leading to high impacts of the Allee effect (e.g., the mating probability will be less than 50% when $N_a < C$ and close to 100% when $N_a \gg C$). It was assumed that eggs do not have their own stage in the model, they are just a transition or a life path of larvae. Eggs hatch into early instar larvae, $N_{l,1}$, to the late instar larvae, $N_{l,2}$, and then to the pupae, N_p , who then become adults, N_a . To obtain the total number of male and female mosquitoes in the population, a 50:50 sex ratio was assumed. To model the female mosquito population only, the total number of mosquito eggs laid per week (total fecundity) was halved where only the proportion, h_e , hatches to early instars. The resultant survival probabilities (Equation 3.1) and the total fecundity (Equation 3.3) were used to obtain population abundances (which were used as one of the main outcomes) for both larvae, pupae and adult mosquitoes. Note that, the survival probability will also incorporate the development rate, meaning that all surviving individuals move to the next stage.

The parameters mentioned in Equations 3.2 and 3.3 were given mean values based on literature, as shown in Table 3.1. The exceptions are the values for the parameters describing the Allee effect (C) and the interaction between negative density dependence and rainfall (β_6), which were given the following values: $C =$

360 (zero value was not included because $C = 0$ did not have an impact on mosquito population dynamics) and $\beta_6 = 1e-06$. The two values 360 and $1e-06$ were chosen because they gave stable population dynamics in the absence of larvicidal intervention. Without intervention, the population stabilised at an average of around 700 female adult mosquitoes. The interaction value $1e-06$ is fixed throughout the simulation, therefore, when mentioning negative density dependence, it will mean the parameter β_1 , throughout the simulation. Similarly, the value for the Allee effect, C , was not informed by the literature, so, initially, its value was set at 360 because it seems to be the neutral value that does not interfere with the population dynamics and was later varied to address specific research questions as explained below in sections 3.2.4, 3.2.5, and 3.2.6. Since one important feature of the Allee effect is its potential increase in stochastic extinction, the model was iterated 100 times and calculated the probability of extinction and the quantiles of the weekly adult mosquito abundances. The model was implemented in R software version 4.3.3 (206) and codes used to produce results is available as supplementary information (see Appendix B.7). In the course of model analysis in R, different initial population sizes for all stages of the mosquito life cycle were used during the analysis. The initial population size for both larval stages was set at 1000 larvae, while for the pupal stage, it was 900 pupae, and for the adult stage, it was 800 mosquitoes. These initial values were chosen based on the effect of negative density dependence (β_1), with a value of $5.5e-05$ (refer to Table 3.1) estimated from an abundance of 1000 larvae.

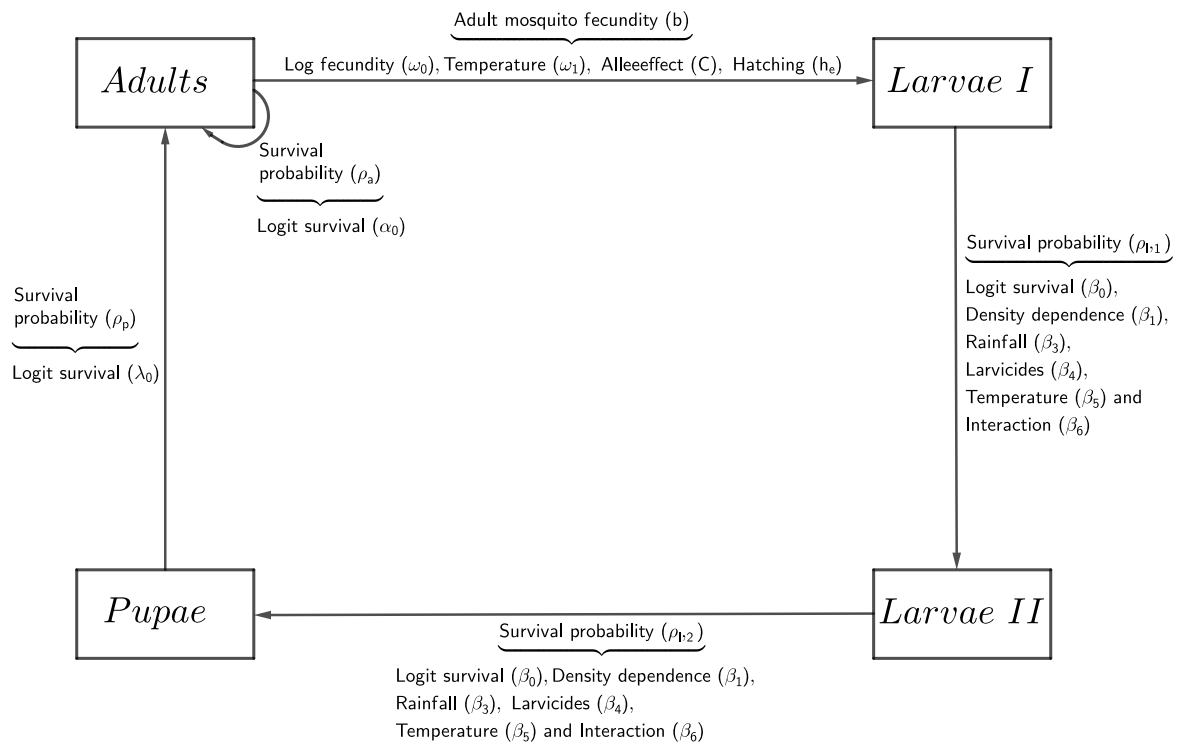


Figure 3.2: Schematic representation of the model showing stages of the mosquito life cycle together with the predictors of the life-history traits. Arrows correspond to the transition from one stage to another. Larvae I correspond to early instar larvae, while Larvae II correspond to late instar larvae.

3.2.3 Leslie Matrix for estimation of adult mosquitoes' population growth rate

The Leslie matrix method is commonly used in ecological studies to predict sizes and growth rates of stable stage-structured populations by using individuals' survival probabilities and fecundity rates in different life cycle stages (207). In this study, the Leslie matrix was utilised to assess the growth rates of the stable adult mosquito populations based on the stage-structured population model developed in subsection 3.2.2. Since it is difficult to observe the growth rate estimates directly from the simulation when the population stabilises because most values will be centred around the same point, the Leslie matrix helps to visualise the growth rate estimates as a smooth straight line. The results here will help to understand how negative density dependence and Allee effects regulate the growth rate of a stable mosquito population over time.

When written in matrix form, $N(t + 1) = LN(t)$ where L is a Leslie matrix and N is the stable population abundances over time such that:

$$\begin{pmatrix} N_{l,1}(t+1) \\ N_{l,2}(t+1) \\ N_p(t+1) \\ N_a(t+1) \end{pmatrix} = \begin{pmatrix} 0 & 0 & 0 & b_r \\ \rho_{l,1} & 0 & 0 & 0 \\ 0 & \rho_{l,2} & 0 & 0 \\ 0 & 0 & \rho_p & \rho_a \end{pmatrix} \begin{pmatrix} N_{l,1}(t) \\ N_{l,2}(t) \\ N_p(t) \\ N_a(t) \end{pmatrix}$$

3.4

The maximum eigenvalue of the matrix L is the growth rate of a stable population over time. The variables from the system 3.4 are described below in Equations 3.5-3.8.

Briefly, the population abundance of new early instar larvae ($N_{l,1}$) over time is defined as

$$N_{l,1}(t+1) = b_r N_a$$

3.5

Where b_r is the per capita fecundity rate (i.e., $b_r = \exp(\omega_0 + \omega_1 T(i, t))$) and N_a is the total number of adult mosquitoes.

Late instar larvae are determined by multiplying survival probability by the total abundance of the early instar larvae, such that:

$$N_{l,2}(t+1) = \rho_{l,1} N_{l,1}$$

3.6

Pupae abundance is the product of survival probability and the total abundance of the late instar larvae, such that:

$$N_p(t+1) = \rho_{l,2} N_{l,2}$$

3.7

The number of adults results from multiplying the pupae survival probability by their total abundance plus the product of adult survival probability and their abundance, such that:

$$N_a(t+1) = \rho_p N_p + \rho_a N_a$$

3.8

Population growth rate was also obtained directly from the simulation model as an average across 100 simulations using the abundance of adult mosquitoes in the formula below.

$$Gr(t) = \frac{N(t+1)}{N(t)}$$

Whereby $Gr(t)$ is the population growth rate and $N(t)$ is the population size at a time t . The theoretical growth rate estimates was initially computed using the Leslie matrix and then compared the estimates with those generated directly at

each time step of the simulation model. A 5% proportion of female adult mosquitoes from the total population of early and late instar larvae (ranging between 0-16000) was used to compute the theoretical growth rate. This proportion was acquired by running Equations 3.1 and 3.2 at equilibrium, resulting in 0 to 800 adults. Since pupae are not density-dependent, their proportion is not necessary in the theoretical simulation. Adult mosquitoes are also not density-dependent, but their proportion is essential for determining the Allee effect.

3.2.4 Role of negative density dependence and Allee effect in regulating mosquito populations

Given that negative density dependence (β_1) and the Allee effect (C) are critical parameters for the mosquito population dynamics, they were varied in three ways. (i) To illustrate the potential impacts of these parameters on the population dynamics, 3 different values (low, medium and high) were set for negative density dependence (DD) and the Allee effect (AE) while maintaining the other parameters constant at the levels shown in Table 3.1, i.e. values that provide stable population dynamics. Negative density dependence was set based on the literature value of $5.5e-05$ (Table 3.1), corresponding to mid-level (DD2). DD2 was then halved to lower level ($2.75e-05$; DD1) and increased four times to a higher level ($2.2e-04$; DD3). These values were chosen purely to illustrate the types of 'extreme' impacts that high and low levels of DD might have on the population dynamics. Similarly, the Allee effect was initially set at 360 as mid-level (AE2, Table 3.1), and then AE2 was halved to lower level (180; AE1) and increased two times to higher level (720; AE3). AE was increased 2 times as opposed to the 4 times increase in DD because the impacts of AE on population dynamics are much stronger, and extinction could be seen by doubling the effect. The table of DD1-3 and AE1-3 combinations is provided in the supplementary information (see Appendix B.4). (ii) To understand the independent effects of both DD and AE on population dynamics, the AE was set to 0 against the three levels of negative density dependence (i.e., DD1, DD2 and DD3). (iii) Finally, given the unknown values for these parameters, all other possible combinations were explored by investigating the impact of a wide range of values on the percentage of population change by varying negative density dependence and the Allee effect mid-levels ($5.5e-05$ and 360, respectively) across the range of values from 90% reduction (>zero effect) to 100% increase (double effect for AE) or 300% (quadruple effect

for DD) increase. The percentage of population change was calculated as an average across 100 simulations. To avoid confounding impacts with treatment, all larvicidal coefficients in Equation 3.2 were set to 0, indicating the absence of an intervention. All combinations of variations of negative density dependence vs the Allee effect are shown in a table as the supplementary information (see Appendix B.4).

3.2.5 Impacts of negative density dependence and Allee effects on sustained and short-termed interventions

As interventions are intended to change population sizes, the role of negative density dependence and the Allee effect were investigated on that change when an intervention is applied either in a sustained way (i.e., once application starts at week 48, it is continuously applied until the end of the simulation at week 193) or short-termed (i.e. single short application lasting 7 months or two short applications lasting 3 months each, separated by 3 months) (see supplementary information in Appendix B.4) . A short-term intervention regime was chosen because it is common for larvicide to be implemented for a few months, e.g., 4 or 5 and then stop the implementation, with potential re-application again in the future. In contrast, the sustained intervention regime is not commonly used due to the high cost of resources but serves to illustrate whether the intervention would have the potential to eliminate the population by preventing the population from bouncing back after suppression. For this, the parameters β_1 and C were set based on similar values as described in the previous subsection 3.2.4. The only difference from subsection 3.2.4 is that in this subsection, the larvicidal coefficient in Equation 3.2 was set to a non-zero value (as shown in Table 3.1). To illustrate the impacts of the intervention on the population dynamics, DD2 and AE2 were varied to explore the wider trade-offs between intervention and DD or AE by exploring the probability of population extinction through varying DD or AE and intervention from 90% reduction to 100% increase. The probability of extinction was calculated as an average across 100 simulations. All combinations of variations of negative density dependence vs the Allee effect, negative density dependence vs larvicides and the Allee effect vs larvicides are shown in separate tables as the supplementary information (see Appendix B.4).

3.2.6 Trade-offs between negative density dependence and the Allee effect

Since the real values of negative density dependence and the Allee effect are unknown, negative density dependence and the Allee effect sizes were varied from 90% reduction to 100% increase on their values set in Table 3.1 (i.e., DD2 and AE2 as described in section 3.2.4), and estimate the population growth rates as an average over 100 simulations. That is to say, the simulation was iterated 100 times, recording the average growth rate over these simulations for each combination of negative density dependence and the Allee effect. A heatmap was used to show the population growth rate across wards for each percentage change in both negative density dependence and the Allee effect. For illustration, the simulation was repeated under four intervention regimes as described in the previous subsection 3.2.5, i.e., (a) without an intervention, (b) double short-termed, (c) single short-termed and (d) sustained intervention (as described in section 3.2.5 and Appendix B.4). Similar process as described in this subsection was repeated to calculate probability of extinction (see more details in Appendix B.6).

Table 3.1: Description and parameter values used in the simulation model, with respective literature sources. Only estimates per week were used during the simulation. How original biological values converted to per week values are shown in Appendix B.8.

Parameter	Parameter descriptions	Literature estimates	Estimates per week	Original (biological) values	Reference
β_0	Logit larval survival when no rainfall and larvicide and centred temperature is 0°C	-1.39-1.39/7-14days	-0.16	0.955/day	(165,208)
β_1	Effect of negative density dependence on larval survival i.e., DD per a thousand larvae	5.5e-05/week	5.5e-05	5.5e-05/week	(165)
β_2	Ratio of the interaction effect and negative density dependence		β_6/β_1	β_6/β_1 per week	-
β_3	Effect of rainfall on larval survival	0.0025/11days	0.0015	0.0025/11days	(209)
β_4	Effect of larvicides on larval survival	0.057/day	0.25	0.25/week	(210)
β_5	Effects of temperature on larval survival	0.0043/3days	0.01	0.0043/3days	(211)
β_6	Interaction effect between larvae and rainfall	-	1e-06	1e-06/week	-
ω_0	Log fecundity when centred temperature is 0 °C	4.19-5.67/cycle	5.2	180/cycle	(212,213)
ω_1	Impact of temperature on the fecundity	-	0.01	-	-
λ_0	Logit pupal survival at centred temperature 0°C	-6.2/day	-0.4	0.97/2days	(208,214)
α_0	Logit adult mosquito survival when temperature is 0 °C	-1.32/3days	0.04	0.95/day	(215,216)
h_e	Eggs hatching rate	0.1 per 3 days	0.23	0.78/day	(217)
C	Strength of mate finding Allee effect (i.e., number of female adults per thousand larvae)	-	360	-	-

3.3 Results

3.3.1 Adult mosquitoes' population growth rate

The stable population growth rate estimates from the Leslie matrix increased with the size of the mosquito population until it reached a maximum size, after which it declined as population size increased. When the population was less than 200 mosquitoes, the growth rate remained below 1, indicating that the Allee effect would be expected below this population size. However, when the population increased between 200 and 600, the growth rate increased above 1, and as the population grew beyond 600, the growth rate decreased (Figure 3.3a). From an average of 100 simulations, the estimated population growth rate was initially inconsistent with the population size and unstable but was later stabilised for a population size bigger than 300. At low population sizes, the growth rate was quite high, with values up to almost 2, but it declined sharply as the population size increased and eventually stabilised at around 1.1 for population sizes above 300. When populations ranged between 150-300 mosquitoes, growth rate estimates were frequently below 1, which could be caused by either the Allee effect or the populations' instability. Additionally, the growth rate seemed to stabilise more, around 1.1 for a population size between 650 and 800 mosquitoes (Figure 3.3b). The fluctuations in growth rates in Figure 3.3 may be due to the high variability in the simulation model, which arises as the current population is influenced by the previous population and unique weekly rainfall and temperature. In contrast, the Leslie matrix did not have this variability; instead, total larvae and adults were pre-defined, with consistent average rainfall and temperature across weeks, creating conditions to maintain stable populations.

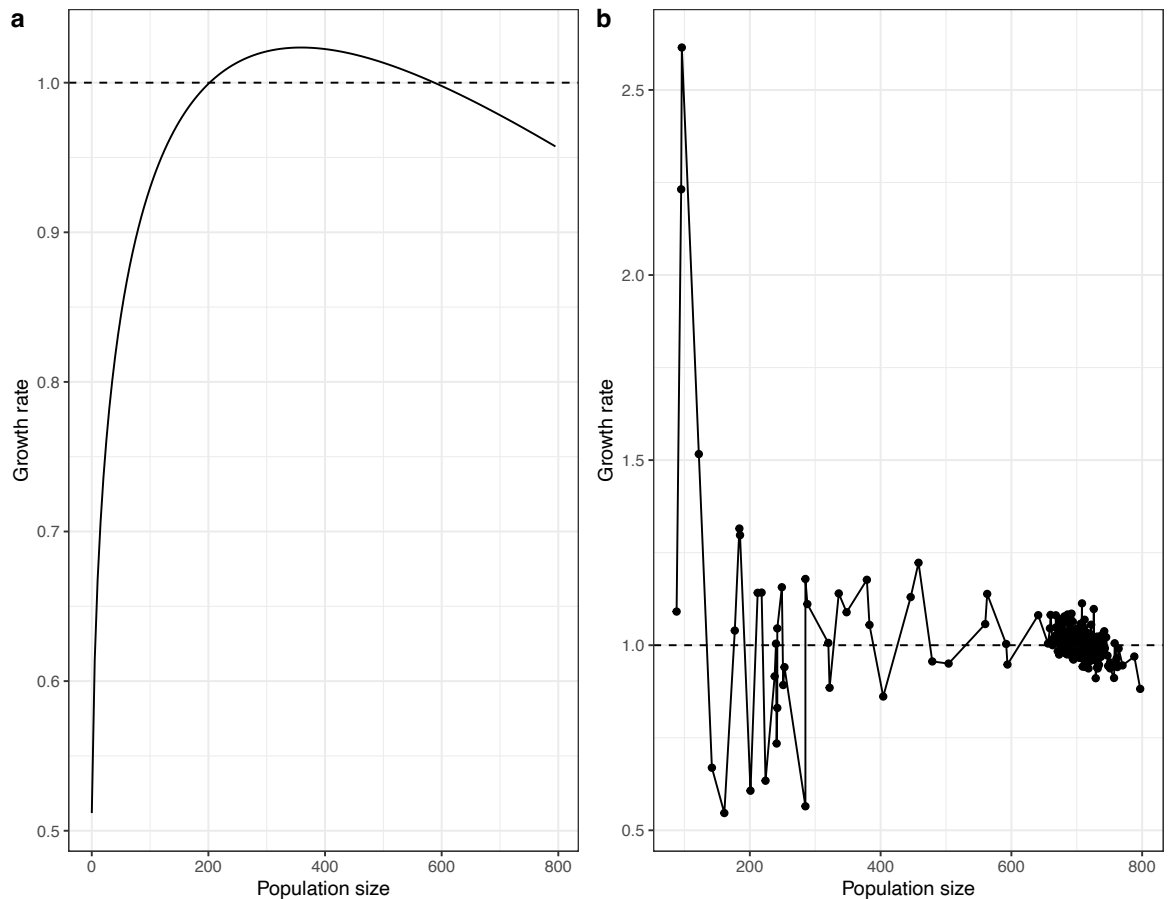


Figure 3.3: Population growth as estimated through (a) a Leslie matrix method and (b) direct calculations from the simulation model (i.e., an average across 100 simulations all initialised at 800 female mosquitoes). The dashed line indicates the threshold of the population growth rate where the population declines when the rate is below this point.

3.3.2 Role of negative density dependence and Allee effect in regulating mosquito populations

While in isolation, lower levels of negative density dependence and the Allee effect did not impact the population size in the long term, their combination at higher levels tended to accelerate the population decline. With the constant Allee effect AE2, lower- and mid-levels of negative density dependence (i.e., DD1 and DD2) resulted in similar population trajectories with initial 104.6% and 29.2% increase followed by a 12.6% and 13.3% decrease before stabilising the population (Figure 3.4a, black and blue lines). However, higher levels of negative density dependence (DD3) and the Allee effect (AE2) resulted in a 100% reduction (i.e., extinction) in the mosquito population just after the 37th week (Figure 3.4a, black and blue lines). Moreover, at DD3 and without the Allee effect (i.e., AE=0), the population declined 90% before stabilising again to an average of 180 mosquitoes and could not decline to extinction by the end of the simulation (Figure 3.4a, red line).

Furthermore, the Allee effect levels AE1, AE2 and negative density dependence level (DD2) resulted in similar population dynamics with initial decreases of 7% and 6.9%, respectively, before populations stabilised at an average of 700 mosquitoes (down from the initial population size of 800) (Figure 3.4b, black or blue lines). On the other hand, at AE3 and DD2, the population initially declined by 41.7% before stabilising at an average of 569 mosquitoes (Figure 3.4b, black or blue lines). In contrast, without negative density dependence (i.e., DD=0), population size increased and exploded irrespective of the Allee effect levels (as shown in Appendix B.5). When negative density dependence increased by more than 100% and the Allee effect by 50%, population size declined to extinction (Figure 3.4c, blue colour). Trajectories for DD1&2 at AE=0 were not shown here because they have the same dynamics as DD1&2 at AE=360, and for similar reasons, other combinations (i.e., DD1&2 vs. AE1&2) were not shown.

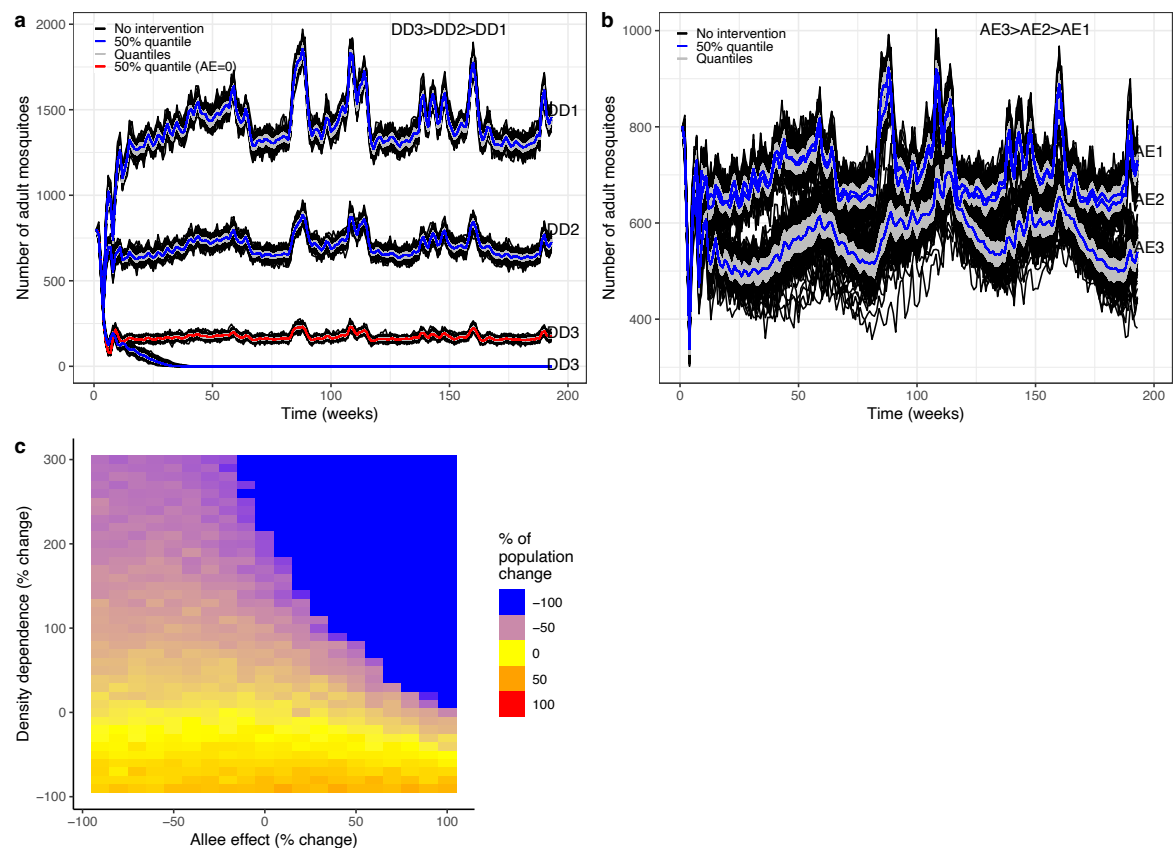


Figure 3.4: Role of DD and AE in regulating mosquito populations without a larvicidal intervention. (a) Three DD levels, $2.75e-05$, $5.5e-05$ and $2.2e-04$, were used, keeping Allee effects constant at 360. The red colour corresponds to DD3 when AE=0, (b) Three AE levels, 180, 360 and 720, were used, keeping DD constant at $5.5e-05$, and (c) Percentage of population change (relative to the initial size of 800 mosquitoes) after 193 weeks when DD and AE mean values $5.5e-05$ and 360 were varied across a range of values from 90% reduction to 100% or 300% increase. The percentage of population change was averaged over 100 simulations.

3.3.3 Impacts of negative density dependence and Allee effects on sustained and short-term interventions

As the duration of intervention increased, the mosquito population decreased in all studied scenarios, but populations only tended to go extinct in the presence of the Allee effect. With the constant Allee effect (AE2) and short-termed intervention (i.e., single short application), the mosquito population was reduced by 39.2% and 74.6% at DD1 and DD2 but bounced back to similar or higher levels, respectively, while at DD3, the population was declined to extinction (Figure 3.5c). With two short applications, the mosquito population was reduced by 39.5% and 55.9% in the first application and 23.6% and 46.7% in the second application at DD1 and DD2, respectively, while in at DD3, the population declined to extinction (Figure 3.5e). The bouncing-back behaviour of the population was solely caused by negative density dependence. When larvicide was applied in a sustained way from week 48 to the end of the simulation in week 193, the mosquito population initially declined by 35.6% at DD1 but then stabilised at an average of 1042 mosquitoes throughout the intervention; however, the population declined to extinction at DD2 and DD3 (Figure 3.5a). With sustained intervention and constant negative density dependence DD2, the mosquito population declined by 32.3% at AE1 before declining to extinction by the end of simulation at AE2 and AE3 (Figure 3.5b). With a single short application at AE1 and AE2, the population size declined by 38.9% and 76.3% but then bounced back to similar or higher levels (Figure 3.5d). In contrast, at AE3, population size declined to extinction, and there was no rebound. With two short applications, the population declined by 55.8%, 60.4% and 99.3% at AE1-3 and bounced back to similar or higher levels in the first short application. Contrarily, in the second short application, population size declined by 16.1% and 46.6% at AE1 and AE2 before declining again to extinction at A3 (Figure 3.5f).

Moreover, the probability of extinction increased with an increasing larvicidal effect, negative density dependence and the Allee effect. Keeping the Allee effect constant and varying negative density dependence and larvicidal effect across a range of values from 90% reduction to 100% increase, the probability of extinction ranged between 0 to 1 (Figure 3.6a). However, only increasing negative density dependence and larvicidal effect by 50% each while keeping the Allee effect constant drove the population to extinction. Similarly, keeping density

dependence constant and varying the Allee effect and larvicidal effect across a range of values from 90% reduction to 100% increase, the probability of extinction ranged between 0.25 to 1 (Figure 3.6b). Surprisingly, increasing the Allee effect by more than 50% while setting the negative density dependence constant would drive the population to extinction even if the larvicidal effect was reduced by 50%. Similarly, given constant negative density dependence, the Allee effect at a 100% increase would require a small larvicidal effort (intervention reduced by 90%) to drive the population to extinction.

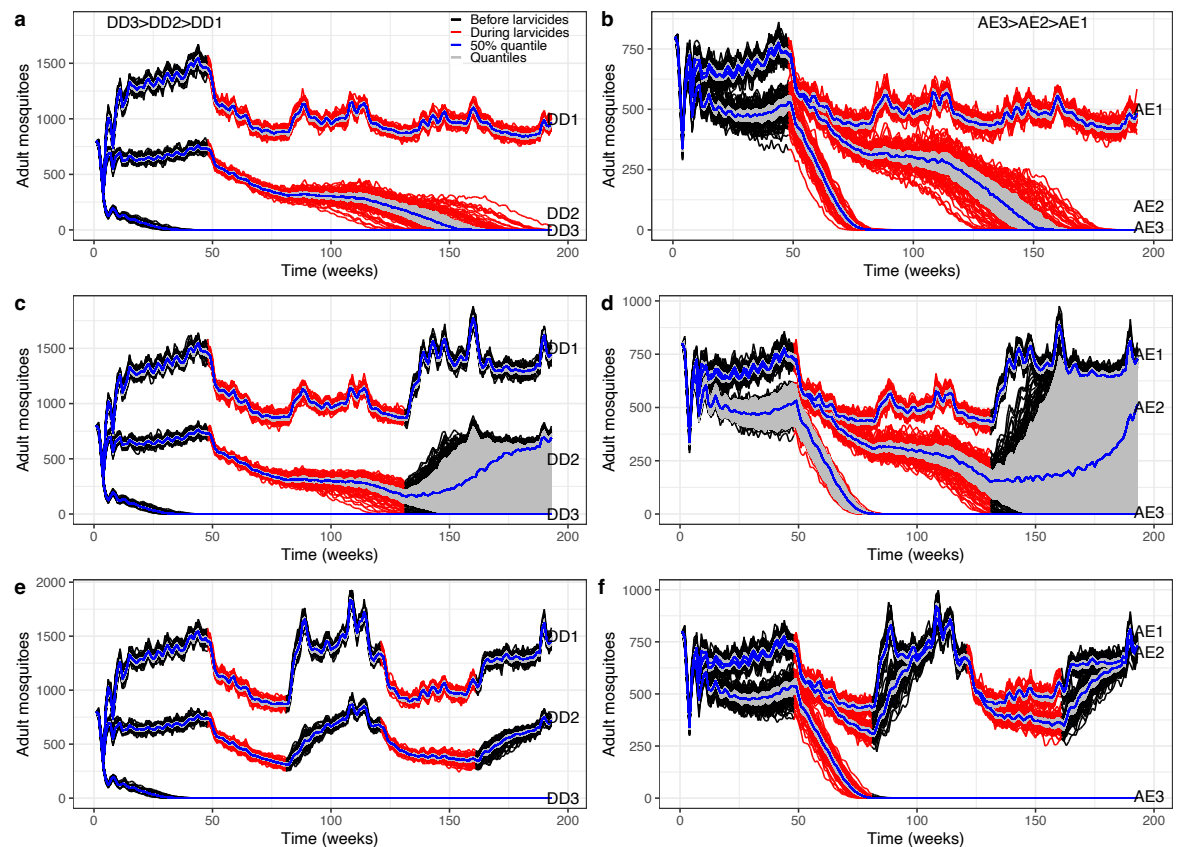


Figure 3.5: Mosquito populations regulated by (a, c, e) negative density dependence at levels $2.75e-05$, $5.5e-05$ and $2.2e-04$ setting the Allee effect (C) constant to 360 and (b, d, f) Allee effects at levels 180, 360 and 720 keeping negative density dependence constant at $5.5e-05$. Larvicidal treatment was applied in three regimes, (a, b) sustained larvicidal application, (c, d) a single short application and (e, f) two short applications.

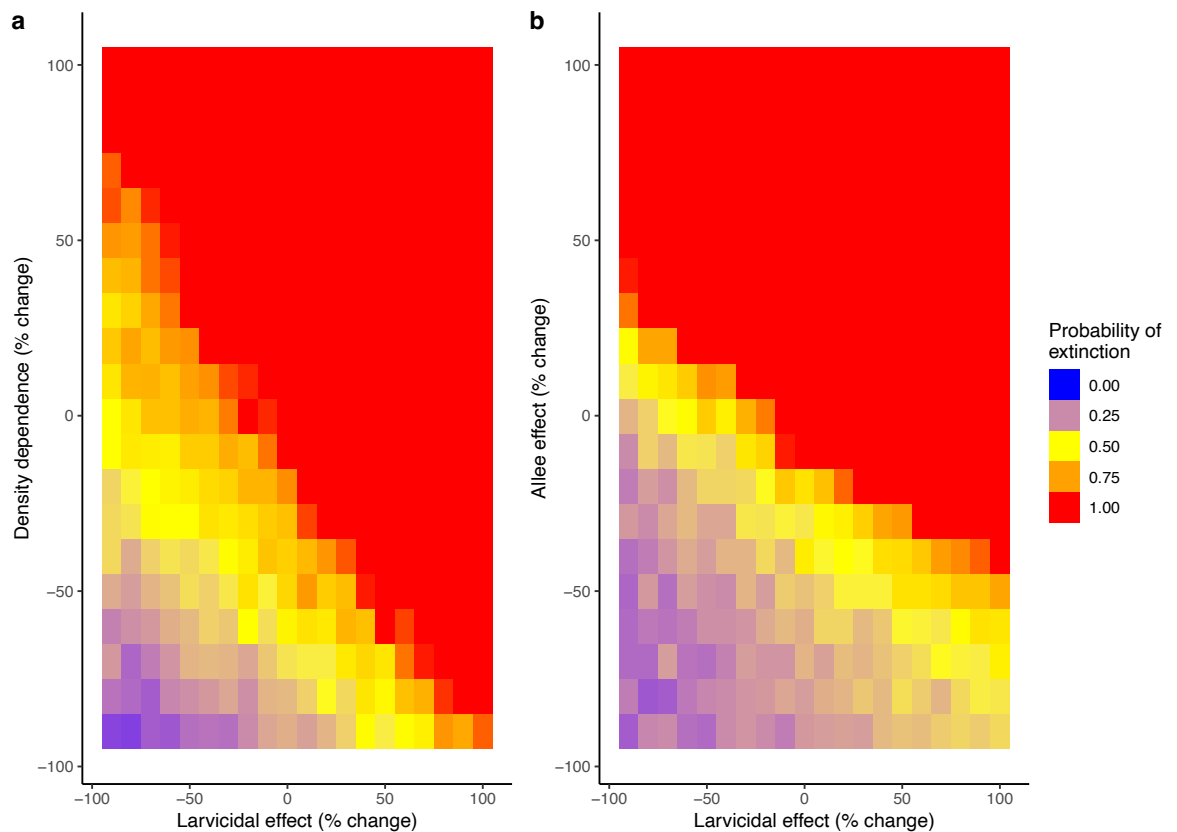


Figure 3.6: Heat maps showing the probability of extinction (averaged over 100 iterations) by week 193 after varying across a range of values from 90% reduction to 100% increase in sustained larvicidal effect size, 0.25, and (a) negative density dependence effect size, $5.5e-05$, setting Allee effect constant or (b) Allee effect size, 360, setting negative density dependence constant.

3.3.4 Trade-offs between negative density dependence and Allee effect in the mosquito population regulation

As negative density dependence and the Allee effect increased, the population growth rates decreased, but the Allee effect tended to accelerate population decline (Figure 3.7). While negative density dependence with less Allee effect (i.e., 90% reduction) could not lead to population growth rates < 1 , higher levels of Allee effect with less negative density dependence (i.e., 90% reduction) caused mosquito population rates to decrease below one, especially with a sustained intervention (Figure 3.7b-d). With lower levels of both negative density dependence and the Allee effect (i.e., mean values $5.5e-05$ and 360, respectively, reduced by 90%), the population was high, making the growth rates increase above 1, with and without larvicidal intervention (Figure 3.7a-d). Without intervention, the population growth rate could not decrease below 1 unless negative density dependence and the Allee effect were both increased by at least 50% (Figure 3.7a). With two short applications of intervention, only a 10% increase in negative density dependence and the Allee effect could drive the population growth rate

below 1 (Figure 3.7b). Similarly, with a single short application of intervention, only keeping negative density dependence and the Allee effect constant could drive the population down at a growth rate below 1 (Figure 3.7c). In Figure 3.7d, the mosquito population growth rate declined to less than 1 without any change in negative density dependence and the Allee effect (i.e., $5.5e-05$ and 360, respectively). However, with nearly no negative density dependence, the population growth rate slowly declined below 1 if and only if the Allee effect was doubled in the presence of single or double short applications of intervention (Figure 3.7b, c). Moreover, when negative density dependence was increased by at least 50%, population growth rates declined below 1 even before reaching a 50% increase in the Allee effect if and only if there is an intervention (Figure 3.7b-d). Furthermore, when negative density dependence and the Allee effect were both increased by at least 50%, their combination drove the growth rate to 0 (Figure 3.7b-d). However, the presence of a sustained intervention accelerated 0 growth rates and made the combination of negative density dependence and the Allee effect become a threat to mosquito populations (Figure 3.7d).

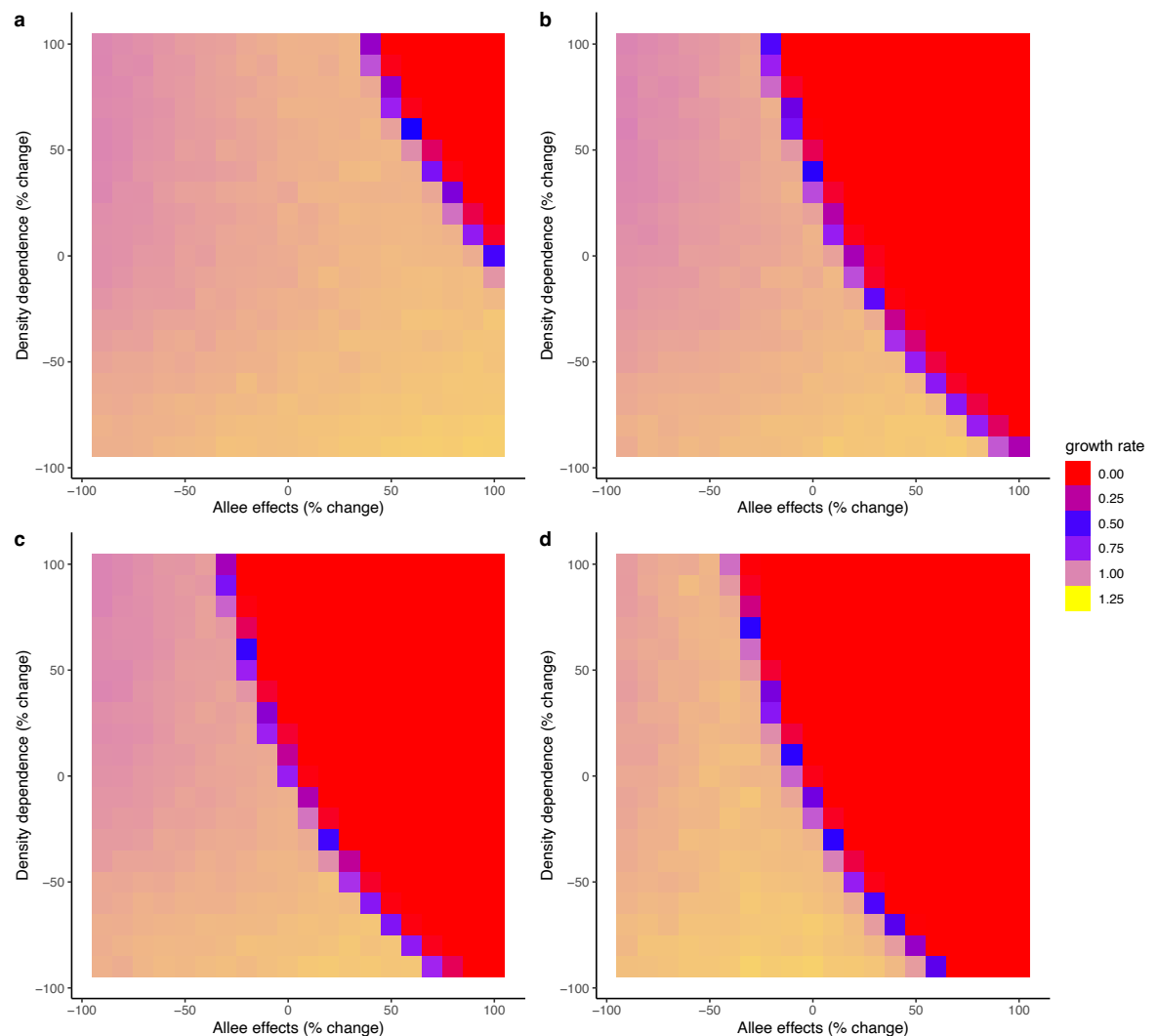


Figure 3.7: Heat maps showing the population growth rates averaged over 100 simulations for each percentage increase or decrease in negative density dependence and the Allee effect mean values, $5.5e-05$ and 360, respectively; (a) without intervention, (b) with two short applications of intervention, (c) single short application of intervention and (d) with sustained intervention.

3.4 Discussion

Understanding the interplay between vector control interventions and malaria mosquito population dynamics is key to making informed decisions and accelerating malaria elimination. While in isolation negative density dependence and the Allee effect did not impact mosquito population in long run, their combination accelerated mosquito population decline. The role of biological processes (i.e., negative density dependence and Allee effects) in regulating mosquito populations may be useful in determining what kind of intervention is needed, how much (i.e., the intensity needed) and when the intervention should be deployed. Sustained application of interventions can activate Allee effects and increase the chance of mosquito populations to extinct while short application of intervention can lead to a population rebound driven by negative density dependence. As both negative density dependence and the Allee effect increase, population growth rates decrease but Allee effect tends to accelerate population decline with increase in duration of intervention. This trade-offs between negative density dependence and the Allee effect in the regulation of mosquito populations provide insights for optimising vector controls. Such insights include the possibility that vector control measures would require fewer resources to achieve large outcomes and the significance of the frequency and duration of larvicidal applications on mosquito population dynamics. To my knowledge, this is the first study to comprehensively evaluate the importance of negative density dependence and the Allee effect and their implications for vector control and malaria elimination.

The estimated population growth rates from the Leslie matrix were low at lower densities and increased with an increase in population density before stabilising and then decreasing again at higher densities. The implications of the increase and decrease in growth rates due to densities suggest that a better time to target mosquitoes with interventions is when their density is lower or declining; this approach may help push the population closer to extinction, rather than waiting

until it stabilises. A reduction in population sizes at high densities is important for vector control as it may facilitate the conditions necessary for the Allee effect to occur. Typically, a population cannot grow indefinitely because the negative density dependence effect eventually regulates its growth, which is consistent with results from this study, where populations exploded when density dependence was set to zero. A population with no negative density dependence may be unrealistic (218,219), especially for mosquitoes, as the survival and development rates of some of their immature stages (e.g., larvae) depend on their population density (90). Zero negative density dependence clearly implies that population regulation is not feasible, whether through density or intervention measures. A modelling study aimed at quantifying the effect of negative density dependence and density independence on population growth rates and survival, utilising both simulated and empirical seabird data, has revealed that the model incorporating negative density dependence better explained the population fluctuations. In contrast, the model based on density independence resulted in biased estimates (220). Similarly, another modelling study examined the importance of negative density dependence on the development and survival of immature mosquitoes using empirical data from the semi-field. Their findings showed that models incorporating negative density dependence accurately reflected the trends in the data, while those without negative density dependence failed to explain the data effectively (95). Amongst the main population regulatory processes (i.e., negative density dependence and Allee effects), negative density dependence is the most studied (90,93,96,221) to understand its implications in regulating malaria mosquito populations at different population densities.

A study reported that with higher larval density, survival declines (i.e., mortality increases) and the development time (time to reach pupal stage) increases (90); in turn, there are few survived larvae experiencing less competition, making the population size increase again. This aligns with the results of this thesis chapter, where populations initially declined to lower- or mid-levels due to negative density dependence and short applications of larvicides but subsequently rebounded to higher levels than before. These findings suggest that interventions such as larvicides should be applied frequently and consistently to effectively reduce mosquito populations. Simply applying interventions for a short period and then discontinuing the treatment is insufficient to drive populations down to extinction. A significant drawback of having short applications of interventions is

that when the intervention ceases, the remaining mosquitoes can recover quickly due to decreased competition for resources. While negative density dependence has been extensively studied (as an example, see these studies (90,93,95,218,222-224)), Allee effects and their implications for regulating small malaria mosquito populations remain largely overlooked. This study is important as it demonstrated scenarios where the Allee effect could influence the effectiveness of larviciding, and the modelling framework developed here could be utilised to explore these effects. This study has shown that a population reduced to low levels can decline further to extinction if the Allee effect kicks in; however, without the Allee effect or an intervention such as larvicides, the population can recover quickly. Similar to what was reported by previous studies, due to less competition for resources, when the mosquito population is reduced to low levels (90,93,96), surviving larvae grow faster to adulthood, and in the end, mosquito populations bounce back to similar or higher levels than what was recorded before. On the contrary, the population declined and reached extinction in the presence of sustained intervention and higher levels of the Allee effect. However, given the low Allee effect, the population grew to similar levels regardless of whether the intervention was short-termed once or twice. These results suggest that the Allee effect requires lower population sizes to take effect, meaning that interventions must not be applied for short terms as doing so may not help to achieve low densities.

Furthermore, without intervention, it was very unlikely to drive the population to extinction unless both negative density dependence and the Allee effect were strongly operating together (e.g., at DD3 and AE3). However, the presence of a sustained larvicidal intervention drove the population to extinction even by mid-levels of negative density dependence and the Allee effect, which was likely to happen as the population declined below the threshold. As reported in (185), a population reduced below the threshold will be driven to extinction, assuming that this population will not strive to survive. It is important to note that negative density dependence or the Allee effect alone did not reduce the population to extinction, even when intervention was sustained for a long period. In contrast, their combination decreased the population to extinction, which was mainly accelerated by the presence of an intervention. Given negative density dependence and the Allee effect, sustained intervention was more effective in driving the population to extinction than short-term intervention. Generally, given

the Allee effect, the probability of population extinction increased with the duration of the intervention. This implied that an intervention such as larvicides could take advantage of these main regulatory mechanisms, specifically the Allee effect, to accelerate malaria elimination and wrap up the endgame. Additionally, it is important to note that findings from this study imply that the scale of regulatory processes is crucial, whereby only high levels of negative density dependence and the Allee effect can lead to smaller population sizes or even population extinction.

Calibrating this model with empirical data is essential for obtaining reliable insights into the presence of Allee effects within wild mosquito populations. However, the calibration process, which seeks to adjust model parameters to accurately reflect real-world observations, faces challenges due to a scarcity of experimental data (225). This lack of data is particularly evident in studies focused on the Allee effect among mosquito populations, leaving a gap in our understanding of these regulatory processes and their implications for malaria vector control and elimination efforts. Since we do not know whether the Allee effect exists in natural mosquito populations, using empirical data collected from low-density settings or conducting Allee effect experiments in the lab, semi-field, or field conditions is suggested. Although it was not considered for this study but conducting a detailed sensitivity analysis to identify which parameters most influence model outcomes would help prioritize data collection and refine the model's accuracy. This study provided explanations, predictions, and estimations of how Allee effects might impact mosquito populations and their consequences on contemporary malaria vector control interventions. Findings from this study can also be used as a stepping-stone for researchers to develop more models incorporating more Allee effect mechanisms that might be operating in mosquito populations to help create ways to study these effects in laboratories, semi-fields, or field conditions. All these extensions are suggested for future considerations in malaria-related research.

3.5 Conclusion

It is crucial to understand the role of ecological dynamics in regulating mosquito populations and how interventions could harness these processes for malaria vector control and elimination efforts. Learning how to exploit the interplay

between vector control interventions and malaria mosquito population dynamics is critical to making the difference between mosquito population persistence and extinction. There is great potential in understanding these regulatory processes to help National malaria control programs and other stakeholders in their efforts to eliminate malaria. Therefore, understanding less studied regulatory processes like Allee effects can support vector controls by highlighting the resilient and vulnerable aspects of the vector's life cycles to different interventions. If present, we can harness Allee effects to accelerate malaria elimination.

Chapter 4 Identifying the Allee effects impacting *Anopheles gambiae* populations in the field

Abstract

Population dynamics are crucial to understand when and how a population may decline and may be pushed to extinction by an intervention. Regulatory mechanisms such as Allee effects, are key factors that influence population dynamics. However, the presence of Allee effects in natural mosquito populations remains largely unknown. This study aimed to assess *An. gambiae* mosquito population dynamics and identify evidence of Allee effects in the field. This was achieved by fitting an age-structured population model developed under a Bayesian state-space modelling (SSM) framework first to simulated data to determine whether our modelling approach could identify Allee effects if they exist. Indeed, the model effectively detected Allee effects, with the true values falling well within the 95% CI of the posterior predictions. The same SSM was then fitted to female adult *An. gambiae* mosquito data from Dar es Salaam, Tanzania, to assess the population dynamics and identify evidence of Allee effects in a natural setting. The results showed no evidence of Allee effects, exhibiting a 0% decrease in total fecundity. The model defined key life history traits such as fecundity, larval and adult survivals and negative density dependence and was able to quantify the impact of larviciding on larval abundances, leading to a 10.5% reduction in larval survival, while negative density dependence resulted in a 7.4% decrease in larval survival at an abundance of 100 larvae. The lack of Allee effects could be because the intervention did not reduce the population enough to trigger it. Although we could not fully discard the existence of Allee effects, their absence may require more sustained control efforts when population sizes are small and difficult to measure. If Allee effects exist, fewer resources could result in better outcomes, similar to deploying more resources.

4.1 Introduction

Despite the recent stagnation and increase in malaria cases, from 2000 to 2015, global malaria deaths decreased by 32% (8). This decline has been attributed primarily to vector control interventions such as insecticide-treated bed nets (ITNs) and indoor residual spraying (IRS) (2), but other supplementary tools, such as larviciding, have had a fundamental role in decreasing malaria infection prevalence, especially in urban settings (47). This has led to mosquito populations declining to low densities in many places (2,226), but it has been challenging for them to be pushed down further to extinction. Population dynamics play a vital role in our understanding of when and how the population can decline and be pushed to extinction stochastically or by an intervention. The two main population regulatory mechanisms are Allee effects, where individuals' fitness reduces as population size declines, leading to a reduced per capita population growth rate (227-229), and negative density dependence, which regulates population by decreasing individual survival as density increases (90,230). Similar to studies on Allee effects in other systems such as mammals (106) and birds (100), the results presented in Chapter 3 have shown that sustained malaria control interventions can 'activate' Allee effects and increase the chance of mosquito populations going into extinction, while short application of these interventions has led to population rebound driven by negative density dependence. But if present these effects are likely to lead to complex trade-offs. Allee effect are difficult to directly estimate in the field and so even the existence of Allee effects remains unknown.

It is reasonably well established (90,91,231) that mosquito population sizes vary due to competition for resources at the larval stage where the per capita growth rate decreases with increasing density, a process known as negative density dependence (95). Biological factors such as negative density dependence and the Allee effect also play an important role in the seasonal dynamics of vector populations as they influence seasonality in vector abundance or act on it through their interaction with abiotic factors (222). Understanding the biological mechanisms of malaria vectors, such as negative density dependence and the Allee effect, is crucial for effectively controlling malaria transmission (135,232). The evidence supporting the existence of Allee effects in other species, such as natural animal populations, is substantial and increasing. A systematic review

study indicated that 77%, 71%, 65%, 71% and 64% out of 25 studies published over three decades from 1976 to 2008 (187) for terrestrial arthropods (107,110-113), aquatic invertebrates (97,108,109), mammals (104-106), birds (98-100) and fishes (101-103), respectively, presented evidence of the existence of Allee effects in natural populations. Similarly, the percentage of Allee effects detected in plant populations was 82% out of 25 studies (187). The Allee effect, which typically operates at low population densities, is caused by various factors, but mate-finding limitation is the most widespread factor (233), which may also be possible to operate in mosquito populations. Mate limitations may lead to a critical population size below which the population declines to extinction (193). Although quantifying the existence and the magnitude of Allee effects in natural systems has been challenging due to data availability and limitations of observing or sampling at low population sizes (102), various methods have been used, including quantifying fitness parameters (denoted as y): i) the proportion of breeding female adults to estimate the probability that a female successfully bred, ii) the number of offspring per adult female, (iii) adult or offspring survival and (iv) the per capita population growth rate, then use linear model (i.e., $y=a + bD$) to test the relationship of each parameter to the density (denoted as D). In the linear model, the parameter b scales the linear term of the fitness function, indicating the Allee effect when $b>0$ (106). Implicitly, similar model (i.e., $y=a + bD$) could be used to identify the Allee effect where y is mortality rates of the prey populations and D predator densities (234). Some of these techniques used for other species cannot be directly applied to mosquitoes, as they solely focused on density as the only factor affecting individual fitness. However, we can adapt these methods by incorporating additional factors determining mosquitos' life history, such as environmental factors (e.g., rainfall, temperature, and humidity) and interventions.

Suppression of malaria vector populations is feasible if appropriate vector control technology is made available and deployed with sufficient coverage. A notable historical example is the Tanzanian Pare-Taveta study area in the 1960s, where *Anopheles funestus* disappeared completely after the application of IRS with dieldrin. However, five years after the spraying stopped, the mosquito populations rebounded and became stable in the region (232). Similarly, in the Santa Isabel province in the Solomon Islands, *Anopheles koliensis* was eliminated through four years of comprehensive malaria vector control interventions, including the use of

ITNs and IRS (148). In addition to the achievements of core malaria vector control interventions, supplementary measures such as larval source management (LSM) have contributed to the historic elimination of *Anopheles gambiae* in various regions over different periods. LSM involves the management of water bodies (i.e., aquatic habitats) to prevent immature stages (i.e., egg, larva, and pupa) from completing their development into adult mosquitoes (55,235,236). LSM encompasses four types: habitat modification (e.g., land reclamation), habitat manipulation (e.g., flushing of water streams), larviciding, and biological control (e.g., introducing predators into aquatic habitats) (236,237). Larviciding, which entails the regular application of biological or chemical insecticides into water bodies, is the most widely practised form of LSM. Larval control played a crucial role in eradicating *An. gambiae* in Brazil during the 1930s and early 1940s, Egypt from early 1942, and the Zambian copper belt between 1930 and 1950 (238). It was hypothesised by Killeen *et al.* that mosquitoes are subjected to the mate-finding Allee effect, wherein individuals fitness is compromised at lower population density or size (232,239). The successful elimination of malaria vectors in different geographical settings (148,232,238) suggests that the effects of vector control interventions could have been enhanced by Allee effects (239). However, it is currently unknown whether Allee effects accompanied these malaria elimination instances in all these settings, but it is possible that these effects accelerated vector extinctions.

In this Chapter, the overall aim was to assess *An. gambiae* mosquito population dynamics and identify the existence of Allee effects in the field by investigating key regulatory mechanisms that might emerge from a large-scale vector control intervention in Dar es Salaam, Tanzania. The dataset from this larviciding control programme in Dar es Salaam is ideally suited for this aim because vector abundance in these settings was low, but malaria transmission persisted at low levels. Additionally, throughout this larviciding programme, malaria prevalence decreased from 28% to less than 2% (41,142), indicating a reduction in vector population abundance, thus, suggesting that Allee effects could be identified from this dataset from Dar es Salaam. Specifically, the aim was to address the following research questions: (i) Can the Bayesian modelling framework adapted from Chapter 3 identify Allee effects, given the available field data characteristics? (ii) Do Allee effects exist in natural *An. gambiae* mosquito populations in Dar es

Salaam? (iii) How does a larvicidal intervention impact the population dynamics of *An. gambiae* mosquitoes in Dar es Salaam? To address the research aims, a Bayesian state-space model (SSM) was first fitted to simulated data and then to field data. The simulated data was used to test if the SSM can identify Allee effects while the field data was consequently used to identify the existence of Allee effects in natural mosquito population and assess the impact of larvicidal intervention on population dynamics of *An. gambiae* mosquitoes in Dar es Salaam.

4.2 Methods

4.2.1 Large-scale larvicidal control programme in Dar es Salaam

The programme targeted 15 wards across 3 municipalities over three phases (time periods) spanning 193 weeks from early 2005 to late 2008 (Figure 4.1a). Baseline data was collected over a total of 47 weeks, with larvicide applications commencing in the 48th week. Larviciding activities took place in the lowest administrative unit known as “ten-cell” (even though it may consist of more than ten houses, the name “ten-cell” has been commonly used). Several ten-cell units form a higher administrative unit called *mtaa* (the plural is *mitaa*, a Swahili word for streets), and the ward is made up of more than one *mtaa*. In the first phase, larvicidal treatment was administered in three wards, which increased to nine wards in the second phase and ultimately expanded to cover all 15 wards in the final phase (Figure 4.1b). The specific larvicides used, their quantities, and the duration of the intervention are detailed elsewhere (41,47,240). In the model, larvicide is represented as a binary variable where 1 indicates the presence of larvicide and 0 indicates its absence.

4.2.2 Longitudinal surveillance of *An. gambiae* in Dar es Salaam

Adult female *An. gambiae* were collected weekly. Each week, Human Landing Catches (HLCs) (82,241), the gold standard method for catching female adult mosquitoes seeking humans for blood feed, were conducted in each *mtaa* across wards to sample female adult mosquitoes before and during the intervention. The total number of *mtaa* for each ward is provided in Appendix C.2 as supplementary

information. Figure 4.1 shows the total number of mosquitoes caught in all traps (a) per ward and (b) across wards.

4.2.3 Simulated data: adult female *An. gambiae* population abundance

The stage-structured population model developed in Chapter 3 was adapted to generate adult female mosquito population abundance data mimicking the dynamics of the long-term entomological surveillance data collected in Dar es Salaam, Tanzania. To simulate the data, the parameter values were fixed to those in Table 4.1. As in the previous chapter, most of these were taken from the literature, including negative density dependence. The exception was Allee effects, which was given a neutral value that does not interfere with the population dynamics (i.e., a value that gave stable population dynamics in the absence of larvicidal intervention). For the time period, the number of wards and larvicidal phases, see more descriptions in subsection 4.2.2 and Figure 4.1. From this model, several datasets were generated (while keeping the ‘observed data’ constant to match with real observed data from the field) with varying proportions of observations (*pobs*) from 0.0001 to 1. For illustration, results section will include *pobs* values of 0.01, 0.1, 0.5 and 1. True population abundances were allowed to vary with *pobs*, while negative density dependence and the Allee effect were also scaled to maintain consistency with data to observe from the simulation. These selections in the *pobs* were made due to our lack of knowledge regarding the actual mosquito population size, which also prevents us from determining the proportion we observe during surveillance. Since population size is a crucial factor for understanding negative density dependence and Allee effects, it was aimed to ensure that these parameters could be quantified irrespective of the *pobs*.

4.2.4 Environmental data

Daily rainfall and temperature data per ward from 2005-2008 were acquired from the Soil and Water Assessment Tool (205). This rainfall data was used to generate two rainfall variables for each ward: i) average weekly rainfall to account for ‘current’ conditions, and ii) 2-week cumulative rainfall to account for the availability of larval habitats due to the amount of water. Similarly, the daily temperature was averaged into the weekly temperature to match the time unit in the model (see subsection 4.2.5.1). Since there was little to no difference in

temperatures between wards the mean weekly temperature was assumed to be equivalent across all fifteen wards in urban Dar es Salaam.

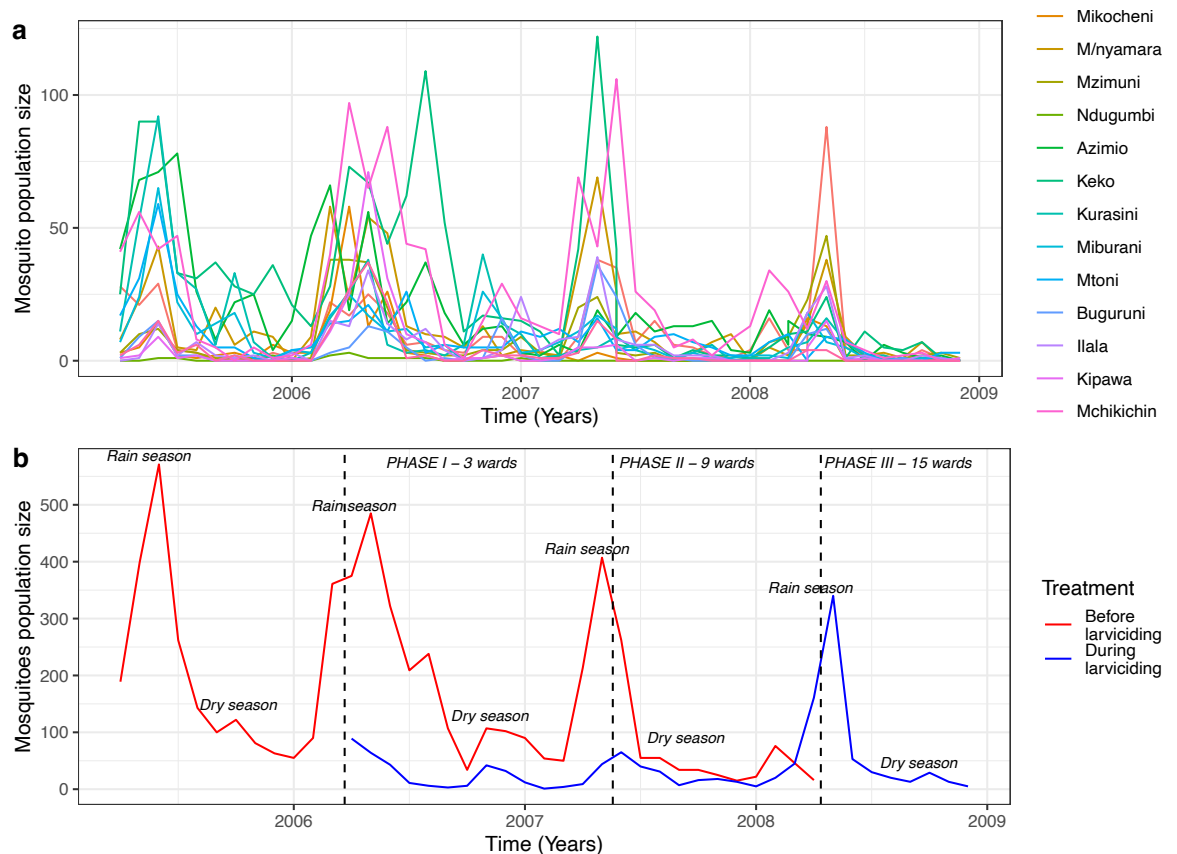


Figure 4.1: Monthly mosquito population abundance data showing (a) the sum of all traps per ward and (b) the sum of all traps across wards before and during a large-scale larvicidal control programme conducted from 2004 to 2008 in three administrative municipalities of Dar es Salaam, Tanzania.

4.2.5 Bayesian state-space models (SSMs)

To explore the mosquito population dynamics, a structured population model was used to implemented under a Bayesian state-space modelling (SSM) framework. The SSM has two components: the process model and the observation process model. The process model of the SSM describes the population dynamics of the mosquitoes through a simplified mosquito life cycle (see Figure 4.2) and is an extension of the stage-structured population model developed in Chapter 3. The observation model of the SSM describes the stochastic process of the female adult mosquito data collection per trap (i.e., *mtaa*) per ward.

4.2.5.1 Biological process: Mosquito life cycle

A simple mosquito life cycle was defined where adult female mosquitoes lay eggs that hatch into early instars, which then develop into late instars. Late instars become pupae and eventually emerge as adult mosquitoes. Each life cycle stage

is linked through or influenced by factors such as fecundity and larval and adult survival, as illustrated in Figure 4.2, and lasts one week. This is an approximation that results in a full life cycle (from being eggs to laying eggs) lasting 4 weeks. Specifically,

Adult survival

Adult female (N_a) survival follows a binomial process and is defined using a linear function S_a , at ward i and week t . The weekly survival probabilities (ρ_a) were defined through an inverse logit transformation of a linear function $S_a(i, t)$ such that:

$$\rho_a(i, t) = \frac{\exp(S_a(i, t))}{1 + \exp(S_a(i, t))}. \quad 4.1$$

Specifically, $S_a(i, t)$ is written as a linear function of weekly mean log odds of adult survival and a random effect such that:

$$S_a(i, t) = \alpha_0 + \varepsilon_i. \quad 4.2$$

$$\varepsilon_i \sim \text{Normal}(0, \sigma_\varepsilon). \quad 4.3$$

where α_0 is the mean logit (i.e., log odds) of adult survival. The prior distribution of adult survival (i.e., inverse logit of α_0) was beta with shape values 12.2 and 11.8. Throughout the text, mean survival values were set as shown in Table 4.1 (which were obtained from literature) and then assigned beta priors to these values before transforming them into log odds (refer Appendix C.6 for a more detailed description of this transformation). The same prior means and variance were then used to calculate shape and rate parameters for beta and gamma distributions as detailed in Appendix C.6. The prior distribution of error term ε at ward i was normal with a mean of 0 and a precision σ_ε . The prior distribution of τ_ε was gamma with a shape and rate of 0.01. The random effect was added in Equation 4.2 to account for unknown variability in the longitudinal surveillance data of adult female *An. gambiae* mosquito abundance between wards such as HLC volunteers, environmental factors, or source of blood meal. The prior distributions for all parameters in the model, as well as their biological explanations, are provided in Table 4.1.

Pupal survival

Pupae survival follows a binomial process, where the weekly pupal survival probability (ρ_p) was determined through an inverse logit transformation of λ_0 , which is structured similarly to Equation 4.1. Specifically, λ_0 is the mean logit of pupal survival. The prior distribution of mean larval survival (i.e., inverse logit of λ_0) was beta with shape values 9.2 and 13.8. The random effect was not included due to the absence of field abundance data for pupae, which would have required a random term to capture the variations between wards and also to avoid over-parameterisation.

Early instar larval survival

The survival of early instars follows a binomial process and is defined using a linear function $S_{l,1}$, in ward i at week t . The weekly early instar larval survival probability ($\rho_{l,1}$) was defined through an inverse logit transformation of a linear function ($S_{l,1}(i, t)$) and was structured similarly to Equation 4.1. Specifically, $S_{l,1}(i, t)$ is written as a function of cumulative rainfall (Q), the total larval density ($N_{l,1}+N_{l,2}$), current rainfall (R), larvicides (LA) and temperature (T) such that:

$$S_{l,1}(i, t) = \beta_0 - \beta_1 \left(1 - \frac{\beta_2 Q(i, t)}{\max(Q)}\right) (N_{l,1}(i, t) + N_{l,2}(i, t)) - \beta_3 R(t) - \beta_4 LA(i, t) + \beta_5 T(t).$$

4.4

where β_0 is the mean logit of larval survival. The prior distribution of mean early instar larval survival (i.e., inverse logit of β_0) was beta with shape values 22.4 and 26.3. The parameters β_1 and β_2 described the impact of negative density dependence on larval survival, which is mainly regulated by cumulative rainfall and larval density. Specifically, β_1 is the effect of larval density ($N_{l,1}+N_{l,2}$) on larval survival, with survival declining at higher densities. The prior distribution of β_1 was gamma with shape 3.03 and rate 5500. These larval densities are driven by the amount of cumulative rainfall, with β_2 representing a probability that captures a potential interaction between the availability of larval habitats and larval density. Here, larval habitat availability is defined as cumulative rainfall (Q) over the past week. For example, if both Q (i.e. 331 mm of rain) and β_2 (i.e., equals 1) are at maximum, the term $1 - \frac{\beta_2 Q(i, t)}{\max(Q)}$ becomes zero, meaning there are

plenty of habitats available, leading to no negative larval density dependence. To allow a positive impact on the strength of negative density dependence, the prior distribution of β_2 was beta with shape values 14 and 6. The effect of current rainfall (R) denoted by β_3 was quantified under the assumption that higher R leads to flooding, which in turn leads to a wash effect on larvae. The prior distribution of β_3 was gamma with shape 1 and rate 100. The parameters β_4 and β_5 are the effects of larvicides (LA) and temperature (T) on larval survival, respectively. The prior distribution of β_4 was gamma with shape 6.3 and rate 25 while the prior distribution of β_5 was normal with a mean of 0.01 and standard deviation of 0.07.

Late instar larval survival

The survival of late instars follows a binomial process and is defined using a linear function $S_{l,2}$, in the ward i at week t . The weekly late instar larval survival probability ($\rho_{l,2}$) was defined through an inverse logit transformation of a linear function ($S_{l,2}(i, t)$) and was structured similarly to Equation 4.1. Specifically, the late instar linear function is written similarly to the linear function of early larval instars (Equation 4.4) i.e., $S_{l,1}(i, t) = S_{l,2}(i, t)$. The larval development stage (which roughly lasts for a maximum of two weeks) was divided into two one-week stages to align with the model development that assumes one week for each stage of the mosquito life cycle. This division allows for the assumption that the survival functions of early and late instar larva stages are the same. This means that early and late larval survival rates share all parameters.

Fecundity

The adult mosquito fecundity makes the transition from adult mosquitoes to eggs and follows a Poisson process with a mean of the number of eggs laid (b) in a ward i at week t , defined through an exponential transformation and regulated by total adult mosquitoes ($N_a(i, t)$) such that:

$$b(i, t) = 0.5 * \exp(\omega_0) * N_a(i, t) * \frac{Na(i, t)}{C + N_a(i, t)}$$

4.5

where ω_0 corresponds to the log of per capita fecundity, i.e., log of number of eggs laid per female mosquito. The prior distribution of ω_0 was gamma with shape 4.59 and rate 0.02. The term $\frac{Na(i, t)}{C + N_a(i, t)}$ corresponds to the Allee effect, which here

is constructed as a probability of mating, where the number of female adults N_a , was scaled by a constant C (hereafter Allee effect parameter). This means that, the greater the value of C relative to N_a , the lesser the mating probability, leading to a lower number of total eggs being laid (i.e., large Allee effects). The prior distribution of C was gamma with shape 1.44 and rate 0.04.

Transitions between life cycle stages

Briefly, the mosquito life cycle begins with eggs hatching into early instar larvae, which then develop into late instar larvae and eventually into pupae before emerging into adult mosquitoes (Figure 4.2). To determine the total number of male and female mosquitoes in the population, a 50:50 sex ratio was assumed. To model the female mosquito population specifically, the total number of mosquito eggs laid per week (total fecundity) was halved. It was also assumed that only a proportion (h_e) of eggs hatch into early instars. The prior distribution of h_e was beta with shape values 7.9 and 26.5. The resultant survival probabilities (Equation 4.1) and total fecundity (Equation 4.5) were used to obtain population abundances (which were used as one of the key model outcomes) for larvae (Equations 4.6&4.7), pupae (Equation 4.8) and adult mosquitoes (Equation 4.9). Note that the survival probabilities will also incorporate the development rate, meaning that surviving individuals move to the next stage.

Specifically, abundances of early instar larvae (Larvae I) were from Poisson distribution with mean $h_e * b$ such that:

$$N_{l,1}(i, t + 1) \sim \text{Poisson}(h_e * b(i, t)).$$

4.6

Abundances of late instar larvae (Larvae II) were from a binomial distribution with mean $N_{l,1}$ and probability $\rho_{l,1}$ such that:

$$N_{l,2}(i, t + 1) \sim B(N_{l,1}(i, t), \rho_{l,1}(i, t)).$$

4.7

Abundances of pupae were from a binomial distribution with mean $N_{l,2}$ and probability $\rho_{l,2}$ such that:

$$N_p(i, t + 1) \sim B(N_{l,2}(i, t), \rho_{l,2}(i, t)).$$

4.8

Total abundances of female adult mosquitoes were from binomial distribution with means N_p and N_a and probabilities ρ_p and ρ_a , respectively, such that:

$$N_a(i, t + 1) \sim B(N_a(i, t), \rho_a(i, t)) + B(N_p(i, t), \rho_p(i, t)).$$

Probability ρ_a defines adults that remain in the system after surviving, and these individuals join those transitioning into adulthood from the pupal stage.

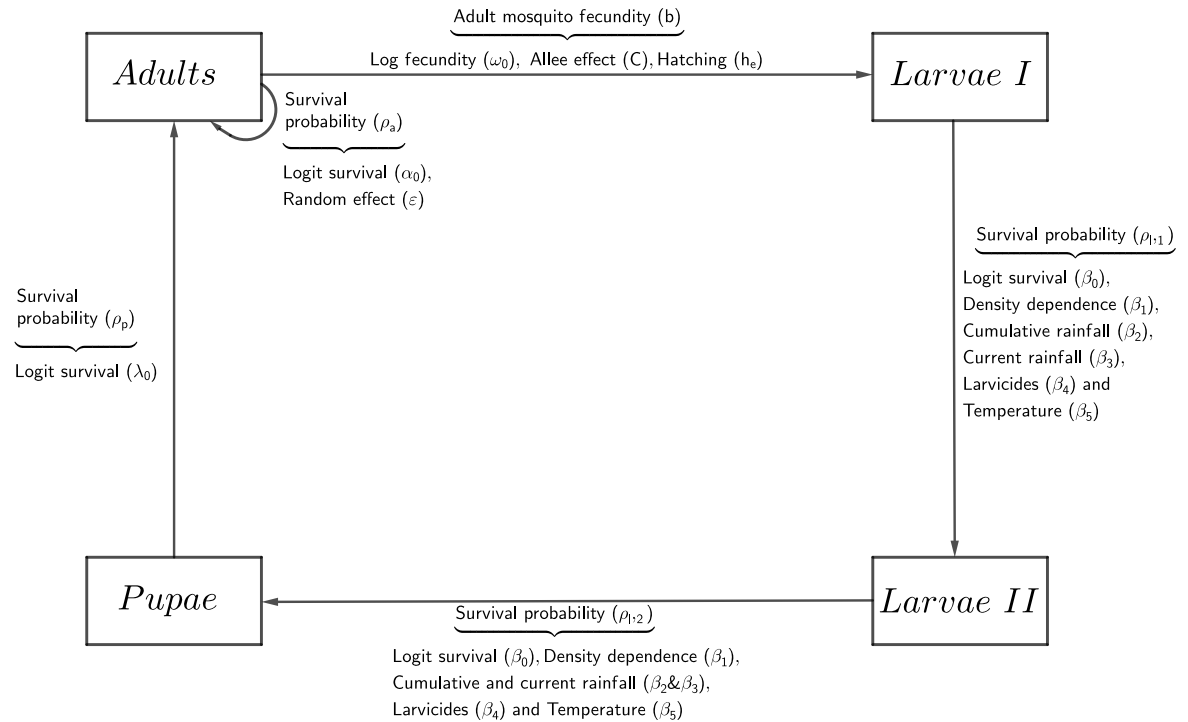


Figure 4.2: Schematic of the life cycle model. At each life stage (i.e., adults, Larvae I, Larvae II and Pupae) mosquitoes transition from one stage to another (arrows) by surviving and some of these transitions (i.e., Larvae I to Larvae II and Larvae II to Pupae) are influenced by ecological factors. The Greek letters reflect the parameters in the model.

4.2.5.2 Observational processes

The observed adult mosquito abundance ($\text{dat}N_a$) was modelled as a Poisson process with the mean defined as the number of adults N_a in the ward i at time t weighted by the *sampling* effort such that

$$\text{dat}N_a(i, t) \sim \text{Pois}(pobs * n_traps(i) * N_a(i, t)).$$

4.9

Where *pobs* refer to the proportion of mosquitoes caught from the true population size of female adult mosquitoes in each ward. Here, only a proportion of female adult mosquitoes are typically trapped. In the field data, *pobs* (i.e., probability of observation or the ratio between observed and simulated population size) were fixed at 0.1, meaning we observed 10% of the true field population. Unfortunately, we do not know the true size of the population, so this number was chosen to minimise *pobs* impact on model convergence and goodness of fit (i.e., we observe

the dynamics better with $pobs=0.1$). While highest values ($pobs>0.1$) could enhance convergence and overall model fit, they might not be realistic in the field (e.g., if $pobs=1$ indicates that we observed entire field population, which is unrealistic). Conversely, setting low values ($pobs\leq 0.01$) results in poorer model convergence and fit. Although this is a shortcoming of this approach, our key results do not seem to be very sensitive to this. In addition, for some results, such as relative change in life history traits, this becomes less important. The remaining variable, n_traps , is the number of traps per ward. In the field data, negative density dependence and the Allee effect were not scaled for $pobs$ (which is different from the approach taken with the simulated data) because we do not know the actual size of the field population, as we are sampling from an unknown population: however, they were both assigned wider priors, which would include the scaled values.

Table 4.1: Description of prior and posterior distributions. For each parameter in the model, a brief description of its biological meaning, the mean values obtained from the literature, and how these were transformed first into weekly values (the time unit of the SSM model) and then as parameters of their corresponding prior distribution are provided. Finally, for the posterior distributions, the mean and 95% credible intervals (CIs) are provided, and to maintain biological meaning, parameter values representing mean survival were transformed into logit (i.e., log odds of survival) using logit function.

Parameter		Prior distribution						Posterior distribution		
No tation	Description	Distribution	Original (biological) values	Mean (per week)	SD	Reference	Additional information regarding the choice and selection of prior distributions	Mean	SD	95% CI
β_0	Logit of larval survival	Beta(22.4, 26.3)	0.95/day	0.46	0.07	(165)	Provides survival information from the same <i>An. gambiae</i> complex	0.3771	1.597e-2	[0.3487,0.4115]
β_1	Negative density dependence on larval survival i.e., DD per a hundred larvae	Gamma(3.03, 5500)	5.5e-04/week	5.5e-4	3.2e-4	(88,165)	Two sources provide information regarding resource competition within <i>Anopheles</i> mosquitoes	1.211e-3	1.886e-4	[8.816e-4,1.614e-3]
β_2	Effect of cumulative rainfall on negative density dependence	Beta(14,6)	0.9601/day	0.7	0.1	(88)	Taken from <i>An. funestus</i> because of scarcity of same information for <i>An. gambiae</i> mosquitoes	0.9770	2.509e-2	[0.9095,0.9997]
β_3	Effect of current rainfall on larval survival	Gamma(1, 100)	0.0025/11days	0.01	0.01	(209,242)	Quantify how current rainfall influences flushing, mortality, and ejection on different larvae stages of <i>An. gambiae</i>	7.094e-5	7.106e-5	[1.662e-6,2.530e-4]

β_4	Effect of larvicides on larval survival	Gamma(6.25,25)	0.25/week	0.25	0.1	(210)	Provide information on <i>An. gambiae</i> and how larvicide affects the survival	0.1727	3.266e-2	[0.1114,0.2398]
β_5	Effect of temperature on larval survival	Normal(0.01,0.07)	0.487/day	0.01	0.07	(88,211)	Temperatures used correspond to ones in Dar and describe direct and indirect impact on larval survival	2.985e-2	5.247e-3	[0.0196,0.0401]
ω_0	Log of per capita fecundity	Gamma(4.6,0.02)	300/cycle	300	140	(212,213)	Used in temperature-dependent model to better understand how climate determines risk	164	1.1572	[122,215]
λ_0	Logit of pupal survival	Beta(9.2,13.8)	0.97/2days	0.4	0.1	(214)	Among few studies with information regarding <i>An. gambiae</i> pupae survival	0.2054	1.796e-3	[0.2025,0.2096]
α_0	Logit of adult mosquito survival	Beta(12.23, 11.76)	0.95/day	0.51	0.1	(215)	Provides same mean survival of adult <i>An. gambiae</i> from two different sites	0.3638	5.491e-2	[0.2711,0.4797]
h_e	Eggs hatching probability	Beta(7.92, 26.50)	0.78/day	0.23	0.07	(217)	Among few studies with information on egg hatching probability	0.1733	1.349e-2	[0.1511,0.2024]
C	Strength of mate finding Allee effect i.e., number of female adults per a hundred larvae	Gamma(1.44, 0.04)	-	36	30	-	Provides stable population when there is no larvicidal intervention	0.0101	8.480e-3	[0.0007,0.0323]

4.2.6 Model fitting and outputs.

The model was fitted to simulated data and then to field data of *An. gambiae* mosquitoes from Dar es Salaam using JAGS software (243) within R software through the *R2jags* and *jagsUI* packages (244,245) (JAGS codes are provided in Appendix C.15 as supplementary information). To achieve convergence, the model was run with 3 chains for 2M iterations, a burn-in of 1M, keeping every 1250th iteration for memory-saving reasons. Chain convergence was visually assessed using trace plots, histograms of prior and posterior distributions, effective sample sizes and the Gelman-Rubin convergence diagnostic using *Rhat* (where $Rhat < 1.1$ means convergence; see Appendix C.7, Appendix C.8, Appendix C.11 and Appendix C.12) (245,246). Prior and posterior means and 95% credible intervals for all parameters are provided in Table 4.1. Posterior predictive check was conducted using autocorrelation as a summary statistic by comparing the autocorrelations of observed (i.e., the simulated data) and posterior predictions (*predNa*). Autocorrelation is an important summary statistic for time series analysis because it shows repeating trends within the data. The autocorrelations were computed using the R function “*acf()*”. Autocorrelation shows the relationship between a variable (here, the weekly adult female mosquito abundance) and itself over a certain period of time. When plotted together, a good model fit would be achieved if the autocorrelations of observed data fall within that of predicted data. The model can estimate parameters if true parameter values used in the simulation (which were also used in the SSM as the mean of the prior distributions) fall within the 95% credible interval of the posterior distributions. To monitor mosquito population abundances, posterior predictions (*predNa*) of the adult mosquito abundances in the ward *i* at the time *t* were obtained similarly to the observation process in equation 4.9 and averaged across the total number of iterations, such that:

$$\text{predN}_a(i, t) \sim \text{Pois}(pobs * n_traps(i) * N_a(i, t)).$$

4.10

4.3 Results

4.3.1 Allee effects are identifiable with simulated data

Overall, the model fitted to simulated data was able to estimate all parameters regardless of the probability of observations (pobs), with the means of the prior distributions (which were also used in the simulation as true parameter values) being within 95% credible intervals (CIs) of the posterior distributions (Figure 4.3), indicating that the model is appropriate and can learn information from the data. This suggests that, if present, the model can effectively identify Allee effects. Unsurprisingly, the most difficult parameter to estimate was the negative density dependence, which was scaled with pobs, and required longer runs to converge.

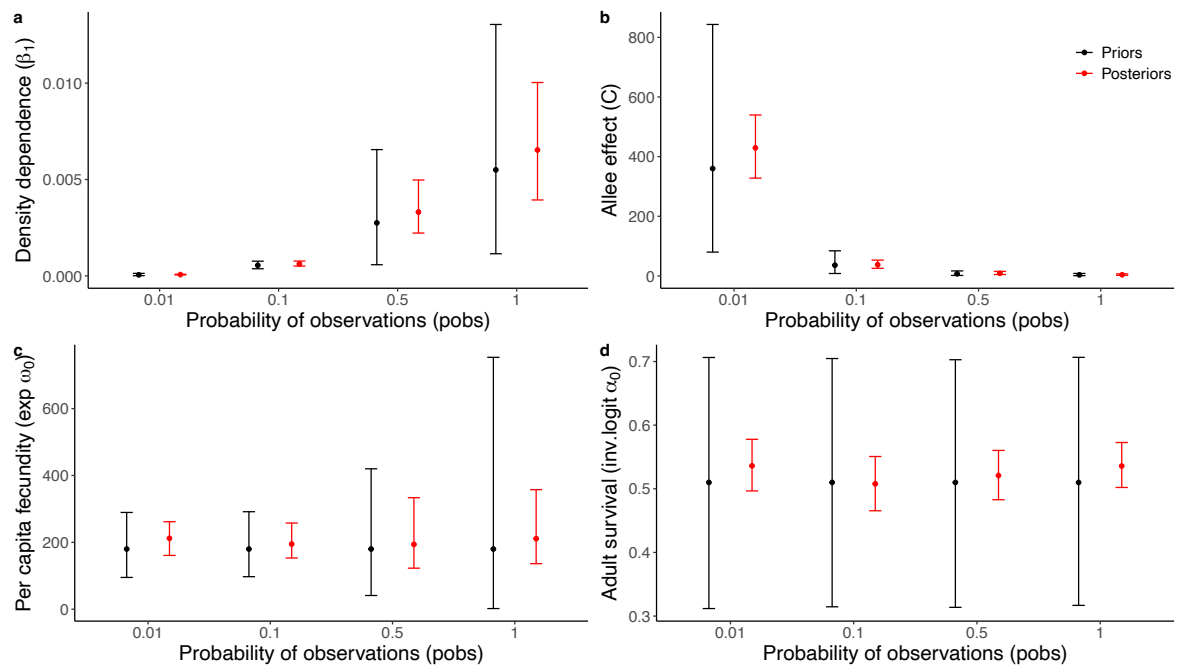


Figure 4.3: An illustration of prior (black) and posterior (red) estimates of (a) negative density dependence, (b) Allee effect, (c) per capita fecundity and (d) adult survival in the y-axis for each of the probability of observations (pobs) in the x-axis. The error bars represent means and 95% CIs of the prior and posterior distributions.

Regardless, the model was able to estimate both negative density dependence and Allee effects. For pobs of 0.1, the true value for the negative density dependence used in the simulation was $5.5e-04$ (Figure 4.4a, red line) and the estimated median of the posterior distribution was $6.5e-04$ (95% CI: $4.37e-04$, $9.65e-04$, Figure 4.4a, solid blue and dashed grey lines); both falling well within the prior distribution (Figure 4.4a, grey histograms) and the true value also fall within the 95% CI of the posterior distribution. Similarly, the true value of the Allee effect used in the simulation was 36 (Figure 4.4b, red line) and the estimated median of the posterior distribution was 39.8 (95% CI: 26.8, 59.0, Figure 4.4b,

solid blue and dashed grey lines); both falling well within the prior distribution (Figure 4.4b, grey histograms) and the true value also fall within 95% CI of the posterior distribution. The histograms showing the true values falling within the 95% CI of posterior distributions for the rest of the parameters are provided in the supplementary information (see Appendix C.8).

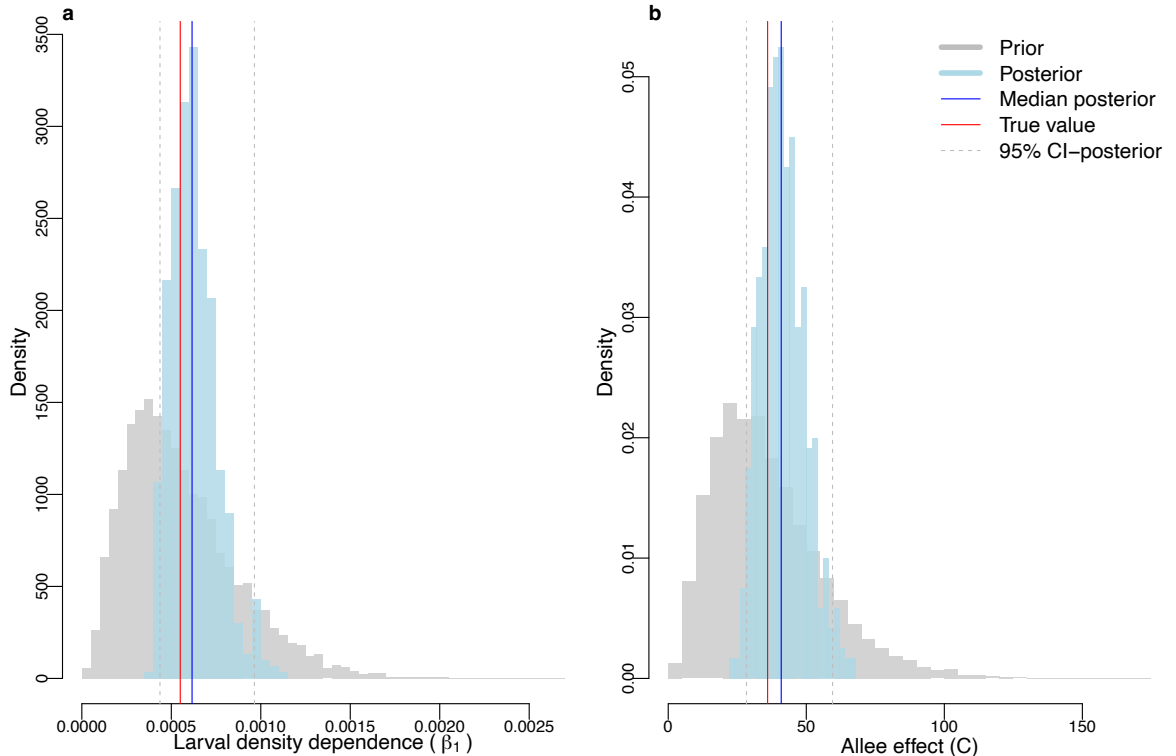


Figure 4.4: Accuracy of model estimates using pobs of 0.1. Histograms of prior (grey) and posterior (light blue) distributions for (a) negative density dependence and (b) the Allee effect with lines indicating the true values (red), median of the posterior distribution (blue) and 95% CIs of the posterior distributions (dashed grey).

4.3.2 Population dynamics of *An. gambiae* mosquitoes in Dar es Salaam

The Bayesian state-space model (SSM) developed here converged well (Rhat and examples of trace plots are provided in Appendix C.11 as supplementary information) and adequately reconstructed the observed population dynamics of female adult *An. gambiae* mosquitoes across all wards (Figure 4.5) and individually for each ward (Figure 4.6). Generally, the seasonal patterns of the data, i.e. peaks in the rainy season and troughs in the dry season, including the timing of starts of the seasons, was relatively well captured by the model as seen by comparing the observed data with the estimated abundances over time across all wards (Figure 4.5 & Figure 4.6). However, the model underestimated some of the highest abundances, especially towards the second half of the data. This was particularly evident when observed data were plotted against mean posterior predictions,

showing that some of the highest numbers (>80) of observed mosquitoes were found to be below the linear line (Figure 4.5b). Additionally, an estimated (predNa) average number of female adult *An. gambiae* mosquitoes across wards is 52. In part, this might be because of the averaging across all wards. Although, this underestimation is less frequent per ward (Figure 4.6), but for wards with strong peaks this remains a challenge.

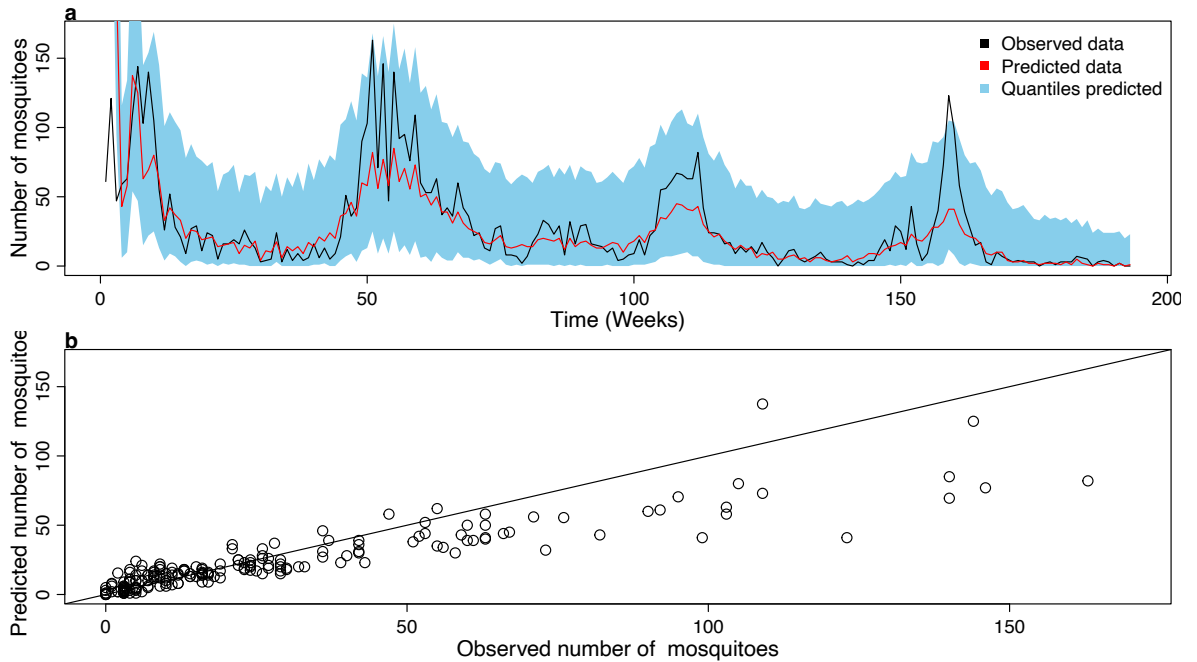


Figure 4.5: (a) Illustration of the reconstruction of the total population abundances of *An. gambiae* adult mosquitoes across all wards: The y-axis is observed (black), predicted mean mosquito population abundance (predNa) (red), 2.5% and 97.5% quantiles (sky blue) of predicted population abundance, while the x-axis is the time in weeks. (b) Goodness of fit: observed vs. predicted total population abundances of *An. gambiae* adult mosquitoes across wards, where the diagonal solid line corresponds to the 1:1 line.

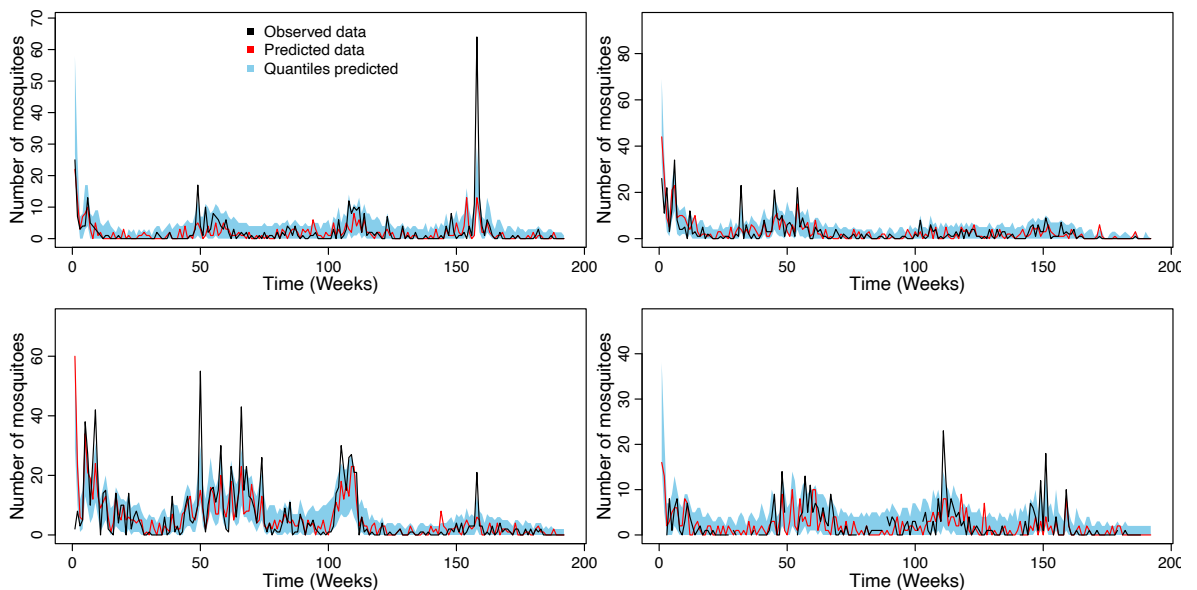


Figure 4.6: Illustration of the reconstruction of the population abundances of *An. gambiae* adult mosquitoes for selected wards. The y-axis is the number of adult mosquitoes, and the x-axis is the time in weeks. The black colour shows the observed data collected in the field

for 193 weeks from April 2005 to December 2008. The red shows the mean mosquito population abundance (predNa) estimated by SSM for a similar time interval with corresponding 2.5% and 97.5% quantiles of estimated population abundance (predNa) (sky blue).

The Bayesian state-space model used here was able to describe the population dynamics of the female adult *An. gambiae* mosquitoes from Dar es Salaam. All key life history traits including, the Allee effect, negative density dependence, environmental variables, and hatching probability were estimated (summaries of the posterior predictions are presented in Table 4.1). The prior vs posterior distribution plots of the life history parameters, negative density dependence, Allee effect, rainfall and temperature are shown in Figure 4.7, while distributions for the rest of the parameters and a complete set of trace plots are provided in Appendix C.11 and Appendix C.12 as supplementary information. Specifically, the estimated mean weekly survival (Figure 4.7, grey histograms) for larvae, pupae and adult mosquitoes are 0.38 (95% CI, 0.35,0.42) (Figure 4.7a), 0.21 (95% CI, 0.20,0.21) (Figure 4.7b), 0.37 (95% CI, 0.27,0.48) (Figure 4.7c), respectively. Of these, mean pupae survival was the least confident parameter as seen by its posterior going against the lower boundary of the prior distribution. The estimated mean weekly per capita fecundity is 164 (95% CI, 122,215) (Figure 4.7d).

The effect of the environmental variables showed that there is no flushing effect on larval survival, while temperature had a positive impact on the overall mean larval survival, where survival increased with increased temperatures. Specifically, estimated mean effect of current rainfall was $7.094e-05$ (95% CI, $1.662e-06$, $2.530e-04$) (Figure 4.7f), which is equivalent to 0.004% (95% CI, 0%, 0.016%) decrease in mean larval survival due current rainfall alone. On the other hand, estimated mean effect of temperature was 0.0299 (95% CI, 0.0196, 0.0401) (Figure 4.7g), which is equivalent to 1.87% (95% CI, 1.20%, 2.53%) increase in mean larval survival due to temperature alone.

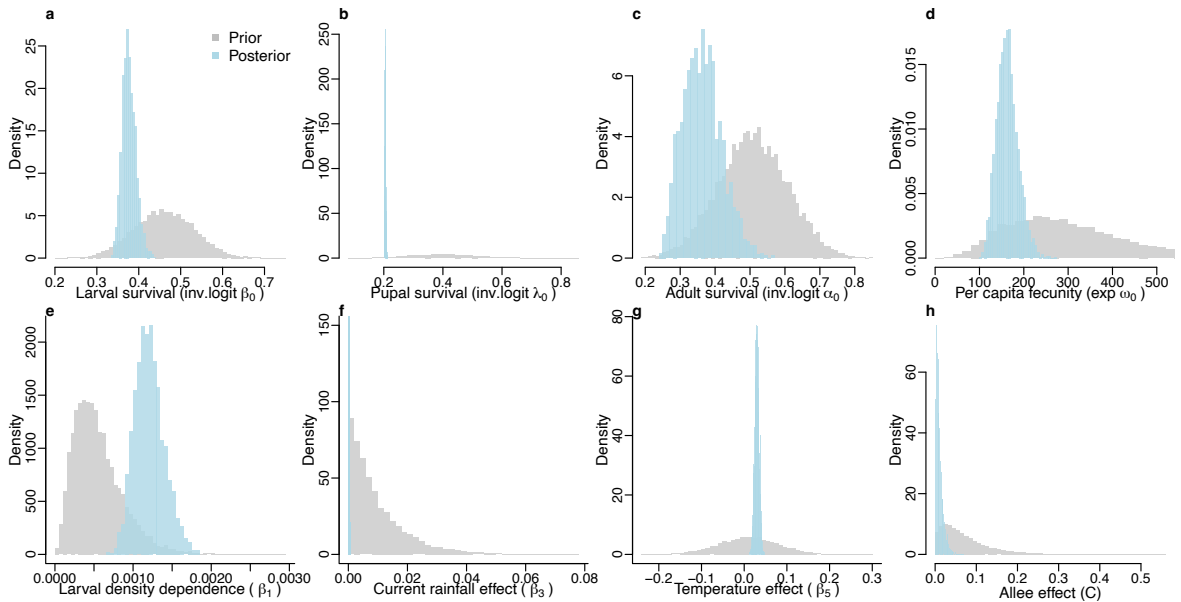


Figure 4.7: Histograms of prior and posterior distributions of selected parameters showing mean (a) larval survival, (b) pupal survival, (c) adult survival, (d) per capita fecundity, the effect of (e) negative density dependence, (f) current rainfall (g) temperature on larval survival and (h) the Allee effect. The grey colour is the prior distribution, and the light blue colour is the posterior distribution.

As expected, the most influential parameter was the effect of negative density dependence on larval survival. The parameter seems to have converged well within the posterior with a mean value of 1.2108×10^{-3} (95% CI, 8.8158×10^{-4} , 1.6136×10^{-3}), but depending on the level of rainfall and larvae density, its impact on larval survival varies. For the mean larval survival of 0.3771/week and larval (early + late instar) abundances of 100 and 500 larvae, negative density dependence reduced mean larval survival by 7.41% (95% CI, 5.44%, 9.75%) and 34.01% (95% CI, 25.75%, 43.45%), respectively (Figure 4.8a). However, this reduction was highly regulated by cumulative rainfall. Across all wards of Dar es Salaam, the amount of minimum cumulative rainfall was 0 mm, maximum (peak during the rainy season) was 331 mm, and medium (lower during the rainy season) rainfall was 31 mm. See rainfall and cumulative rainfall amounts in Appendix C.3 and Appendix C.4. To illustrate how rainfall impacted negative density dependence and overall mean larval survival, here details of the impacts of these two amounts for cumulative rainfall are provided as follows: at a medium cumulative rainfall for Dar es Salam (i.e., 31 mm), an abundance of 100 larvae reduced mean larval survival by 6.74% (95% CI, 4.94%, 8.87%), while an abundance of 500 larvae decreased mean larval survival by 31.24% (95% CI, 32.50%, 40.05%) (Figure 4.8b). At a maximum cumulative rainfall (i.e., 331 mm), an abundance of 100 larvae reduced mean larval survival by 0.17% (95% CI, 0.002%, 0.67%), while an abundance of 500 larvae decreased the larval survival by 0.85% (95% CI, 0.01%,

3.33%) (Figure 4.8c). The impact of negative density dependence alone on mean larval survival was assessed by using average of 100 larvae (and its fivefold increase) because of the probability of observations of 0.1 ($pobs=0.1$), which indicates that we maintain an average of 10 larvae by sampling 10% from an unknown average population of 100 mosquitoes. In general, lower cumulative rainfall resulted in higher density dependence, while maximum rainfall resulted in lower or no density dependence. Although we were able to estimate well the density dependence parameter, we found it very sensitive to the probability of observations ($pobs$). This means that lower $pobs$ lead to low peaks of abundance and poor convergence of the negative density dependence parameter, which in turn affects overall model convergence.

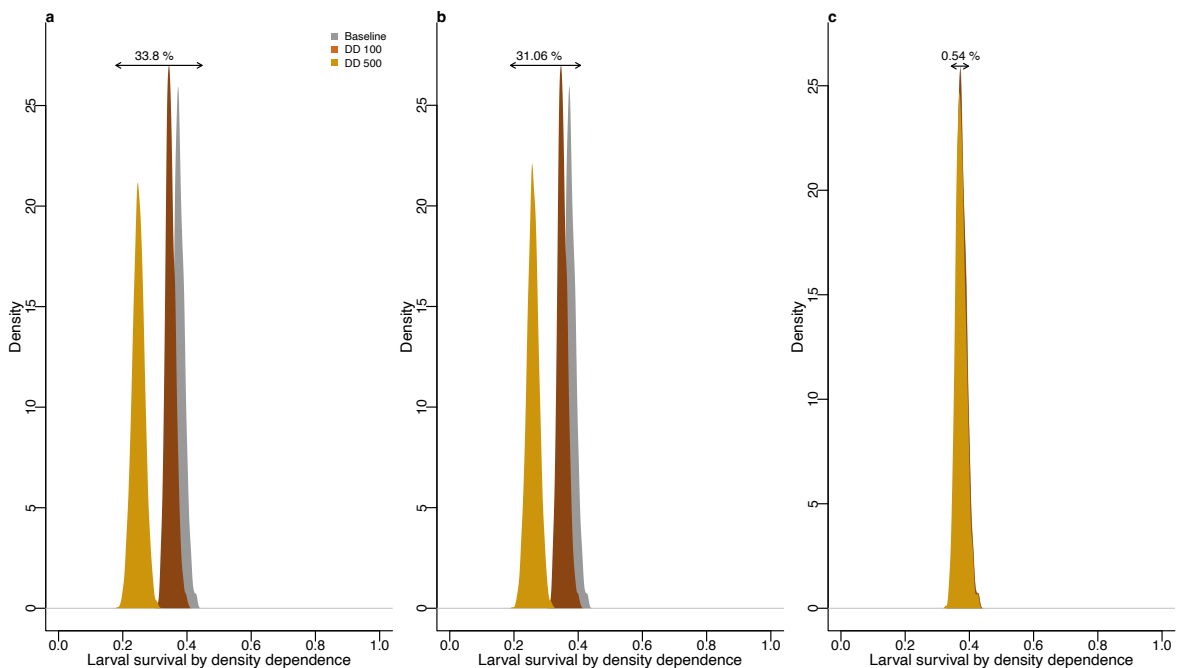


Figure 4.8: Effects of negative density dependence on mean larval survival as regulated by cumulative rainfall of (a) 0 mm (no rainfall), (b) 31 mm (medium across the year or lower during the rainy season), and (c) 331 mm (maximum/peak during the rainy season), all at different larval abundances. The grey colour is the mean larval survival, the brown colour is survival at 100 larvae, and the dark golden colour is survival at 500 larvae.

4.3.3 Allee effects could not be identified from the Dar es Salaam field data

There were no Allee effects identified in female adult *An. gambiae* mosquito data from Dar es Salaam, Tanzania. This is reflected by posterior predictions of the Allee effects parameter (C), which was pushed against 0 with a median of 0.0101 (95% CI, 0.0007, 0.0323) (Figure 4.9a, light blue colour). It is also reflected in the unchanged total fecundity, where the estimated total fecundity per week was 8528 (i.e., a per capita fecundity of 164 multiplied by a total of 52 female adult

mosquitoes) without the Allee effect (Figure 4.9b, grey colour): this was similar to the estimated total fecundity in the presence of the Allee effect (Figure 4.9b, red colour). The percentage decrease in total fecundity due to the Allee effect was 0. These results show that there is no evidence supporting the presence of the Allee effect in the mosquito population data from Dar es Salaam.

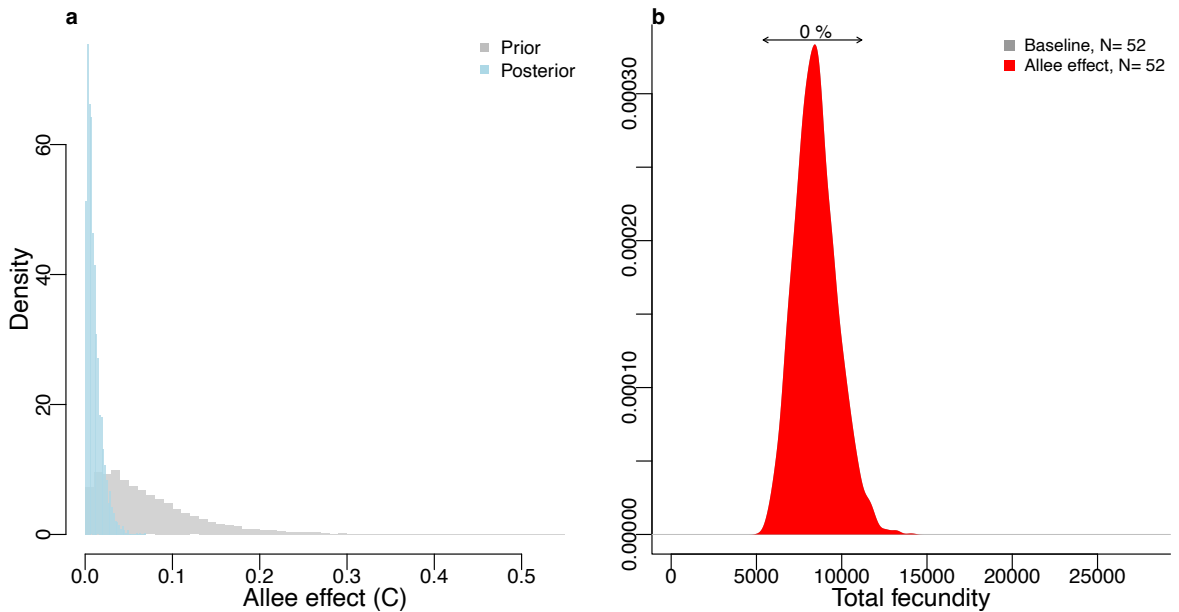


Figure 4.9: The evidence of whether Allee effects exist in the *An. gambiae* mosquito population in Dar es Salaam. Panel (a) shows priors in grey colour and posterior predictions in light blue colour for the Allee effect, C. Panel (b) shows the predicted overall mean fecundity in grey colour and overall predicted fecundity after the Allee effect in red colour, all based on an estimated average number of female adult mosquitoes across wards and weeks (i.e., N=52).

4.3.4 Larvicidal in Dar es Salam decreased mosquito abundance through reductions in larval survival

The introduction of larvicides in Dar es Salam successfully reduced female adult *An. gambiae* mosquitoes across all wards of Dar es Salaam across the different intervention phases, with 22.41% fewer mosquitoes by the end of the first phase (i.e., 107th week, Figure 4.10b), 62.07% by the end of the second phase (i.e., 154th week, Figure 4.10b) and 98.28% by the end of the third phase (i.e., 193rd week, Figure 4.10b). This reduction was driven by a decrease in larvae survival of 10.5% (95% CI, 6.88%, 14.47%; Figure 4.10a) from mean larval survival of 0.38 (95% CI, 0.35, 0.41; grey colour in Figure 4.10a) without larvicides effect compared to mean larval survival of 0.34 (95% CI, 0.31, 0.37; red colour in Figure 4.10a) due to larvicides.

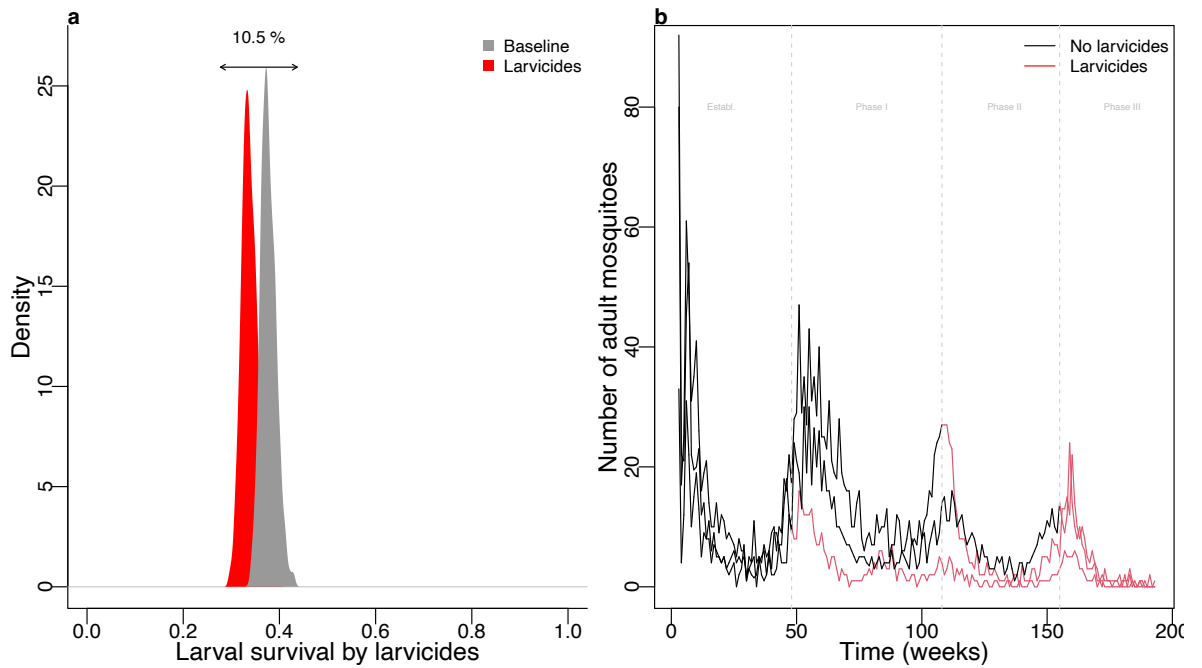


Figure 4.10: The effects of larvicides alone on larvae: (a) Histogram of estimated mean survival with (red) and without (grey) larvicides and (b) the estimated female adult mosquito abundance averaged across wards before (black) and during (red) the larvicidal programme, where each line represents the abundance per each phase of larvicide application which included a total of 3, 6, and 6 wards in the first, second and third phase, respectively.

4.4 Discussion

Regulatory mechanisms such as negative density dependence and Allee effects are fundamental for regulating population dynamics. However, the presence of Allee effects and their importance in regulating natural malaria mosquito populations remain largely unknown. Understanding Allee effects is important as it would help to enhance the effectiveness of vector control interventions and accelerate malaria elimination efforts by increasing the risk of stochastic vector extinction. To address this, a Bayesian state-space modelling framework (SSM) was developed and fitted to simulated data to identify whether the model can effectively determine the Allee effect. The framework was then fitted to field surveillance data from Dar es Salam collected during the successful large-scale larvicidal intervention to assess population dynamics and identify the presence of Allee effects in the field.

To our knowledge, this study is the first to test for the existence of Allee effects in malaria-transmitting mosquitoes in natural field settings. The developed model framework effectively identified the Allee effect in simulated data but did not find evidence of it in the field data from Dar es Salaam, Tanzania. Unlike in species such as wild animal populations where Allee effects exist (104,187), to date, no study has demonstrated evidence of Allee effects in any malaria vector species. Of course, this might be true because this is the first study to look for evidence of Allee effects in the natural mosquito population and it did not find such evidence in the Dar es Salaam setting. However, there are also other reasons for why Allee effects were not detected here. It is possible that in Dar es Salaam the population was not reduced enough to create necessary conditions for Allee effects to occur. Intrinsic or extrinsic factors, such as negative density dependence, environmental factors and vector control measures, led to a decline in mosquito population abundance (88), but the population persisted at low levels. There is still uncertainty about the amount of intervention and effort needed to reduce the natural mosquito population to levels low enough to trigger Allee effects. Although there was no Allee effect evident in Dar es Salaam data, this study laid a foundation for future research in investigating and identifying Allee effects in natural settings with low mosquito population abundance. Section 5.2 below provides a detailed information suggesting ways on how we can adapt present and

future malaria vector control programmes based on the presence or absence of regulatory mechanisms particularly Allee effects.

The absence of Allee effects is regrettable for malaria control. It will not only mean that population will not stochastically go into extinction but that sustained control efforts will be required even at very low population sizes. With surveillance being increasingly complicated at low population sizes, rebounds could occur frequently. Since we cannot completely exclude the existence of Allee effects, there is a need to design studies that can support detection of Allee effects in malaria vectors. This can be achieved through more controlled experiments in semi-field systems (SFS) that would facilitate assessing various mechanisms underlying Allee effects, such as mate limitation and predation. In these controlled environments, monitoring of population regulation processes will be more straightforward; for example, we can track the number of males in female chambers and observe how often mating occurs between males and females. Moreover, introducing predators could provide us with an opportunity to assess whether predation leads to Allee effects in malaria mosquitoes. Developing a framework to identify types of data necessary for detecting Allee effects would be beneficial, as there is currently no consensus on the required data or established experimental design for its collection. It is also proposed to divide adult stage into gravid (i.e., egg-laying) and non-gravid mosquitoes, setting that Allee effects only impact gravid mosquitoes (i.e., the development rate from non-gravid to gravid is affected by Allee effects). Additionally, to identify the presence of Allee effects using data from settings that eliminated mosquitoes, specifically focusing on periods just before elimination occurred (i.e., periods immediately preceding the elimination events): this will help to determine whether the elimination was influenced by Allee effects.

It is well known that *Anopheles* mosquito populations tend to increase during the rainy season and decrease or nearly disappear during the dry season (247-250), but the mechanisms and life history strategies behind these observed patterns are less studied. The population dynamics of *An. gambiae* mosquitoes in Dar es Salaam are believed to be mainly influenced by environmental factors such as rainfall and temperature due to the hot and humid climatic conditions (140,141). This study further supported these findings and provided some mechanistic insights for them. Specifically, cumulative rainfall and temperature positively impact larval survival,

while current rainfall leads to a flush-out effect that reduces larval survival, similar to what reported elsewhere (242,251-253).

The Bayesian state-space model (SSM) fitted to field female mosquito data from Dar es Salaam successfully predicted life history parameters of mosquitoes, including larval, pupal and adult survivals, as well as per capita fecundity. However, some of the life history parameters, particularly mean pupae survival, produced lower estimate that was pushed towards lower bound. This could be due to trade-offs in some parameters for which we were not able to capture the full mechanism. For example, with the SSM fitted to the simulated data, trade-offs existed between parameters related to Allee effects and negative density dependence versus population abundance and probability observations (pobs). Although, other parameters linked to larvae, pupae, and adult survival and fecundity remained consistent with changes in population abundance and pobs, other trade-offs between total mosquito fecundity and mean larval survival, where an increase in fecundity led to a decrease in larval survival are also well known (254). This reduction in larval survival occurred because a higher fecundity leads to a greater number of larvae, which are then subject to negative density dependence regulation. Conversely, lower fecundity leads to a smaller number of larvae, which are then associated with an increase in their survival because they experience less negative density dependence. These findings are consistent with previous studies that have shown a negative correlation between the number of eggs laid by female mosquitoes and the subsequent survival of larvae (254).

It was also found in this study that larvicidal control in Dar es Salam reduced the population size by an average of 60.92%. Importantly, this reduction was driven by a reduction in larval survival of 10.50%. Other studies have also demonstrated a notable decrease in the population of *An. gambiae* in urban Dar es Salaam due to similar large-scale community-based larvicidal control intervention (41,47). Effectiveness of vector control interventions, such as larviciding, is normally influenced by the ecology of a particular mosquito species, implying that the same intervention may not have a similar impact on multiple species (88). While larviciding effectively reduced larval survival as expected, quantifying this impact beyond population abundance is challenging. Being able to quantify mechanisms that regulate population dynamics paves the way to evaluate whether interventions in the field are typically performing as expected in laboratory

conditions or semi-field systems. The World Health Organisation (60), recommends tools with combined or dual-action interventions such as new nets treated with pyrethroid-pyriproxyfen or pyrethroid-chlorfenapyr. While in this chapter we assessed the impact of a single intervention, it provides a foundation to which we can assess the mechanisms of multi-action tools.

The results of the model showed that negative density dependence plays a critical role in population dynamics of *An. gambiae* mosquitoes. This has also been shown in a modelling study by White *et al.* which revealed the importance of the presence of negative density dependence during the larval stages of *An. gambiae* mosquitoes in the Garki District of Nigeria (92) for the overall dynamics of the population (92). However, measuring the magnitude of negative density dependence continues to be a challenge without knowing population sizes. Here, the trade-offs with the probability of observations (pobs), where the mean estimates increased with increasing pobs, were problematic. However, the overall dynamics matching the data, the ability of the model to converge all parameters and also because the estimates are consistent with other studies such as (88) and (255), provide some support. Unlike in other *Anopheles* species such as *An. funestus*, where little is known about the effect of negative density dependence due to their ecology and reliance on large and semi or permanent breeding habitats (88,256), negative density dependence in *An. gambiae* (90), which prefer temporary or small larval habitats (e.g., small water pools, which tend to appear and disappear frequently in time and space, particularly in urban settings (204)), is well known.

The findings align with a previous study that larval habitat availability increases with higher cumulative rainfall, leading to reduced or no negative density dependence (257). On the other hand, a possible reason for the absence of impact from current rainfall could be that it was neither heavy nor persistent enough to cause flooding, which is consistent with previous studies (258,259). Again, this study aligns with the previous studies that *Anopheles* mosquito development and survival are temperature-dependent (212,251). Since mosquitoes do not persist at temperatures below 16 °C (212,260,261), this study did not consider the negative impact because data had no such low values and typically in Dar es Salaam temperature ranges 24-28 °C (262), which favours mosquito survival.

There was generally poor model fit associated with low probability of observations ($p_{obs} \leq 0.01$), at a regional level. However, when looking individually at each ward, some wards fit better than others, suggesting a lot of variation in the dynamics between wards. This between-ward variability might be one of the reasons for a less good fit at the population level. The poor model fitting might also be caused by the trade-offs between p_{obs} and negative density dependence, especially when observing from a large unknown population. This trade-off affected estimation of female adult mosquito population sizes, with abundance decreasing at lower p_{obs} and increasing at higher p_{obs} . Additionally, the lack of a close match might be because we are comparing mean across multiple predictions with a single observed data series. In general, p_{obs} are linked with negative density dependence, yet we don't know well what their relationship is, whether it is a linear or non-linear relationship. Understanding this relationship is important, as it will help us understand how to develop surveillance programmes that will capture populations at the levels we want. To improve model fit and increase estimates in population abundance, we need to increase p_{obs} , which would allow sampling from a small unknown population and consequently increase model performance, but we need to be cautious not to increase p_{obs} to a level that might be unrealistic. We can also improve model performance by increasing the number of iterations where lower p_{obs} would require more iterations for better model convergence. Alternatively, additional mechanics such as the influence of environmental factors like rainfall can improve the model fitting; thus, this requires further work. It is also suggested that future work to incorporate performance curves for each of the mosquito life history parameters to visually represent and assess model performance. We note that the estimate of the Allee effect does not seem to change regardless of p_{obs} .

One of the limitations of this study is that it only used a dataset from a single setting, which may not be sufficient to provide evidence of Allee effects. Therefore, it is suggested to fit the model to data sets from multiple settings with low mosquito population densities. Another limitation is that the study only focused on a single malaria mosquito species, i.e., *An. gambiae*, therefore, it is suggested to take into account other species with similar characteristics. Additionally, the study only fitted the model to adult mosquito abundances, so it is suggested to incorporate fitting the model to data from other stages of the mosquito's life cycle, particularly the larval abundance data. On the other hand,

it is suggested to treat p_{obs} as a parameter of the model, so that the model can be given enough freedom to feasibly select from the distribution of p_{obs} . Lastly, while the study focused on the impact of a single intervention, this modelling framework is generalisable and can be further used to incorporate more data on combined interventions, such as insecticide-treated nets or indoor residual spraying.

4.5 Conclusion

The model's capability to detect Allee effects using the simulated data could be fundamentally important for identifying the presence of Allee effects when fitted to data from various low-density settings. At present, there is no evidence of Allee effects in the entomological surveillance data from Dar es Salaam, Tanzania. It is possible that the intervention did not reduce the population enough to a level at which Allee effects could kick in (i.e., to trigger Allee effects) or that there are no Allee effects in *Anopheles* populations. This modelling study provided a valuable framework that can be used for identifying Allee effects but also the mechanistic impacts of interventions using routine surveillance data collected from different settings with low mosquito population densities.

Chapter 5 General Discussion and Conclusions

Malaria is the leading vector-borne disease worldwide, claiming the lives of over a million individuals, with more than 75% of these deaths occurring in children under five years old (1,8,263). While malaria vaccines are available, they are not yet widely implemented (264). Consequently, vector control remains the most effective method for reducing malaria transmission and plays a crucial role in malaria control and elimination strategies (35). Through a combination of computer simulations and modelling of field data, my PhD research has provided valuable tools that can improve malaria vector control and enhance elimination efforts by informing the evaluation and assessment of interventions in semi-field and field settings; but also, by highlighting potential impacts of some key population regulatory mechanisms such as Allee effects and the trade-offs might have with negative density dependence as population declines. The developed tools are advantageous not only to improving malaria vector control but also can be more widely utilised to inform the control of vectors responsible for other diseases such as dengue fever, yellow fever, and chikungunya.

5.1 The role of simulations for evaluating vector control interventions.

My PhD research contributed a simulation-based power analysis framework to enhance the design of vector control experiments in SFS and used simulations to understand the role of understudied population regulatory mechanisms in *Anopheles* mosquitoes and the impact their trade-offs might have for vector control. More generally for the malaria field, simulation approaches have many advantages, such as providing support for decision-making and guiding policy directions, understanding vector ecology and population dynamics in mosquito research, or predicting transmissions in vector-borne disease. Some examples include Runge *et al.* who used simulations to assess council-specific impact of anti-malaria interventions to support malaria strategic planning efforts in Tanzania (265). Depinay *et al.* developed a simulation model focused on the ecology and population dynamics of African *Anopheles* to predict malaria transmission (128). In western Kenya, Stuckey *et al.* simulated malaria epidemiology and vector control strategies to facilitate planning for malaria control and elimination processes (266). While all these simulation-based studies were targeted against

malaria vector control and elimination strategies, simulations can also effectively be utilised in planning for control of other vector-borne diseases such as Dengue (267,268), Zika (269,270) and lymphatic filariasis (271,272). Simulations have played a significant role in historical and contemporary research activities because of their ability to predict outcomes across diverse quantitative research fields, including ecology (273), epidemiology (274) and entomology (275). For malaria vector control, simulations can help identify what kinds of data are needed from field experiments to assess the impact of population regulation mechanisms or the effectiveness of interventions or their combinations.

Similar to data-driven approaches such as the Bayesian state-space models used in this PhD thesis, which are typically important as they help us to learn anything about the real world (although they are computationally intensive as they require powerful computers and typically suffer from parameter estimation problems (276)), simulations are also important in terms of availability of computers and software needed for their implementation. In addition to determine sample sizes, combining simulations (since simulations can help to generate data that mirror dynamics of real experiments) with experimental approaches throughout all stages of field trials can also increase the quality and quantity of data by helping identify variables and potential challenges before data collection begins, e.g., through sensitivity analysis. Conducting sensitivity analysis is fundamental as it directs data collection efforts toward the most sensitive parameters by assessing how variations in these parameters influence the simulation output (277). Contemporary malaria vector control interventions, such as new generations of bed nets treated with pyrethroid-pyriproxyfen, pyrethroid-chlorfenapyr, or piperonyl butoxide-pyrethroid combinations (278,279), necessitate rigorous testing in the SFS before any small or large-scale field trials. This iterative testing process in SFS underscores the need for well-designed semi-field experiments (SFEs) to produce reliable results, and one way of doing this is by ensuring that experiments are adequately powered. The application of power analysis in SFEs is quite uncommon; this trend is attributed to the insufficient knowledge among researchers to perform necessary statistical calculations (280) and lack of software (84). Additionally, simulation results derived from mosquito population dynamics models could be used as the power analysis to inform experiments in both SFS and field settings, for instance, guiding sample size calculations or

intervention effects estimations. While other power analysis tools exist, they are often underutilised; however, as new and innovative vector control interventions emerge and the interest in eliminating malaria continues to grow, it is anticipated that these tools will become increasingly prevalent among researchers. Moreover, the power analysis framework developed in this PhD project is expected to play a crucial role in both contemporary and future research studies.

5.2 Implications of vector population regulation for malaria vector control efforts

Being able to consider mosquito population regulation factors in malaria vector control strategies is important not only to support short-term reductions of mosquito populations but crucially to ensure sustainable and effective interventions that would adapt to the naturally varying dynamics of mosquitoes. (92,281). As it was showed in Chapter 3 and Chapter 4, this is because understanding population regulation can help disentangle underlying mechanisms such as negative density dependence and Allee effects that have consequences for how we perceive each stage of the mosquito life cycle. However, their quantification using empirical data remains quite difficult (230). Partly this may be because there is an interplay with abiotic factors such as temperature and rainfall that can also play a crucial role in regulating populations and driving seasonal patterns, as well as influencing individual life history traits (282,283). From a control perspective, this interplay is important because it allows us to decide how and when to intervene, along with determining the type of intervention. My work has shown that Allee effects, despite being understudied, are important as they can profoundly impact population dynamics, and if we can learn how to leverage it, we can enhance elimination efforts, especially when vector control interventions such as larvicides decrease the population to a level where Allee effects can kick in and stochastically collapse the population. When planning present and future malaria vector control programmes, it is essential to consider Allee effects as fewer resources might achieve outcomes compared to huge investments. Exploring diverse approaches, such as modelling data from diverse ecological settings or targeting gravid mosquitoes, is essential to better understand Allee effects in malaria mosquitoes. Despite these promising theoretical findings, empirically the presence of the Allee effect could not be determined in the local mosquito population from Dar es Salaam. However, it is

important to note that it is too early in drawing a definitive conclusion about the absence of the Allee effect at this stage because only data from a single setting, where the population might not have been small enough, was tested. Finding ways to monitor and assess low mosquito population abundances becomes ever more important as we achieve control success, for example in Zanzibar (284-286) and Rwanda (287-290). These circumstances can create an opportunity to detect Allee effects more readily.

The World Health Organisation suggests incorporating vector biology into vector control, as successful vector control depends much on a comprehensive understanding of vector ecology (291); consequently, population regulatory mechanisms should become a key component of this approach. For instance, we know that in the absence of negative density dependence, population sizes would be much larger. Therefore, it is essential to start planning when to intervene relative to these regulatory mechanisms, particularly when the population is unstable, just before it reaches its peak, or during a decline. Although surveillance becomes challenging as the population decreases, this moment might be most important because two scenarios might happen: (i) further declines could occur, potentially leading to Allee effects, or (ii) the population might recover due to negative density dependence, something that we want to prevent. Allee effects have been documented across a range of biological systems, including birds (98-100), fish (101-103), mammals (104-106), reptiles or amphibians (107) and other aquatic (97,108,109) and terrestrial invertebrates (110-113). We can learn lessons for malaria vector control from these systems where they could identify Allee effects. Examples of lessons include introducing predators in both immature and adult stages, discouraging female mosquito feeding success and releasing transgenic mosquitoes. Beyond negative density dependence and Allee effects, other mechanisms regulating mosquito populations exist, including ageing, predation (sometimes categorised as one of the causative mechanisms of Allee effects (292)) and migration. There is potential and need to explore other mechanisms of how populations are regulated in natural environments and the implications this has for malaria vector control and elimination efforts. For example, ageing is the gradual decline in the physical condition of the body which leads to the decrease in immune proficiency and alters key life stages such as reproduction output (293,294). Together these affect overall population dynamics

but also vectorial capacity and transmission of diseases (294-296). Similarly, migration; movement of mosquitoes over long distances can be accelerated by wind patterns, which can carry them from one geographical location to another, seeking suitable conditions for breeding and feeding (297-299). For example, a study has shown that persistence of malaria in the Sahel where surface water is absent for up to eight months is due to *Anopheles* mosquitoes migrating over long distances (298). Therefore, identifying and controlling sources of migratory mosquitoes is necessary for successful vector control programmes and elimination efforts (298).

5.3 Leveraging population dynamics modelling for effective malaria vector control

Population dynamics models provide an understanding of how populations change over time, e.g., vector populations, species communities, and ecosystems, as they define the system's complexity without directly disrupting it (121,122). They can also be used to identify the ecological behaviours of a population, provide predictions of current and future trends of populations and estimate parameter space where empirical data is absent or limited. Because of their strength in providing descriptions, explanations, and predictions of phenomena (such as growth, reproduction, or disease transmission from one stage to another), population dynamics models have been used to estimate the impact of vector control interventions (e.g., (92,123,300)). Consequently, they have been used by researchers, national malaria control programs, and policymakers to inform decision-making for malaria control programs (301,302). In this thesis, a framework has been developed, that quantified mosquito life histories and, importantly, the impacts of interventions on these life history parameters. This framework provides underlying mechanisms of action of interventions. While these mechanisms are often well known from laboratory studies, in semi-field and especially field settings, the environments and local ecologies interact, thus, what we observe in the laboratory might not translate in the field. However, with larviciding, the mechanisms were very well known, in that it leads to the reduction of larval survival, for other interventions; the mode of action is not as clearly defined. These models were developed before to determine the impact of intervention in the semi-field systems (255); however, they have never been tried for a similar objectives in field settings. In addition, an overall reduction in

mosquito population was generally quantified by assessing the mechanisms leading to that reduction. This framework is generalisable for any intervention but could be even more useful for combined or dual-action interventions as it has the ability to quantify effects on different life history parameters. Beyond determining the mechanism of action of interventions, understanding variation in the life history of populations could provide insights into population vulnerabilities, which we can leverage for vector control strategies. The same modelling framework developed here can be used to quantify the impact of these factors in controlled laboratory settings or semi-field systems. Recent advancements in innovative technologies, such as gene drive, are emerging as promising measures for vector control and malaria elimination (303,304). By integrating these innovative technologies with population dynamics modelling, we can better predict their substantial outcomes, identify essential information for their improvement, and inform the optimal implementation strategies for these technologies. Apart from malaria vector control, population dynamics models have also been used to inform control of other vectors, including agricultural pest management (305,306), tick control (307), tsetse fly management (308,309), and control of *Simulium damnosum s.l* which causes onchocerciasis (also known as river blindness disease) (310).

5.4 Future work

The development of a unified pipeline to inform the design of interventions and guide the collection of data across all levels of intervention testing (i.e., from laboratory to semi-field and field settings), and then analyse the data to assess the efficiency of the interventions would be an important step change in how we conduct interventions and assessments. Additionally, it is essential to develop a dynamic feedback framework where different types of simulations provide feedback to the field, and field trials, in turn, offer insights back into the simulations. This iterative feedback loop is vital for enhancing the quality, accuracy, effectiveness and continuous improvement of simulations while simultaneously optimising the deployment of interventions in the field.

Developing a framework to identify types of data necessary for detecting Allee effects would be beneficial, as there is currently no consensus on the required data or established experimental design for its collection. It is also proposed to divide adult stage into gravid (i.e., egg-laying) and non-gravid mosquitoes, setting

that Allee effects only impact gravid mosquitoes (i.e., the development rate from non-gravid to gravid is affected by Allee effects). Additionally, to identify the presence of Allee effects using data from settings that eliminated mosquitoes, specifically focusing on periods just before elimination occurred (i.e., periods immediately preceding the elimination events): this will help to determine whether the elimination was influenced by Allee effects.

Moreover, it is proposed that future research explore mosquito's life history parameters and their potential non-linear relationships with environmental variables. Considering non-linear relationships reflects the complexities of ecological and climatic interactions necessary for vector control and control interventions. Due to the increasing potential of new technologies, it is proposed the use of population dynamics models to inform the impact of gene drive technology in malaria and malaria vector control. Lastly, it is proposed to create awareness at the stakeholder levels, including researchers, communities and policymakers, about the effect of population regulation factors that can contradict predictions and outcomes of field trials.

5.5 Conclusions

This PhD work covered multiple aspects, from the evaluation to the assessment of malaria vector control interventions through the use of theoretical and statistical modelling approaches. Ways to improve the designs of vector control semi-field experiments through the use of simulation-based power analysis methods were demonstrated. Since power analysis methods are not commonly used due to a lack of technical knowledge and software, the framework and R tutorials developed here will help researchers better understand and investigate step-by-step the trade-offs between the power of their studies and resource allocation. Additionally, the work involved modelling the population dynamics of *An. gambiae* mosquitoes will help researchers to understand the trade-offs between negative density dependence and Allee effects and their underlying consequences for malaria vector control. Lastly, Bayesian state-space models have been developed and fitted to the field data to assess the evidence of the Allee effect in natural *An. gambiae* mosquito populations. Although interventions are very important in regulating vector population dynamics, it has been demonstrated that negative density dependence alongside sustained interventions also play a paramount role

in reducing vector abundances. While there was no evidence of the Allee effect in the *An. gambiae* mosquito populations in Dar es Salaam, this study cannot generalise that Allee effects never exist in malaria mosquitoes; instead, it suggests that more data from different settings with low densities must be tested. The methods and findings presented in this PhD will help future research to evaluate vector control interventions in semi-field systems and assess their efficacies in field settings by determining the trade-offs between statistical power and resource allocation, as well as identifying the mechanisms that regulate mosquito populations.

Chapter 6 List of Appendices

Appendix A Supplementary materials for Chapter 2

Appendix A.1 List of articles selected for a simple review of the use of power to justify the sample size.

Here is the list of articles selected for simple review to assess whether they used power analysis to justify their sample size. A total of 38 articles (19 from Malaria Journal and 19 from Parasites & Vectors) published between 2020 to 2023 that comprise SFE studies (n=25) or hut trials (n=13) which would have been eligible for power analysis were selected. In the Malaria Journal 26% of articles used power while 74% did not, and in the Journal of Parasite & Vectors power 32% used power while 68% did not. Total in both journals combined, 29% of articles used power while 71% did not.

1. Vajda, É.A., Saeung, M., Ross, A. *et al.* A semi-field evaluation in Thailand of the use of human landing catches (HLC) versus human-baited double net trap (HDN) for assessing the impact of a volatile pyrethroid spatial repellent and pyrethroid-treated clothing on *Anopheles minimus* landing. *Malar J* 22, 202 (2023). <https://doi.org/10.1186/s12936-023-04619-x>
2. Muyaga, L.L., Meza, F.C., Kahamba, N.F. *et al.* Effects of vegetation densities on the performance of attractive targeted sugar baits (ATSBs) for malaria vector control: a semi-field study. *Malar J* 22, 190 (2023). <https://doi.org/10.1186/s12936-023-04625-z>
3. Chanda, J., Wagman, J., Chanda, B. *et al.* Feeding rates of malaria vectors from a prototype attractive sugar bait station in Western Province, Zambia: results of an entomological validation study. *Malar J* 22, 70 (2023). <https://doi.org/10.1186/s12936-023-04491-9>
4. Gleave, K., Guy, A., Mechan, F. *et al.* Impacts of dual active-ingredient bed nets on the behavioural responses of pyrethroid resistant *Anopheles gambiae* determined by room-scale infrared video tracking. *Malar J* 22, 132 (2023). <https://doi.org/10.1186/s12936-023-04548-9>
5. Swai, J.K., Kibondo, U.A., Ntabaliba, W.S. *et al.* CDC light traps underestimate the protective efficacy of an indoor spatial repellent against bites from wild *Anopheles arabiensis* mosquitoes in Tanzania. *Malar J* 22, 141 (2023). <https://doi.org/10.1186/s12936-023-04568-5>
6. Mmbando, A.S., Mponzi, W.P., Ngowo, H.S. *et al.* Small-scale field evaluation of transfluthrin-treated eave ribbons and sandals for the control of malaria vectors in rural Tanzania. *Malar J* 22, 43 (2023). <https://doi.org/10.1186/s12936-023-04476-8>
7. Yohana, R., Chisulumi, P.S., Kidima, W. *et al.* Anti-mosquito properties of *Pelargonium roseum* (Geraniaceae) and *Juniperus virginiana* (Cupressaceae) essential oils against dominant malaria vectors in Africa. *Malar J* 21, 219 (2022). <https://doi.org/10.1186/s12936-022-04220-8>

8. Govoetchan, R., Fongnikin, A., Syme, T. *et al.* VECTRONE™ T500, a new broflanilide insecticide for indoor residual spraying, provides prolonged control of pyrethroid-resistant malaria vectors. *Malar J* **21**, 324 (2022). <https://doi.org/10.1186/s12936-022-04336-x>
9. Mmbando, A.S., Bradley, J., Kazimbaya, D. *et al.* The effect of light and ventilation on house entry by *Anopheles arabiensis* sampled using light traps in Tanzania: an experimental hut study. *Malar J* **21**, 36 (2022). <https://doi.org/10.1186/s12936-022-04063-3>
10. Tambwe, M.M., Moore, S., Hofer, L. *et al.* Transfluthrin eave-positioned targeted insecticide (EPTI) reduces human landing rate (HLR) of pyrethroid resistant and susceptible malaria vectors in a semi-field simulated peridomestic space. *Malar J* **20**, 357 (2021). <https://doi.org/10.1186/s12936-021-03880-2>
11. Kaindo, E.W., Mmbando, A.S., Shirima, R. *et al.* Insecticide-treated eave ribbons for malaria vector control in low-income communities. *Malar J* **20**, 415 (2021). <https://doi.org/10.1186/s12936-021-03945-2>
12. Mbuba, E., Odufuwa, O.G., Tenywa, F.C. *et al.* Single blinded semi-field evaluation of MAÏA® topical repellent ointment compared to unformulated 20% DEET against *Anopheles gambiae*, *Anopheles arabiensis* and *Aedes aegypti* in Tanzania. *Malar J* **20**, 12 (2021). <https://doi.org/10.1186/s12936-020-03461-9>
13. Osoro, J.K., Machani, M.G., Ochomo, E. *et al.* Insecticide resistance exerts significant fitness costs in immature stages of *Anopheles gambiae* in western Kenya. *Malar J* **20**, 259 (2021). <https://doi.org/10.1186/s12936-021-03798-9>
14. Nignan, C., Niang, A., Maïga, H. *et al.* Comparison of swarming, mating performance and longevity of males *Anopheles coluzzii* between individuals fed with different natural fruit juices in laboratory and semi-field conditions. *Malar J* **19**, 173 (2020). <https://doi.org/10.1186/s12936-020-03248-y>
15. Martin, N.J., Nam, V.S., Lover, A.A. *et al.* The impact of transfluthrin on the spatial repellency of the primary malaria mosquito vectors in Vietnam: *Anopheles dirus* and *Anopheles minimus*. *Malar J* **19**, 9 (2020). <https://doi.org/10.1186/s12936-019-3092-4>
16. Sangoro, O.P., Gavana, T., Finda, M. *et al.* Evaluation of personal protection afforded by repellent-treated sandals against mosquito bites in south-eastern Tanzania. *Malar J* **19**, 148 (2020). <https://doi.org/10.1186/s12936-020-03215-7>
17. Cribellier, A., Spitzen, J., Fairbairn, H. *et al.* Lure, retain, and catch malaria mosquitoes. How heat and humidity improve odour-baited trap performance. *Malar J* **19**, 357 (2020). <https://doi.org/10.1186/s12936-020-03403-5>
18. Kemibala, E.E., Mafra-Neto, A., Dekker, T. *et al.* A zooprophyllaxis strategy using L-lactic acid (Abate) to divert host-seeking malaria vectors from human host to treated non-host animals. *Malar J* **19**, 52 (2020). <https://doi.org/10.1186/s12936-020-3136-9>
19. Musa, J.J., Moore, S., Moore, J. *et al.* Long-lasting insecticidal nets retain bio-efficacy after 5 years of storage: implications for malaria control programmes. *Malar J* **19**, 110 (2020). <https://doi.org/10.1186/s12936-020-03183-y>
20. Zahouli, J.Z.B., Dibo, J.D., Diakaridia, F. *et al.* Semi-field evaluation of the space spray efficacy of Fludora Co-Max EW against wild insecticide-resistant *Aedes aegypti* and *Culex quinquefasciatus* mosquito populations from Abidjan, Côte d'Ivoire. *Parasites Vectors* **16**, 47 (2023). <https://doi.org/10.1186/s13071-022-05572-5>

21. Maasayi, M.S., Machange, J.J., Kamande, D.S. *et al.* The MTego trap: a potential tool for monitoring malaria and arbovirus vectors. *Parasites Vectors* **16**, 212 (2023). <https://doi.org/10.1186/s13071-023-05835-9>
22. Tia, I.Z., Barreaux, A.M.G., Oumbouke, W.A. *et al.* Efficacy of a ‘lethal house lure’ against *Culex quinquefasciatus* from Bouaké city, Côte d’Ivoire. *Parasites Vectors* **16**, 300 (2023). <https://doi.org/10.1186/s13071-023-05883-1>
23. Tambwe, M.M., Kibondo, U.A., Odufuwa, O.G. *et al.* Human landing catches provide a useful measure of protective efficacy for the evaluation of volatile pyrethroid spatial repellents. *Parasites Vectors* **16**, 90 (2023). <https://doi.org/10.1186/s13071-023-05685-5>
24. Sarwar, M.S., Jahan, N., Ali, A. *et al.* Establishment of *Wolbachia* infection in *Aedes aegypti* from Pakistan via embryonic microinjection and semi-field evaluation of general fitness of resultant mosquito population. *Parasites Vectors* **15**, 191 (2022). <https://doi.org/10.1186/s13071-022-05317-4>
25. Njoroge, M.M., Hiscox, A., Saddler, A. *et al.* Less is more: repellent-treated fabric strips as a substitute for full screening of open eave gaps for indoor and outdoor protection from malaria mosquito bites. *Parasites Vectors* **15**, 259 (2022). <https://doi.org/10.1186/s13071-022-05384-7>
26. Pauly, I., Jakoby, O. & Becker, N. Efficacy of native cyclopoid copepods in biological vector control with regard to their predatory behavior against the Asian tiger mosquito, *Aedes albopictus*. *Parasites Vectors* **15**, 351 (2022). <https://doi.org/10.1186/s13071-022-05460-y>
27. Mbewe, N.J., Rowland, M.W., Snetselaar, J. *et al.* Efficacy of bednets with dual insecticide-treated netting (Interceptor® G2) on side and roof panels against *Anopheles arabiensis* in north-eastern Tanzania. *Parasites Vectors* **15**, 326 (2022). <https://doi.org/10.1186/s13071-022-05454-w>
28. Kibondo, U.A., Odufuwa, O.G., Ngonyani, S.H. *et al.* Influence of testing modality on bioefficacy for the evaluation of Interceptor® G2 mosquito nets to combat malaria mosquitoes in Tanzania. *Parasites Vectors* **15**, 124 (2022). <https://doi.org/10.1186/s13071-022-05207-9>
29. Tambwe, M.M., Saddler, A., Kibondo, U.A. *et al.* Semi-field evaluation of the exposure-free mosquito electrocuting trap and BG-Sentinel trap as an alternative to the human landing catch for measuring the efficacy of transfluthrin emanators against *Aedes aegypti*. *Parasites Vectors* **14**, 265 (2021). <https://doi.org/10.1186/s13071-021-04754-x>
30. Bokore, G.E., Svenberg, L., Tamre, R. *et al.* Grass-like plants release general volatile cues attractive for gravid *Anopheles gambiae* sensu stricto mosquitoes. *Parasites Vectors* **14**, 552 (2021). <https://doi.org/10.1186/s13071-021-04939-4>
31. Njoroge, M.M., Fillinger, U., Saddler, A. *et al.* Evaluating putative repellent ‘push’ and attractive ‘pull’ components for manipulating the odour orientation of host-seeking malaria vectors in the peri-domestic space. *Parasites Vectors* **14**, 42 (2021). <https://doi.org/10.1186/s13071-020-04556-7>
32. Nambunga, I.H., Msugupakulya, B.J., Hape, E.E. *et al.* Wild populations of malaria vectors can mate both inside and outside human dwellings. *Parasites Vectors* **14**, 514 (2021). <https://doi.org/10.1186/s13071-021-04989-8>
33. Tambwe, M.M., Moore, S.J., Chilumba, H. *et al.* Semi-field evaluation of freestanding transfluthrin passive emanators and the BG sentinel trap as a “push-pull control strategy” against *Aedes aegypti* mosquitoes. *Parasites Vectors* **13**, 392 (2020). <https://doi.org/10.1186/s13071-020-04263-3>

34. Sippy, R., Rivera, G.E., Sanchez, V. *et al.* Ingested insecticide to control *Aedes aegypti*: developing a novel dried attractive toxic sugar bait device for intra-domiciliary control. *Parasites Vectors* **13**, 78 (2020). <https://doi.org/10.1186/s13071-020-3930-9>
35. Hughes, A., Lissenden, N., Viana, M. *et al.* *Anopheles gambiae* populations from Burkina Faso show minimal delayed mortality after exposure to insecticide-treated nets. *Parasites Vectors* **13**, 17 (2020). <https://doi.org/10.1186/s13071-019-3872-2>
36. Kathet, S., Sudi, W., Mwingira, V. *et al.* Efficacy of 3D screens for sustainable mosquito control: a semi-field experimental hut evaluation in northeastern Tanzania. *Parasites Vectors* **16**, 417 (2023). <https://doi.org/10.1186/s13071-023-06032-4>
37. Cozzarolo, CS., Pigeault, R., Isaïa, J. *et al.* Experiment in semi-natural conditions did not confirm the influence of malaria infection on bird attractiveness to mosquitoes. *Parasites Vectors* **15**, 187 (2022). <https://doi.org/10.1186/s13071-022-05292-w>
38. Fongnikin, A., Houeto, N., Agbevo, A. *et al.* Efficacy of Fludora® Fusion (a mixture of deltamethrin and clothianidin) for indoor residual spraying against pyrethroid-resistant malaria vectors: laboratory and experimental hut evaluation. *Parasites Vectors* **13**, 466 (2020). <https://doi.org/10.1186/s13071-020-04341-6>

Appendix B Supplementary materials for Chapter 3

Appendix B.1 Dynamics of female adult *An. gambiae* mosquito data from the field

This figure was brought here because it represents the dynamics that was mimicked in the development of state-structured population model in Chapter 3.

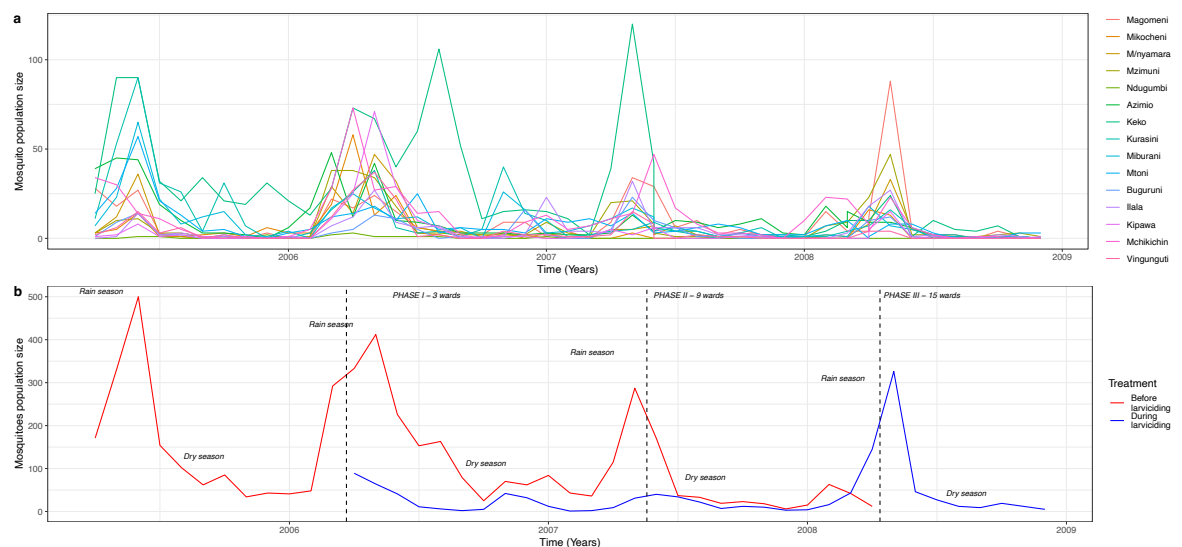


Figure B.1: An illustration of the adult *An. gambiae* mosquito population abundances aggregated monthly from 2005-2009 (a) per ward and (b) across wards before and during large-scale larvicidal control in Dar es Salaam, Tanzania.

Appendix B.2 Weekly rainfall across wards during the large scale larvicidal control programme in Dar es Salaam

This figure brought here to show how dynamics of data simulated from the model in Chapter 3 match the dynamics of the rainfall (none centred).

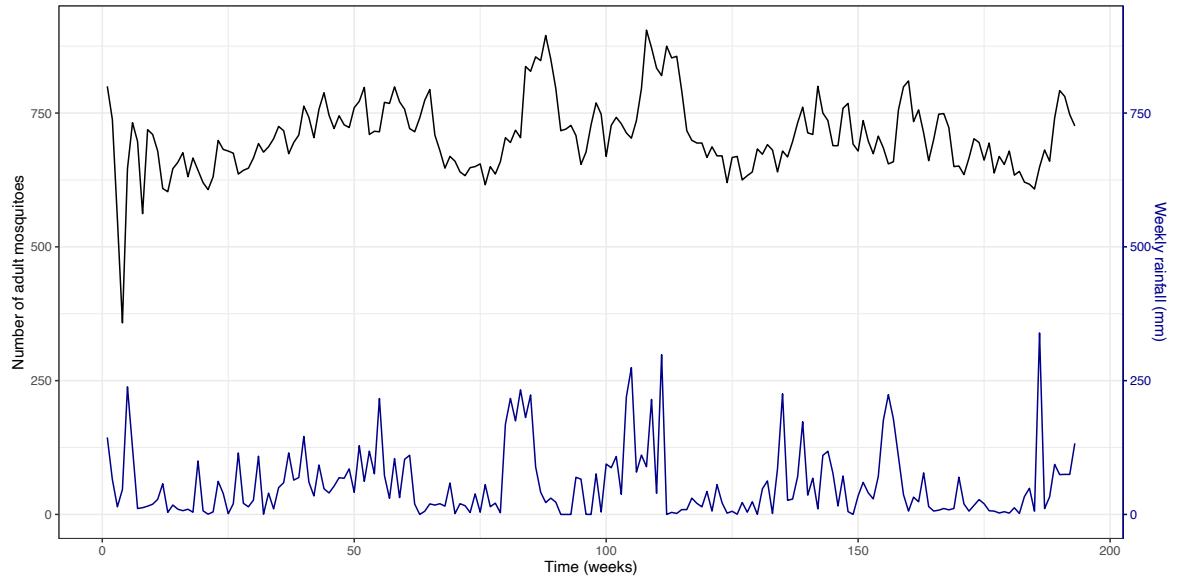


Figure B.2: Average weekly rainfall across wards (black) and population dynamics without intervention (blue) during the large-scale larvicidal control in Dar es Salaam, Tanzania.

Appendix B.3 Figure showing centered average weekly rainfall across wards (black) and population dynamics without intervention (blue) during the large-scale larvicidal control in Dar es Salaam, Tanzania

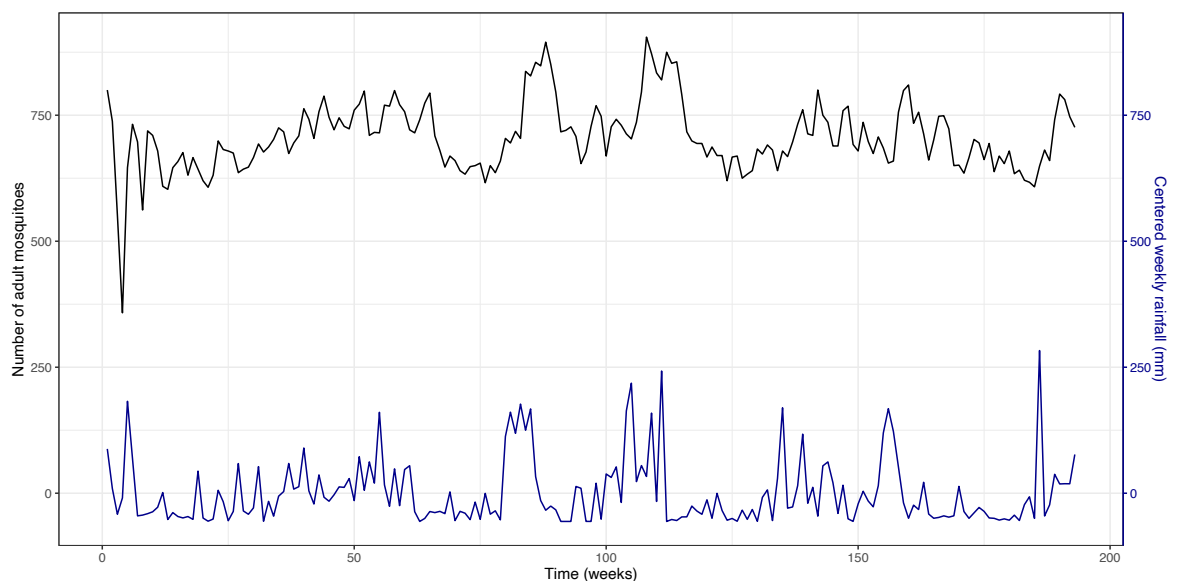


Figure B.3: Illustration of how dynamics of data simulated from the model in Chapter 3 match the dynamics of the centred rainfall.

Appendix B.4 Tables of selected combinations of negative density dependence (DD), the Allee effect variations (AE) and Larvicides application (LA)

Table B.4.1: Study variables and scenarios used for sustained and short-termed intervention

Study variables and scenarios		Simulated values			
Sustained larvicidal intervention		48 th to 193 rd week			
Short-termed larvicidal intervention (single short application)		48 th to 130 th week			
Short-termed larvicidal intervention (two short applications)		48 th to 80 th and 121 st to 150 th week			
Negative density dependence levels i.e., DD1, DD2 and DD3 (when Allee effect set to 360)		0, 2.75e-05, 5.5e-05, 2.2e-04			
The Allee effect levels i.e., AE1, AE2 and AE3 (when negative density dependence set to 5.5e-05)		0, 180, 360 and 720			
All combinations of negative density dependence and the Allee effect variations (AE,DD)					
The Allee effect (AE)	Negative density dependence (DD)				
		0	2.75e-05	5.5e-05	2.2e-04
	0	(0,0)	(0, 2.75e-05)	(0, 5.5e-05)	(0, 2.2e-04)
	180	(180,0)	(180, 2.75e-05)	(180, 5.5e-05)	(180, 2.2e-04)
	360	(360,0)	(360, 2.75e-05)	(360, 5.5e-05)	(360, 2.2e-04)
	720	(720,0)	(720, 2.75e-05)	(720, 5.5e-05)	(720, 2.2e-04)

Table B.4.2: Table of all combinations of variations in negative density dependence and the Allee effect varied from 100% increase to 100% decrease

AE \ DD	0	36	72	108	144	180	216	252	288	324	360	396	432	468	504	540	576	612	648	684	720
---------	---	----	----	-----	-----	-----	-----	-----	-----	-----	------------	-----	-----	-----	-----	-----	-----	-----	-----	-----	-----

5.5 e- 06	5.5 e- 06, 0	5.5 e- 06, 36	5.5 e- 06, 72	5.5 e- 06, 108	5.5 e- 06, 144	5.5 e- 06, 180	5.5 e- 06, 216	5.5 e- 06, 252	5.5 e- 06, 288	5.5 e- 06, 324	5.5 e- 06, 360	5.5 e- 06, 396	5.5 e- 06, 432	5.5 e- 06, 468	5.5 e- 06, 504	5.5 e- 06, 540	5.5 e- 06, 576	5.5 e- 06, 612	5.5 e- 06, 648	5.5 e- 06, 684	5.5 e- 06, 720
1.1 e- 05	1.1 e- 05, 0	1.1 e- 05, 36	1.1 e- 05, 72	1.1 e- 05, 108	1.1 e- 05, 144	1.1 e- 05, 180	1.1 e- 05, 216	1.1 e- 05, 252	1.1 e- 05, 288	1.1 e- 05, 324	1.1 e- 05, 360	1.1 e- 05, 396	1.1 e- 05, 432	1.1 e- 05, 468	1.1 e- 05, 504	1.1 e- 05, 540	1.1 e- 05, 576	1.1 e- 05, 612	1.1 e- 05, 648	1.1 e- 05, 684	1.1 e- 05, 720
1.6 5- 05	1.6 5- 05, 0	1.6 5- 05, 36	1.6 5- 05, 72	1.6 5- 05, 108	1.6 5- 05, 144	1.6 5- 05, 180	1.6 5- 05, 216	1.6 5- 05, 252	1.6 5- 05, 288	1.6 5- 05, 324	1.6 5- 05, 360	1.6 5- 05, 396	1.6 5- 05, 432	1.6 5- 05, 468	1.6 5- 05, 504	1.6 5- 05, 540	1.6 5- 05, 576	1.6 5- 05, 612	1.6 5- 05, 648	1.6 5- 05, 684	1.6 5- 05, 720
2.2 e- 05	2.2 e- 05, 0	2.2 e- 05, 36	2.2 e- 05, 72	2.2 e- 05, 108	2.2 e- 05, 144	2.2 e- 05, 180	2.2 e- 05, 216	2.2 e- 05, 252	2.2 e- 05, 288	2.2 e- 05, 324	2.2 e- 05, 360	2.2 e- 05, 396	2.2 e- 05, 432	2.2 e- 05, 468	2.2 e- 05, 504	2.2 e- 05, 540	2.2 e- 05, 576	2.2 e- 05, 612	2.2 e- 05, 648	2.2 e- 05, 684	2.2 e- 05, 720
2.7 5e- 05	2.7 5e- 05, 0	2.7 5e- 05, 36	2.7 5e- 05, 72	2.7 5e- 05, 108	2.7 5e- 05, 144	2.7 5e- 05, 180	2.7 5e- 05, 216	2.7 5e- 05, 252	2.7 5e- 05, 288	2.7 5e- 05, 324	2.7 5e- 05, 360	2.7 5e- 05, 396	2.7 5e- 05, 432	2.7 5e- 05, 468	2.7 5e- 05, 504	2.7 5e- 05, 540	2.7 5e- 05, 576	2.7 5e- 05, 612	2.7 5e- 05, 648	2.7 5e- 05, 684	2.7 5e- 05, 720
3.3 e- 05	3.3 e- 05, 0	3.3 e- 05, 36	3.3 e- 05, 72	3.3 e- 05, 108	3.3 e- 05, 144	3.3 e- 05, 180	3.3 e- 05, 216	3.3 e- 05, 252	3.3 e- 05, 288	3.3 e- 05, 324	3.3 e- 05, 360	3.3 e- 05, 396	3.3 e- 05, 432	3.3 e- 05, 468	3.3 e- 05, 504	3.3 e- 05, 540	3.3 e- 05, 576	3.3 e- 05, 612	3.3 e- 05, 648	3.3 e- 05, 684	3.3 e- 05, 720
3.8 5e- 05	3.8 5e- 05, 0	3.8 5e- 05, 36	3.8 5e- 05, 72	3.8 5e- 05, 108	3.8 5e- 05, 144	3.8 5e- 05, 180	3.8 5e- 05, 216	3.8 5e- 05, 252	3.8 5e- 05, 288	3.8 5e- 05, 324	3.8 5e- 05, 360	3.8 5e- 05, 396	3.8 5e- 05, 432	3.8 5e- 05, 468	3.8 5e- 05, 504	3.8 5e- 05, 540	3.8 5e- 05, 576	3.8 5e- 05, 612	3.8 5e- 05, 648	3.8 5e- 05, 684	3.8 5e- 05, 720

4.4 e- 05	4.4 e- 05, 0	4.4 e- 05, 36	4.4 e- 05, 72	4.4 e- 05, 108	4.4 e- 05, 144	4.4 e- 05, 180	4.4 e- 05, 216	4.4 e- 05, 252	4.4 e- 05, 288	4.4 e- 05, 324	4.4 e- 05, 360	4.4 e- 05, 396	4.4 e- 05, 432	4.4 e- 05, 468	4.4 e- 05, 504	4.4 e- 05, 540	4.4 e- 05, 576	4.4 e- 05, 612	4.4 e- 05, 648	4.4 e- 05, 684	4.4 e- 05, 720
4.9 5e- 05	4.9 5e- 05, 0	4.9 5e- 05, 36	4.9 5e- 05, 72	4.9 5e- 05, 108	4.9 5e- 05, 144	4.9 5e- 05, 180	4.9 5e- 05, 216	4.9 5e- 05, 252	4.9 5e- 05, 288	4.9 5e- 05, 324	4.9 5e- 05, 360	4.9 5e- 05, 396	4.9 5e- 05, 432	4.9 5e- 05, 468	4.9 5e- 05, 504	4.9 5e- 05, 540	4.9 5e- 05, 576	4.9 5e- 05, 612	4.9 5e- 05, 648	4.9 5e- 05, 684	4.9 5e- 05, 720
5.5 e- 05	5.5 e- 05, 0	5.5 e- 05, 36	5.5 e- 05, 72	5.5 e- 05, 108	5.5 e- 05, 144	5.5 e- 05, 180	5.5 e- 05, 216	5.5 e- 05, 252	5.5 e- 05, 288	5.5 e- 05, 324	5.5 e- 05, 360	5.5 e- 05, 396	5.5 e- 05, 432	5.5 e- 05, 468	5.5 e- 05, 504	5.5 e- 05, 540	5.5 e- 05, 576	5.5 e- 05, 612	5.5 e- 05, 648	5.5 e- 05, 684	5.5 e- 05, 720
6.0 5e- 05	6.0 5e- 05, 0	6.0 5e- 05, 36	6.0 5e- 05, 72	6.0 5e- 05, 108	6.0 5e- 05, 144	6.0 5e- 05, 180	6.0 5e- 05, 216	6.0 5e- 05, 252	6.0 5e- 05, 288	6.0 5e- 05, 324	6.0 5e- 05, 360	6.0 5e- 05, 396	6.0 5e- 05, 432	6.0 5e- 05, 468	6.0 5e- 05, 504	6.0 5e- 05, 540	6.0 5e- 05, 576	6.0 5e- 05, 612	6.0 5e- 05, 648	6.0 5e- 05, 684	6.0 5e- 05, 720
6.6 e- 05	6.6 e- 05, 0	6.6 e- 05, 36	6.6 e- 05, 72	6.6 e- 05, 108	6.6 e- 05, 144	6.6 e- 05, 180	6.6 e- 05, 216	6.6 e- 05, 252	6.6 e- 05, 288	6.6 e- 05, 324	6.6 e- 05, 360	6.6 e- 05, 396	6.6 e- 05, 432	6.6 e- 05, 468	6.6 e- 05, 504	6.6 e- 05, 540	6.6 e- 05, 576	6.6 e- 05, 612	6.6 e- 05, 648	6.6 e- 05, 684	6.6 e- 05, 720
7.1 5e- 05	7.1 5e- 05, 0	7.1 5e- 05, 36	7.1 5e- 05, 72	7.1 5e- 05, 108	7.1 5e- 05, 144	7.1 5e- 05, 180	7.1 5e- 05, 216	7.1 5e- 05, 252	7.1 5e- 05, 288	7.1 5e- 05, 324	7.1 5e- 05, 360	7.1 5e- 05, 396	7.1 5e- 05, 432	7.1 5e- 05, 468	7.1 5e- 05, 504	7.1 5e- 05, 540	7.1 5e- 05, 576	7.1 5e- 05, 612	7.1 5e- 05, 648	7.1 5e- 05, 684	7.1 5e- 05, 720
7.7 e- 05	7.7 e- 05, 0	7.7 e- 05, 36	7.7 e- 05, 72	7.7 e- 05, 108	7.7 e- 05, 144	7.7 e- 05, 180	7.7 e- 05, 216	7.7 e- 05, 252	7.7 e- 05, 288	7.7 e- 05, 324	7.7 e- 05, 360	7.7 e- 05, 396	7.7 e- 05, 432	7.7 e- 05, 468	7.7 e- 05, 504	7.7 e- 05, 540	7.7 e- 05, 576	7.7 e- 05, 612	7.7 e- 05, 648	7.7 e- 05, 684	7.7 e- 05, 720

8.2 5e- 05	8.2 5e- 05, 0	8.2 5e- 05, 36	8.2 5e- 05, 72	8.2 5e- 05, 108	8.2 5e- 05, 144	8.2 5e- 05, 180	8.2 5e- 05, 216	8.2 5e- 05, 252	8.2 5e- 05, 288	8.2 5e- 05, 324	8.2 5e- 05, 360	8.2 5e- 05, 396	8.2 5e- 05, 432	8.2 5e- 05, 468	8.2 5e- 05, 504	8.2 5e- 05, 540	8.2 5e- 05, 576	8.2 5e- 05, 612	8.2 5e- 05, 648	8.2 5e- 05, 684	8.2 5e- 05, 720
8.8 e- 05	8.8 e- 05, 0	8.8 e- 05, 36	8.8 e- 05, 72	8.8 e- 05, 108	8.8 e- 05, 144	8.8 e- 05, 180	8.8 e- 05, 216	8.8 e- 05, 252	8.8 e- 05, 288	8.8 e- 05, 324	8.8 e- 05, 360	8.8 e- 05, 396	8.8 e- 05, 432	8.8 e- 05, 468	8.8 e- 05, 504	8.8 e- 05, 540	8.8 e- 05, 576	8.8 e- 05, 612	8.8 e- 05, 648	8.8 e- 05, 684	8.8 e- 05, 720
9.3 5e- 05	9.3 5e- 05, 0	9.3 5e- 05, 36	9.3 5e- 05, 72	9.3 5e- 05, 108	9.3 5e- 05, 144	9.3 5e- 05, 180	9.3 5e- 05, 216	9.3 5e- 05, 252	9.3 5e- 05, 288	9.3 5e- 05, 324	9.3 5e- 05, 360	9.3 5e- 05, 396	9.3 5e- 05, 432	9.3 5e- 05, 468	9.3 5e- 05, 504	9.3 5e- 05, 540	9.3 5e- 05, 576	9.3 5e- 05, 612	9.3 5e- 05, 648	9.3 5e- 05, 684	9.3 5e- 05, 720
9.9 e- 05	9.9 e- 05, 0	9.9 e- 05, 36	9.9 e- 05, 72	9.9 e- 05, 108	9.9 e- 05, 144	9.9 e- 05, 180	9.9 e- 05, 216	9.9 e- 05, 252	9.9 e- 05, 288	9.9 e- 05, 324	9.9 e- 05, 360	9.9 e- 05, 396	9.9 e- 05, 432	9.9 e- 05, 468	9.9 e- 05, 504	9.9 e- 05, 540	9.9 e- 05, 576	9.9 e- 05, 612	9.9 e- 05, 648	9.9 e- 05, 684	9.9 e- 05, 720
1.0 45e -4	1.0 45e -4, 0	1.0 45e -4, 36	1.0 45e -4, 72	1.0 45e -4, 108	1.0 45e -4, 144	1.0 45e -4, 180	1.0 45e -4, 216	1.0 45e -4, 252	1.0 45e -4, 288	1.0 45e -4, 324	1.0 45e -4, 360	1.0 45e -4, 396	1.0 45e -4, 432	1.0 45e -4, 468	1.0 45e -4, 504	1.0 45e -4, 540	1.0 45e -4, 576	1.0 45e -4, 612	1.0 45e -4, 648	1.0 45e -4, 684	1.0 45e -4, 720
1.1 e- 04	1.1 e- 04, 0	1.1 e- 04, 36	1.1 e- 04, 72	1.1 e- 04, 108	1.1 e- 04, 144	1.1 e- 04, 180	1.1 e- 04, 216	1.1 e- 04, 252	1.1 e- 04, 288	1.1 e- 04, 324	1.1 e- 04, 360	1.1 e- 04, 396	1.1 e- 04, 432	1.1 e- 04, 468	1.1 e- 04, 504	1.1 e- 04, 540	1.1 e- 04, 576	1.1 e- 04, 612	1.1 e- 04, 648	1.1 e- 04, 684	1.1 e- 04, 720

Table B.4.3: Table of all combinations of variations in negative density dependence and the larvicides varied from 100% increase to 100% decrease

LA	0	0.02 5	0.05 0	0.07 5	0.10 0	0.12 5	0.15 0	0.17 5	0.20 0	0.22 5	0.2 50	0.27 5	0.30 0	0.32 5	0.35 0	0.37 5	0.40 0	0.42 5	0.45 0	0.47 5	0.5 00
----	---	-----------	-----------	-----------	-----------	-----------	-----------	-----------	-----------	-----------	-------------------	-----------	-----------	-----------	-----------	-----------	-----------	-----------	-----------	-----------	-----------

DD																						
5.5 e- 06	5.5 e- 6,0	5.5 e- 6,0. 025	5.5 e- 6,0. 050	5.5 e- 6,0. 075	5.5 e- 6,0. 100	5.5 e- 6,0. 125	5.5 e- 6,0. 15	5.5 e- 6,0. 175	5.5 e- 6,0. 2	5.5 e- 6,0. 225	5.5 e- 6,0. .25	5.5 e- 6,0. 275	5.5 e- 6,0. 3	5.5 e- 6,0. 325	5.5 e- 6,0. 35	5.5 e- 6,0. 375	5.5 e- 6,0. 4	5.5 e- 6,0. 425	5.5 e- 6,0. 45	5.5 e- 6,0. 475	5.5 e- 6,0. .5	
1.1 e- 05	1.1 e- 5,0	1.1 e- 5,0. 025	1.1 e- 5,0. 050	1.1 e- 5,0. 075	1.1 e- 5,0. 100	1.1 e- 5,0. 125	1.1 e- 5,0. 15	1.1 e- 5,0. 175	1.1 e- 5,0. 200	1.1 e- 5,0. 225	1.1 e- 5,0. .25	1.1 e- 5,0. 275	1.1 e- 5,0. 3	1.1 e- 5,0. 325	1.1 e- 5,0. 35	1.1 e- 5,0. 375	1.1 e- 5,0. 4	1.1 e- 5,0. 425	1.1 e- 5,0. 45	1.1 e- 5,0. 475	1.1 e- 5,0. .5	
1.6 5- 05	1.6 5e- 05, 0	1.65 e- 05,0 .025	1.65 e- 05,0 .05	1.65 e- 05,0 .075	1.65 e- 05,0 .1	1.65 e- 05,0 .125	1.65 e- 05,0 .15	1.65 e- 05,0 .175	1.65 e- 05,0 .2	1.65 e- 05,0 .225	1.6 5e- 05,0 .25	1.65 e- 05,0 .275	1.65 e- 05,0 .300	1.65 e- 05,0 .325	1.65 e- 05,0 .350	1.65 e- 05,0 .375	1.65 e- 05,0 .400	1.65 e- 05,0 .425	1.65 e- 05,0 .45	1.65 e- 05,0 .475	1.6 5e- 05, 0.5	
2.2 e- 05	2.2 e- 05, 0	2.2 e- 05,0 .025	2.2 e- 05,0 .050	2.2 e- 05,0 .075	2.2 e- 05,0 .100	2.2 e- 05,0 .125	2.2 e- 05,0 .150	2.2 e- 05,0 .175	2.2 e- 05,0 .200	2.2 e- 05,0 .225	2.2 e- 5,0 .25	2.2 e- 05,0 .275	2.2 e- 05,0 .300	2.2 e- 05,0 .325	2.2 e- 05,0 .350	2.2 e- 05,0 .375	2.2 e- 05,0 .400	2.2 e- 05,0 .425	2.2 e- 05,0 .450	2.2 e- 05,0 .475	2.2 e- 05, 0.5	
2.7 5e- 05	2.7 5e- 05, 0	2.75 e- 05,0 .025	2.75 e- 05,0 .050	2.75 e- 05,0 .075	2.75 e- 05,0 .100	2.75 e- 05,0 .125	2.75 e- 05,0 .150	2.75 e- 05,0 .175	2.75 e- 05,0 .200	2.75 e- 05,0 .225	2.7 5e- 05,0 .25	2.75 e- 05,0 .275	2.75 e- 05,0 .300	2.75 e- 05,0 .325	2.75 e- 05,0 .350	2.75 e- 05,0 .375	2.75 e- 05,0 .400	2.75 e- 05,0 .425	2.75 e- 05,0 .450	2.75 e- 05,0 .475	2.7 5e- 05, 0.5	
3.3 e- 05	3.3 e- 05, 0	3.3 e- 05,0 .025	3.3 e- 05,0 .050	3.3 e- 05,0 .075	3.3 e- 05,0 .100	3.3 e- 05,0 .125	3.3 e- 05,0 .150	3.3 e- 05,0 .175	3.3 e- 05,0 .200	3.3 e- 05,0 .225	3.3 e- 5,0 .25	3.3 e- 05,0 .275	3.3 e- 05,0 .300	3.3 e- 05,0 .325	3.3 e- 05,0 .350	3.3 e- 05,0 .375	3.3 e- 05,0 .400	3.3 e- 05,0 .425	3.3 e- 05,0 .450	3.3 e- 05,0 .475	3.3 e- 05, 0.5	
3.8 5e- 05	3.8 5e- 05, 0	3.85 e- 05,0 .025	3.85 e- 05,0 .050	3.85 e- 05,0 .075	3.85 e- 05,0 .100	3.85 e- 05,0 .125	3.85 e- 05,0 .150	3.85 e- 05,0 .175	3.85 e- 05,0 .200	3.85 e- 05,0 .225	3.8 5e- 05,0 .25	3.85 e- 05,0 .275	3.85 e- 05,0 .300	3.85 e- 05,0 .325	3.85 e- 05,0 .350	3.85 e- 05,0 .375	3.85 e- 05,0 .400	3.85 e- 05,0 .425	3.85 e- 05,0 .450	3.85 e- 05,0 .475	3.8 5e- 05, 0.5	

4.4 e- 05	4.4 e- 05, 0	4.4 e- 5,0. 025	4.4 e- 5,0. 050	4.4 e- 5,0. 075	4.4 e- 5,0. 100	4.4 e- 5,0. 125	4.4 e- 5,0. 150	4.4 e- 5,0. 175	4.4 e- 5,0. 200	4.4 e- 5,0. 225	4.4 e- 5,0 .25	4.4 e- 5,0. 275	4.4 e- 5,0. 300	4.4 e- 5,0. 325	4.4 e- 5,0. 350	4.4 e- 5,0. 375	4.4 e- 5,0. 400	4.4 e- 5,0. 425	4.4 e- 5,0. 450	4.4 e- 5,0. 475	4.4 e- 5,0 .50
4.9 5e- 05	4.9 5e- 05, 0	4.95 e- 05,0 .025	4.95 e- 5,0. 050	4.95 e- 5,0. 075	4.95 e- 5,0. 100	4.95 e- 5,0. 125	4.95 e- 5,0. 150	4.95 e- 05,0 .175	4.95 e- 05,0 .200	4.95 e- 05,0 .225	4.9 5e- 5,0 .25	4.95 e- 05,0 .275	4.95 e- 05,0 .300	4.95 e- 05,0 .325	4.95 e- 05,0 .350	4.95 e- 05,0 .375	4.95 e- 05,0 .400	4.95 e- 05,0 .425	4.95 e- 05,0 .450	4.95 e- 05,0 .475	4.9 5e- 5,0 .5
5.5 e- 05	5.5 e- 05, 0	5.5 e- 5,0. 025	5.5 e- 5,0. 050	5.5 e- 5,0. 075	5.5 e- 5,0. 100	5.5 e- 5,0. 125	5.5 e- 5,0. 150	5.5 e- 5,0. 175	5.5 e- 5,0. 200	5.5 e- 5,0. 225	5.5 e- 5,0 .25	5.5 e- 5,0. 275	5.5 e- 5,0. 300	5.5 e- 5,0. 325	5.5 e- 5,0. 350	5.5 e- 5,0. 375	5.5 e- 5,0. 400	5.5 e- 5,0. 425	5.5 e- 5,0. 450	5.5 e- 5,0. 475	5.5 e- 5,0 .5
6.0 5e- 05	6.0 5e- 05, 0	6.05 e- 5,0. 025	6.05 e- 5,0. 050	6.05 e- 5,0. 075	6.05 e- 05,0 .100	6.05 e- 05,0 .125	6.05 e- 05,0 .150	6.05 e- 05,0 .175	6.05 e- 05,0 .200	6.05 e- 05,0 .225	6.0 5e- 5,0 .25	6.05 e- 05,0 .275	6.05 e- 05,0 .300	6.05 e- 05,0 .325	6.05 e- 05,0 .350	6.05 e- 05,0 .375	6.05 e- 05,0 .400	6.05 e- 05,0 .425	6.05 e- 05,0 .450	6.05 e- 05,0 .475	6.0 5e- 5,0 .5
6.6 e- 05	6.6 e- 05, 0	6.6 e- 05,0 .025	6.6 e- 05,0 .050	6.6 e- 05,0 .075	6.6 e- 05,0 .100	6.6 e- 05,0 .125	6.6 e- 05,0 .150	6.6 e- 05,0 .175	6.6 e- 05,0 .200	6.6 e- 05,0 .225	6.6 e- 5,0 .25	6.6 e- 05,0 .275	6.6 e- 05,0 .300	6.6 e- 05,0 .325	6.6 e- 05,0 .350	6.6 e- 05,0 .375	6.6 e- 05,0 .400	6.6 e- 05,0 .425	6.6 e- 05,0 .450	6.6 e- 05,0 .475	6.6 e- 05,0 .5
7.1 5e- 05	7.1 5e- 05, 0	7.15 e- 05,0 .025	7.15 e- 05,0 .050	7.15 e- 05,0 .075	7.15 e- 05,0 .100	7.15 e- 05,0 .125	7.15 e- 05,0 .150	7.15 e- 05,0 .175	7.15 e- 05,0 .200	7.15 e- 05,0 .225	7.1 5e- 5,0 .25	7.15 e- 05,0 .275	7.15 e- 05,0 .300	7.15 e- 05,0 .325	7.15 e- 05,0 .350	7.15 e- 05,0 .375	7.15 e- 05,0 .400	7.15 e- 05,0 .425	7.15 e- 05,0 .450	7.15 e- 05,0 .475	7.1 5e- 5,0 .5
7.7 e- 05	7.7 e- 05, 0	7.7 e- 05,0 .025	7.7 e- 05,0 .050	7.7 e- 05,0 .075	7.7 e- 05,0 .100	7.7 e- 05,0 .125	7.7 e- 05,0 .150	7.7 e- 05,0 .175	7.7 e- 05,0 .200	7.7 e- 05,0 .225	7.7 e- 5,0 .25	7.7 e- 05,0 .275	7.7 e- 05,0 .300	7.7 e- 05,0 .325	7.7 e- 05,0 .350	7.7 e- 05,0 .375	7.7 e- 05,0 .400	7.7 e- 05,0 .425	7.7 e- 05,0 .450	7.7 e- 05,0 .475	7.7 e- 05,0 .5

8.2 5e- 05	8.2 5e- 05, 0	8.25 e- 05,0 .025	8.25 e- 05,0 .050	8.25 e- 05,0 .075	8.25 e- 05,0 .100	8.25 e- 05,0 .125	8.25 e- 05,0 .150	8.25 e- 05,0 .175	8.25 e- 05,0 .200	8.25 e- 05,0 .225	8.2 5e- 5,0 .25	8.25 e- 05,0 .275	8.25 e- 05,0 .300	8.25 e- 05,0 .325	8.25 e- 05,0 .350	8.25 e- 05,0 .375	8.25 e- 05,0 .400	8.25 e- 05,0 .425	8.25 e- 05,0 .450	8.25 e- 05,0 .475	8.2 5e- 5,0 .5
8.8 e- 05	8.8 e- 05, 0	8.8 e- 05,0 .025	8.8 e- 05,7 2 .075	8.8 e- 05,0 .075	8.8 e- 05,0 .100	8.8 e- 05,0 .125	8.8 e- 05,0 .150	8.8 e- 05,0 .175	8.8 e- 05,0 .200	8.8 e- 05,0 .225	8.8 e- 5,0 .25	8.8 e- 05,0 .275	8.8 e- 05,0 .300	8.8 e- 05,0 .325	8.8 e- 05,0 .350	8.8 e- 05,0 .375	8.8 e- 05,0 .400	8.8 e- 05,0 .425	8.8 e- 05,0 .450	8.8 e- 05,0 .475	8.8 e- 5,0 .5
9.3 5e- 05	9.3 5e- 05, 0	9.35 e- 05,0 .025	9.35 e- 05,0 .050	9.35 e- 05,0 .075	9.35 e- 05,0 .100	9.35 e- 05,0 .125	9.35 e- 05,0 .150	9.35 e- 05,0 .175	9.35 e- 05,0 .200	9.35 e- 05,0 .225	9.3 5e- 5,0 .25	9.35 e- 05,0 .275	9.35 e- 05,0 .300	9.35 e- 05,0 .325	9.35 e- 05,0 .350	9.35 e- 05,0 .375	9.35 e- 05,0 .400	9.35 e- 05,0 .425	9.35 e- 05,0 .450	9.35 e- 05,0 .475	9.3 5e- 5,0 .5
9.9 e- 05	9.9 e- 05, 0	9.9 e- 05,0 .025	9.9 e- 05,0 .050	9.9 e- 05,0 .075	9.9 e- 05,0 .100	9.9 e- 05,0 .125	9.9 e- 05,0 .150	9.9 e- 05,0 .175	9.9 e- 05,0 .200	9.9 e- 05,0 .225	9.9 e- 5,0 .25	9.9 e- 05,0 .275	9.9 e- 05,0 .300	9.9 e- 05,0 .325	9.9 e- 05,0 .350	9.9 e- 05,0 .375	9.9 e- 05,0 .400	9.9 e- 05,0 .425	9.9 e- 05,0 .450	9.9 e- 05,0 .475	9.9 e- 5,0 .5
1.0 45e -4	1.0 45e - 4,0	1.04 5e- 4,0. 025	1.04 5e- 4,0. 050	1.04 5e- 4,0. 075	1.04 5e- 4,0. 100	1.04 5e- 4,0. 125	1.04 5e- 4,0. 150	1.04 5e- 4,0. 175	1.04 5e- 4,0. 200	1.04 5e- 4,0. 225	1.0 45e - 4,0 .25	1.04 5e- 4,0. 275	1.04 5e- 4,0. 300	1.04 5e- 4,0. 325	1.04 5e- 4,0. 350	1.04 5e- 4,0. 375	1.04 5e- 4,0. 400	1.04 5e- 4,0. 425	1.04 5e- 4,0. 450	1.04 5e- 4,0. 475	1.0 - 4,0 .5
1.1 e- 04	1.1 e- 04, 0	1.1 e- 04,0 .025	1.1 e- 04,0 .050	1.1 e- 04,0 .075	1.1 e- 04,0 .100	1.1 e- 04,0 .125	1.1 e- 04,0 .150	1.1 e- 04,0 .175	1.1 e- 04,0 .200	1.1 e- 04,0 .225	1.1 e- 4,0 .25	1.1 e- 04,0 .275	1.1 e- 04,0 .300	1.1 e- 04,0 .325	1.1 e- 04,0 .350	1.1 e- 04,0 .375	1.1 e- 04,0 .400	1.1 e- 04,0 .425	1.1 e- 04,0 .450	1.1 e- 04,0 .475	1.1 e- 04, 0.5

Table B.4.4: Table of all combinations of variations in the Larvicides and the Allee effect varied from 100% increase to 100% decrease

A E LA	0	36	72	108	144	180	216	252	288	324	360	396	432	468	504	540	576	612	648	684	720
0	0,0	0,3 6	0,7 2	0,10 8	0,14 4	0,18 0	0,21 6	0,25 2	0,28 8	0,32 4	0,3 60	0,39 6	0,43 2	0,46 8	0,50 4	0,54 0	0,57 6	0,61 2	0,64 8	0,68 4	0,72 0
0. 02 5	0.0 25, 0	0.0 25, 36	0.0 25, 72	0.02 5,10 8	0.02 5,14 4	0.02 5,18 0	0.02 5,21 6	0.02 5,25 2	0.02 5,28 8	0.02 5,32 4	0.02 5,3 60	0.02 5,39 6	0.02 5,43 2	0.02 5,46 8	0.02 5,50 4	0.02 5,54 0	0.02 5,57 6	0.02 5,61 2	0.02 5,64 8	0.02 5,68 4	0.02 5,72 0
0. 05	0.0 5,0	0.0 5,3 6	0.0 5,7 2	0.05 ,108	0.05 ,144	0.05 ,180	0.05 ,216	0.05 ,252	0.05 ,288	0.05 ,324	0.05 ,360	0.05 ,396	0.05 ,432	0.05 ,468	0.05 ,504	0.05 ,540	0.05 ,576	0.05 ,612	0.05 ,648	0.05 ,684	0.05 ,720
0. 07 5	0.0 75, 0	0.0 75, 36	0.0 75, 72	0.07 5,10 8	0.07 5,14 4	0.07 5,18 0	0.07 5,21 6	0.07 5,25 2	0.07 5,28 8	0.07 5,32 4	0.07 5,3 60	0.07 5,39 6	0.07 5,43 2	10.0 75,4 68	0.07 5,50 4	0.07 5,54 0	0.07 5,57 6	0.07 5,61 2	0.07 5,64 8	0.07 5,68 4	0.07 5,72 0
0. 10	0.1 0,0	0.1 ,36	0.1 ,72	0.1, 108	0.1, 144	0.1, 180	0.1, 216	0.1, 252	0.1, 288	0.1, 324	0.1, 360	0.1, 396	0.1, 432	0.1, 468	0.1, 504	0.1, 540	0.1, 576	0.1, 612	0.1, 648	0.1, 684	0.1, 720
0. 12 5	0.1 25, 0	0.1 25, 36	0.1 25, 72	0.12 5,10 8	0.12 5,14 4	0.12 5,18 0	0.12 5,21 6	0.12 5,25 2	0.12 5,28 8	0.12 5,32 4	0.12 5,3 60	0.12 5,39 6	0.12 5,43 2	0.12 5,46 8	0.12 5,50 4	0.12 5,54 0	0.12 5,57 6	0.12 5,61 2	0.12 5,64 8	0.12 5,68 4	0.12 5,72 0
0. 15 0	0.1 50, 0	0.1 50, 36	0.1 50, 72	0.15 0,10 8	0.15 0,14 4	0.15 0,18 0	0.15 0,21 6	0.15 0,25 2	0.15 0,28 8	0.15 0,32 4	0.15 0,3 60	0.15 0,39 6	0.15 0,43 2	0.15 0,46 8	0.15 0,50 4	0.15 0,54 0	0.15 0,57 6	0.15 0,61 2	0.15 0,64 8	0.15 0,68 4	0.15 0,72 0
0. 17 5	0.1 75, 0	0.1 75, 36	0.1 75, 72	0.17 5,10 8	0.17 5,14 4	0.17 5,18 0	0.17 5,21 6	0.17 5,25 2	0.17 5,28 8	0.17 5,32 4	0.17 5,3 60	0.17 5,39 6	0.17 5,43 2	0.17 5,46 8	0.17 5,50 4	0.17 5,54 0	0.17 5,57 6	0.17 5,61 2	0.17 5,64 8	0.17 5,68 4	0.17 5,72 0
0. 20 0	0.2 00, 0	0.2 00, 36	0.2 00, 72	0.20 0,10 8	0.20 0,14 4	0.20 0,18 0	0.20 0,21 6	0.20 0,25 2	0.20 0,28 8	0.20 0,32 4	0.20 0,3 60	0.20 0,39 6	0.20 0,43 2	0.20 0,46 8	0.20 0,50 4	0.20 0,54 0	0.20 0,57 6	0.20 0,61 2	0.20 0,64 8	0.20 0,68 4	0.20 0,72 0

0.475	0.475,0	0.475,36	0.475,72	0.475,108	0.475,144	0.475,180	0.475,216	0.475,252	0.475,288	0.475,324	0.475,360	0.475,396	0.475,432	0.475,468	0.475,504	0.475,540	0.475,576	0.475,612	0.475,648	0.475,684	0.475,720
0.475	0.475,0	0.475,36	0.475,72	0.475,108	0.475,144	0.475,180	0.475,216	0.475,252	0.475,288	0.475,324	0.475,360	0.475,396	0.475,432	0.475,468	0.475,504	0.475,540	0.475,576	0.475,612	0.475,648	0.475,684	0.475,720

Appendix B.5 Population without negative density dependence

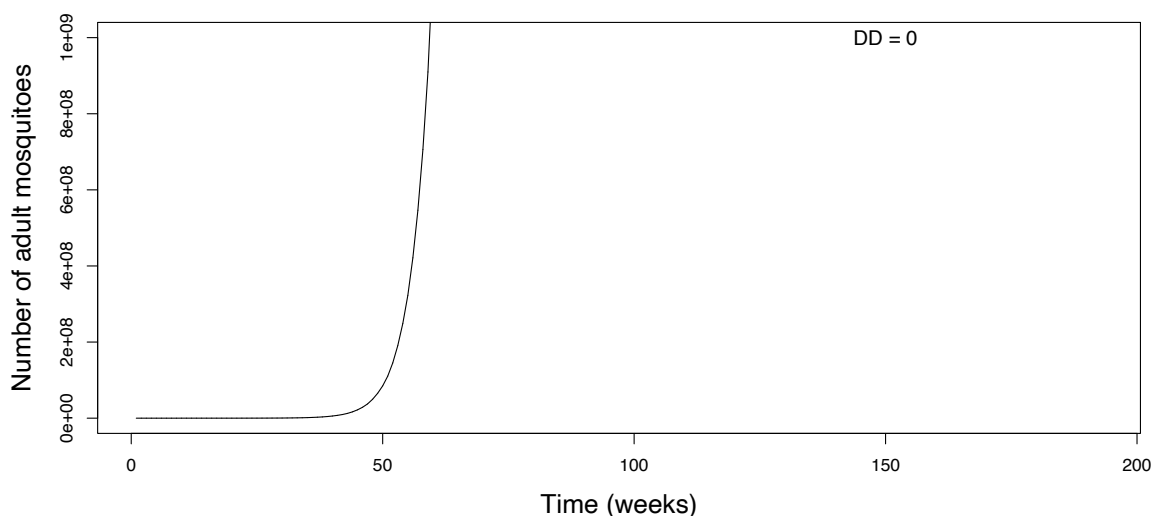


Figure B.5: This figure shows a population that exploded to infinity size when there was no negative density dependence (i.e., $\beta_1=0$).

Appendix B.6 Trade-offs between the negative density dependence and the Allee effects by probability of extinction

Since the real values of negative density dependence and the Allee effect are unknown, negative density dependence and the Allee effect sizes were varied from 100% reduction to 100% increase (Appendix B.4, Table B.4.2) on their values set in Table 3.1 (i.e., DD2 and AE2 in Appendix B.4, Table B.4.1) and estimated the probability of extinction. A heatmap was used to show the probability of extinction across wards for each percentage change in both negative density dependence and the Allee effect. For illustration, the simulation was repeated under three intervention regimes as described in the previous subsection i.e., (a) without an intervention, (b) single short-termed, (c) double short-termed and (c) sustained intervention (see Appendix B.4, Table B.4.1).

As negative density dependence and the Allee effect increased, the probability of extinction also increased but the Allee effect seemed to accelerate population extinction (Figure B.6). While negative density dependence in the absence of the Allee effect cannot lead the population to extinction, the Allee effect without negative density dependence can drive the mosquito population to extinction, especially with a sustained intervention (Figure B.6). In the absence of negative

density dependence and the Allee effect (i.e., mean values $5.5e-05$ and 360 respectively reduced by 100%), the probability of extinction was 0 with and without larvicidal intervention (Figure B.6a-d). Without intervention, the population could not go extinct unless negative density dependence and the Allee effect are both increased by at least 50% (Figure B.6a). With a single short-term intervention, only a 30% increase in negative density dependence while keeping the Allee effect constant could drive the population to extinction with a probability of extinction ranging between 0.75 and 1.0 (Figure B.6b). Similarly, with two short-term interventions, only a 10% increase in negative density dependence while keeping the Allee effect constant could drive the population to extinction with a probability of extinction equalled to 1 (Figure B.6d). In Figure B.6d, the mosquito population declined to extinction with a probability of extinction starting from 0.75 when both negative density dependence and the Allee effect (i.e., $5.5e-05$ and 360, respectively) increased by at least 5% with a sustained intervention. However, with nearly no negative density dependence, population size slowly declined to extinction if and only if the Allee effect was increased by 50% in the presence of larvicidal intervention (Figure B.6c,d). Moreover, if negative density dependence is increased by at least 50%, population size declines to extinct even before reaching a 50% increase in the Allee effect given there is an intervention (Figure B.6b-d). Furthermore, when negative density dependence and the Allee effect were both increased by at least 50%, their combination drove the population to extinction (Figure B.6b-d). However, the presence of a sustained intervention accelerated extinction and made the combination of negative density dependence and the Allee effect become a threat to mosquito populations (Figure B.6d).

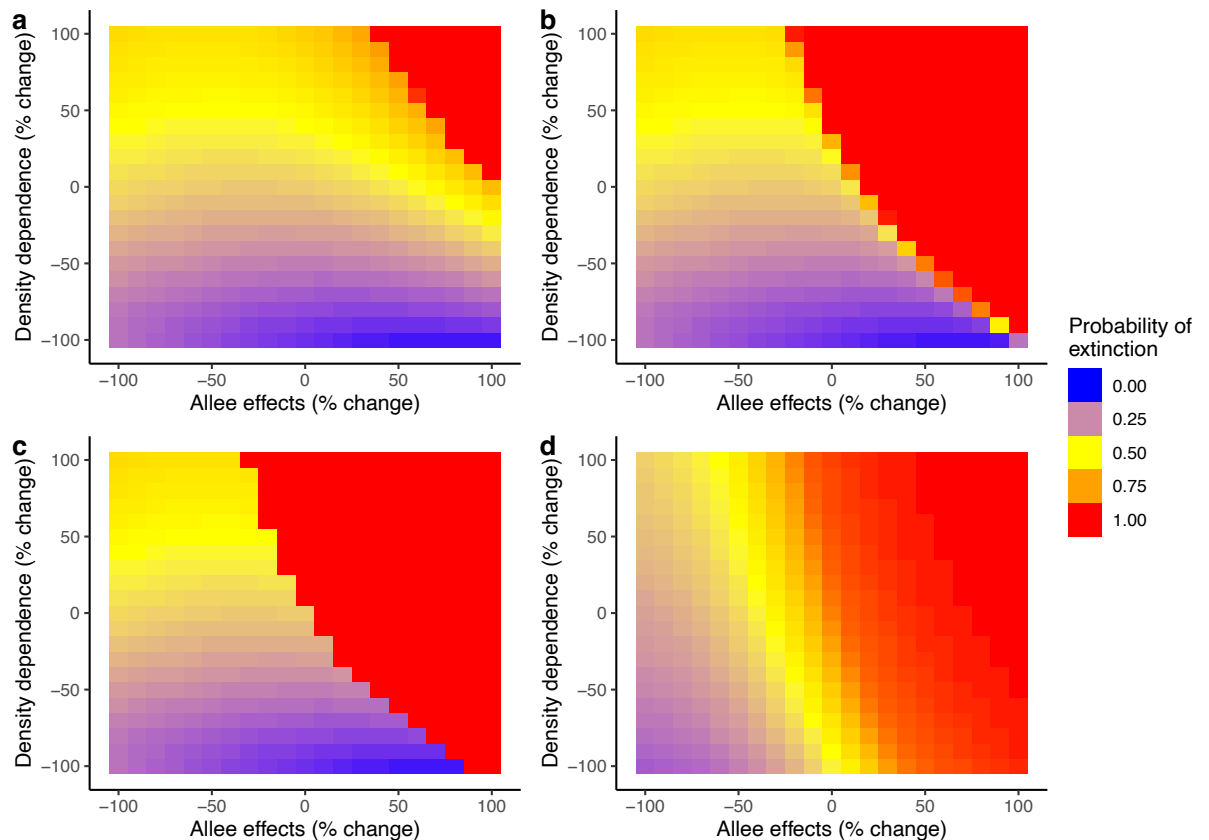


Figure B.6: Heat maps showing the probability of extinction for each percentage increase or decrease in negative density dependence and Allee effect mean values, $5.5e-05$ and 360, respectively; (a) without intervention, (b) with single short application of intervention, (c) two short applications of intervention and (d) sustained intervention.

Appendix B.7 R script for a simulation model in Chapter 3

```

tmax=193 #Maximum time
Nwards=15 #Number of compartments i.e., wards in our case
#Read rainfall and temperature data
rainfall = read.csv("weekly_rainfall.csv") #Read rainfall data
temperature = read.csv("weekly_Temperature.csv") #Read temperature data
R = as.data.frame(rainfall[,2]-56, drop=TRUE) #Write rainfall as a data
frame
Te = as.data.frame(temperature[,2]-27, drop=TRUE) #Write rainfall as a d
ata frame
#State vectors
Na<-matrix(0, Nwards, tmax) # Adult state vectors
Nl1<-matrix(0, Nwards, tmax) # Early instars state vectors
Nl2<-matrix(0, Nwards, tmax) # Late instars state vectors
Np<-matrix(0, Nwards, tmax) # Pupae state vectors
#Growth rate
Gr <- matrix(0,Nwards, tmax)
#Observation process
#Create empty matrix with Nas in datNaPois for Poisson process
datNaPois <- matrix(NA,Nwards, tmax)
datNaPois[1:Nwards]<-800
#Create empty matrix with Nas in datNaNB for negative binomial process
datNaNB <- matrix(NA,Nwards, tmax)
datNaNB[1:Nwards]<-800
# #Define initial values
Nl1[1:Nwards]<-1000 #Initialisation with earrly instars

```

```

Nl2[1:Nwards]<-1000      #Initialisation with late instars
Np[1:Nwards]<-900       #Initialisation with pupae
Na[1:Nwards]<-800       #Initialisation with female adults
# Definition and duration of experimental treatments
LA<-matrix(0, Nwards, tmax)
LA[1:3, 48:tmax]<-0 #First phase of larviciding
LA[4:9,108:tmax]<-0 #Second phase of larviciding
LA[10:15,155:tmax]<-0 #Third phase of larviciding
simulation_function <- function(
  beta0, #Logit of baseline early instar larval survival
  beta1, #Negative density dependence on early instar larval survival
  beta2, #constant defining sensitivity to rainfall in early instar larval survival
  beta3, #Interaction between late instars and rainfall on the survival early instars
  beta4, #Effect of larvicides on early instar larval survival
  beta5, #Sensitivity of temperature to early instar larval survival
  beta6, #Ratio between beta3 and beta1 i.e., beta3/beta1
  lambda0, #Logit of baseline pupa survival
  omega0, #Log per capita fecundity
  omega1, #Constant defining sensitivity of temperature to fecundity rate
  alpha0, #Logit of baseline adult survival
  he, #Hatching rate
  C, #Population size that scale Allee effect
  stochastic #Runs the simulation as stochastic when TRUE and deterministic when FALSE
){
  require("abind")
  #Define a loop for survivals and fecundity for total larvae, pupae and adults
  for(t in 2:tmax)
  {
    #Survival rates of early and late instars, pupae and adults
    s11<-plogis(beta0-beta1*(1-beta6*R[t-1,])*(Nl1[,t-1] + Nl2[,t-1])-beta4*LA[,t-1]+beta5*Te[t,])
    s12<-plogis(beta0-beta1*(1-beta6*R[t-1,])*(Nl1[,t-1] + Nl2[,t-1])-beta4*LA[,t-1]+beta5*Te[t,])
    sp<-plogis(lambda0)
    sa<-plogis(alpha0)
    #Survivors
    #Late instar larvae: Early to late instars
    Nl2[,t]<-
      if (stochastic) {
        rbinom(Nwards,Nl1[,t-1],s11)
      } else{
        Nl1[,t-1]*s11
      }
    #Pupae: Late instars to pupae
    Np[,t]<-
      if (stochastic) {
        rbinom(Nwards,Nl2[,t-1],s12)
      } else{
        Nl2[,t-1]*s12
      }
    #Total adults: from survived adults plus emerged from pupae
    Na[,t]<-
      if (stochastic) {

```

```

    rbinom(Nwards,Na[,t-1],sa)+rbinom(Nwards,Np[,t-1],sp)
  } else{
    Na[,t-1]*sa + Np[,t-1]*sp
  }
  #Fecundity rate: total number of eggs laid
  b<-exp(omega0+omega1*Te[t,])*Na[,t-1]*(Na[,t-1]/(C+Na[,t-1]))
  #Early instars: Eggs hatched to early instar larvae
  N11[,t]<-
  if (stochastic) {
    rpois(Nwards, 0.5*he*b)
  } else{
    0.5*he*b
  }
  Gr[,t-1] <- Na[,t]/(Na[,t-1]+1) #growth rate
} # End of time t Loop
abind(LA=LA, N11=N11, N12=N12, Np=Np, Na=Na, Gr=Gr, along = 3)
} #End of simulation function

```

Appendix B.8 Conversion of original parameters values to values per week

One common challenge in calculating parameter values is the conversion of their observed or original values to a standardized time base e.g., values per week. This can be done as follow:

$$\text{Parameter value per week} = (\text{original biological value})^{\frac{7 \text{ days}}{t_0 \text{ days}}}$$

Where t_0 is the original or observed time interval such as per one, two or three days etc.

Appendix C Supplementary materials for Chapter 4

Appendix C.1 Female adult mosquito data from data from Dar es Salaam, Tanzania, aggregated weekly

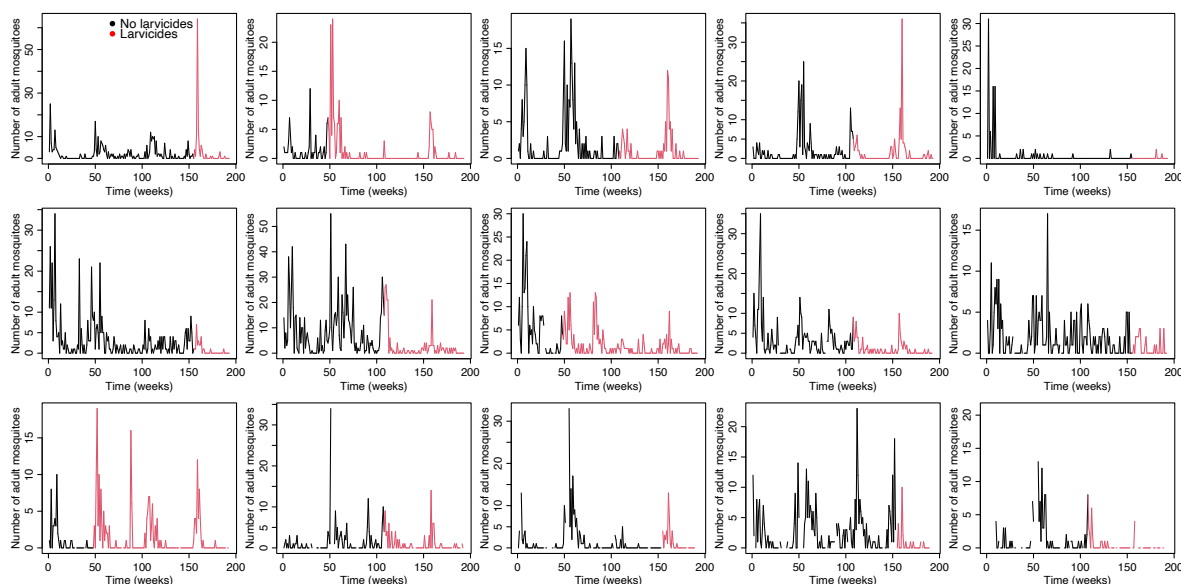


Figure C.1: An illustration of adult *Anopheles gambiae* mosquito population abundances aggregated weekly for a total of 193 weeks from 2005-2009 for each ward before and during large-scale larvicidal control in Dar es Salaam, Tanzania.

Appendix C.2 Total number of traps per each ward

Table C.2: Total number of Human Landing Catches (HLC) traps (i.e., *mitaa*) for each of the wards before and during large-scale larvicidal control in Dar es Salaam

No	1	2	3	4	5	6	7	8	9	10	11	12	13	14	15
Ward name	Magome ni	Mikocheni	Mwananyamara	Mzimuni	Ndungubi	Azi mi o	Ke ko	Kur asi ni	Mib ura ni	Mt on i	Bug uru ni	Il al a	Kip aw a	Mchi kich ini	Ving ung uti
Traps	5	3	6	4	4	7	5	5	5	4	4	4	4	3	4

Appendix C.3 Weekly current rainfall per ward

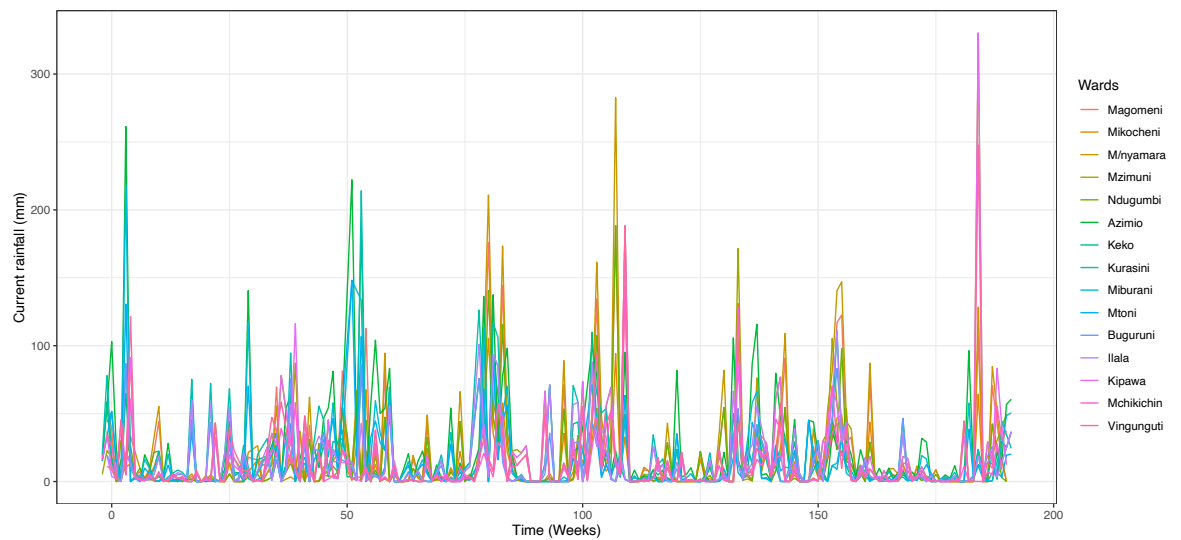


Figure C.3: Showing weekly current rainfall data per ward used during the large-scale larvicidal control intervention in Dar es Salaam, Tanzania.

Appendix C.4 Weekly cumulative rainfall for each ward

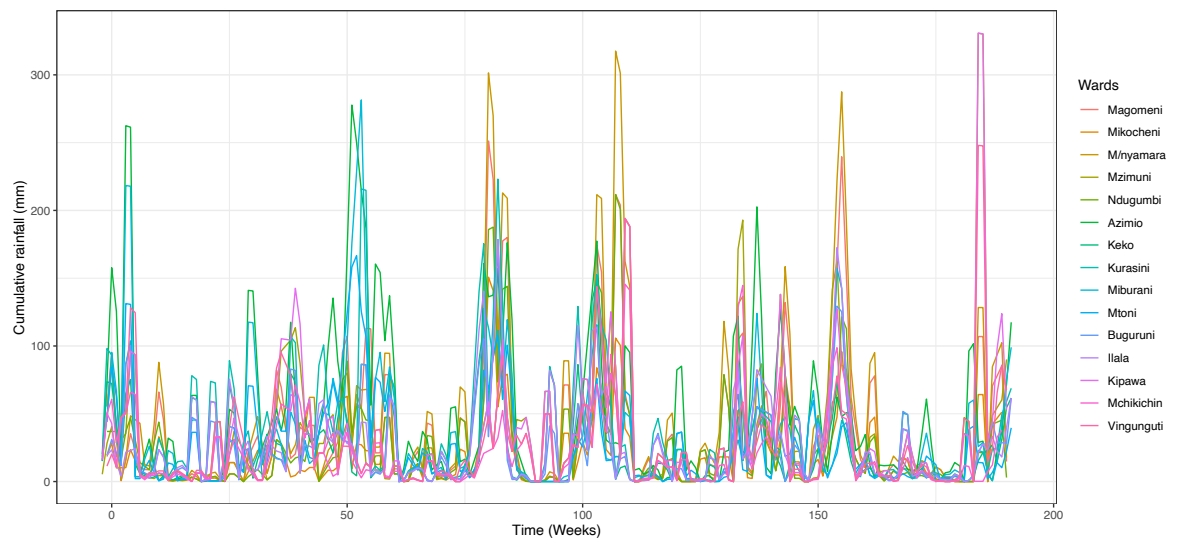


Figure C.4: weekly cumulative rainfall data per ward used during the large-scale larvicidal control intervention in Dar es Salaam, Tanzania.

Appendix C.5 Average weekly temperature across wards

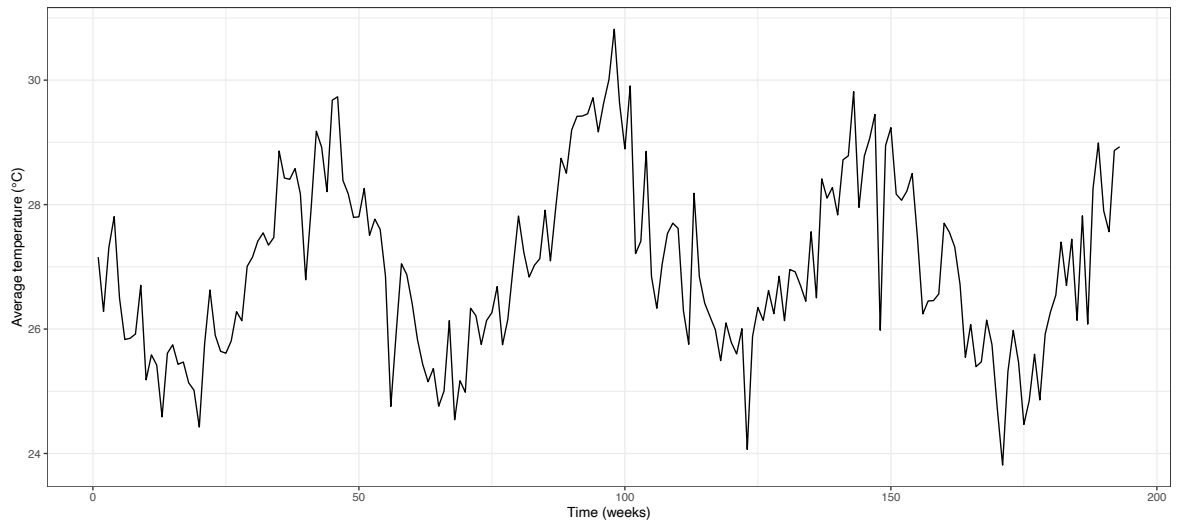


Figure C.5: An average temperature across wards during the large-scale larvicidal control in Dar es Salaam, Tanzania

Appendix C.6 Representation of statistical distributions shape or rate parameters of priors using means and variances

Mean log odds of survival (L) are transformed into probability of survival through time step inverse logit (P) (i.e., $P = \text{inv.logit}(L)$). The prior distribution of P was beta with shape parameters α and β . The shape parameters are determined by using P and variance (V) such that:

$$P \sim \text{Beta}(\alpha, \beta).$$

where $\alpha = \left(\frac{P}{V}\right) (P - P^2 - V)$ and $\beta = \left(\frac{1-P}{V}\right) (P - P^2 - V)$. Then P is changed into L such that:

$$L = \text{logit}(P) = \log\left(\frac{P}{1-P}\right).$$

Given P and V are mean and variance, respectively, shape and rate parameters of gamma distribution parameters were calculated as follows:

$$\alpha = \frac{P^2}{V}$$

$$\beta = \frac{P}{V}$$

Appendix C.7 Trace plots of model fitting using the simulated data

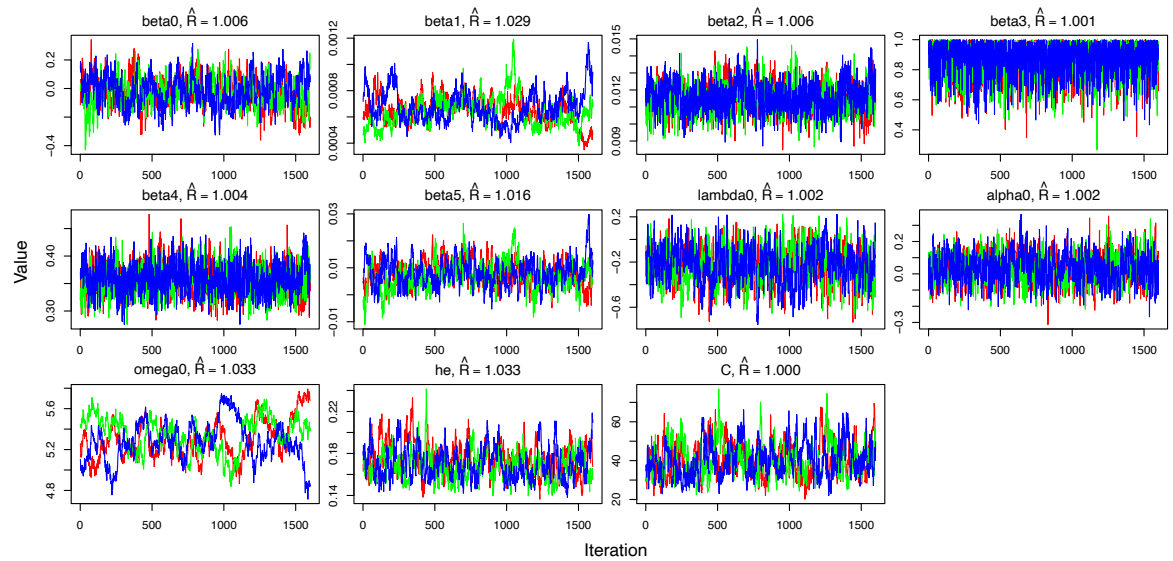


Figure C.7: Trace plots after model fitting using the simulated data and pobs of 0.1. Note that plot beta2 should be named beta3 and plot beta3 should be named beta2.

Appendix C.8 Prior and posterior distributions of model fitting using the simulated data

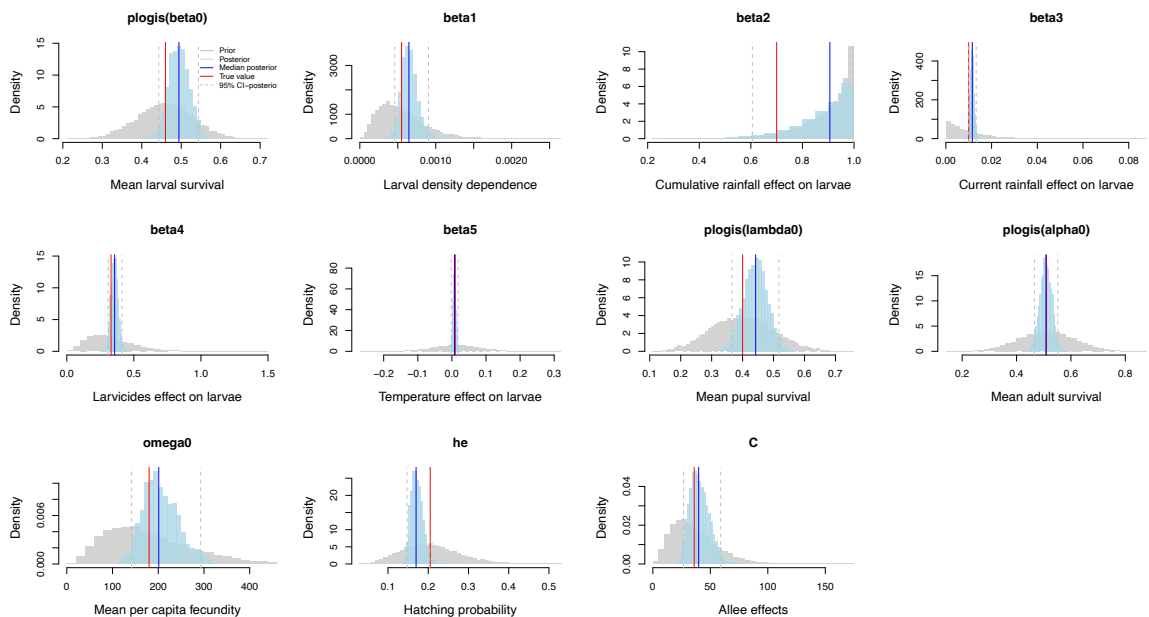


Figure C.8: Goodness of fit: Histograms showing prior (grey) and posterior (sky blue) distributions of the model fitting using the simulated data and pobs of 0.1. Red and blue colours are means of the prior (which are also true parameter values) and posterior distributions while grey dashed lines show the 95% CI of quantiles of the posterior distribution.

Appendix C.9 Observed vs. predicted adult mosquito averaged across wards

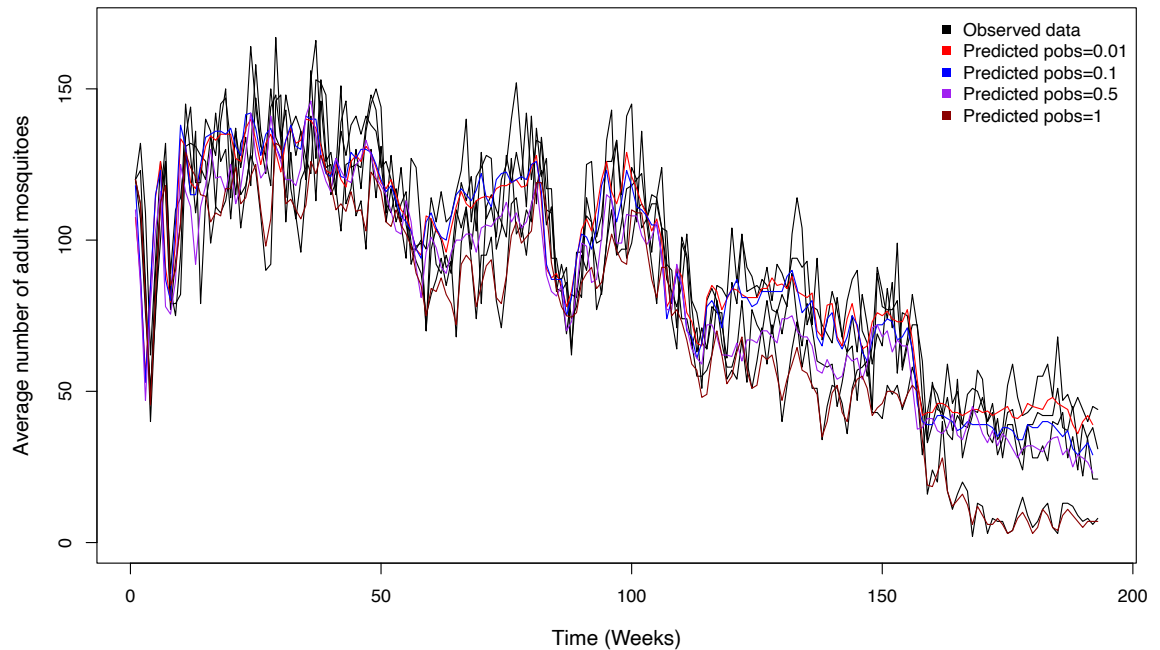


Figure C.9: Goodness of fit: Observed (i.e., simulated) vs. estimated data averaged across wards for each probability of observations (pobs) after the Bayesian state-space model was fitted to the simulated data.

Appendix C.10 ACFs for the simulated data

After removing the primary trends in the population abundance, the autocorrelation function (ACFs) of the observed adult mosquitoes (black colour) mostly falls within the ACFs of the predicted adult mosquitoes (red colour). The autocorrelation function (ACFs) of the observed adult mosquitoes (black colour) mostly falls within the ACFs of the predicted adult mosquitoes

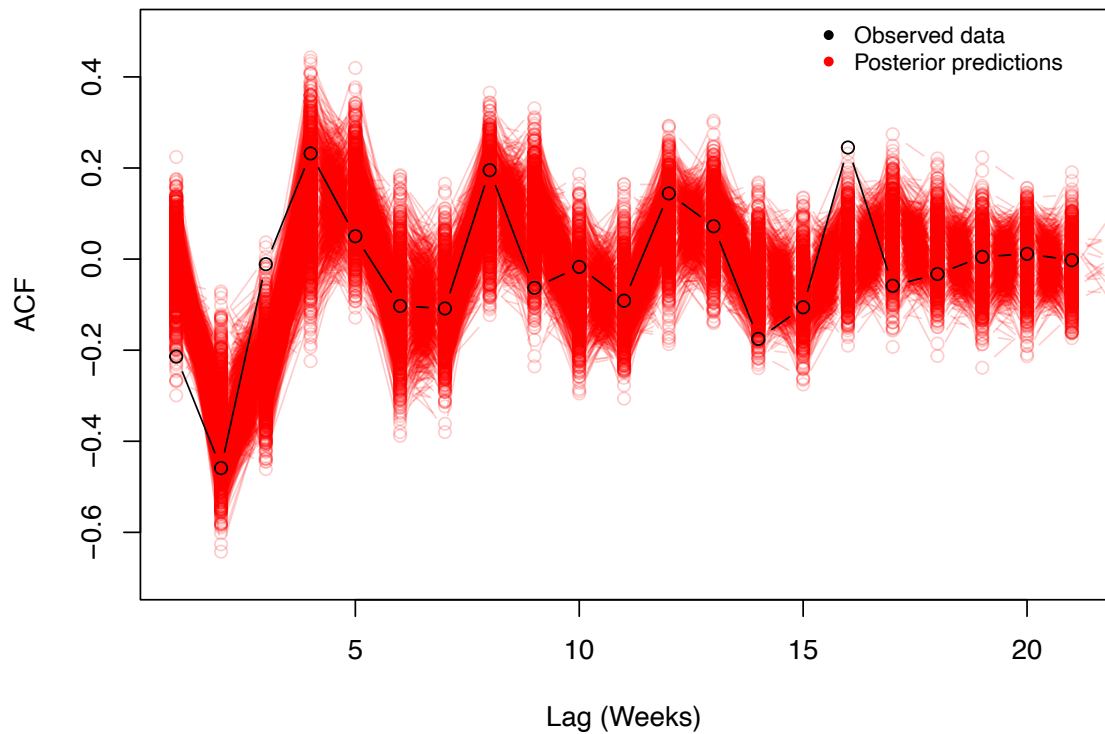


Figure C.10: Goodness of fit: Observed versus posterior predicted ACF values for weekly detrended adult mosquito densities for 22 lags. The black lines and points are the ACF for observed mosquitoes from the human landing catches while the red lines and points show ACF values for predicted mosquitoes.

Appendix C.11 Trace plots of model fitted to field data

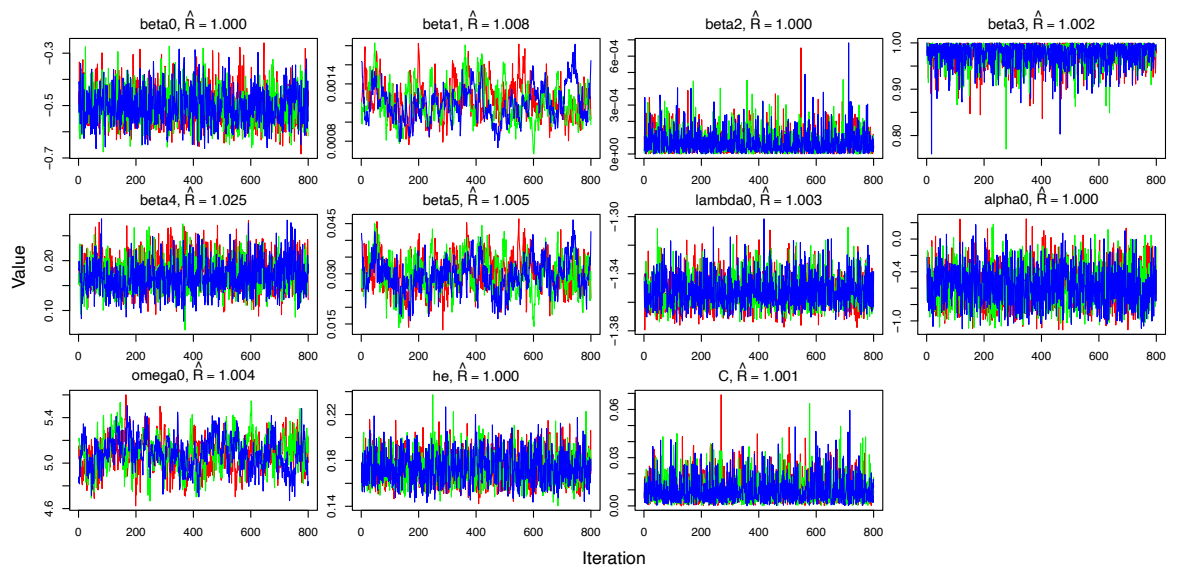


Figure C.11: Panels showing trace plots after model was fitted to the female adult *An. gambiae* data from a large-scale larvicidal control in Dar es Salaam, Tanzania. Note that plot beta2 should be named beta3 and plot beta3 should be named beta2.

Appendix C.12 Prior vs. posterior distribution of model fitting using field data

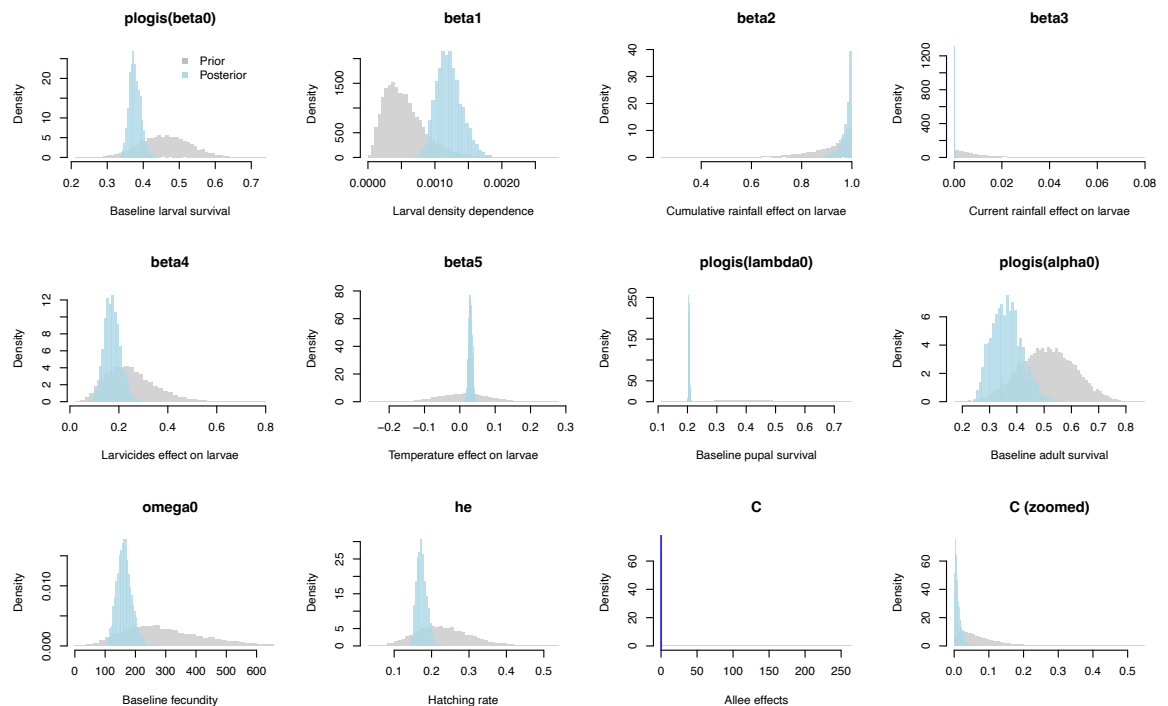


Figure C.12: Histograms showing prior vs posterior distributions after the model was fitted to the female adult *An. gambiae* data from large-scale larvicidal control in Dar es Salaam, Tanzania.

Appendix C.13 Observed vs. estimated mosquitoes for each ward

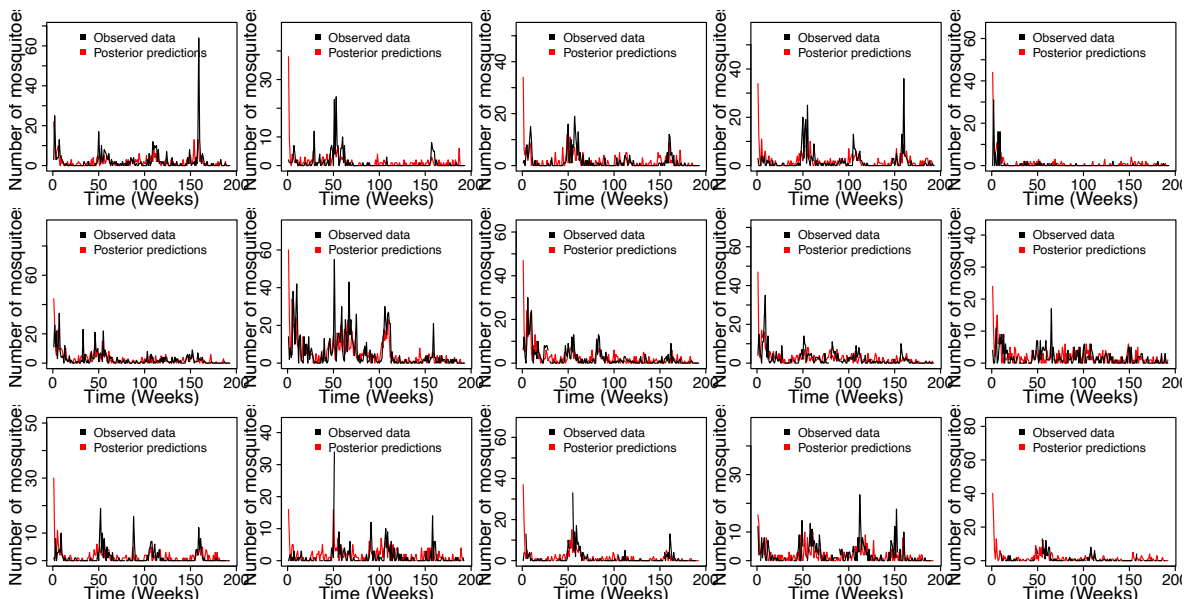


Figure C.13: Panels showing observed (black) vs. estimated (red) adult female *An. gambiae* mosquito population dynamics for each of 15 wards in Dar es Salaam, Tanzania, for pobs of 0.1.

Appendix C.14 Observed vs. estimated mosquitoes across wards

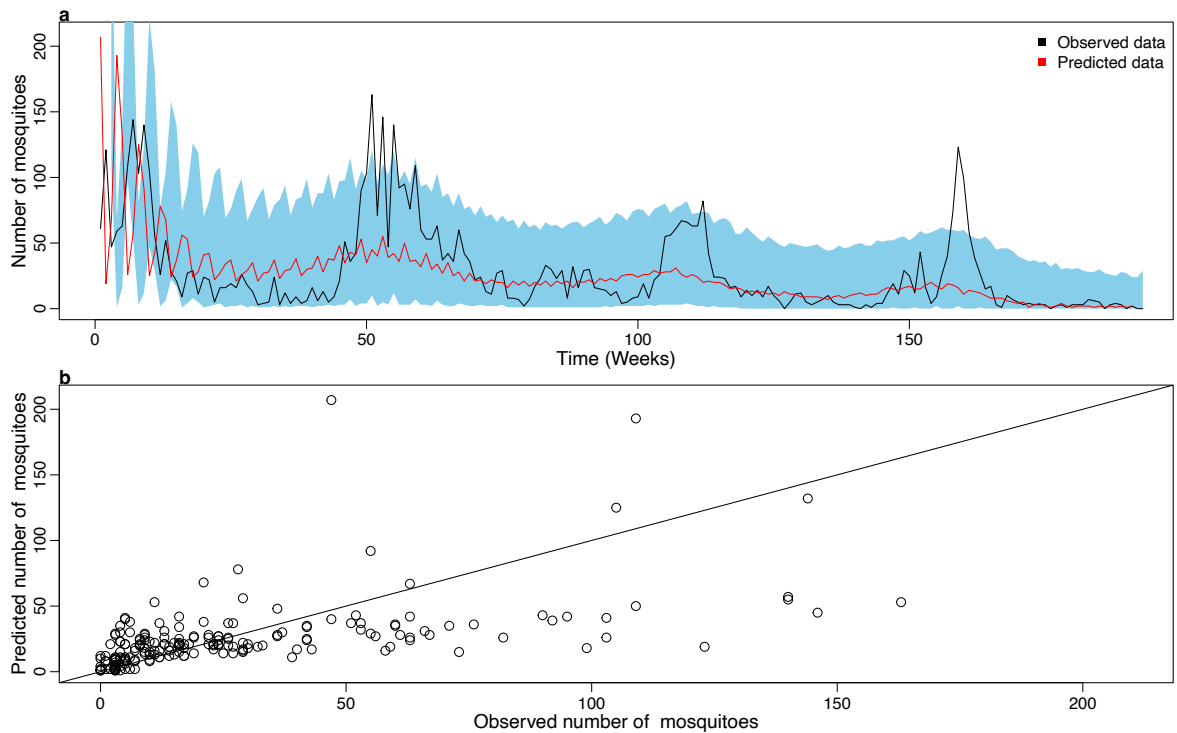


Figure C.14: Illustration of the reconstruction of the total population abundances of *An. gambiae* adult mosquitoes across all wards for pobs of 0.01: The y-axis is observed (black), predicted mean mosquito population abundance (predNa) (red), 2.5% and 97.5% quantiles (sky blue) of predicted population abundance, while the x-axis is the time in weeks. (b) Goodness of fit: observed vs. predicted total population abundances of *An. gambiae* adult mosquitoes across wards, where the diagonal solid line corresponds to the 1:1 line.

Appendix C.15 Bayesian state-space model JAGS code

```
#Model starts here
model{
  for(i in 1:Nwards){
    #Set initial conditions
    Nl1[i,1]<-round(30/pobs); Nl2[i,1]<-round(30/pobs); Np[i,1]<-
round(28/pobs);
    Na[i,1]<-round(28/pobs); predNa[i,1]<-Na[i,1];
    pNa[i,1]<-round(14/pobs); aNa[i,1]<-round(14/pobs);

    #Add uncertainty in adult survival at each ward
    saE[i]~dnorm(0,tau.saE)
    for(t in 2:tmax){
#Early instar larval survival is density, rainfall, temperature and treatment
dependent
      logit(sl1[i,t])<-beta0-beta1*(1-beta3*datRcum[i,t-
1]/330.8189)*(Nl1[i,t-1]+Nl2[i,t-1]) - beta2*datR[i,t-1] - beta4*LA[i,t-1] +
beta5*datT[t,]
#Late instar larval survival is density, rainfall, temperature and treatment
dependent
```

```

logit(sl2[i,t])<-beta0-beta1*(1-beta3*datRcum[i,t-
1]/330.8189)*(NL1[i,t-1]+NL2[i,t-1]) - beta2*datR[i,t-1] - beta4*LA[i,t-1] +
beta5*datT[t,]
# Pupal survival probability
logit(sp[i,t])<-lambda0 #+ spE[i]
# Adult survival probability
logit(sa[i,t])<-alpha0 + saE[i]
# SURVIVORS
# Late instar larvae: from survived early instars
NL2[i,t]~dbin(sl1[i,t], NL1[i,t-1])
# Pupae: from survived late instars
Np[i,t]~dbin(sl2[i,t], NL2[i,t-1])
# Adults: pupae that survive this stage become adults
pNa[i,t]~dbin(sp[i,t], Np[i,t-1])
# Adults: that were in the system and survived
aNa[i,t]~dbin(sa[i,t], Na[i,t-1])
# Total adults: adults that were in the system and
survive, plus those coming into adulthood from pupal state
Na[i,t]~ dsum(pNa[i,t],aNa[i,t])
# Total fecundity is dependent on Allee effects
b[i,t]<-exp(omega0)*Na[i,t-1]*(Na[i,t-1]/(C+Na[i,t-1]))
#Total eggs laid
# Female eggs hatched to early instar larvae at a
hatching probability of "he"
NL1[i,t]~dpois(0.5*he*b[i,t])
#Stochasticity in the observation of adults in the experiment
#Observation process model: Observation likelihoods against real data
#Poisson process
datNa[i,t] ~ dpois(pobs*mitaa[i]*Na[i,t])
#Posterior predictions
predNa[i,t] ~ dpois(pobs*mitaa[i]*Na[i,t])
} #End of time t loop

} #End of ward i loop

#Priors on early and late instar LARVAL SURVIVAL: Mean larval survival
mu.beta0<- 0.46
var.beta0<- 0.005
alpha.beta0<- (mu.beta0/var.beta0)*(mu.beta0-pow(mu.beta0,2)-var.beta0)
beta.beta0<- ((1-mu.beta0)/var.beta0)*(mu.beta0-pow(mu.beta0,2)-var.beta0)
beta0line~dbeta(alpha.beta0,beta.beta0)
beta0<- log(beta0line/(1-beta0line))

#Negative density dependence in early and late instar larval survival
mu.beta1<- 0.0055*pobs
var.beta1<- 0.00001*pobs*pobs
alpha.beta1<- pow(mu.beta1,2)/var.beta1
beta.beta1<- mu.beta1/var.beta1
beta1~dgamma(alpha.beta1,beta.beta1)

#Effect of rainfall on early and late instar larval survival
mu.beta2<- 0.01

```

```

var.beta2<- 0.0001
alpha.beta2<- pow(mu.beta2,2)/var.beta2
beta.beta2<- mu.beta2/var.beta2
beta2~dgamma(alpha.beta2,beta.beta2)

#Effect of interaction between early and late instars and rainfall
mu.beta3<- 0.7
var.beta3<- 0.01
alpha.beta3<- (mu.beta3/var.beta3)*(mu.beta3-pow(mu.beta3,2)-var.beta3)
beta.beta3<- ((1-mu.beta3)/var.beta3)*(mu.beta3-pow(mu.beta3,2)-var.beta3)
beta3~dbeta(7.2,0.8) #dbeta(alpha.beta3,beta.beta3)

#Effect of larvicides on early and late instar larval survival
mu.beta4<- 0.25
var.beta4<- 0.03
alpha.beta4<- pow(mu.beta4,2)/var.beta4
beta.beta4<- mu.beta4/var.beta4
beta4~dgamma(alpha.beta4,beta.beta4)

#Effect of temperature on early instar larval survival
mu.beta5<- 0.01
sd.beta5<- 0.07 #0.05 #0.1
beta5~dnorm(mu.beta5,1/(sd.beta5)^2)

#Priors on PUPAL SURVIVAL: Mean pupal survival
mu.lambda0<- 0.4
var.lambda0<- 0.01
alpha.lambda0<- (mu.lambda0/var.lambda0)*(mu.lambda0-pow(mu.lambda0,2)-
var.lambda0)
beta.lambda0<- ((1-mu.lambda0)/var.lambda0)*(mu.lambda0-
pow(mu.lambda0,2)-var.lambda0)
lambda0line~dbeta(alpha.lambda0,beta.lambda0)
lambda0<- log(lambda0line/(1-lambda0line))

#Priors on ADULT SURVIVAL: Mean adult survival
mu.alpha0<- 0.51
var.alpha0<- 0.01
alpha.alpha0<- (mu.alpha0/var.alpha0)*(mu.alpha0-pow(mu.alpha0,2)-
var.alpha0)
beta.alpha0<- ((1-mu.alpha0)/var.alpha0)*(mu.alpha0-pow(mu.alpha0,2)-
var.alpha0)
alpha0line~dbeta(alpha.alpha0,beta.alpha0)
alpha0<- log(alpha0line/(1-alpha0line))

#Priors on FECUNDITY: Mean per capita fecundity
mu.omega0<- 300
sd.omega0<- 140
alpha.omega0<- pow(mu.omega0,2)/pow(sd.omega0,2)
beta.omega0<- mu.omega0/pow(sd.omega0,2)
omega0line~dgamma(alpha.omega0,beta.omega0)
omega0<- log(omega0line)

```

```
#Eggs hatching probability
mu.he<- 0.23
var.he<- 0.005
alpha.he<- (mu.he/var.he)*(mu.he-pow(mu.he,2)-var.he)
beta.he<- ((1-mu.he)/var.he)*(mu.he-pow(mu.he,2)-var.he)
he~dbeta(alpha.he,beta.he)

#Priors of ALLEE EFFECTS
mu.C<- 3.6/pobs
sd.C<- 3/pobs
alpha.C<- pow(mu.C,2)/pow(sd.C,2)
beta.C<- mu.C/pow(sd.C,2)
C~dgamma(alpha.C,beta.C)

#Uncertainty in adult survival at each ward
tau.saE<- 1/pow(sigma.saE,2)
sigma.saE~dgamma(0.01,0.01)
} #END model
```

List of References

1. World malaria report 2024 [Internet]. [cited 2024 Dec 23]. Available from: <https://www.who.int/teams/global-malaria-programme/reports/world-malaria-report-2024>
2. Bhatt S, Weiss DJ, Cameron E, Bisanzio D, Mappin B, Dalrymple U, et al. The effect of malaria control on *Plasmodium falciparum* in Africa between 2000 and 2015. *Nature*. 2015 Oct;526(7572):207-11.
3. Okumu FO, Moore SJ. Combining indoor residual spraying and insecticide-treated nets for malaria control in Africa: a review of possible outcomes and an outline of suggestions for the future. *Malaria Journal*. 2011 Jul 28;10(1):208.
4. Bhattarai A, Ali AS, Kachur SP, Mårtensson A, Abbas AK, Khatib R, et al. Impact of Artemisinin-Based Combination Therapy and Insecticide-Treated Nets on Malaria Burden in Zanzibar. *PLOS Medicine*. 2007 Nov 6;4(11):e309.
5. West PA, Protopopoff N, Wright A, Kivaju Z, Tigererwa R, Mosha FW, et al. Indoor Residual Spraying in Combination with Insecticide-Treated Nets Compared to Insecticide-Treated Nets Alone for Protection against Malaria: A Cluster Randomised Trial in Tanzania. *PLOS Medicine*. 2014 Apr 15;11(4):e1001630.
6. Okumu F, Finda M. Key Characteristics of Residual Malaria Transmission in Two Districts in South-Eastern Tanzania—Implications for Improved Control. *The Journal of Infectious Diseases*. 2021 May 1;223(Supplement_2):S143-54.
7. World malaria report 2016 [Internet]. [cited 2024 Aug 12]. Available from: <https://www.who.int/publications/i/item/9789241511711>
8. World malaria report 2023 [Internet]. [cited 2024 Jul 1]. Available from: <https://www.who.int/teams/global-malaria-programme/reports/world-malaria-report-2023>
9. World malaria report 2020 [Internet]. [cited 2024 Aug 12]. Available from: <https://www.who.int/publications/i/item/9789240015791>
10. World malaria report 2021 [Internet]. [cited 2022 May 31]. Available from: <https://www.who.int/teams/global-malaria-programme/reports/world-malaria-report-2021>
11. World malaria report 2022 [Internet]. [cited 2024 Jul 16]. Available from: <https://www.who.int/publications/i/item/9789240064898>

12. Cowman AF, Healer J, Marapana D, Marsh K. Malaria: biology and disease. *Cell*. 2016;167(3):610-24.
13. Miller LH, Ackerman HC, Su X zhuan, Wellem TE. Malaria biology and disease pathogenesis: insights for new treatments. *Nature medicine*. 2013;19(2):156-67.
14. Raghavendra K, Barik TK, Reddy BN, Sharma P, Dash AP. Malaria vector control: from past to future. *Parasitology research*. 2011;108(4):757-79.
15. Robert V, Macintyre K, Keating J, Trape JF, Duchemin JB, Warren M, et al. Malaria transmission in urban sub-Saharan Africa. *The American journal of tropical medicine and hygiene*. 2003;68(2):169-76.
16. Abossie A, Demissew A, Getachew H, Tsegaye A, Degefa T, Habtamu K, et al. Higher outdoor mosquito density and Plasmodium infection rates in and around malaria index case households in low transmission settings of Ethiopia: Implications for vector control. *Parasites & Vectors*. 2024 Feb 6;17(1):53.
17. Abel L, Kimachas E, Omollo E, Nalianya E, Chepkwony T, Kipkoech J, et al. Relationship between malaria vector survival, infectivity and insecticide treated net use in western Kenya [Internet]. 2024 [cited 2024 Sep 12]. Available from: <https://www.researchsquare.com/article/rs-4090984/v1>
18. Matthews J, Bethel A, Osei G. An overview of malarial Anopheles mosquito survival estimates in relation to methodology. *Parasites Vectors*. 2020 Dec;13(1):233.
19. Nzioki I, Machani MG, Onyango SA, Kabui KK, Githeko AK, Ochomo E, et al. Differences in malaria vector biting behavior and changing vulnerability to malaria transmission in contrasting ecosystems of western Kenya. *Parasites & Vectors*. 2023 Oct 21;16(1):376.
20. Odero JI, Abong'o B, Moshi V, Ekodir S, Harvey SA, Ochomo E, et al. Early morning anopheline mosquito biting, a potential driver of malaria transmission in Busia County, western Kenya. *Malaria Journal*. 2024 Mar 4;23(1):66.
21. White NJ, Pukrittayakamee S, Hien TT, Faiz MA, Mokuolu OA, Dondorp AM. Malaria. *The Lancet*. 2014 Feb 22;383(9918):723-35.
22. Cohuet A, Harris C, Robert V, Fontenille D. Evolutionary forces on *Anopheles*: what makes a malaria vector? *Trends in Parasitology*. 2010 Mar 1;26(3):130-6.

23. WHO recommends groundbreaking malaria vaccine for children at risk [Internet]. [cited 2022 Jun 10]. Available from: <https://www.who.int/news/item/06-10-2021-who-recommends-groundbreaking-malaria-vaccine-for-children-at-risk>
24. Malaria vaccine implementation programme [Internet]. [cited 2024 Aug 12]. Available from: <https://www.who.int/initiatives/malaria-vaccine-implementation-programme>
25. Sanou A. The ecology and behaviour of insecticide resistant malaria vectors and implications for control in Burkina Faso [Internet] [PhD]. University of Glasgow; 2020 [cited 2024 Sep 12]. Available from: <https://theses.gla.ac.uk/81392/>
26. Warrell, D.A, Gilles, H.M. Essential Malariology. Fourth Edition. New York, NY: CRC Press, Taylor & Francis Group; 2002. 373 p.
27. Christiansen-Jucht CD, Parham PE, Saddler A, Koella JC, Basáñez MG. Larval and adult environmental temperatures influence the adult reproductive traits of *Anopheles gambiae* s.s. *Parasites Vectors*. 2015 Dec;8(1):456.
28. Azam FB, Carney RM, Kariev S, Nallan K, Subramanian M, Sampath G, et al. Classifying stages in the gonotrophic cycle of mosquitoes from images using computer vision techniques. *Sci Rep*. 2023 Dec 13;13(1):22130.
29. Ejeta D. Mating Behavior and Gonotrophic Cycle in *Anopheles gambiae* Complex and their Significance in Vector Competence and Malaria Vector Control. *Journal of Biomedical Research & Environmental Sciences*. 2022 Jan 1;3:031-43.
30. Xing Y, Liu J, Guo Z. A discrete-time mathematical model of stage-structured mosquito populations. *Advances in Difference Equations*. 2019 Dec 12;2019(1):518.
31. Malaria vector control [Internet]. [cited 2024 Jul 1]. Available from: <https://www.who.int/teams/global-malaria-programme/prevention/vector-control>
32. Global vector control response 2017-2030 [Internet]. [cited 2024 Jun 11]. Available from: <https://www.who.int/publications-detail-redirect/9789241512978>
33. Tizifa TA, Kabaghe AN, McCann RS, van den Berg H, Van Vugt M, Phiri KS. Prevention Efforts for Malaria. *Curr Trop Med Rep*. 2018 Mar 1;5(1):41-50.

34. Glunt KD, Blanford JI, Paaijmans KP. Chemicals, Climate, and Control: Increasing the Effectiveness of Malaria Vector Control Tools by Considering Relevant Temperatures. *PLOS Pathogens*. 2013 Oct 3;9(10):e1003602.
35. Malaria vector control [Internet]. [cited 2023 Aug 17]. Available from: <https://www.who.int/teams/global-malaria-programme/prevention/vector-control>
36. Makungu C, Stephen S, Kumburu S, Govella NJ, Dongus S, Hildon ZJL, et al. Informing new or improved vector control tools for reducing the malaria burden in Tanzania: a qualitative exploration of perceptions of mosquitoes and methods for their control among the residents of Dar es Salaam. *Malaria Journal*. 2017 Oct 11;16(1):410.
37. Mwalimu CD, Lazaro SN, Kisinza WN, Magesa SM, Kiware SS. The impact of Indoor Residual Spraying (IRS) withdrawal in the Lake Zone Regions in Mainland Tanzania. Should Tanzania withdrawal its IRS program? [Internet]. 2023 [cited 2024 Aug 12]. Available from: <https://www.researchsquare.com/article/rs-2888818/v1>
38. Tungu P, Kabula B, Nkya T, Machafuko P, Sambu E, Batengana B, et al. Trends of insecticide resistance monitoring in mainland Tanzania, 2004-2020. *Malaria Journal*. 2023 Mar 17;22(1):100.
39. Finda MF, Moshi IR, Monroe A, Limwagu AJ, Nyoni AP, Swai JK, et al. Linking human behaviours and malaria vector biting risk in south-eastern Tanzania. *PLOS ONE*. 2019 Jun 3;14(6):e0217414.
40. TZ-DHSMIS. Tanzania Demographic and Health Survey and Malaria Indicator Survey 2022 - Key Indicators Report (English). 2022 [cited 2023 Aug 23]; Available from: <https://dhsprogram.com/publications/publication-PR144-Preliminary-Reports-Key-Indicators-Reports.cfm>
41. Maheu-Giroux M, Castro MC. Impact of Community-Based Larviciding on the Prevalence of Malaria Infection in Dar es Salaam, Tanzania. *PLOS ONE*. 2013 Aug 14;8(8):e71638.
42. Pates HV, Lines JD, Keto AJ, Miller JE. Personal protection against mosquitoes in Dar es Salaam, Tanzania, by using a kerosene oil lamp to vaporize transfluthrin. *Medical and Veterinary Entomology*. 2002;16(3):277-84.
43. Killeen GF, Govella NJ, Mlacha YP, Chaki PP. Suppression of malaria vector densities and human infection prevalence associated with scale-up of mosquito-proofed housing in Dar es Salaam, Tanzania: re-analysis of an

- observational series of parasitological and entomological surveys. *The Lancet Planetary Health*. 2019 Mar;3(3):e132-43.
44. Mboma ZM, Dillip A, Kramer K, Koenker H, Greer G, Lorenz LM. 'For the poor, sleep is leisure': understanding perceptions, barriers and motivators to mosquito net care and repair in southern Tanzania. *Malaria Journal*. 2018 Oct 22;17(1):375.
45. Msellemu D, Shemdoe A, Makungu C, Mlacha Y, Kannady K, Dongus S, et al. The underlying reasons for very high levels of bed net use, and higher malaria infection prevalence among bed net users than non-users in the Tanzanian city of Dar es Salaam: a qualitative study. *Malaria Journal*. 2017 Oct 23;16(1):423.
46. Sleeping Safely in Tanzania | Hopkins Bloomberg Public Health Magazine [Internet]. [cited 2024 Sep 23]. Available from: <https://magazine.publichealth.jhu.edu/2011/sleeping-safely-in-tanzania>
47. Geissbühler Y, Kannady K, Chaki PP, Emidi B, Govella NJ, Mayagaya V, et al. Microbial Larvicide Application by a Large-Scale, Community-Based Program Reduces Malaria Infection Prevalence in Urban Dar Es Salaam, Tanzania. *PLOS ONE*. 2009 Mar 31;4(3):e5107.
48. Mazigo HD, Mboera LEG, Rumisha SF, Kweka EJ. Malaria mosquito control in rice paddy farms using biolarvicide mixed with fertilizer in Tanzania: semi-field experiments. *Malar J* [Internet]. 2019 Jul 8 [cited 2021 Feb 18];18. Available from: <https://www.ncbi.nlm.nih.gov/pmc/articles/PMC6615286/>
49. Antonio-Nkondjio C, Sandjo NN, Awono-Ambene P, Wondji CS. Implementing a larviciding efficacy or effectiveness control intervention against malaria vectors: key parameters for success. *Parasites Vectors*. 2018 Dec;11(1):57.
50. WHO guidelines for malaria - 16 October 2023 [Internet]. [cited 2024 Jul 1]. Available from: <https://app.magicapp.org/#/guideline/LwRMXj/section/LGDAon>
51. Gachelin G, Garner P, Ferroni E, Verhave JP, Opinel A. Evidence and strategies for malaria prevention and control: a historical analysis. *Malaria Journal*. 2018 Feb 27;17(1):96.
52. World Health Organization. Larval source management: a supplementary malaria vector control measure: an operational manual [Internet]. Geneva: World Health Organization; 2013 [cited 2022 Jun 3]. Available from: <https://apps.who.int/iris/handle/10665/85379>

53. Majambere S, Lindsay SW, Green C, Kandeh B, Fillinger U. Microbial larvicides for malaria control in The Gambia. *Malaria Journal*. 2007 Jun 7;6(1):76.
54. Tusting LS, Thwing J, Sinclair D, Fillinger U, Gimnig J, Bonner KE, et al. Mosquito larval source management for controlling malaria. *Cochrane Database Syst Rev*. 2013 Aug 29;2013(8):CD008923.
55. García GA, Fuseini G, Donfack OT, Wofford RN, Nlang JAM, Efiri PB, et al. The need for larval source management accompanying urban development projects in malaria endemic areas: a case study on Bioko Island. *Malaria Journal*. 2022 Nov 14;21(1):328.
56. Imbahale SS, Githeko A, Mukabana WR, Takken W. Integrated mosquito larval source management reduces larval numbers in two highland villages in western Kenya. *BMC Public Health*. 2012 May 18;12(1):362.
57. Fillinger U, Ndenga B, Githeko A, Lindsay SW. Integrated malaria vector control with microbial larvicides and insecticide-treated nets in western Kenya: a controlled trial. *Bull World Health Org*. 2009 Sep 1;87(9):655-65.
58. Tungu PK, Michael E, Sudi W, Kisinza WW, Rowland M. Efficacy of interceptor® G2, a long-lasting insecticide mixture net treated with chlorfenapyr and alpha-cypermethrin against *Anopheles funestus*: experimental hut trials in north-eastern Tanzania. *Malaria Journal*. 2021 Apr 9;20(1):180.
59. Tchouakui M, Thiomela RF, Nchoutpouen E, Menze BD, Ndo C, Achu D, et al. High efficacy of chlorfenapyr-based net Interceptor® G2 against pyrethroid-resistant malaria vectors from Cameroon. *Infectious Diseases of Poverty*. 2023 Aug 29;12(1):81.
60. WHO publishes recommendations on two new types of insecticide-treated nets [Internet]. [cited 2024 Jul 1]. Available from: <https://www.who.int/news/item/14-03-2023-who-publishes-recommendations-on-two-new-types-of-insecticide-treated-nets>
61. Accrombessi M, Cook J, Dangbenon E, Yovogan B, Akpovi H, Sovi A, et al. Efficacy of pyriproxyfen-pyrethroid long-lasting insecticidal nets (LLINs) and chlorfenapyr-pyrethroid LLINs compared with pyrethroid-only LLINs for malaria control in Benin: a cluster-randomised, superiority trial. *The Lancet*. 2023 Feb 11;401(10375):435-46.
62. Grisales N, Lees RS, Maas J, Morgan JC, Wangrawa DW, Guelbeogo WM, et al. Pyriproxyfen-treated bed nets reduce reproductive fitness and longevity of

- pyrethroid-resistant *Anopheles gambiae* under laboratory and field conditions. *Malaria Journal*. 2021 Jun 22;20(1):273.
63. Ng'habi K, Viana M, Matthiopoulos J, Lyimo I, Killeen G, Ferguson HM. Mesocosm experiments reveal the impact of mosquito control measures on malaria vector life history and population dynamics. *Scientific Reports*. 2018 Sep 17;8(1):13949.
64. Souza DK, Thomas R, Bradley J, Leyrat C, Boakye DA, Okebe J. Ivermectin treatment in humans for reducing malaria transmission. *Cochrane Database Syst Rev*. 2021 Jun 29;2021(6):CD013117.
65. Lovett B, Bilgo E, Millogo SA, Ouattarra AK, Sare I, Gnambani EJ, et al. Transgenic *Metarhizium* rapidly kills mosquitoes in a malaria-endemic region of Burkina Faso. *Science*. 2019 May 31;364(6443):894-7.
66. Baldini F, Segata N, Pompon J, Marcenac P, Robert Shaw W, Dabiré RK, et al. Evidence of natural *Wolbachia* infections in field populations of *Anopheles gambiae*. *Nat Commun*. 2014 Jun 6;5(1):3985.
67. Bier E. Gene drives gaining speed. *Nat Rev Genet*. 2022 Jan;23(1):5-22.
68. Derua YA, Kweka EJ, Kisinza WN, Githeko AK, Moshia FW. Bacterial larvicides used for malaria vector control in sub-Saharan Africa: review of their effectiveness and operational feasibility. *Parasites Vectors*. 2019 Dec;12(1):426.
69. WHO Efficacy Testing Guidelines for Vector Control Products | WHO - Prequalification of Medical Products (IVDs, Medicines, Vaccines and Immunization Devices, Vector Control) [Internet]. [cited 2024 Nov 15]. Available from: <https://extranet.who.int/prequal/vector-control-products/who-efficacy-testing-guidelines-vector-control-products>
70. Ferguson HM, Ng'habi KR, Walder T, Kadungula D, Moore SJ, Lyimo I, et al. Establishment of a large semi-field system for experimental study of African malaria vector ecology and control in Tanzania. *Malar J*. 2008 Aug 20;7(1):158.
71. Ferguson HM, Ng'habi KR, Walder T, Kadungula D, Moore SJ, Lyimo I, et al. Establishment of a large semi-field system for experimental study of African malaria vector ecology and control in Tanzania. *Malaria Journal*. 2008 Aug 20;7(1):158.
72. Onen H, Kaindoa EW, Nkya J, Limwagu A, Kaddumukasa MA, Okumu FO, et al. Semi-field experiments reveal contrasted predation and movement patterns

- of aquatic macroinvertebrate predators of *Anopheles gambiae* larvae. *Malaria Journal*. 2025 Jan 9;24(1):4.
73. Mahenge HH, Muyaga LL, Nkya JD, Kafwenji AD, Mwalugelo YA, Kahamba NF, et al. Semi-field evaluation of aquatic predators for the control of *Anopheles funestus* in rural south-eastern Tanzania. *Malaria Journal*. 2024 Aug 2;23(1):228.
74. Shirima RS, Katusi GC, Mmbando AS, Fanuel G, Aslanis D, Kadam S, et al. Semi-field evaluation of electrocuting eave tubes for the control of endophagic mosquitoes in south-east Tanzania. *Parasites & Vectors*. 2024 Aug 20;17(1):349.
75. Kathet S, Sudi W, Mwingira V, Tungu P, Aalto M, Hakala T, et al. Efficacy of 3D screens for sustainable mosquito control: a semi-field experimental hut evaluation in northeastern Tanzania. *Parasites & Vectors*. 2023 Nov 15;16(1):417.
76. Muyaga LL, Meza FC, Kahamba NF, Njalambaha RM, Msugupakulya BJ, Kaindoa EW, et al. Effects of vegetation densities on the performance of attractive targeted sugar baits (ATSBs) for malaria vector control: a semi-field study. *Malar J*. 2023 Jun 21;22(1):190.
77. Mwanga EP, Mmbando AS, Mrosso PC, Stica C, Mapua SA, Finda MF, et al. Eave ribbons treated with transfluthrin can protect both users and non-users against malaria vectors. *Malar J*. 2019 Sep 18;18(1):314.
78. Vajda ÉA, Ross A, Saeung M, Pongsiri A, Mclver DJ, Tatarsky A, et al. The effect of novel mosquito bite prevention tools on *Anopheles minimus* landing and key secondary endpoints: semi-field evaluations in Thailand. *Malaria Journal*. 2024 Dec 18;23(1):387.
79. Vajda ÉA, Saeung M, Ross A, Mclver DJ, Tatarsky A, Moore SJ, et al. A semi-field evaluation in Thailand of the use of human landing catches (HLC) versus human-baited double net trap (HDN) for assessing the impact of a volatile pyrethroid spatial repellent and pyrethroid-treated clothing on *Anopheles minimus* landing. *Malaria Journal*. 2023 Jul 3;22(1):202.
80. Meza FC, Tenywa FC, Ashall S, Okumu FO, Moore SJ, Tripet F. Scalable camera traps for measuring the attractiveness of sugar baits for controlling malaria and dengue vectors. *Parasites & Vectors*. 2024 Dec 3;17(1):499.
81. Rique HL, Menezes HSG, Melo-Santos MAV, Silva-Filha MHNL. Evaluation of a long-lasting microbial larvicide against *Culex quinquefasciatus* and *Aedes*

- aegypti under laboratory and a semi-field trial. *Parasites & Vectors*. 2024 Sep 14;17(1):391.
82. Tambwe MM, Kibondo UA, Odufuwa OG, Moore J, Mpelepele A, Mashauri R, et al. Human landing catches provide a useful measure of protective efficacy for the evaluation of volatile pyrethroid spatial repellents. *Parasites & Vectors*. 2023 Mar 7;16(1):90.
83. Knols BG, Njiru BN, Mathenge EM, Mukabana WR, Beier JC, Killeen GF. MalariaSphere: A greenhouse-enclosed simulation of a natural *Anopheles gambiae* (Diptera: Culicidae) ecosystem in western Kenya. *Malar J*. 2002 Dec 18;1(1):19.
84. Johnson PCD, Barry SJE, Ferguson HM, Müller P. Power analysis for generalized linear mixed models in ecology and evolution. *Methods in Ecology and Evolution*. 2015;6(2):133-42.
85. Miles J. A framework for power analysis using a structural equation modelling procedure. *BMC Medical Research Methodology*. 2003 Dec 11;3(1):27.
86. Faul F, Erdfelder E, Lang AG, Buchner A. G*Power 3: A flexible statistical power analysis program for the social, behavioral, and biomedical sciences. *Behavior Research Methods*. 2007 May 1;39(2):175-91.
87. Juliano SA. POPULATION DYNAMICS. *moco*. 2007 Jul;23(sp2):265-75.
88. Ngowo HS, Okumu FO, Hape EE, Mshani IH, Ferguson HM, Matthiopoulos J. Using Bayesian state-space models to understand the population dynamics of the dominant malaria vector, *Anopheles funestus* in rural Tanzania. *Malaria Journal*. 2022 Jun 3;21(1):161.
89. Courchamp F, Clutton-Brock T, Grenfell B. Inverse density dependence and the Allee effect. *Trends in ecology & evolution*. 1999;14(10):405-10.
90. Muriu SM, Coulson T, Mbogo CM, Godfray HCJ. Larval density dependence in *Anopheles gambiae* ss, the major African vector of malaria. *Journal of Animal Ecology*. 2013;82(1):166-74.
91. Gimnig JE, Ombok M, Otieno S, Kaufman MG, Vulule JM, Walker ED. Density-Dependent Development of *Anopheles gambiae* (Diptera: Culicidae) Larvae in Artificial Habitats. *Journal of Medical Entomology*. 2002 Jan 1;39(1):162-72.
92. White MT, Griffin JT, Churcher TS, Ferguson NM, Basáñez MG, Ghani AC. Modelling the impact of vector control interventions on *Anopheles gambiae* population dynamics. *Parasites Vectors*. 2011 Dec;4(1):153.

93. Lyimo EO, Takken W, Koella JC. Effect of rearing temperature and larval density on larval survival, age at pupation and adult size of *Anopheles gambiae*. *Entomologia Experimentalis et Applicata*. 1992;63(3):265-71.
94. Schneider P, Takken W, McCall PJ. Interspecific competition between sibling species larvae of *Anopheles arabiensis* and *An. gambiae*. *Medical and Veterinary Entomology*. 2000;14(2):165-70.
95. Walker M, Robert MA, Childs LM. The importance of density dependence in juvenile mosquito development and survival: A model-based investigation. *Ecological Modelling*. 2021 Jan 15;440:109357.
96. Russell TL, Lwetoijera DW, Knols BG, Takken W, Killeen GF, Ferguson HM. Linking individual phenotype to density-dependent population growth: the influence of body size on the population dynamics of malaria vectors. *Proceedings of the Royal Society B: Biological Sciences*. 2011;278(1721):3142-51.
97. Tobin PC, Berec L, Liebhold AM. Exploiting Allee effects for managing biological invasions. *Ecology letters*. 2011;14(6):615-24.
98. Oro D, Martínez-Abraín A, Paracuellos M, Nevado JC, Genovart M. Influence of density dependence on predator-prey seabird interactions at large spatio-temporal scales. *Proceedings of the Royal Society B: Biological Sciences*. 2005 Nov 8;273(1584):379-83.
99. Marvelde L te, Meininger PL, Flamant R, Dingemanse NJ. Age-Specific Density-Dependent Survival in Mediterranean Gulls *Larus melanocephalus*. *arde*. 2009 Oct;97(3):305-12.
100. Li M, Dong R, Tuohetahong Y, Li X, Zhang H, Ye X, et al. Impact of Allee effects on the establishment of reintroduction populations of endangered species: The case of the Crested Ibis. *Global Ecology and Conservation*. 2022 Jun 1;35:e02103.
101. Perälä T, Hutchings JA, Kuparinen A. Allee effects and the Allee-effect zone in northwest Atlantic cod. *Biology Letters*. 2022 Feb 2;18(2):20210439.
102. Perälä T, Kuparinen A. Detection of Allee effects in marine fishes: analytical biases generated by data availability and model selection. *Proceedings of the Royal Society B: Biological Sciences*. 2017 Aug 30;284(1861):20171284.
103. Winter AM, Vasilyeva N, Vladimirov A. Spawner weight and ocean temperature drive Allee effect dynamics in Atlantic cod, *Gadus morhua*:

- inherent and emergent density regulation. *Biogeosciences*. 2023 Sep 13;20(17):3683-716.
104. Nagel R, Stainfield C, Fox-Clarke C, Toscani C, Forcada J, Hoffman JI. Evidence for an Allee effect in a declining fur seal population. *Proceedings of the Royal Society B* [Internet]. 2021 Mar 31 [cited 2023 Nov 10]; Available from: <https://royalsocietypublishing.org/doi/10.1098/rspb.2020.2882>
105. McLellan BN, Serrouya R, Wittmer HU, Boutin S. Predator-mediated Allee effects in multi-prey systems. *Ecology*. 2010;91(1):286-92.
106. Angulo E, Roemer GW, Berec L, Gascoigne J, Courchamp F. Double Allee Effects and Extinction in the Island Fox. *Conservation Biology*. 2007;21(4):1082-91.
107. Gaston MA, Fuji A, Weckerly FW, Forstner MRJ. Potential Component Allee Effects and Their Impact on Wetland Management in the Conservation of Endangered Anurans. *PLoS One*. 2010 Apr 9;5(4):e10102.
108. Berec L, Angulo E, Courchamp F. Multiple Allee effects and population management. *Trends in Ecology & Evolution*. 2007 Apr 1;22(4):185-91.
109. Kramer AM, Drake JM. Experimental demonstration of population extinction due to a predator-driven Allee effect. *Journal of Animal Ecology*. 2010;79(3):633-9.
110. Tobin PC, Robinet C, Johnson DM, Whitmire SL, Bjørnstad ON, Liebhold AM. The role of Allee effects in gypsy moth, *Lymantria dispar* (L.), invasions. *Population Ecology*. 2009;51(3):373-84.
111. Luque GM, Giraud T, Courchamp F. Allee effects in ants. *Journal of Animal Ecology*. 2013;82(5):956-65.
112. Kuussaari M, Saccheri I, Camara M, Hanski I. Allee Effect and Population Dynamics in the Glanville Fritillary Butterfly. *Oikos*. 1998;82(2):384-92.
113. Robinet C, Lance DR, Thorpe KW, Onufrieva KS, Tobin PC, Liebhold AM. Dispersion in Time and Space Affect Mating Success and Allee Effects in Invading Gypsy Moth Populations. *Journal of Animal Ecology*. 2008;77(5):966-73.
114. Courchamp F, Woodroffe R, Roemer G. Removing Protected Populations to Save Endangered Species. *Science*. 2003 Nov 28;302(5650):1532-1532.
115. Coonan, T. J. Recovery plan for island foxes (*Urocyon littoralis*) on the northern Channel Islands. Channel Islands National Park, Ventura, California.

- 2001; Available from:
<https://corpora.tika.apache.org/base/docs/govdocs1/271/271872.pdf>
116. Latta B, Driscoll D, Linticum J, Jackman R, Doney G. Capture and translocation of golden eagles from the California Channel Islands to mitigate depredation of endemic island foxes. 2005 Jan 1;
117. Coonan T, Rutz K, Garcelon D, Latta B, Gray M, Aschehoug E. Progress in island fox recovery efforts on the northern Channel Islands. 2005 Jan 1;
118. Rozikov UA, Boxonov ZS. A Discrete-Time Dynamical System of Wild Mosquito Population with Allee Effects. *DNC*. 2024 Sep;13(03):495-506.
119. Goswami M, Bhattacharyya P, Tribedi P. Allee effect: the story behind the stabilization or extinction of microbial ecosystem. *Archives of Microbiology*. 2017;199(2):185-90.
120. Zhou SR, Wang G. Allee-like effects in metapopulation dynamics. *Mathematical Biosciences*. 2004;189(1):103-13.
121. Gertsev VI, Gertseva VV. Classification of mathematical models in ecology. *Ecological Modelling*. 2004;178(3-4):329-34.
122. Malaria GP to RB, Chitnis N, Schpira A, Smith D, Hay SI, Smith T, et al. Mathematical modelling to support malaria control and elimination [Internet]. World Health Organization; 2010 [cited 2024 Sep 16]. Available from: <https://iris.who.int/handle/10665/87051>
123. Kiware SS, Chitnis N, Tatarsky A, Wu S, Castellanos HMS, Gosling R, et al. Attacking the mosquito on multiple fronts: Insights from the Vector Control Optimization Model (VCOM) for malaria elimination. *PLOS ONE*. 2017 Dec 1;12(12):e0187680.
124. Wu SL, Henry JM, Citron DT, Ssebuliba DM, Nsumba JN, C HMS, et al. Spatial dynamics of malaria transmission. *PLOS Computational Biology*. 2023 Jun 12;19(6):e1010684.
125. Lu J, Li J. Dynamics of stage-structured discrete mosquito population models. *Journal of Applied Analysis & Computation*. 2011 Feb 13;1.
126. Ngwa GA. On the Population Dynamics of the Malaria Vector. *Bull Math Biol*. 2006 Nov 1;68(8):2161-89.
127. Lutambi AM, Penny MA, Smith T, Chitnis N. Mathematical modelling of mosquito dispersal in a heterogeneous environment. *Mathematical Biosciences*. 2013 Feb 1;241(2):198-216.

128. Depinay JMO, Mbogo CM, Killeen G, Knols B, Beier J, Carlson J, et al. A simulation model of African Anopheles ecology and population dynamics for the analysis of malaria transmission. *Malar J.* 2004 Jul 30;3(1):29.
129. Okuneye K, Abdelrazec A, Gumel AB. Mathematical analysis of a weather-driven model for the population ecology of mosquitoes. *MBE.* 2018 Feb 1;15(1):57-93.
130. Christiansen-Jucht C, Erguler K, Shek CY, Basáñez MG, Parham PE. Modelling *Anopheles gambiae* s.s. Population Dynamics with Temperature- and Age-Dependent Survival. *International Journal of Environmental Research and Public Health.* 2015 Jun;12(6):5975-6005.
131. Abdelrazec A, Gumel AB. Mathematical assessment of the role of temperature and rainfall on mosquito population dynamics. *J Math Biol.* 2017 May 1;74(6):1351-95.
132. Ezanno P, Aubry-Kientz M, Arnoux S, Cailly P, L'Ambert G, Toty C, et al. A generic weather-driven model to predict mosquito population dynamics applied to species of *Anopheles*, *Culex* and *Aedes* genera of southern France. *Preventive Veterinary Medicine.* 2015 Jun 1;120(1):39-50.
133. El Moustaid F, Johnson LR. Modeling Temperature Effects on Population Density of the Dengue Mosquito *Aedes aegypti*. *Insects.* 2019 Nov;10(11):393.
134. Biswas SK, Ghosh U, Sarkar S. Mathematical model of zika virus dynamics with vector control and sensitivity analysis. *Infectious Disease Modelling.* 2020 Jan 1;5:23-41.
135. Abiodun GJ, Maharaj R, Witbooi P, Okosun KO. Modelling the influence of temperature and rainfall on the population dynamics of *Anopheles arabiensis*. *Malaria Journal.* 2016 Jul 15;15(1):364.
136. Marshall JM, White MT, Ghani AC, Schlein Y, Muller GC, Beier JC. Quantifying the mosquito's sweet tooth: modelling the effectiveness of attractive toxic sugar baits (ATSB) for malaria vector control. *Malar J.* 2013 Aug 23;12(1):291.
137. Chitnis N, Schapira A, Smith T, Steketee R. Comparing the Effectiveness of Malaria Vector-Control Interventions Through a Mathematical Model. *The American Journal of Tropical Medicine and Hygiene.* 2010 Aug 5;83(2):230-40.
138. Hickey GL, Grant SW, Dunning J, Siepe M. Statistical primer: sample size and power calculations—why, when and how?†. *European Journal of Cardio-Thoracic Surgery.* 2018 Jul 1;54(1):4-9.

139. Sheppard CRC. How Large should my Sample be? Some Quick Guides to Sample Size and the Power of Tests. *Marine Pollution Bulletin*. 1999 Jun 1;38(6):439-47.
140. Govella NJ, Chaki PP, Mpangile JM, Killeen GF. Monitoring mosquitoes in urban Dar es Salaam: Evaluation of resting boxes, window exit traps, CDC light traps, Ifakara tent traps and human landing catches. *Parasites Vectors*. 2011 Dec;4(1):40.
141. Dongus S, Nyika D, Kannady K, Mtasiwa D, Mshinda H, Gosoni L, et al. Urban agriculture and Anopheles habitats in Dar es Salaam, Tanzania. *Geospatial Health*. 2009 May 1;3(2):189-210.
142. Maheu-Giroux M, Castro MC. Attribution of reductions in malaria prevalence in Dar es Salaam, Tanzania. *The Lancet Planetary Health*. 2019 Jun 1;3(6):e246.
143. Chaki PP, Dongus S, Fillinger U, Kelly A, Killeen GF. Community-owned resource persons for malaria vector control: enabling factors and challenges in an operational programme in Dar es Salaam, United Republic of Tanzania. *Human Resources for Health*. 2011 Sep 28;9(1):21.
144. Monroe A, Mihayo K, Okumu F, Finda M, Moore S, Koenker H, et al. Human behaviour and residual malaria transmission in Zanzibar: findings from in-depth interviews and direct observation of community events. *Malaria Journal*. 2019 Jul 1;18(1):220.
145. Thomsen EK, Koimbu G, Pulford J, Jamea-Maiasa S, Ura Y, Keven JB, et al. Mosquito Behavior Change After Distribution of Bednets Results in Decreased Protection Against Malaria Exposure. *The Journal of Infectious Diseases*. 2017 Mar 1;215(5):790-7.
146. Kisinza WN, Nkya TE, Kabula B, Overgaard HJ, Massue DJ, Mageni Z, et al. Multiple insecticide resistance in *Anopheles gambiae* from Tanzania: a major concern for malaria vector control. *Malaria Journal*. 2017 Oct 30;16(1):439.
147. Musiime AK, Smith DL, Kilama M, Rek J, Arinaitwe E, Nankabirwa JI, et al. Impact of vector control interventions on malaria transmission intensity, outdoor vector biting rates and *Anopheles* mosquito species composition in Tororo, Uganda. *Malar J*. 2019 Dec 27;18:445.
148. Bugoro H, Iro'ofa C, Mackenzie DO, Apairamo A, Hevalao W, Corcoran S, et al. Changes in vector species composition and current vector biology and

- behaviour will favour malaria elimination in Santa Isabel Province, Solomon Islands. *Malaria Journal*. 2011 Sep 30;10(1):287.
149. Derua YA, Alifrangis M, Hosea KM, Meyrowitsch DW, Magesa SM, Pedersen EM, et al. Change in composition of the *Anopheles gambiae* complex and its possible implications for the transmission of malaria and lymphatic filariasis in north-eastern Tanzania. *Malar J*. 2012 Jun 8;11(1):188.
150. Kitau J, Oxborough RM, Tungu PK, Matowo J, Malima RC, Magesa SM, et al. Species Shifts in the *Anopheles gambiae* Complex: Do LLINs Successfully Control *Anopheles arabiensis*? *PLOS ONE*. 2012 Mar 16;7(3):e31481.
151. Gari T, Lindtjørn B. Reshaping the vector control strategy for malaria elimination in Ethiopia in the context of current evidence and new tools: opportunities and challenges. *Malaria Journal*. 2018 Dec 5;17(1):454.
152. Killeen GF, Seyoum A, Gimnig JE, Stevenson JC, Drakeley CJ, Chitnis N. Made-to-measure malaria vector control strategies: rational design based on insecticide properties and coverage of blood resources for mosquitoes. *Malaria Journal*. 2014 Apr 16;13(1):146.
153. Beier JC, Keating J, Githure JI, Macdonald MB, Impoinvil DE, Novak RJ. Integrated vector management for malaria control. *Malar J*. 2008 Dec 11;7(1):S4.
154. Raghavendra K, Barik TK, Sharma P, Bhatt RM, Srivastava HC, Sreehari U, et al. Chlorfenapyr: a new insecticide with novel mode of action can control pyrethroid resistant malaria vectors. *Malaria Journal*. 2011 Jan 25;10(1):16.
155. Protopopoff N, Mosha JF, Messenger LA, Lukole E, Charlwood JD, Wright A, et al. Effectiveness of piperonyl butoxide and pyrethroid-treated long-lasting insecticidal nets (LLINs) versus pyrethroid-only LLINs with and without indoor residual spray against malaria infection: third year results of a cluster, randomised controlled, two-by-two factorial design trial in Tanzania. *Malaria Journal*. 2023 Oct 3;22(1):294.
156. Devine GJ, Perea EZ, Killeen GF, Stancil JD, Clark SJ, Morrison AC. Using adult mosquitoes to transfer insecticides to *Aedes aegypti* larval habitats. *Proceedings of the National Academy of Sciences*. 2009 Jul 14;106(28):11530-4.
157. Lovett B, Bilgo E, Diabate A, St. Leger R. A review of progress toward field application of transgenic mosquitoicidal entomopathogenic fungi. *Pest Management Science*. 2019;75(9):2316-24.

158. Bilgo E, Lovett B, Bayili K, Millogo AS, Saré I, Dabiré RK, et al. Transgenic *Metarhizium pingshaense* synergistically ameliorates pyrethroid-resistance in wild-caught, malaria-vector mosquitoes. *PLOS ONE*. 2018 Sep 7;13(9):e0203529.
159. Smith DR, Hardy ICW, Gammell MP. Power rangers: no improvement in the statistical power of analyses published in *Animal Behaviour*. *Animal Behaviour*. 2011 Jan 1;81(1):347-52.
160. Taborsky M. Sample Size in the Study of Behaviour. *Ethology*. 2010;116(3):185-202.
161. Hayes RJ, Bennett S. Simple sample size calculation for cluster-randomized trials. *International Journal of Epidemiology*. 1999 Apr 1;28(2):319-26.
162. Green P, MacLeod CJ. SIMR: an R package for power analysis of generalized linear mixed models by simulation. *Methods in Ecology and Evolution*. 2016;7(4):493-8.
163. Bolker BM. Ecological Models and Data in R. In: *Ecological Models and Data in R* [Internet]. Princeton University Press; 2008 [cited 2023 Aug 22]. Available from:
<https://www.degruyter.com/document/doi/10.1515/9781400840908/html>
164. Martin JGA, Nussey DH, Wilson AJ, Réale D. Measuring individual differences in reaction norms in field and experimental studies: a power analysis of random regression models. *Methods in Ecology and Evolution*. 2011;2(4):362-74.
165. Ng'habi K, Viana M, Matthiopoulos J, Lyimo I, Killeen G, Ferguson HM. Mesocosm experiments reveal the impact of mosquito control measures on malaria vector life history and population dynamics. *Sci Rep*. 2018 Sep 17;8(1):13949.
166. Bates D, Mächler M, Bolker B, Walker S. Fitting Linear Mixed-Effects Models Using lme4. *Journal of Statistical Software*. 2015 Oct 7;67:1-48.
167. Kipingu AM, Lwatoejera DW, Ng'habi KR, Kiware SS, Viana M, Johnson PCD. A power analysis framework to aid the design of robust semi-field vector control experiments: R and RMarkdown tutorials for short- and long-term semi-field experiments testing single and combined interventions. 2024 Jun 19 [cited 2024 Jun 19]; Available from: <https://zenodo.org/records/11186504>

168. R Core Team. R: A Language and Environment for Statistical Computing [Internet]. Vienna, Austria: R Foundation for Statistical Computing; 2024. Available from: <https://www.R-project.org/>
169. Wickham H. ggplot2: Elegant Graphics for Data Analysis. Springer-Verlag New York; 2016.
170. Wickham H, François R, Henry L, Müller K, Vaughan D, Software P, et al. `_dplyr: A Grammar of Data Manipulation_`. R package version 1.1.2 [Internet]. 2023 [cited 2024 Jun 19]. Available from: <https://CRAN.R-project.org/package=dplyr>
171. Hartig F. `_DHARMA: Residual Diagnostics for Hierarchical (Multi-Level / Mixed) Regression Models_`. R package version 0.4.6, <<https://CRAN.R-project.org/package=DHARMA>>. 2022 Sep 8;
172. Bakker M, Wicherts JM. Outlier removal, sum scores, and the inflation of the type I error rate in independent samples t tests: The power of alternatives and recommendations. *Psychological Methods*. 2014;19(3):409-27.
173. Dai F, Hossain MA, Wang Y. State of the Art in Parallel and Distributed Systems: Emerging Trends and Challenges. *Electronics*. 2025 Jan;14(4):677.
174. Farlow R, Russell TL, Burkot TR. Nextgen Vector Surveillance Tools: sensitive, specific, cost-effective and epidemiologically relevant. *Malar J*. 2020 Nov 25;19(1):432.
175. Kenea O, Balkew M, Tekie H, Gebre-Michael T, Deressa W, Loha E, et al. Comparison of two adult mosquito sampling methods with human landing catches in south-central Ethiopia. *Malaria Journal*. 2017 Jan 13;16(1):30.
176. Mbuba E, Odufuwa OG, Tenywa FC, Philipo R, Tambwe MM, Swai JK, et al. Single blinded semi-field evaluation of MAÏA® topical repellent ointment compared to unformulated 20% DEET against *Anopheles gambiae*, *Anopheles arabiensis* and *Aedes aegypti* in Tanzania. *Malar J*. 2021 Jan 6;20:12.
177. Li L, Rysavy MA, Bobashev G, Das A. Comparing methods for risk prediction of multicategory outcomes: dichotomized logistic regression vs. multinomial logit regression. *BMC Medical Research Methodology*. 2024 Oct 31;24(1):261.
178. Sutradhar SC, Neerchal NK, Morel JG. A goodness-of-fit test for overdispersed binomial (or multinomial) models. *Journal of Statistical Planning and Inference*. 2008 May 1;138(5):1459-71.
179. Malaria [Internet]. [cited 2023 Aug 17]. Available from: <https://www.who.int/news-room/questions-and-answers/item/malaria>

180. Bolnick DI, Amarasekare P, Araújo MS, Bürger R, Levine JM, Novak M, et al. Why intraspecific trait variation matters in community ecology. *Trends in ecology & evolution*. 2011;26(4):183-92.
181. Ferguson HM, Govella NJ. Impacts of climate change on malaria vector control in Africa. In: *Planetary health approaches to understand and control vector-borne diseases* [Internet]. Wageningen Academic; 2023 [cited 2024 Feb 21]. p. 387-421. Available from: <https://brill.com/edcollchap-ooa/book/9789004688650/BP000024.xml>
182. World Health Organization. *Global vector control response 2017-2030*. Geneva; 2017.
183. Brady OJ, Godfray HCJ, Tatem AJ, Gething PW, Cohen JM, McKenzie FE, et al. Adult vector control, mosquito ecology and malaria transmission. *International health*. 2015 Mar;7(2):121-9.
184. Musiba RM, Tarimo BB, Monroe A, Msaky D, Ngowo H, Mihayo K, et al. Outdoor biting and pyrethroid resistance as potential drivers of persistent malaria transmission in Zanzibar. *Malar J*. 2022 Dec;21(1):172.
185. Fadai NT, Simpson MJ. Population Dynamics with Threshold Effects Give Rise to a Diverse Family of Allee Effects. *Bull Math Biol*. 2020 Jun 12;82(6):74.
186. Albery GF, Becker DJ, Firth JA, Silk M, Sweeny AR, Wal EV, et al. Density-dependent network structuring within and across wild animal systems [Internet]. *bioRxiv*; 2024 [cited 2024 Aug 26]. p. 2024.06.28.601262. Available from: <https://www.biorxiv.org/content/10.1101/2024.06.28.601262v1>
187. Kramer AM, Dennis B, Liebhold AM, Drake JM. The evidence for Allee effects. *Popul Ecol*. 2009 Jul 1;51(3):341-54.
188. Levin DA, Kelley CD, Sarkar S. Enhancement of Allee effects in plants due to self-incompatibility alleles. *Journal of Ecology*. 2009;97(3):518-27.
189. Kunin WE. Population Size and Density Effects in Pollination: Pollinator Foraging and Plant Reproductive Success in Experimental Arrays of Brassica Kaber. *Journal of Ecology*. 1997;85(2):225-34.
190. Stephens PA, Sutherland WJ, Freckleton RP. What Is the Allee Effect? *Oikos*. 1999;87(1):185-90.
191. Morris DW. Measuring the Allee Effect: Positive Density Dependence in Small Mammals. *Ecology*. 2002;83(1):14-20.
192. Drake, J. M., Kramer, A. M. Allee Effects. *Nature Education*. 2011;3(10):3.

193. Fauvergue X. A review of mate-finding Allee effects in insects: from individual behavior to population management. *Entomologia Experimentalis et Applicata*. 2013;146(1):79-92.
194. Sharov AA, Liebhold AM, Ravlin FW. Prediction of Gypsy Moth (Lepidoptera: Lymantriidae) Mating Success from Pheromone Trap Counts. *Environmental Entomology*. 1995 Oct 1;24(5):1239-44.
195. Tcheslavskaja K, Brewster CC, Sharov AA. Mating Success of Gypsy Moth (Lepidoptera: Lymantriidae) Females in Southern Wisconsin. 2002;35(1):8.
196. Robinet C, Liebhold A, Gray D. Variation in developmental time affects mating success and Allee effects. *Oikos*. 2007;116(7):1227-37.
197. Tobin PC, Robinet C, Johnson DM, Whitmire SL, Bjørnstad ON, Liebhold AM. The role of Allee effects in gypsy moth, *Lymantria dispar* (L.), invasions. *Population Ecology*. 2009;51(3):373-84.
198. Venette RC, Hutchison WD. Invasive Insect Species: Global Challenges, Strategies & Opportunities. *Front Insect Sci*. 2021;1:650520.
199. Walker M, Blackwood JC, Brown V, Childs LM. Modelling Allee effects in a transgenic mosquito population during range expansion. *Journal of Biological Dynamics*. 2019 Mar 15;13(sup1):2-22.
200. Li J. Modeling of mosquitoes with dominant or recessive Transgenes and Allee effects. *MBE*. 2009 Dec 31;7(1):99-121.
201. Gascoigne J, Berec L, Gregory S, Courchamp F. Dangerously few liaisons: a review of mate-finding Allee effects. *Popul Ecol*. 2009 Jul 1;51(3):355-72.
202. Zhao Z, Pang L, Song X, Wang D, Li Q. Impact of the impulsive releases and Allee effect on the dispersal behavior of the wild mosquitoes. *J Appl Math Comput*. 2022 Jun 1;68(3):1527-44.
203. Gambhir M, Singh BK, Michael E. Chapter One - The Allee Effect and Elimination of Neglected Tropical Diseases: A Mathematical Modelling Study. In: Anderson RM, Basáñez MG, editors. *Advances in Parasitology*. Academic Press; 2015. p. 1-31. (Mathematical Models for Neglected Tropical Diseases: Essential Tools for Control and Elimination, Part A; vol. 87).
204. Fillinger U, Kannady K, William G, Vanek MJ, Dongus S, Nyika D, et al. A tool box for operational mosquito larval control: preliminary results and early lessons from the Urban Malaria Control Programme in Dar es Salaam, Tanzania. *Malaria Journal*. 2008 Jan 25;7(1):20.

205. CFSR Global Weather Data for SWAT 1979-2014 | SWAT | Soil & Water Assessment Tool [Internet]. [cited 2022 Oct 4]. Available from: <https://swat.tamu.edu/data/cfsr>
206. R Core Team. *_R: A Language and Environment for Statistical Computing_*. R Foundation for Statistical Computing, Vienna, Austria. 2024; Available from: <https://www.R-project.org/>
207. Monte L. Characterisation of a nonlinear Leslie matrix model for predicting the dynamics of biological populations in polluted environments: Applications to radioecology. *Ecological Modelling*. 2013 Jan 10;248:174-83.
208. Mwangangi JM, Muturi EJ, Shililu J, Muriu SM, Jacob B, Kabiru EW, et al. Survival of immature *Anopheles arabiensis* (Diptera: Culicidae) in aquatic habitats in Mwea rice irrigation scheme, central Kenya. *Malar J*. 2006 Dec;5(1):114.
209. Koenraadt CJM, Githeko AK, Takken W. The effects of rainfall and evapotranspiration on the temporal dynamics of *Anopheles gambiae* s.s. and *Anopheles arabiensis* in a Kenyan village. *Acta Tropica*. 2004 Apr 1;90(2):141-53.
210. Vantaux A, Ouattarra I, Lefèvre T, Dabiré KR. Effects of larvicidal and larval nutritional stresses on *Anopheles gambiae* development, survival and competence for *Plasmodium falciparum*. *Parasit Vectors*. 2016 Apr 23;9:226.
211. Christiansen-Jucht CD, Parham PE, Saddler A, Koella JC, Basáñez MG. Larval and adult environmental temperatures influence the adult reproductive traits of *Anopheles gambiae* s.s. *Parasites Vectors*. 2015 Dec;8(1):456.
212. Beck-Johnson LM, Nelson WA, Paaijmans KP, Read AF, Thomas MB, Bjørnstad ON. The Effect of Temperature on *Anopheles* Mosquito Population Dynamics and the Potential for Malaria Transmission. Costa FTM, editor. *PLoS ONE*. 2013 Nov 14;8(11):e79276.
213. Lyimo EO, Takken W. Effects of adult body size on fecundity and the pre-gravid rate of *Anopheles gambiae* females in Tanzania. *Medical and Veterinary Entomology*. 1993;7(4):328-32.
214. Edillo FE, Touré YT, Lanzaro GC, Dolo G, Taylor CE. Survivorship and Distribution of Immature *Anopheles gambiae* s.l. (Diptera: Culicidae) in Banambani Village, Mali. *J Med Entomol*. 2004 May 1;41(3):333-9.
215. Charlwood JD, Smith T, Billingsley PF, Takken W, Lyimo EOK, Meuwissen JHET. Survival and infection probabilities of anthropophagic anophelines from

- an area of high prevalence of *Plasmodium falciparum* in humans. Bull Entomol Res. 1997 Oct;87(5):445-53.
216. Midega JT, Mbogo CM, Mwambi H, Wilson MD, Ojwang G, Mwangangi JM, et al. Estimating Dispersal and Survival of *Anopheles gambiae* and *Anopheles funestus* Along the Kenyan Coast by Using Mark-Release-Recapture Methods. J Med Entomol. 2007 Nov;44(6):923-9.
217. Impoinvil DE, Cardenas GA, Gihture JI, Mbogo CM, Beier JC. Constant Temperature and Time Period Effects on *Anopheles Gambiae* Egg Hatching. J Am Mosq Control Assoc. 2007 Jun;23(2):124-30.
218. Gebreyohannes DT, Houlahan JE. Weak evidence of density dependent population regulation when using the ability of two simple density dependent models to predict population size. Sci Rep. 2024 Feb 29;14(1):5051.
219. Population Limiting Factors | Learn Science at Scitable [Internet]. [cited 2024 Nov 4]. Available from: <https://www.nature.com/scitable/knowledge/library/population-limiting-factors-17059572/>
220. Tenan S, Tavecchia G, Oro D, Pradel R. Assessing the effect of density on population growth when modeling individual encounter data. Ecology. 2019;100(3):e02595.
221. Basáñez MG, Razali K, Renz A, Kelly D. Density-dependent host choice by disease vectors: epidemiological implications of the ideal free distribution. Transactions of the Royal Society of Tropical Medicine and Hygiene. 2007;101(3):256-69.
222. Solano N, Herring EC, Hintz CW, Newberry PM, Schatz AM, Walker JW, et al. Mosquito population dynamics is shaped by the interaction among larval density, season, and land use [Internet]. bioRxiv; 2024 [cited 2024 Oct 21]. p. 2024.06.08.598043. Available from: <https://www.biorxiv.org/content/10.1101/2024.06.08.598043v1>
223. Russell TL, Lwetoijera DW, Knols BGJ, Takken W, Killeen GF, Ferguson HM. Linking individual phenotype to density-dependent population growth: the influence of body size on the population dynamics of malaria vectors. Proceedings of the Royal Society B: Biological Sciences. 2011 Mar 9;278(1721):3142-51.
224. Churcher TS, Dawes EJ, Sinden RE, Christophides GK, Koella JC, Basáñez MG. Population biology of malaria within the mosquito: density-dependent

- processes and potential implications for transmission-blocking interventions. *Malaria Journal*. 2010 Nov 4;9(1):311.
225. Villaverde AF, Pathirana D, Fröhlich F, Hasenauer J, Banga JR. A protocol for dynamic model calibration. *Briefings in Bioinformatics*. 2022 Jan 1;23(1):bbab387.
226. World malaria report 2015 [Internet]. [cited 2024 Dec 24]. Available from: <https://www.who.int/publications/i/item/9789241565158>
227. Vercken E, Groussier G, Lamy L, Mailleret L. The hidden side of the Allee effect: correlated demographic traits and extinction risk in experimental populations. *Peer Community Journal* [Internet]. 2021 [cited 2024 Oct 21];1. Available from: <https://peercommunityjournal.org/articles/10.24072/pcjournal.41/>
228. Gascoigne J. A theoretical and experimental study of Allee effects. *Dissertations, Theses, and Masters Projects* [Internet]. 2003 Jan 1; Available from: <https://scholarworks.wm.edu/etd/1539616659>
229. Gascoigne J, Lipcius RN. Allee effects in marine systems. *Marine Ecology Progress Series*. 2004;269:49-59.
230. DeSiervo MH, Ayres MP, Culler LE. Quantifying the nature and strength of intraspecific density dependence in Arctic mosquitoes. *Oecologia*. 2021 Aug 1;196(4):1061-72.
231. Gilles JRL, Lees RS, Soliban SM, Benedict MQ. Density-Dependent Effects in Experimental Larval Populations of *Anopheles arabiensis* (Diptera: Culicidae) Can Be Negative, Neutral, or Overcompensatory Depending on Density and Diet Levels. *Journal of Medical Entomology*. 2011 Mar 1;48(2):296-304.
232. Killeen GF, Seyoum A, Sikaala C, Zomboko AS, Gimnig JE, Govella NJ, et al. Eliminating malaria vectors. *Parasites & Vectors*. 2013 Jun 7;6(1):172.
233. Luque GM, Vayssade C, Facon B, Guillemaud T, Courchamp F, Fauvergue X. The genetic Allee effect: a unified framework for the genetics and demography of small populations. *Ecosphere*. 2016;7(7):e01413.
234. Clutton-Brock TH, Gaynor D, McIlrath GM, Maccoll ADC, Kansky R, Chadwick P, et al. Predation, group size and mortality in a cooperative mongoose, *Suricata suricatta*. *Journal of Animal Ecology*. 1999;68(4):672-83.
235. Gowelo S, McCann RS, Koenraadt CJM, Takken W, van den Berg H, Manda-Taylor L. Community factors affecting participation in larval source

- management for malaria control in Chikwawa District, Southern Malawi. *Malaria Journal*. 2020 Jun 2;19(1):195.
236. McCann RS, van den Berg H, Diggle PJ, van Vugt M, Terlouw DJ, Phiri KS, et al. Assessment of the effect of larval source management and house improvement on malaria transmission when added to standard malaria control strategies in southern Malawi: study protocol for a cluster-randomised controlled trial. *BMC Infectious Diseases*. 2017 Sep 22;17(1):639.
237. World Health Organization. Larval source management: a supplementary malaria vector control measure: an operational manual [Internet]. Geneva: World Health Organization; 2013 [cited 2024 Mar 20]. Available from: <https://iris.who.int/handle/10665/85379>
238. Killeen GF, Fillinger U, Kiche I, Gouagna LC, Knols BG. Eradication of *Anopheles gambiae* from Brazil: lessons for malaria control in Africa? *The Lancet Infectious Diseases*. 2002 Oct 1;2(10):618-27.
239. Killeen GF, Kiware SS, Okumu FO, Sinka ME, Moyes CL, Massey NC, et al. Going beyond personal protection against mosquito bites to eliminate malaria transmission: population suppression of malaria vectors that exploit both human and animal blood. *BMJ Glob Health*. 2017 Apr;2(2):e000198.
240. A tool box for operational mosquito larval control: preliminary results and early lessons from the Urban Malaria Control Programme in Dar es Salaam, Tanzania | *Malaria Journal* | Full Text [Internet]. [cited 2023 Aug 19]. Available from: <https://malariajournal.biomedcentral.com/articles/10.1186/1475-2875-7-20>
241. Gimnig JE, Walker ED, Otieno P, Kosgei J, Olang G, Ombok M, et al. Incidence of Malaria among Mosquito Collectors Conducting Human Landing Catches in Western Kenya. *The American Journal of Tropical Medicine and Hygiene*. 2013 Feb 6;88(2):301-8.
242. Paaijmans KP, Wandago MO, Githeko AK, Takken W. Unexpected High Losses of *Anopheles gambiae* Larvae Due to Rainfall. Carter D, editor. *PLoS ONE*. 2007 Nov 7;2(11):e1146.
243. JAGS - Just Another Gibbs Sampler [Internet]. [cited 2024 Mar 6]. Available from: <https://mcmc-jags.sourceforge.io/>
244. Su Y, Yajima, M. `_R2jags: Using R to Run 'JAGS'_`. R package version 0.7-1. 2021; Available from: <https://CRAN.R-project.org/package=R2jags>

245. Kellner K. `_jagsUI`: A Wrapper Around 'rjags' to Streamline 'JAGS' Analyses_. R package version 1.5.2. 2021; Available from: <https://CRAN.R-project.org/package=jagsUI>
246. `gelman.diag`: Gelman and Rubin's convergence diagnostic in coda: Output Analysis and Diagnostics for MCMC [Internet]. [cited 2024 Mar 6]. Available from: <https://rdrr.io/cran/coda/man/gelman.diag.html>
247. Fillinger U, Sonye G, Killeen GF, Knols BGJ, Becker N. The practical importance of permanent and semipermanent habitats for controlling aquatic stages of *Anopheles gambiae sensu lato* mosquitoes: operational observations from a rural town in western Kenya. *Tropical Medicine & International Health*. 2004;9(12):1274-89.
248. Baldini F, Viana M. Dried out but alive: how mosquitoes survive 8 months. *Trends in Parasitology*. 2023 Jan 1;39(1):1-3.
249. Faiman R, Yaro AS, Dao A, Sanogo ZL, Diallo M, Samake D, et al. Isotopic evidence that aestivation allows malaria mosquitoes to persist through the dry season in the Sahel. *Nat Ecol Evol*. 2022 Nov;6(11):1687-99.
250. Zhou G, Munga S, Minakawa N, Githeko AK, Yan G. Spatial Relationship between Adult Malaria Vector Abundance and Environmental Factors in Western Kenya Highlands. *The American Journal of Tropical Medicine and Hygiene*. 2007 Jul 1;77(1):29-35.
251. Christiansen-Jucht C, Parham PE, Saddler A, Koella JC, Basáñez MG. Temperature during larval development and adult maintenance influences the survival of *Anopheles gambiae s.s.* 2014;10.
252. Fukui S, Kuwano Y, Ueno K, Atsumi K, Ohta S. Modeling the effect of rainfall changes to predict population dynamics of the Asian tiger mosquito *Aedes albopictus* under future climate conditions. *PLOS ONE*. 2022 May 25;17(5):e0268211.
253. Benedum CM, Seidahmed OME, Eltahir EAB, Markuzon N. Statistical modeling of the effect of rainfall flushing on dengue transmission in Singapore. *PLoS Negl Trop Dis*. 2018 Dec 6;12(12):e0006935.
254. Vézilier J, Nicot A, Gandon S, Rivero A. Plasmodium infection decreases fecundity and increases survival of mosquitoes. *Proc Biol Sci*. 2012 Oct 7;279(1744):4033-41.
255. Ng'habi K, Viana M, Matthiopoulos J, Lyimo I, Killeen G, Ferguson HM. Mesocosm experiments reveal the impact of mosquito control measures on

- malaria vector life history and population dynamics. *Sci Rep*. 2018 Dec;8(1):13949.
256. Nambunga IH, Ngowo HS, Mapua SA, Hape EE, Msugupakulya BJ, Msaky DS, et al. Aquatic habitats of the malaria vector *Anopheles funestus* in rural south-eastern Tanzania. *Malaria Journal*. 2020 Jun 23;19(1):219.
257. McCann RS, Messina JP, MacFarlane DW, Bayoh MN, Vulule JM, Gimnig JE, et al. Modeling larval malaria vector habitat locations using landscape features and cumulative precipitation measures. *International Journal of Health Geographics*. 2014 Jun 6;13(1):17.
258. Tsegaye A, Demissew A, Hawaria D, Abossie A, Getachew H, Habtamu K, et al. *Anopheles* larval habitats seasonality and environmental factors affecting larval abundance and distribution in Arjo-Didessa sugar cane plantation, Ethiopia. *Malaria Journal*. 2023 Nov 15;22(1):350.
259. Kweka EJ, Zhou G, Munga S, Lee MC, Atieli HE, Nyindo M, et al. Anopheline Larval Habitats Seasonality and Species Distribution: A Prerequisite for Effective Targeted Larval Habitats Control Programmes. *PLOS ONE*. 2012 Dec 18;7(12):e52084.
260. Bayoh MN, Lindsay SW. Effect of temperature on the development of the aquatic stages of *Anopheles gambiae sensu stricto* (Diptera: Culicidae). *Bulletin of Entomological Research*. 2003 Sep;93(5):375-81.
261. Bayoh MN, Lindsay SW. Temperature-related duration of aquatic stages of the Afrotropical malaria vector mosquito *Anopheles gambiae* in the laboratory. *Medical and Veterinary Entomology*. 2004;18(2):174-9.
262. Ndetto EL, Matzarakis A. Basic analysis of climate and urban bioclimate of Dar es Salaam, Tanzania. *Theor Appl Climatol*. 2013 Oct 1;114(1):213-26.
263. Vector-borne diseases [Internet]. [cited 2023 Nov 8]. Available from: <https://www.who.int/news-room/fact-sheets/detail/vector-borne-diseases>
264. Malaria vaccines (RTS,S and R21) [Internet]. [cited 2024 Nov 14]. Available from: <https://www.who.int/news-room/questions-and-answers/item/q-a-on-rts-s-malaria-vaccine>
265. Runge M, Snow RW, Molteni F, Thawer S, Mohamed A, Mandike R, et al. Simulating the council-specific impact of anti-malaria interventions: A tool to support malaria strategic planning in Tanzania. *PLoS One*. 2020 Feb 19;15(2):e0228469.

266. Stuckey EM, Stevenson JC, Cooke MK, Owaga C, Marube E, Oando G, et al. Simulation of malaria epidemiology and control in the highlands of western Kenya. *Malaria Journal*. 2012 Oct 29;11(1):357.
267. De Lima TFM, Lana RM, De Senna Carneiro TG, Codeço CT, Machado GS, Ferreira LS, et al. DengueME: A Tool for the Modeling and Simulation of Dengue Spatiotemporal Dynamics. *International Journal of Environmental Research and Public Health*. 2016 Sep;13(9):920.
268. Zhang X, He H, Wang K, Zhu H. Dynamics and Simulations of Impulsive Population Models Involving Integrated Mosquito Control Strategies and Fractional Derivatives for Dengue Control. *Fractal and Fractional*. 2024 Nov;8(11):624.
269. Helikumi M, Lolika PO, Makau KA, Ndambuki MC, Mhlanga A. Modeling Zika Virus Disease Dynamics with Control Strategies. *Informatics*. 2024 Dec;11(4):85.
270. Suparit P, Wiratsudakul A, Modchang C. A mathematical model for Zika virus transmission dynamics with a time-dependent mosquito biting rate. *Theoretical Biology and Medical Modelling*. 2018 Aug 1;15(1):11.
271. Stolk WA, de Vlas SJ, Borsboom GJJM, Habbema JDF. LYMFASIM, a simulation model for predicting the impact of lymphatic filariasis control: quantification for African villages. *Parasitology*. 2008 Nov;135(13):1583-98.
272. Plaisier AP, Subramanian S, Das PK, Souza W, Lapa T, Furtado AF, et al. The LYMFASIM simulation program for modeling lymphatic filariasis and its control. *Methods Inf Med*. 1998 Jan;37(1):97-108.
273. Petrovskii S, Petrovskaya N. Computational ecology as an emerging science. *Interface Focus*. 2012 Jan 5;2(2):241.
274. Brauer F. Mathematical epidemiology: Past, present, and future. *Infectious Disease Modelling*. 2017 Feb 4;2(2):113.
275. Lippi CA, Mundis SJ, Sippy R, Flenniken JM, Chaudhary A, Hecht G, et al. Trends in mosquito species distribution modeling: insights for vector surveillance and disease control. *Parasites & Vectors*. 2023 Aug 28;16(1):302.
276. Auger-Méthé M, Field C, Albertsen CM, Derocher AE, Lewis MA, Jonsen ID, et al. State-space models' dirty little secrets: even simple linear Gaussian models can have estimation problems. *Sci Rep*. 2016 May 25;6(1):26677.
277. Restif O, Hayman DTS, Pulliam JRC, Plowright RK, George DB, Luis AD, et al. Model-guided fieldwork: practical guidelines for multidisciplinary research on

- wildlife ecological and epidemiological dynamics. *Ecology Letters*. 2012;15(10):1083-94.
278. Moshia JF, Matowo NS, Kulkarni MA, Messenger LA, Lukole E, Mallya E, et al. Effectiveness of long-lasting insecticidal nets with pyriproxyfen-pyrethroid, chlorfenapyr-pyrethroid, or piperonyl butoxide-pyrethroid versus pyrethroid only against malaria in Tanzania: final-year results of a four-arm, single-blind, cluster-randomised trial. *The Lancet Infectious Diseases*. 2024 Jan 1;24(1):87-97.
279. Böhmert AL, Logan RAE, Portwood NM, Hartke J, Ingham VA. A descriptive review of next-generation insecticide-treated bed nets for malaria control. *Front Malar* [Internet]. 2024 May 28 [cited 2024 Nov 9];2. Available from: <https://www.frontiersin.org/journals/malaria/articles/10.3389/fmala.2024.1337572/full>
280. Serdar CC, Cihan M, Yücel D, Serdar MA. Sample size, power and effect size revisited: simplified and practical approaches in pre-clinical, clinical and laboratory studies. *Biochem Med (Zagreb)*. 2021 Feb 15;31(1):010502.
281. Juliano SA. Population Dynamics. *J Am Mosq Control Assoc*. 2007;23(2 Suppl):265-75.
282. Afrane YA, Githeko AK, Yan G. The ecology of Anopheles mosquitoes under climate change: case studies from the effects of deforestation in East African highlands. *Annals of the New York Academy of Sciences*. 2012;1249(1):204-10.
283. Asgarian TS, Moosa-Kazemi SH, Sedaghat MM. Impact of meteorological parameters on mosquito population abundance and distribution in a former malaria endemic area, central Iran. *Heliyon*. 2021 Dec 1;7(12):e08477.
284. Monroe A, Msaky D, Kiware S, Tarimo BB, Moore S, Haji K, et al. Patterns of human exposure to malaria vectors in Zanzibar and implications for malaria elimination efforts. *Malaria Journal*. 2020 Jun 22;19(1):212.
285. Mkali HR, Lalji SM, Al-mafazy A wahid, Joseph JJ, Mwaipape OS, Ali AS, et al. How Real-Time Case-Based Malaria Surveillance Helps Zanzibar Get a Step Closer to Malaria Elimination: Description of Operational Platform and Resources. *Glob Health Sci Pract*. 2023 Oct 30;11(5):e2200522.
286. Ali MH, Kitau J, Ali AS, Al-Mafazy A wahid, Tegegne SG, Ussi O, et al. Malaria elimination in Zanzibar: where next? *Pan Afr Med J*. 2023 Jun 18;45(Suppl 1):7.

287. Murindahabi MM, Takken W, Misago X, Niyituma E, Umupfasoni J, Hakizimana E, et al. Monitoring mosquito nuisance for the development of a citizen science approach for malaria vector surveillance in Rwanda. *Malaria Journal*. 2021 Jan 10;20(1):36.
288. Murindahabi MM, Takken W, Hakizimana E, van Vliet AJH, Poortvliet PM, Mutesa L, et al. A handmade trap for malaria mosquito surveillance by citizens in Rwanda. *PLoS One*. 2022 May 11;17(5):e0266714.
289. Murindahabi MM, Asingizwe D, Poortvliet PM, van Vliet AJH, Hakizimana E, Mutesa L, et al. A citizen science approach for malaria mosquito surveillance and control in Rwanda. *NJAS - Wageningen Journal of Life Sciences*. 2018 Nov 1;86-87:101-10.
290. Murindahabi MM, Hoseni A, Corné Vreugdenhil LC, van Vliet AJH, Umupfasoni J, Mutabazi A, et al. Citizen science for monitoring the spatial and temporal dynamics of malaria vectors in relation to environmental risk factors in Ruhuha, Rwanda. *Malaria Journal*. 2021 Dec 3;20(1):453.
291. vector-biology-ppt.pdf [Internet]. [cited 2024 Nov 30]. Available from: https://www.who.int/docs/default-source/wrindia/presentations-webinar-on-vector-control-strategies/vector-biology-ppt.pdf?sfvrsn=7029d78b_2
292. Gascoigne JC, Lipcius RN. Allee effects driven by predation. *Journal of Applied Ecology*. 2004;41(5):801-10.
293. Gilbert SF. Aging: The Biology of Senescence. In: *Developmental Biology* 6th edition [Internet]. Sinauer Associates; 2000 [cited 2024 Nov 12]. Available from: <https://www.ncbi.nlm.nih.gov/books/NBK10041/>
294. Barr JS, Martin LE, Tate AT, Hillyer JF. Warmer environmental temperature accelerates aging in mosquitoes, decreasing longevity and worsening infection outcomes. *Immunity & Ageing*. 2024 Sep 11;21(1):61.
295. Somé BM, Guissou E, Da DF, Richard Q, Choisy M, Yameogo KB, et al. Mosquito ageing modulates the development, virulence and transmission potential of pathogens. *Proceedings of the Royal Society B: Biological Sciences*. 2024 Jan 3;291(2014):20232097.
296. Johnson BJ, Hugo LE, Churcher TS, Ong OTW, Devine GJ. Mosquito Age Grading and Vector-Control Programmes. *Trends in Parasitology*. 2020 Jan 1;36(1):39-51.

297. Atieli HE, Zhou G, Zhong D, Wang X, Lee M chieh, Yaro AS, et al. Wind-assisted high-altitude dispersal of mosquitoes and other insects in East Africa. *Journal of Medical Entomology*. 2023 Jul 1;60(4):698-707.
298. Huestis DL, Dao A, Diallo M, Sanogo ZL, Samake D, Yaro AS, et al. Windborne long-distance migration of malaria mosquitoes in the Sahel. *Nature*. 2019 Oct;574(7778):404-8.
299. Yaro AS, Linton YM, Dao A, Diallo M, Sanogo ZL, Samake D, et al. Diversity, composition, altitude, and seasonality of high-altitude windborne migrating mosquitoes in the Sahel: Implications for disease transmission. *Front Epidemiol [Internet]*. 2022 Oct 13 [cited 2024 Nov 12];2. Available from: <https://www.frontiersin.org/journals/epidemiology/articles/10.3389/fepid.2022.1001782/full>
300. Briët OJT, Impoinvil DE, Chitnis N, Pothin E, Lemoine JF, Frederic J, et al. Models of effectiveness of interventions against malaria transmitted by *Anopheles albimanus*. *Malaria Journal*. 2019 Aug 1;18(1):263.
301. Runge M, Molteni F, Mandike R, Snow RW, Lengeler C, Mohamed A, et al. Applied mathematical modelling to inform national malaria policies, strategies and operations in Tanzania. *Malaria Journal*. 2020 Mar 2;19(1):101.
302. Golumbeanu M, Yang GJ, Camponovo F, Stuckey EM, Hamon N, Mondy M, et al. Leveraging mathematical models of disease dynamics and machine learning to improve development of novel malaria interventions. *Infectious Diseases of Poverty*. 2022 Jun 4;11(1):61.
303. Hammond A, Pollegioni P, Persampieri T, North A, Minuz R, Trusso A, et al. Gene-drive suppression of mosquito populations in large cages as a bridge between lab and field. *Nat Commun*. 2021 Jul 28;12(1):4589.
304. Naidoo K, Oliver SV. Gene drives: an alternative approach to malaria control? *Gene Ther*. 2024 Jul 22;1-13.
305. Gilioli G, Pasquali S, Marchesini E. A modelling framework for pest population dynamics and management: An application to the grape berry moth. *Ecological Modelling*. 2016 Jan 24;320:348-57.
306. Lustig A, James A, Anderson D, Plank M. Pest control at a regional scale: Identifying key criteria using a spatially explicit, agent-based model. *Journal of Applied Ecology*. 2019;56(7):1515-27.

307. Porter R, Norman R, Gilbert L. Controlling tick-borne diseases through domestic animal management: a theoretical approach. *Theor Ecol.* 2011 Aug 1;4(3):321-39.
308. Longbottom J, Caminade C, Gibson HS, Weiss DJ, Torr S, Lord JS. Modelling the impact of climate change on the distribution and abundance of tsetse in Northern Zimbabwe. *Parasites & Vectors.* 2020 Oct 19;13(1):526.
309. Liana YA, Shaban N, Mlay G, Phibert A. African Trypanosomiasis Dynamics: Modelling the Effects of Treatment, Education, and Vector Trapping. *International Journal of Mathematics and Mathematical Sciences.* 2020;2020(1):3690472.
310. Routledge I, Walker M, Cheke RA, Bhatt S, Nkot PB, Matthews GA, et al. Modelling the impact of larviciding on the population dynamics and biting rates of *Simulium damnosum* (s.l.): implications for vector control as a complementary strategy for onchocerciasis elimination in Africa. *Parasites Vectors.* 2018 May 29;11(1):316.